Message du Vice Doyen de la Recherche

Chers Collègues, Chers Amis,

Je vous souhaite la bienvenue à la sixième édition de la Journée de Recherche CHUV qui touche cette année la thématique de la *Médecine Régénérative*. Cette thématique est particulièrement intégrative puisqu'elle intéresse biologistes, médecins, ingénieurs et chimistes et constitue l'exemple même du domaine pluridisciplinaire qui réunit les chercheurs du CHUV, de l'UNIL et de l'EPFL, et que notre Faculté souhaite promouvoir.

La médecine régénérative touche pratiquement tous les domaines de la médecine, puisque elle se consacre en grande partie à la compréhension de la biologie des cellules souches dont la fonction physiologique détermine la nature et le fonctionnement de chaque tissu mais dont la dysfonction peut être à l'origine d'un vaste diapason de maladies, allant de maladies dégénératives jusqu'au cancer. Les questions fondamentales quand au traitement de nombreuses affections dans lesquelles le régénération tissulaire est affectée d'une manière directe ou indirecte sont restées jusqu'ici sans réponse : comment réparer des lésions du système nerveux qui sont à l'origine d'une para- ou d'une tétraplégie ? Comment contrecarrer la progression de myopathies qui causent le décès dans l'adolescence ? Comment manipuler un greffon d'organe de manière à ce qu'il ne soit pas rejeté sans que l'on doive recourir à un traitement immunosuppresseur lourd de conséquences ? Comment identifier les cellules cancéreuses qui constituent le moteur de la progression tumorale et qu'il faut cibler sur le plan thérapeutique ?

La compréhension des propriétés et du fonctionnement des cellules souches d'une part, et celle des molécules qui constituent la matrice extracellulaire tissulaire de l'autre, permettent d'anticiper des progrès sans précédent dans de multiples domaines de la médecine. En premier lieu viennent les affections touchant les tissus dont la capacité de régénération est limitée. Le traitement des maladies dégénératives des systèmes nerveux, musculaire et squelettique, ainsi que celui des conséquences de lésions traumatiques, qui présentaient un défi insurmontable, commencent a laisser entrevoir des perspectives inimaginables jusqu'à il y a relativement peu de temps. La possibilité de régénerer les tissus nerveux et musculaire et d'y corriger des défauts innés ou acquis, même si elle nécessite encore un long travail de mise au point, ne relève plus de la science-fiction.

De même, l'identification de cellules initiatrices de multiples types de cancer commence à devenir une réalité. Les questions liées à la nature et aux propriétés des ces cellules et à la manière de les cibler de façon à bloquer leur dissémination et de renverser la croissances des lésions métastatiques sont maintenant abordables.

La résolution de l'ensemble de ces questions nécessite une approche pluridisciplinaire comprenant non seulement des biologistes et des médecins mais aussi des chimistes, des bioinformaticiens des physiciens et des ingénieurs. La qualité et la complémentarité de chercheurs du CHUV, de l'UNIL et de l'EPFL placent Lausanne dans une situation particulièrement favorable pour y apporter des contributions significatives.

J'aimerais remercier les membres du comité scientifique pour avoir établi le programme stimulant et de très haute qualité auquel vous êtes conviés. Je vous souhaite de passer une excellente journée et vous adresse mes meilleures salutations.

Ivan Stamenkovic
Vice Doyen de la Recherche

UNIL | Université de Lausanne
Faculté de biologie et de médecine

Comité d'organisation 2008

Yvan Arsenijevic, Thérapie génique et biologie des cellules souches, Hôp.Ophtal.

Yann Barrandon, Dynamique des cellules souches, EPFL

Vassily Hatzimanikatis, Biotechnologie computationnelle des systèmes, EPFL

Jeffrey Hubbell, Médecine régénérative et de pharmacobiologie, EPFL

Brigitte Jolles-Haeberli, Hôpital Orthopédique

Thierry Pedrazzini, Médecine interne, CHUV

Ivan Stamenkovic, Institut de pathologie, CHUV

Melody Swartz, Mécanobiologie et de morphogenèse, EPFL

Administration de la Recherche :

Jovan Mirkovitch

Anne Tricot

Coraline Fraga

CHUV RESEARCH DAY 2008

Thursday, January 17th, 2008

"Regenerative Medicine"

08:30 **Presentation of the 2008 Research Day**
Professor Ivan Stamenkovic, Vice Dean for Research

08:45 **Keynote speaker 1**

Professor Philippe Menasché
Department of Cardio-Vascular Surgery
Hôpital Européen G. Pompidou, Paris
"Promises and pitfalls of skeletal myoblast therapy"

09:30 **Coffee & Posters**

10:30 **6 short talks**

12:00 **Keynote speaker 2**

Professor Giulio Cossu
Stem Cell Research Institute, Milano
"Towards a cell therapy for muscular dystrophy"

12:45 **Lunch, Coffee & Posters**

14:00 **Keynote speaker 3**

Professor Michele De Luca
Department of Biomedical Sciences, Modena
Epithelial Stem Cell Research Centre, Venice
"Epithelial stem cells and regenerative medicine"

14:45 **6 short talks**

16:15 **Coffee & Posters**

17:00 **Keynote speaker 4**

Professor Lior Gepstein
Dept of Physiology & Biophysics, Technion – Haifa, Israel
"Myocardial Regeneration by Human Embryonic Stem Cells"

17:45 **Poster Prizes Ceremony**

18:00 **Apéritif & Buffet**

ATTENDANCE IS FREE - NO REGISTRATION IS NECESSARY

NOTE: Posters will be displayed from
Wednesday January 16st early morning to Friday January 18th early morning.

12 short talks

Schedule	Names, departments	Titles
Morning		
10h30 - 10h45	**Boris Hinz** Laboratoire de biophysique cellulaire - EPFL	*"The myofibroblast - friend and foe in tissue regeneration"*
10h45 – 11h00	**Matthias Lutolf** Laboratoire de cellules souches et bioengineering - EPFL	*"Bioengineering artificial stem cell niches".*
11h00 – 11h15	**Corinne Kostic** Unité de thérapie génique et biologie des cellules souches – Hôpital Ophtalmique	*"Gene therapy preclinical studies for Leber congenital amaurosis"*
11h15 – 11h30	**Anne Zurn** Chirurgie expérimentale - CHUV	*"Delayed peripheral nerve priming improves regeneration of sensory axons into the spinal cord following dorsal root injury."*
11h30 – 11h45	**Meta Djojosubroto** Unité de thérapie génique et biologie des cellules souches – Hôpital Ophtalmique	*"Increased chromosomal aberrations and transformation of adult mouse retinal stem cells"*
11h45 – 12h00	**Paola Bonfanti** Chirurgie expérimentale - CHUV & Laboratoire de dynamique des cellules souches - EPFL	*"Thymic epithelial cells have skin potency"*
Afternoon		
14h45 – 15h00	**Dominique Pioletti** Laboratoire de biomécanique en orthopédie - EPFL	*"In Vivo evaluation of human cells as allogenic cell source for tissue engineering"*
15h00 – 15h15	**Mikaël Martino** Laboratoire de médecine régénérative et de pharmacobiologie - EPFL	*"Controlling mesenchymal stem cells response to biomaterials with recombinant integrin-specific fibronectin fragments"*
15h15 – 15h30	**Dela Golshayan** Nephrologie et Centre de Transplantation d'organes - CHUV	*"Mechanisms of Allograft rejection and tolerance in transplantation"*
15h30 - 15h45	**Jonathan Bloch** Médecine Interne - CHUV	*"Spleen derived vascular progenitor cell transfer restores metabolic and vascular insulin sensitivity in high-fat diet insulin resistant mice"*
15h45 - 16h00	**Marc-Etienne Roehrich** Cardiologie – CHUV	*"Immunophenotypical analysis of putative cardiac progenitor cells isolated based on high ALDH activity from adult mouse and human hearts"*
16h00 – 16h15	**Mohamed Nemir** Dpt de Médecine - CHUV	*"Control of cardiac integrity via the Notch1 receptor pathway".*

EHU
Environnement Humain

Key cognitive and collaborative aptitudes in ambulance people

[1]Arial M., [2]Benoît D., [1]Danuser B.

Institute for Work and Health[1], Clinique Bois-Cerf Hirslanden[2]

The aim of our study was to identify and document some key cognitive aptitudes used by ambulance people in emergency situations. Better knowing such aptitudes is necessary for a school of ambulance people in order to improve the selection and education of students. The idea was to better consider real work activity requirements and characteristics, and to develop and implement genuine educational content and selection tools. We followed the work activity of ambulance professionals involved in real emergency situations. Some interventions were filmed and post-analyzed. We completed and validated our analysis by means of interviews with ambulance personnel. We selected some video sequences and used them as a support for the interviews. We identified and documented many different key aptitudes like orientation and spatial sense, the capacity to perform complex cognitive tasks and delicate manipulations in the context of divided attention, as well as diverse aptitudes relevant in collaborative work.

Keywords: Ambulance personnel, emergency, work requirements, aptitudes, education, vocational training, personnel selection.

Le couple et l'infertilité: liens entre l'acceptation du diagnostic, la relation conjugale et le stress d'être infertile

[1]Maillard F., [1]Abbet E., [1]Darwiche J., [2]Favez N., [3]Germond M., [1]Guex P.

Service de Psychiatrie de Liaison - DP-CHUV[1], Unité de Recherche du Centre d'Etude de la Famille - DP-CHUV[2], Centre de Procréation Médicalement Assistée, Lausanne[3]

Introduction

Cette recherche a pour but d'évaluer, de manière longitudinale, comment les couples passent de l'étape de l'infertilité à l'étape de la parentalité suite à un traitement de procréation médicalement assistée. L'hypothèse générale est que l'acceptation du diagnostic d'infertilité par les couples facilite le déroulement de la transition à la parentalité. Les résultats présentés dans ce poster se focalisent sur les liens entre l'acceptation du diagnostic, la relation conjugale et le stress perçu lié à l'infertilité.

Matériel et Méthode

La recherche comporte trois sessions : 1) avant le début du traitement de Fécondation In Vitro ; 2) au 5ème mois de grossesse ; 3) lorsque le bébé a 9 mois. A chaque session, les couples participent à une interview semi-structurée au sujet de leur histoire d'infertilité. L'acceptation du diagnostic est analysée sur la base du discours du couple et donne lieu à un codage individuel (adaptation du "*Reaction to Diagnosis Interview*", Marvin, 1993). Ce codage distingue les personnes "résolues" par rapport à leur diagnostic d'infertilité des personnes "non résolues". Les couples remplissent également deux questionnaires : l'*Echelle d'Ajustement Dyadique* (Spanier, 1976) et un questionnaire sur le stress perçu par rapport à la situation d'infertilité (*Fertility Problem Inventory* , Newton,1999).

Résultats

Les résultats concernent le premier temps de recherche (avant le traitement de Fécondation In Vitro). La satisfaction conjugale est plus élevée chez les personnes "résolues" que chez les "non résolues" ($t(78) = 2.85$, $p = 0.006$). De plus, le stress lié à l'infertilité est moins élevé chez les personnes "résolues" que chez les "non résolues" ($t(78) = -2.37$, $p = 0.020$). Autrement dit, les personnes qui sont satisfaites de leur vie de couple et peu stressées par rapport à la situation d'infertilité sont aussi celles qui acceptent mieux leur diagnostic d'infertilité.

Conclusions

Cette étude a l'avantage d'inclure des données qualitatives et des résultats issus de questionnaires validés. Son intérêt réside dans le fait qu'elle permet d'identifier des facteurs de risque, tels que le manque de satisfaction conjugale et le stress lié au fait d'être infertile, qui peuvent entraver l'acceptation du diagnostic d'infertilité. L'objectif suivant consistera à évaluer le déroulement de la transition à la parentalité des personnes "résolues" et "non résolues" afin de savoir si la non acceptation du diagnostic d'infertilité complique l'accès à la parentalité.

Carbon Isotopic Ratio Analysis by GC/C/IRMS for the Detection of Gamma-hydroybutyric Acid (GHB) Administration to Human.

[1]Saudan C., [1]Augsburger M., [1]Mangin P., [1]Saugy M.

Institut Universitaire de Médecine Légale[1]

To suggest an alternative to the use of GHB (gamma-hydroxybutyrate) interpretative concentration cut-offs, the detection of exogenous GHB in urine specimens was investigated by means of gas chromatography/combustion/isotope ratio mass spectrometry (GC/C/IRMS). GHB was isolated from urinary matrix by successive purification on Oasis MCX and Bond Elute SAX SPE cartridges prior to HPLC fractioning using an Atlantis dC18 column eluted with a mixture of formic acid and methanol. Subsequent intramolecular esterification of GHB leading to the formation of γ-butyrolactone (GBL) was achieved to avoid introduction of additional carbon atoms for carbon isotopic ratio analysis. The evidence of exogenous GHB may be established from the determination of $^{13}C/^{12}C$ ratios of several GHB standard compounds and GHB in samples of subjects exposed to the drug compared to those obtained for endogenous GHB urine samples containing GHB of endogenous origin at concentration levels less than 10 mg/L.

Occupational and non-occupational exposure of non-smokers to Environmental Tobacco Smoke in Switzerland : Preliminary Results of an Original Campaig

[1]Huynh C., [2]Moix J., [2]Dubuis A.

Institut Romand de Santé au Travail (IST)[1], Ligue Valaisanne contre les Maladies Pulmonaires et pour la Prévention (LVPP)[2]

A passive sampling device called Monitor of NICotine or "MoNIC", was constructed and evaluated by IST laboratory for determining nicotine in Environmental Tobacco Smoke (ETS). Vapour nicotine was passively collected on a potassium bisulfate treated glass fibre filter as collection medium. Analysis of amount of nicotine on the treated filter by gas chromatography equipped with Thermoionic-Specific Detector (GC-TSD) after liquid-liquid extraction of 1mL of 5N NaOH : 1 mL of n-heptane saturated with NH_3 using quinoline as internal standard. Based on nicotine amount of 0.2 mg/cigarette as reference, the inhaled Cigarette Equivalents (CE) by non-smokers can be calculated. Using the detected CE on the badge for non-smokers, and comparing with amount of nicotine and cotinine level in saliva of both smokers and exposed non-smokers (N=49), we can confirm the use of the CE concept for estimating exposure to ETS.

The Valais CIPRET (Center of information and prevention of the addiction to smoking), is going to organize a big campaign on the subject of the passive addiction to smoking entitled "Smoked passive, we suffer from it, we die from it ". This campaign will take place in 2007 and has for objective to inform clearly the population of Valais of the dangerousness of the passive smoke. More than 1'500 MoNIC badges were gracefully distributed to Swiss population to perform a self-monitoring of population exposure level to ETS, expressed in term of CE. Non-stimulated saliva were also collected to determine ETS biomarkers nicotine/cotinine levels of participating volunteers.

Preliminary results of different levels of CE in occupational and non-occupational situations in relation with ETS were presented in this study.

Possible origins of undetectable EPO in urine samples

[1]Lamon S., [1]Robinson N., [1]Sottas P.-E., [2]Henry H., [3]Kamber M., [1]Mangin P., [1]Saugy M.

Laboratoire suisse d'Analyse du Dopage - IUML - CHUV[1], Laboratoire central de Chimie Clinique - CHUV[2], Swiss Federal Office of Sport[3]

Erythropoietin (EPO) is a native human glycoprotein hormone, which main physiological effect is the induction of erythrocytosis and the consequent improvement of blood oxygen-carrying capacity. Because an increase of the number of erythrocytes enhances athletic performances in endurance sports, the use of synthetic (recombinant) forms of EPO is prohibited by the World Anti-Doping Code. Currently, the routine-used test, based on isoelectric focusing (IEF) of urinary EPO in polyacrylamide gels followed by double-blotting[1], allows to distinguish between endogenous and recombinant EPOs. However, approximately 15 % of all EPO tests carried out in anti-doping laboratories yield undetectable EPO profiles. An EPO profile is considered undetectable if no endogenous or recombinant EPO can be detected in a sample using the classical IEF-based test. In order to determine the possible origins of undetectable EPO profiles in athletes' urine, data obtained from a large number of official anti-doping urine tests aimed at detecting recombinant EPO were analyzed. In addition to physiological parameters representing potential causes for lack of EPO detection, the possible usage of proteasic adulterants to evade doping detection was also considered.

All EPO analyses were performed using a classical EPO isoelectric focusing test [1]. The potential usage of exogenous proteases in urine was screened using a Western blotting based method targeting some of the tryspsin-digested urinary albumin fragments.

Statistical analyses indicated that EPO undetectability in urine can be explained by at least two physiological characteristics: low EPO concentrations in the sample and very low or very high urine specific gravities. More interestingly, the addition of very small quantities of protease in urine was shown to remove all traces of EPOs. This finding led to the development of a simple, specific and sensitive test based on albumin digestion that reveals proteasic activity.

In carrying out this work, it was aimed to highlight the causes of the high percentage of undetectable EPO profiles resulting from the classical anti-doping test. As expected, it was demonstrated that urine physiological characteristics clearly affect the detectability of an EPO profile. Additionally, in order to substantiate the rumors circulating among top level endurance athletes about adulterants that can alter the EPO test, potential exogenous causes were also considered. To this aim, a model based on trypsin, a very common protease, was developed to illustrate protein degradation. As simple addition of minute amounts of protease can also lead to undetectable EPO profiles, a cheating athlete could thus easily dissimulate a minuscule amount of protease powder and add it to his or her urine sample at some point during the collection procedure. Using the proposed test, an urine sample could then be rapidly analyzed for possible protease adulteration and the protease identified based on the observed albumin patterns without having to isolate the enzyme itself. Such an approach may prove extremely useful since proteases in solution are known to disappear overtime due to autolysis. At the same time, the use of Western blots as a means to detect polypeptides makes it possible to devise highly sensitive screening protocols requiring only small volumes of the urine samples. Finally, it was shown that such urine manipulation can be effectively countered by the addition to the sample of a concentrated cocktail of protease inhibitors, covering a large pH range. Therefore, this work has clear practical implications with regards to the improvement of the entire anti-doping control procedure.

[1] Lasne F, de Ceaurriz J. Recombinant erythropoietin in urine. Nature 2000; 405:635.

Système d'information pour les études cliniques du CHUV

Petter A.

Mathématicien EPFL - OIH

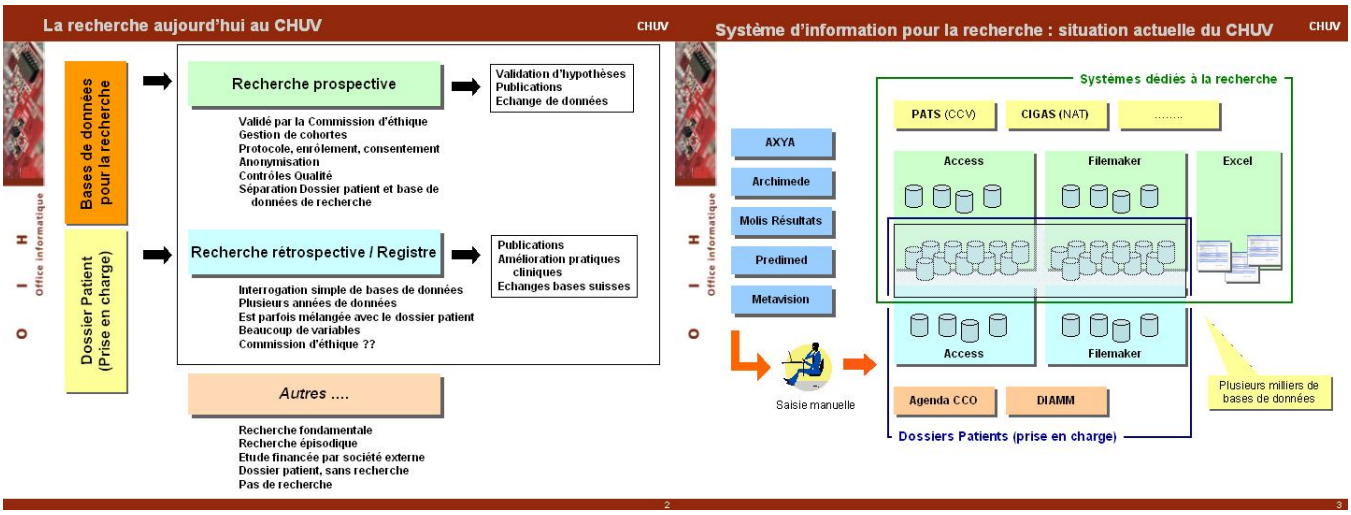

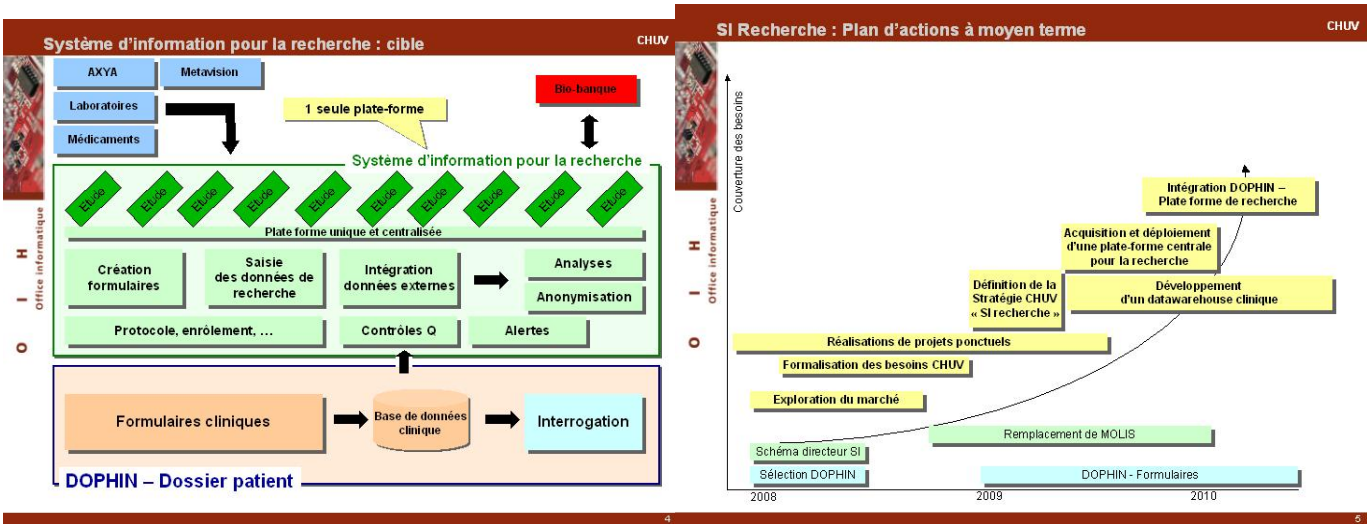

Health at work and risk factors related to ergonomics; some results from the Swiss sample of the 4th European working conditions survey

[1]Arial M., [1]Guillemin M., [2]Faouzi M., [1]Danuser B.

Institute for Work and Health[1], Institut universitaire de médecine sociale et préventive[2]

Introduction

The European Foundation for the improvement of living and working conditions conducts a survey every 5 years since 1990. The foundation also offers the possibility to non-EU countries to be included in the survey: in 2005, Switzerland took part for the first time in the fourth edition of this survey. The Institute for Work and Health (IST) has been associated to the Swiss project conducted under the leadership of the SECO and the Fachhochschule Nordwestschweiz. The survey covers different aspects of work like job characteristics and employment conditions, health and safety, work organization, learning and development opportunities, and the balance between working and non-working life (Parent-Thirion, Fernandez Macias, Hurley, & Vermeylen, 2007). More particularly, one question assesses the worker's self-perception of the effects of work on health. We identified (for the Swiss sample) several factors affecting the risk to report health problems caused by work.

The Swiss sample includes 1040 respondents. Selection of participants was based on a random multi-stage sampling and was carried out by M.I.S Trend S.A. (Lausanne). Participation rate was 59%. The database was weighted by household size, gender, age, region of domicile, occupational group, and economic sector. Specially trained interviewers carried out the interviews at the respondents home. The survey was carried-out between the 19th of September 2005 and the 30th of November 2005.

As detailed in (Graf et al., 2007), 31% of the Swiss respondents identify work as the cause of health problems they experience. Most frequently reported health problems include back pain (18%), stress (17%), muscle pain (13%), and overall fatigue (11%). Ergonomic aspects associated with higher risk of reporting health problems caused by work include frequent awkward postures (odds ratio [OR] 4.7, 95% confidence interval [CI] 3.1 to 5.4), tasks involving lifting heavy loads (OR 2.7, 95% CI 2.0 to 3.6) or lifting people (OR 2.2, 95% CI 1.4 to 3.5), standing or walking (OR 1.4, 95% CI 1.1 to 1.9), as well as repetitive movements (OR 1.7, 95% CI 1.3 to 2.3).

These results highlight the need to continue and intensify the prevention of work related health problems in occupations characterized by risk factors related to ergonomics.

References

Graf, M., Pekruhl, U., Korn, K., Krieger, R., Mücke, A., & Zölch, M. (2007). *Quatrième enquête Européenne sur les conditions de travail en 2005; résultats choisis du point de vue de la Suisse* SECO Secrétariat d'Etat à l'économie.

Parent-Thirion, A., Fernandez Macias, E., Hurley, J., & Vermeylen, G. (2007). *Fourth European Working Conditions Survey* Luxembourg: Office for Official Publications of the European Communities.

Acknowledgment and health in police officers

[1]Arial M., [1]Gonik V., [1]Danuser B.

Institute for Work and Health[1]

The way colleagues and supervisors acknowledge specific contribution and efforts of individuals is crucial for occupational mental health and well being. It contributes to improve the self image of employees and it gives a sense to the activities performed. We carried out a study about occupational health in police officers with a special emphasis on acknowledgment and reward.

A questionnaire was sent to 1000 police officers working for a cantonal administration in Switzerland. In total, 695 participants answered the questionnaire. We used the French version of the Langner's questionnaire on psychiatric symptoms to identify cases characterized by potential mental health problems. Multiple choice items (6 modalities ranging from "*not at all*" to "*tremendously*") to measure acknowledgment were used. Answers were later dichotomized (low annoyance- high annoyance). Questions we used are: "Do you feel annoyed due to a lack of support and attention from your supervisors?" "Do you feel annoyed because the authorities (politics, judges, etc.) have a low consideration of your occupation?" "Do you feel annoyed due to a low appreciation by the public?" and "Do you feel annoyed due to a lack of acknowledgment by the hierarchy?".

The score for psychiatric symptoms was high for 86 police officers for whom health might be at risk. Acknowledgment aspects associated with a high score for psychiatric symptoms are : high annoyance due to a lack of support and attention from supervisors (odds ratio [OR] 3.2, 95% confidence interval [CI] 2.0 to 5.1), high annoyance because authorities seems to have a low consideration for police officers (OR 2.7, 95% CI 1.7 to 4.3), high annoyance due to a low appreciation by the public (OR 1.8, 95% CI 1.2 to 2.9), and high annoyance due to a lack of acknowledgment by the hierarchy (OR 3.0, 95% CI 1.9 to 4.8).

Preserving mental health in occupations characterized by high emotional demand is challenging. The results from our study suggest that appropriate acknowledgment might contribute to the prevention of mental health problems. Further research should address a potential causal relation of acknowledgment on mental health.

3D Cell and Hydrogel Microarray Printing via Commercial Inkjet Printers

[1]Ranga A., [1]Lutolf M.

Laboratory for Stem Cell Bioengineering, EPFL[1]

In order for stem cells to realize their potential for therapeutic use, a better understanding of the mechanisms controlling self-renewal or differentiation into specific lineages is needed. Synthetic approaches in extracellular matrix design now allow us to engineer matrix functionality with potentially unparalleled control over cell function. The goal of this research has been to develop novel methodologies to conduct high-throughput combinatorial experiments of 3D cell/biomaterial interactions.

An HP DeskJet 660C printer was modified by removing its external shell, adding a microscope slide platform and washing the ink cartridge. The Z number (a measure of "printability") of cartridge ink and solutions of various poly(ethylene glycol) (PEG) concentrations was characterized by surface tension and viscosity tests. Solutions of 15% PEG were found to match the Z number of the original ink, and were chosen for subsequent experiments. MDA cells were added to the acrylate-terminated PEG solutions to arrive at a final cell concentration of 1E6 cells/ml. The solution was printed in various patterns, and the precursors were photopolymerized by visible light. Viewed under microscope, the printed dot arrays clearly demonstrated the presence of cells. Viability and proliferation assays were conducted to assess the impact of the printing process on cell behavior.

This is the first study to have successfully patterned a solution combining cells and photopolymerizable hydrogel precursor solution. The use of this method with various cell types and functionalized 3D artificial stem cell microenvironments has the potential to provide new insights into stem cell regulation by signals from their niche.

Assessment of Diesel exhaust particulate exposure and surface characteristics in association with levels of oxidative stress biomarkers

[1]Setyan A., [1]Sauvain J.-J., [1]Riediker M., [2]Rossi M., [1]Guillemin M.

Institut universitaire romand de Santé au Travail[1], Ecole Polytechnique Fédérale de Lausanne[2]

Exposure to PM_{10} and $PM_{2.5}$ (particulate matter with aerodynamic diameter smaller than 10 μm and 2.5 μm, respectively) is associated with a range of adverse health effects, including cancer, pulmonary and cardiovascular diseases. Surface characteristics (chemical reactivity, surface area) are considered of prime importance to understand the mechanisms which lead to harmful effects. A hypothetical mechanism to explain these adverse effects is the ability of components (organics, metal ions) adsorbed on these particles to generate Reactive Oxygen Species (ROS), and thereby to cause oxidative stress in biological systems (Donaldson *et al.*, 2003). ROS can attack almost any cellular structure, like DNA or cellular membrane, leading to the formation of a wide variety of degradation products which can be used as a biomarker of oxidative stress.

The aim of the present research project is to test whether there is a correlation between the exposure to Diesel Exhaust Particulate (DEP) and the oxidative stress status. For that purpose, a survey has been conducted in real occupational situations where workers were exposed to DEP (bus depots).

Different exposure variables have been considered:

- particulate number, size distribution and surface area (SMPS);
- particulate mass - $PM_{2.5}$ and PM_4 (gravimetry);
- elemental and organic carbon (coulometry);
- total adsorbed heavy metals - iron, copper, manganese (atomic adsorption);
- surface functional groups present on aerosols (Knudsen flow reactor). (Demirdjian *et al.*, 2005).

Several biomarkers of oxidative stress (8-hydroxy-2'-deoxyguanosine and several aldehydes) have been determined either in urine or serum of volunteers.

Results obtained during the sampling campaign in several bus depots indicated that the occupational exposure to particulates in these places was rather low (40-50 $\mu g/m^3$ for PM_4). Size distributions indicated that particles are within the nanometric range. Surface characteristics of sampled particles varied strongly, depending on the bus depot. They were usually characterized by high carbonyl and low acidic sites content.

Among the different biomarkers which have been analyzed within the framework of this study, mean levels of 8-hydroxy-2'-deoxyguanosine and several aldehydes (hexanal, heptanal, octanal, nonanal) increased during two consecutive days of exposure for non-smokers.

In order to bring some insight into the relation between the particulate characteristics and the formation of ROS by-products, biomarkers levels will be discussed in relation with exposure variables.

This project is financed by the Swiss State Secretariat for Education and Research. It is conducted within the framework of the COST Action 633 "Particulate Matter – Properties Related to Health Effects".

Demirdjian B., Rossi M. J. (2005). *Atmos. Chem. Phys. Discuss.*, 5, 607 – 654.

Donaldson K., Stone V., Borm P. J., Jimenez L. A., Gilmour P. S., Schins R. P., Knaapen A. M., Rahman I., Faux S. P., Brown D. M., MacNee W. (2003). *Free Radical Biol. Med.*, 34, 1369-1382.

Music performance anxiety among full-time music students

[1]Gomez P., [1]Studer R., [1]Arial M., [1]Danuser B.

Institut de Santé au Travail[1]

Introduction

Music performance anxiety (MPA, often referred to as “stage fright”) is one of the leading severe medical problems among musicians. For about 15-25% of musicians MPA is a serious problem. Particularly high levels of MPA are observed among music students. Musical performance can induce negative emotions, including anxiety, which in some individuals can approach extreme levels of terror and take the form of panic attack, impair the quality of the performance, lead to avoidance of performance situations, and consequently have debilitating effects on the career. Coping efforts used by musicians in their attempts to manage MPA, such as sedatives, alcohol, and β-blockers can have deleterious health side-effects. Music ranks high in the cultural and economic life of Switzerland. In ten university music schools, students from all around the world are educated to become professional musicians. Despite the importance of musical education in Switzerland, data concerning the phenomenon of MPA are largely lacking.

Goal and Methods

The main goal of this research was to survey the occurrence, experience, and management of MPA among full-time music students in French Swiss conservatories. A questionnaire was developed based on the literature and interviews with music students and teachers and distributed to all the students of the conservatories of Fribourg, Geneva, Lausanne, and Neuchâtel in the spring 2007. 194 students (61% women) returned the questionnaire.

Results

The size of the problem: MPA is a major problem for 1/3 of the students (ranks 3 and 4).

MPA is not a problem for me	0	1	2	3	4	MPA is a major problem for me
	4%	24%	41%	19%	12%	

The consequences of MPA: 22% and 35% of the students think that they have failed exams and auditions, respectively, because of MPA. Further, 25% of the students have already avoided performing and 11% have interrupted public performances because of MPA.

Coping with MPA: 90% of the students have never used alcohol prior to performing, whereas 97% and 81%, respectively, have never used recreation drugs and medication. The majority of students use relaxation exercises, respiratory exercises, and meditation techniques to prepare themselves. About ¾ of the students think that the use of alcohol and recreational drugs to manage MPA is never justified. 53% of the students think that the use of medication is justified on some occasions.

Need for information and support: 66% of the students would like to receive more support and help to cope with music performance situations. This support should mainly come from their teachers and specialists. 53% of the students know nothing or little about possible means for the management of MPA. About 50% consider themselves not at all or little informed about the possible risks associated with the consumption of alcohol, recreational drugs, and medication for the management of performance situations. 89% would like to know more about MPA and 94% think that this topic should be discussed much more in their musical education at the conservatory.

Conclusions

The results of this survey indicate that MPA is a major problem for 1/3 of the students with serious consequences on their career. There is a huge need for more information and support on how to manage the stress due to performance situations. The use of alcohol, recreational drugs, and medication is modest but the students are poorly informed about possible side-effects of these coping strategies. It seems clear that more should be done in the French Swiss conservatories about music performance anxiety to inform, educate, and prepare the students for their future professional career.

Comparison of a direct immunoassay (N Latex CDT) and capillary electrophoresis for the determination of carbohydrate-deficient transferrin

[1]Augsburger M., [1]Sporkert F., [1]Dovat M., [1]Favrat B., [1]Mangin P.

Institut Universitaire de Médecine Légale - CHUV[1]

In several scientific investigations, a strong relationship between increasing blood alcohol concentration (BAC) in drivers and increasing risk of road accident has been irrefutably shown, in particular the seminal Grand Rapids study. Objective laboratory evidence of heavy drinking is needed in medico-legal cases for identifying individuals with alcohol problems and for monitoring abstinence from alcohol when offenders reapply for a driving license. Carbohydrate-deficient transferrin (CDT) is nowadays considered as the most specific marker of alcohol abuse among others such as gamma-glutamyltransferase (GGT), mean corpuscular volume (MCV), or serum aminotransferases (AST and ALT).

Several methods for CDT determination have been described and are used by laboratories. The use of high performance liquid chromatography (HPLC) or capillary electrophoresis (CE) has been recommended because these methods allow separation and identification of the different transferrin isoforms, in particular the CDT. Recently, a direct immunoassay has been developed and commercialized (N Latex CDT; Dade Behring). This new method is based on a monoclonal antibody that measures specifically the transferrin isoforms lacking 1 or 2 N-glycan chains (asialo-, monosialo-, and disialotransferrin). Simultaneously, total transferrin (Tf) is determined in order to express the CDT results as a percentage of Tf.

The present study aims at comparing a large number of determinations (n = 538) of CDT by CE and N Latex immunoassay. To separate and measure CDT by CE (CDT : sum of asialo-, monosialo-, and disialotransferrin), a previously described and validated CE method with the Ceofix CDT reagent (Analis) on a Hewlett Packard 3D-CE instrument was used. Subjects were Swiss drivers referred to the Institute of Forensic Medicine because of driving while under the alcohol influence or because of reapplying for a driving license. These subjects were recruited in 2003, 2004, 2006, and 2007. No selection has been made concerning the alcohol consumption of the subjects, resulting in a wide population including teetotalers, occasional drinkers, and regular high alcohol consumers. As observed in other studies dealing with drivers under the influence of alcohol or drugs, males (91%) heavily predominate over females (9%). The mean age of the subjects is 41 ± 13 (S.D.) years.

N Latex CDT results ranges from 0.8% to 10.7%, and 75% of the results are less than 2.3%. CDT CE results ranges from 0.2% to 18.9%, and 75% of the results are less than 1.4%. The results show a good correlation between CE and N Latex CDT (r^2=0.84; $p<0.001$), and a good concordance (93%) in terms of positive-negative samples (CE cutoff value : 1.7% and N Latex CDT cutoff value : 2.5%). N Latex CDT results from samples with genetic transferrin variants (n = 9) give similar results than those obtained with CE.

This study support the use of N Latex CDT test as a specific enough alternative to CE methods.

Fast screening of 115 doping agents in urine using 96-well plate solid phase extraction and UPLC-qTOF-MS

[1,2]Badoud F., [1,2]Grata E., [1]Perrenoud L., [1]Mateus-Avois L., [1]Saugy M., [2]Rudaz S., [2]Veuthey J.-L.

LAD-IUML[1], LCAP-UNIGE[2]

More than 150'000 urine samples are analysed per year over the world for doping control. During major sporting events, analyses results are required within 24 or 48 hours after samples reception meaning that analysis time must be as short as possible. The analytes separation needs to be powerful, fast and as generic as possible since each sample is screened for a large amount of substances forbidden by the World Anti Doping Agency (WADA). Therefore, the entire analytical process, including sample preparation, analyte separation, selective detection and data analysis need to be optimized.

The aim of this study is to analyze in a fast gradient (3 minutes) 115 doping agents excreted under their free form in urine, including diuretics, masking agents, β-blockers, stimulants, narcotics, agents with anti-oestrogenic activity, aromatase inhibitors, anabolic steroids and β_2-adrenergic agonists. Regarding sample preparation, off-line solid phase extraction (SPE) on mixed mode cation exchange (Waters® Oasis MCX) was selected. This simple, rapid and automatic method allows a purification of urine matrix by removing the usual interfering substances like salts, proteins and fatty acids. For analyte separation, ultra performance liquid chromatography (UPLC™) technology using columns packed with small particles (< 2 μm) offers the opportunity to obtain short analysis time, while maintaining efficiency and sensitivity [1]. An analytical BEH C18 column (Waters® Acquity, 50 mm × 2.1 mm, 1.7 μm) was used for liquid chromatography with a linear gradient of water/acetonitrile containing 0.1% formic acid in 3 minutes. Due to the peaks thinness (3 sec), high acquisition rates detector afforded by a quadrupole time of flight (qTOF) mass spectrometry is required for selective detection. Moreover, qTOF gives a second dimension to chromatography, by measuring exact mass of analytes.

Basic and neutral compounds were analysed in positive electrospray ionisation mode (ESI), whereas acidic molecules were detected in negative mode. Mass spectrometry sensitivity was evaluated by measuring limit of detection of the 115 investigated substances diluted in mobile phase and an average value of 10 ng/mL was reached for most of the compounds. The urinary matrix effect was evaluated.

References

[1] Nguyen D.T.T., Guillarme D., Rudaz S., Veuthey J.L., J. Chromatogr. A. (2006) 1128, 105-13.

AIDS Prevention: Consensus and dissension regarding the meaning of messages

[1]Singy P., Spencer B., Bourquin C., Prikhodkine A., Schaffter M., Guex P.

DP-CHUV[1]

Aim: In Western Europe, HIV/AIDS prevention has been based on the provision of information intended to lead the public to voluntarily adapt their behaviour so as to avoid the risk of virus transmission. Whether conveyed in a written or oral form, the messages of prevention are essentially verbal. Sociolinguistic research confirms that, even within a given culture, the meaning attributed to lexical items varies. It was hypothesised that understandings of the terms used in HIV/AIDS prevention in French-speaking Switzerland would vary, and research was undertaken to identify the level and nature of this variation both between and among those who transmit (prevention providers) and those who receive (the public) the messages.

Method/issue: All HIV/AIDS prevention material available in French-speaking Switzerland in 2004 was assembled and a corpus of 50 key documents identified. Two series of lexical items were generated from this corpus: one composed of technical terms potentially difficult to understand, and the other, of terms used in everyday language with implicit, and therefore potentially variable, meaning. The two lists of terms were investigated in qualitative interviews in stratified purposive samples of the general public (n=60) and prevention providers (n=30), using standard socio-linguistic methodology. A further quantitative study (CATI) in the general population (17 – 49 yrs.; n=500) investigated understandings of 15 key prevention terms found in the qualitative research to have been associated with high levels of dissension.

Results/comments: Selected aspects of the results will be presented. In illustration: meanings attributed to the different terms in both the public and the providers varied. For example, when a relationship is described as “stable”, this may be understood as implying exclusive sexual relations or long duration, with an interaction between the two traits; the term “sexual intercourse” may or may not be used to refer to oral sex; “making love” may or may not necessarily include an act of penetration; the pre-ejaculate is qualified by some as sperm, and by others not… Understanding of frequently used “technical” terms in prevention was far from universal; for example, around only a half of respondents understood the meaning of “safer sex”. Degree of understanding of these terms was linked to education, whereas variability in meaning in everyday language was not linked to socio-economic variables.

Discussion: Findings indicate the need for more awareness regarding the heterogeneity of meaning around the terms regularly used in prevention. Greater attention should be paid to the formulation of prevention messages, and providers should take precautions to ensure that the meanings they wish to convey are those perceived by the receivers of their messages. Wherever possible, terms used should be defined and meanings rendered explicit.

Preventive Communication with sub-Saharan Migrants: Complemetary roles of French and African Languages

[1]Weber O., [1]Sulstarova B., [1]Pascal S., [2]Patrice G.

Liaison Psychiatry - CHUV[1], Psychiatric Department - CHUV[2]

Introduction:

Francophone Sub-Saharan migrants represent a segment of the migrant population living in Switzerland which is particularly threatened by HIV/AIDS. The current official AIDS prevention strategy favours the use of native African languages over French. Yet, prior research suggests that this opinion might not completely be shared by the target population. An ongoing study carried out by a team of sociolinguists and physicians addresses among other things the question of the way in which the multilingualism of this ethnically and socially heterogeneous population should be taken into account in preventive activities.

Methods:

46 semi-directive interviews with francophone Sub-Saharan migrants were carried out and subsequently transcribed (sample cf. table). The results of this poster are based on quantitative and qualitative discourse analysis of these transcripts.

Results :

A majority of interviewees reported the use of African languages when talking about HIV/AIDS with friends belonging to their migrant communities. Women and people with non-academic education were especially numerous in this case. However, roughly one respondent out of two perceived code-switching towards French as a means to lessen taboo effects in talk on sexual matters. Even though they were less fluent in French than men, women more frequently recognized this phenomenon. Moreover, approximately half of the interviewees considered that French should be used for HIV/AIDS prevention because of a lack of precise technical terms in African languages.

Conclusion :

Our findings suggest that African languages and French can play complementary roles in HIV/AIDS prevention addressed to French-speaking sub-Saharan migrant communities. Even though African languages, are highly appreciated by sub-Saharan migrants and apparently preponderant in casual in-group conversations different types of code-switching between African languages and French could be used to facilitate discussions on taboo subjects like AIDS and sexuality. The use of French could also increase the chance for the interlocutors to find precise terms when speaking about technical topics. Observed tendencies of social variation in our results also suggest that prevention projects should pay attention to the social heterogeneity of migrant target populations, especially as far as gender is concerned.

Limitations in migrants' access to psychiatric care : what is the staff of the Lausanne Psychiatric Department concerned with ?

[1]Weber O., [1]Daphne R., [1]Florence F., [1]Pascal S., [1]Patrice G.

Psychiatric Department - CHUV[1]

Background:
Migrants' access to psychiatric health services is a crucial but little-known issue. The Lausanne University Department of Psychiatry is currently undertaking a project in order to understand migrants' mental health careers and to improve quality of care through institutional changes and teaching. In a long-term perspective, better awareness of migrants' situations and problems should help psychiatric services to prepare for the challenges they will have to face in the increasingly multicultural societies of the 21st century.

Objective and method:
A qualitative study was carried out in the Lausanne Psychiatric Department in order to investigate the teams and the heads of the medical and nursing staff of the migrants' situation with regard to psychiatric care. Semi-directive interviews were carried out with 33 persons in charge and 22 teams of the department (282 participants). Interviewer notes were submitted to qualitative thematic content analysis.

Results:
Five factors were mentioned by numerous clinical heads and teams of the Lausanne Psychiatric Department as limiting migrants' access to psychiatric services :
- Strong stigmatisation of mental illness and psychiatry in some migrant communities
- Migrants' difficulties in understanding the pertinence of some of the proposed treatments
- Complex admissions procedures for asylum seekers and undocumented migrants
- Precarious legal status of the patient seems incompatible with long term care
- Legal and financial limitations on follow-up care (job prospects, housing, residential care, etc.)

Four other factors were only marginally brought up :
- Communication barriers and lack of a clear procedure for collaboration with interpreters
- Reticence to refer non French-speaking patients for psychiatric care on the part of partner institutions
- Reduction of financial aid for asylum seekers during hospitalisation
- Migrant workers' reluctance to take time off from a job they are afraid to lose

Conclusion:
Surprisingly, obstacles as important as poverty, isolation and other typical social factors of the post-migratory phase were given little attention in comparison with cultural differences. Similarly, there was limited awareness of the negative impact of language barriers on access.
Namely with regard to the observations of this study, de Lausanne Psychiatric Department adopted several measures, (i) including supervision in transcultural psychiatry and social dimensions of migration, (ii) reinforced liaison with Appartenances (Centre offering psychotherapy to migrants), (iii) training of the entire staff in working with interpreters, (iv) clarification of the admissions procedures and (v) improving the staff's awareness of social and legal aspects of migration through itinerant information sessions.

Drug-facilitated crime – Unexpected poisoning with the rodenticide Alpha Chloralose

[1]Sporkert F., [2]Augsburger M., [2]Schrag B., [2]Mangin P.

IUML[1], Institute Universitaire de Médecine Légale[2]

Drug-facilitated crime – Unexpected poisoning with the rodenticide Alpha-Chloralose

Frank Sporkert, Marc Augsburger, Conxita Brandt and Patrice Mangin

Institute of Legal Medicine, University of Lausanne, Rue du Bugnon 21, 1018 Lausanne, Switzerland

A 36 year old man was taken to the institute for an autopsy. Before his death, the deceased had been hospitalized several times with epilepsy-like symptoms. Autopsy findings could not explain the cause of death.

Toxicological analysis resulted in the detection of alpha-chloralose, flunarizine and amitriptyline in urine, gastric content and peripheral blood. Alpha-chloralose (Glucochloral), 1,2-O-(2,2,2-trichloroethylidene)-alpha-D-glucofuranose, is used as rodenticide and as hypnotic in animal experiments.

Alpha-chloralose was quantified in postmortem blood, in plasma from one hospital, in urine, and gastric content after liquid-liquid extraction and GC-MS analysis in SIM mode. Following concentration were obtained: peripheral postmortem blood 20 mg/l, urine 410 mg/l, and gastric content 0.52 g (total amount). Flunarizine and amitriptyline were found in therapeutic concentrations. Finally, the cause of death was explained as a result of a chloralose administration.

In order to verify whether the epilepsy-like symptoms could be explained by repeated administration of alpha-chloralose, a GC-MS detection method for the determination of chloralose in hair analysis was developed. After hair extraction with a methanol/water mixture and derivatization with trifluoroacetic anhydride, chloralose was detected in SCAN- and SIM-mode using negative chemical ionization (NCI). Segmental hair analysis yielded alpha-chloralose concentrations of about 400 ng/mg for each segment suggesting a repetitive exposure to alpha-chloralose. The results of hair analysis supported the assumption of the police that the man was exposed to and poisoned by this rarely used rodenticide.

Alpha-chloralose was also confirmed in a white powder found several weeks later by police investigations in the house of the deceased.

The wife was found guilty and condemned to 18 years imprisonment.

Keywords: chloralose, rodenticide, impoisoning, drug facilitated crime, hair analysis

ENA
Environnement Naturel

Environnement Naturel/ENA-1

Exposure to bioaerosols in poultry houses at different stages of fattening; use of real-time PCR for airborne bacterial quantification.

[1]Oppliger A., [1]Charrière N., [1]Droz P.-O., [1]Rinsoz T.

Institut universitaire romand de santé au travail[1]

Previous studies have demonstrated that poultry-house workers are exposed to very high levels of organic dust and consequently have an increased prevalence of adverse respiratory symptoms. However, the influence of the age of broilers, on bioaerosol concentrations has not been investigated. To evaluate the evolution of bioaerosol concentration during the fattening period, bioaerosol parameters (inhalable dust, endotoxin and bacteria) were measured in 12 poultry confinement buildings in Switzerland, at 3 different stages of the birds' growth; Samples of air taken from within the breathing zones of individual poultry-house employees as they caught the chickens ready to be transported for slaughter, were also analysed. Quantitative PCR (Q-PCR) was used to assess the quantity of total airborne bacteria and total airborne *Staphylococcus* species. Bioaerosol levels increased significantly during the fattening period of the chickens. During the task of catching mature birds, the mean inhalable dust concentration for a worker was 31 ± 4.7 mg/m^3, and endotoxin concentration was 11'080 ± 3436 UE/m^3 air, more than ten-fold higher than the Swiss occupational recommended value (1000 UE/m^3). The mean exposure level of bird catchers to total bacteria and *Staphylococcus* species measured by Q-PCR is also very high, respectively reaching values of 72 (± 11) x10^7 cells/m^3 air and 70 (± 16) x10^6/m^3 air. It was concluded that in the absence of wearing protective breathing apparatus, chicken catchers in Switzerland risk exposure beyond recommended limits for all measured bioaerosol parameters. Moreover, the use of Q-PCR to estimate total and specific numbers of airborne bacteria is a promising tool for evaluating any modifications intended to improve the safety of current working practices.

GEN
Gènes et Environnement

Identifying factors that influence the STR DNA typing success for touched objects

[1]Castella V., [1]Mangin P.

Institute of Legal Medicine - CHUV[1]

Contacts stains collected on handled objects, touched surfaces or worn clothes typically contain minute amounts of DNA and are therefore less exploited than other stains, such as those containing saliva or blood. In this study, 1739 contact traces from real casework were analyzed to determine their analysis success rate and relevance to the case. More DNA was recovered when stains were collected with the double swab technique (mean [DNA] of 0.494 ng/µl), rather than with single swabs (mean [DNA] of 0.312 ng/µl). After being amplified with the SGM Plus STR multiplex kit, 26% of the contact stains had DNA profiles suitable for the Swiss DNA database. Out of the 398 DNA profiles sent to the DNA database, 49 matched crime scene DNA profiles and 136 matched DNA profiles from individuals, including one policeman. These results confirm that, when carefully collected, analyzed and interpreted, contact stains have a high potential to help solving crimes.

The UNIL Protein Analysis Facility

Quadroni M.

Centre Integratif de Genomique

The UNIL Protein Analysis Facility

The PAF (Protein Analysis Facility) is a service and research laboratory specialized in the analysis of proteins and proteomes.

The primary mission of the PAF is to support the local academic community and to function as a catalyst in the application of advanced technologies to analyse protein expression and function.

The PAF is affiliated to the CIG (Center of Integrative Genomics) and is presently organised on two laboratories hosted respectively by the Department of Biochemistry (DB) as well as the CIG itself. For the 2D-PAGE activity the platform can count on the support of a network of labs.
The platform has been created in 2002 thanks to contributions from the the same institute, the University of Lausanne and a very generous donation by the Leenardts Foundation.

Service activities:

* advisory and technical support for local groups that want to undertake proteomics projects.
* protein identification by mass spectrometry in simple or complex mixtures (shotgun proteomics).
* protein separation and profiling by two-dimensional electrophoresis.
* analysis of post-translational modifications (phosphorylation and others).

Goals of research and development

* to implement new technologies for the qualitative and quantitative comparative analysis of proteomes.
* collaborate with local investigators on selected biological research projects.

Teaching

We provide courses at the master and postgraduate level to disseminate the knowledge of proteomics technologies among students and researchers.

Link : **www.unil.ch/paf**

Caractérisation par puce à ADN à haute résolution d'un chromosome 8 surnuméraire en anneau en mosaïque.

[1]NIEI F., [1]Martinet D.

Service de Génétique Médicale-CHUV[1]

Nous rapportons dans cette observation l'apport des puces à ADN à haute résolution pour la caractérisation d'un chromosome surnuméraire en anneau. Il a été possible de mettre en évidence une trisomie 8 partielle dont le taux de mosaïcisme dans les lymphocytes avait été estimé à 21%. Cette anomalie a été identifiée chez un enfant de 5 ans avec un retard de développement prédominant au niveau du langage associé à quelques traits autistiques. A remarquer comme anomalies mineures : de grandes oreilles, une mauvaise dentition et des doigts « boudinés ».

L'analyse du caryotype en bande G (550 bandes) avait révélé un caryotype en mosaïque avec des métaphases normales et des métaphases avec un anneau chromosomique surnuméraire. L'utilisation combinée de sondes de peinture chromosomique, de sondes centromériques alpha-satellites et de sondes subtélomériques sur des préparations métaphasiques avait montré que cet anneau surnuméraire était dérivé du chromosome 8 avec son centromère mais dépourvu de ses deux régions 8pter et 8qter. Par les outils classiques à disposition, il n'avait pas été possible d'aller plus loin dans la définition de la structure de ce dérivé du chromosome 8. A ce jour, de nombreuses descriptions à la fois cytogénétiques et cliniques ont été rapportées dans la littérature concernant des patients avec un chromosome 8 surnuméraire sous forme de marqueur ou d'anneau dans un contexte de mosaïque cellulaire variable. Il existe une grande hétérogénéité phénotypique allant de l'absence de symptomatologie à des signes cliniques compatibles avec ceux de la trisomie 8 en mosaïque. Nous avons étudié le cas présenté par une puce à ADN à haute résolution d'oligonucléotides d'Agilent™ 244K afin de préciser la région du chromosome 8 impliquée dans cet anneau, et de déterminer s'il était possible de détecter une variation du nombre de copies génomiques associé à un faible taux de mosaïcisme. La puce à ADN est composée de 230 000 sondes représentant les régions codantes et non condantes du génome humain dont 10960 sondes retrouvées sur le chromosome 8. Les données obtenues ont permis d'identifier avec précision la portion du chromosome 8 surnuméraire impliqué dans l'anneau s'étendant des extrémités 8p23.1 à 8q11.23 (chr8 : 8,117,271 bp..55,634,100 bp). Dans cette région de 47 Mb, 349 gènes dont 150 gènes OMIM, sont répertoriés dans les bases de données (NCBI, build 36.2). La recherche de cet anneau du chromosome 8 par FISH (sonde centromérique) chez la mère s'est avérée négative (prélèvement du père non disponible).

L'utilisation de la puce à ADN à haute résolution dans le cas présenté a permis d'une part de caractériser avec rapidité (3 jours) et précision le contenu génique de l'anneau surnuméraire dérivé du chromosome 8 et d'autre part de déterminer la sensibilité de cette technique dans un cas avec un faible taux de mosaïque (21%). Ces données pourraient aider à établir des relations génotypes-phénotypes grâce à la détermination des gènes impliqués dans ce type de remaniement chromosomique.

Transcription Profiling of an in Vitro Model for Epidermolytic Hyperkeratosis

[1]Obarzanek-Fojt M., [2]Favre B., [2]Hohl D.

Service of Dermatology and Venereology - CHUV[1], ervice of Dermatology and Venereology - CHUV[2]

Epidermolytic hyperkeratosis (EHK) is an autosomal dominant transmitted skin disorder. The phenotype of the disease is heterogeneous and characterized by hyperkeratosis of the stratum corneum, frequent blistering, scaling and redness. Mutations responsible for EHK occur in keratin 1 or keratin 10 gene. Both genes encode structural intermediate filament proteins which dimerize and form a scaffold for the cells in the suprabasal layers of the epidermis. To understand the mechanisms underlying EHK phenotype we used an in vitro model and searched for important changes in gene expression. Keratinocytes, isolated from either healthy volunteers or patients with diagnosed EHK and mutations in K10 gene, were cultivated in defined keratinocyte serum-free low Ca^{2+} medium. Cells at passage number 4 were used for analysis. Differentiation was induced by low to high Ca^{2+} shift. Total RNA was isolated from keratinocytes at two different stages, end of proliferation (day 0) and late differentiation (day 7). Transcriptomes were analyzed using GeneChip® Human Genome U133A 2.0 Array (Affymetrix). Results showed significant down-regulation of some genes specific for differentiation, i.e. loricrin, in diseased versus normal keratinocytes, confirming disturbances in the formation of the cornified envelope. Desmocollin1 and desmoglein1, membrane glycoproteins connecting the keratin filaments between cells, were also down-regulated in differentiated EHK keratinocytes. In contrast S100A7 gene, known to be over-expressed in psoriatic lesions, was up-regulated in the diseased keratinocytes. These results indicate that cultured diseased keratinocytes can recapitulate in vitro some of the abnormalities observed in vivo and could help for the understanding of the molecular mechanisms of EHK.

Indirect markers of blood doping

[1]ROBINSON N., [1]ROBINSON N., [1]MANGIN P., [1]SAUGY M.

IUML[1]

Today, only the discovery of an exogenous substance in the body of the athlete can lead to a disciplinary sanction. However, the level of evidence provided by indirect markers of altered erythropoïesis can be high enough to differentiate between natural variations and blood doping. Forensic techniques for the evaluation of the evidence, and more particularly Bayesian networks, allow anti-doping authorities to take into account firstly the natural variations of indirect markers of blood doping – through a mathematical formalism based on probabilities -, and secondly the complexity due to the multiplicity of causes and confounding effects – through a distributed and flexible graphical representation. The information embodied in an athlete's biological passport may be sufficient to present a case to a disciplinary panel.

Potassium secretion by cortical collecting duct (CCD) cells: Effects of mineralocorticoid on ROMK expression and K+ secretion in a CCD cell line

[1]Fodstad H., [1]Gonzalez-Rodriguez E., [1]Bron S., [1]Gaeggeler H., [1]Guisan B., [1]Rossier B., [1]Horisberger J.-D.

Department of Pharmacology and Toxicology[1]

In the distal nephron, the cortical collecting duct (CCD) plays a key role in the regulated K^+ secretion, which is mediated mainly through ROMK channels located in the apical membrane. Several factors (Na^+, pH, mineralocorticoids) are known to modulate K^+ secretion in the CCD, but the regulation of urinary K^+ excretion with regards to K^+ balance is still poorly understood. We took advantage of a recently established mouse CCD cell line ($mCCD_{cl1}$) to investigate the regulation of K^+ secretion by mineralocorticoid. We first verified the role of ROMK in K^+ secretion by showing that tertiapin-Q, a ROMK-specific inhibitory peptide, inhibited up to 95% of the barium-sensitive current with an apparent affinity of 4.1 nM. Overnight exposure to 100 nM aldosterone did not significantly change the barium-sensitive current, while it did increase Na^+ transport measured as the amiloride-sensitive short-circuit current. By qRT-PCR we measured the effect of aldosterone on ROMK mRNA levels by exposing the mCCD cells to 0.3 or 300 nM aldosterone for 1 and 3 hours, respectively. All ROMK isoforms presented with a significant down-regulation on the mRNA level, ranging from 15% (0.3 nM, 1h) to 45% (300 nM, 3h), upon treatment with aldosterone ($p<0.05$, $n = 7$ or 8). In conclusion, under transepithelial voltage clamp at -60 mV, $mCCD_{cl1}$ cells demonstrate a significant barium-sensitive K^+ current in the secretory direction, which under these conditions is not significantly modulated by aldosterone. However, on the mRNA level ROMK expression is slightly, but significantly down-regulated already after 1 hour exposure to 0.3 nM aldosterone. This suggests that the ROMK gene expression response to aldosterone is an early mineralocorticoid receptor effect, which possibly works as a preventative mechanism to avoid excessive K^+ loss which would otherwise result from the increased electrogenic Na^+ transport and associated depolarisation of the apical membrane in the CCD.

Implication of ENaC-mediated sodium fluxes in wound healing.

[1]Suarez P., [1]Charles R.-P., [1]Hummler E.

Pharmacology and Toxicology - UNIL[1]

The skin is composed of several layers and forms a barrier that prevents body dehydration and intrusion of pathogens. In a previous study of mice deficient of the alphaENaC subunit, we showed that ENaC is required for differentiation processes in skin. In recent studies, when keratinocytes from alphaENaC knockout mice were isolated and exposed to an electric field, we find that they exhibit a different migration behaviour compared to wild-type keratinocytes.

The aim of the study is to investigate the role of ENaC in wound healing. For this purpose, we use a conditional knockout mouse model, which specifically abrogates the alphaENaC subunit expression in the basal layer and thereby abolishes the whole channel activity in the epidermis.

In these animals, we performed wound healing studies and determined the closure rate of full thickness wounds in function of time. Our data revealed a tendency to delayed wound closure in conditional knockout mice but did not reach statistically significance. Histological sections may show an altered skin remodeling in knockout animals. Further physiological studies and genetic analysis will allow use to show that ENaC is an important gene for wound repair.

Predicting response of HIV patients using SNP-drug interactions

[1]Marek D., [2]Tarr P., [3]Telenti A., [4]Beckmann J., [1]Bergmann S.

Department of Medical Genetics, University of Lausanne; Swiss Institute of Bioinformatics[1], Infectious Diseases Service, CHUV, Lausanne[2], Institute of Microbiology, University of Lausanne; Infectious Diseases Service, CHUV, Lausanne[3], Department of Medical Genetics, University of Lausanne; Medical Genetics Service, CHUV, Lausanne[4]

Understanding why some HIV patients treated with antiretroviral therapy develop adverse side effects, such as dyslipidemia, is one of the goals of pharmacogenetics. We analyzed a dataset from the Swiss HIV cohort containing about 4700 measurements of lipid levels from 438 patients that underwent different treatments (up to 5 out of 18 drugs), as well as their genotype for 20 SNPs in genes involved in lipid transport and metabolism.
Using a linear regression model, taking the genotypes of the SNPs and the usage of the drugs as independent features, we were able to explain about 19% of the variance of the triglyceride levels (corrected for sex and age).
We then extended our model to contain also SNP-drug interaction terms. In order to avoid over fitting we only included a fraction of the 360 possible interactions. To this end, we first tested 360 minimal models allowing only for a single SNP-drug interaction. We then included into the full model only those interactions whose significance was above a threshold. Interestingly, the addition of only 60 SNP-drug interactions raised the variance explained by the model to 28%. This value was never reached by a random pick of 60 interaction terms. These findings reveal that while the independent effects of the SNPs and the drugs explain part of the changes observed in lipid levels, interactions of some SNPs and drugs significantly improve the fitting of the data. Our two-stage approach provides a simple yet efficient method to select relevant SNP-drugs interactions and can be extended to integrate other type of interactions (e.g. SNP-SNP or drug-drug). It generates a robust framework for predicting the lipid responses of new patients based on their genotype and a choice of treatment.

The Evolutionary History of the CD209 (DC-SIGN) Family in Human and Non-Human Primates.

[1]Ortiz M., [1]Zhang K., [1]Telenti A.

Insitute of Microbiolgy - CHUV[1]

Keywords: Evolutionary analysis, Comparative genetics, Host genetics

Background. The CD209 family of C-lectin receptors includes DC-SIGN (encoded by *CD209*), L-SIGN (encoded by *CD209L*), and CD209L2. Their function depends on a carbohydrate-recognition domain separated from a transmembrane region by a neck made up of several repeats. The importance of these receptors in pathogen recognition, and of dendritic cells in pathogenesis of HIV infection, makes these genes an excellent model for evolutionary genetic analysis to (i) assess their evolutionary history in primates, (ii) identify amino acids under positive selection, and (iii) guide functional studies.

Methods. *CD209* family coding sequences were generated by sequencing (n=17) or compiled (NCBI, n=15) for 14 primates (great apes, gibbons, Old World and New World monkeys) representing 40 million years of evolution. We performed phylogenetic analysis using Bayesian inference and analyzed nucleotide substitution patterns using codon-based maximum likelihood procedures as implemented in the codeml tool of the P.A.M.L software.

Results. The evolutionary pattern of *CD209* and *CD209L2* is consistent with purifying selection (K_A/K_S values 0.43 and 0.35 respectively). However, detailed analysis identified a limited number of branches under positive selection, in particular in gibbons. *CD209L2* has been recently lost in humans and gorilla. *CD209L*, resulting from a duplication of *CD209*, is absent in monkeys and truncated in orang-utan. *CD209L* is under relaxing purifying selection (K_A/K_S=0.52). L-SIGN alanine 88, located in the first neck repeat is under positive selection (post probl. P=0.99). In addition, threonine 319, and alanine 393, in the C-lectin domain, were identified with lower confidence (P=0.90 and P=0.93, respectively). These two L-SIGN residues map at the protein surface surrounding the region that contains critical residues involved in carbohydrate interactions.

Conclusions. Evolutionary analysis of *CD209* genes identifies a complex pattern of apparent redundancy (gene absence and gene loss) in the context of a pattern of gene conservation. The degree of purifying selection may reflect the need to faithfully recognize different pathogen motifs and a number of self-antigens. However, it may constrain in the capacity of response to specific pathogens, such as retroviruses, through adaptive mechanisms of positive selection. The identification of specific residues under positive selection at the L-SIGN C-lectin domain should be followed by functional analysis.

Genetic Variation in Accessory Metabolic Pathways is Associated with Extreme Efavirenz Exposure in Individuals with Impaired CYP2B6 Function

[1]di Iulio J., [1]Rotger M., [1]Lubomirov R., [2]Decosterd L.-A., [3]Eap C., [1]Telenti A.

Institute of Microbiology - CHUV[1], Division of Clinical Pharmacology - CHUV[2], Biochemistry and Clinical Psychopharmacology Unit - Cery Hospital[3]

Key words: Pharmacogenetics, Efavirenz, Metabolism

Introduction: The antiretroviral drug efavirenz (EFV) presents wide interindividual variability in exposure. This is explained to a great extent by polymorphisms of *CYP2B6*, coding for the isoenzyme responsible for EFV metabolism. When CYP2B6 function is impaired, CYP3A isoenzymes may control the rate of 8-hydroxylation, and CYP2A6 may modulate an alternative pathway to 7-hydroxy-EFV. We hypothesize that genetic variability in these accessory pathways may contribute to the remaining, unexplained variability in EFV exposure in subjects with limited CYP2B6 function.

Methods: Participants (n=167), fully characterized for *CYP2B6* variation, were genotyped for the decreased function alleles *CYP3A4*1B*, *CYP3A5*3*, **6*, &**7*; and for the increased function alleles *CYP3A7*1C* & **2* by Taqman allelic discrimination. *CYP2A6* was assessed by (i) full resequencing (promoter region, all 9 exons and exon-intron boundaries) of the gene in a well characterized subgroup of 21 subjects homozygous for a loss/diminished function *CYP2B6* allele (**6, *11, *18, *27* or **28*), and (ii) by genotyping loss of function *CYP2A6* alleles and by determining the gene copy number in the complete study population.

Results: Analysis of the 146 subjects without impaired CYP2B6 function did not reveal a correlation between the *CYP3A* family, *CYP2A6* genotype and EFV exposure. However, a significant correlation was observed between *CYP3A4*1B* allele and high EFV exposure among CYP2B6 slow metabolizers. Median log10 EFV AUC values for carriers of *3A4*1B* (n=6) was 2.48 μg*h/ml, versus 2.12 for non-carriers (n=15), *p*=0.016. Resequencing of *CYP2A6* revealed 16 polymorphisms in the exons,16 in the exon-intron boundaries, and 1 in the promoter region. Median log10 EFV AUC values for subjects (n=5) with alleles associated with decreased 2A6 function (*2A6*7, *9, *17*) was 2.50 μg*h/ml, versus 2.15 for non-carriers (n=16), *p*=0.018. Combining CYP3A4 and 2A6 information provided the best discrimination of subjects with extreme EFV AUC: median log10 EFV AUC was 2.46 μg*h/ml for CYP2B6 slow metabolizers with reduced CYP3A4/2A6 function (n=8), 2.11 for CYP2B6 slow metabolizers (n=13), and 1.65 for the reference population (all common alleles, n=53).

Conclusions: In the setting of limited CYP2B6 function, functional polymorphisms in accessory metabolic pathways may contribute to extremely high EFV exposure. However, functional studies are needed to confirm these associations because of a strong confounding factor of ethnicity.

Analysis of the Expression and Function of LY6/PLAUR Proteins in the Differentiation Program of Keratinocytes

[1]Favre B., [1]Obarzanek-Fojt M., [1]Hohl D.

Service of Dermatology and Venereology[1]

Lymphocyte antigen 6/plasminogen activator, urokinase receptor (LY6/PLAUR) proteins are GPI-anchored or secreted extracellular protein-protein interaction modules. Only the function of CD59 and PLAUR among this family comprising at least 30 members is well known. In the epidermis several LY6/PLAUR proteins, in addition to PLAUR, are expressed, suggesting that they play an important role for skin homeostasis. As a first step toward the understanding of their function we have analyzed their expression in the skin by qualitative and quantitative PCR, in situ hybridization (ISH) and gene expression profiling during differentiation of cultured keratinocytes. Four LY6/PLAUR genes were up-regulated during differentiation, SLURP1, LYNX1B, LYPD3 and LY6G6C. ISH analysis revealed that both SLURP1 and LYNX1B were mainly transcribed in the granular layer. In contrast LY6D gene was only expressed in the basal and spinous layers. However, in cultured cells LY6D was not expressed in proliferating keratinocytes while immunofluorescence analysis on skin sections revealed the presence of LY6D all over the epidermis. Taken together these results indicate that LY6D is a marker of postmitotic keratinocytes. To understand more specifically the function of SLURP1 we cultured normal human keratinocytes and keratinocytes isolated from patients suffering from Mal de Meleda, a genetic palmoplantar disease caused by mutations in the gene encoding SLURP1, and performed gene expression profiling. Several genes were up or down regulated in diseased versus normal keratinocytes. These results suggest that a knock down approach could be envisaged for the analysis of the function of other LY6/PLAUR proteins in the differentiation process of keratinocytes.

Souris génétiquement modifiées

[1]Porret A., [2]Anne-marie M., [2]Edith H.

UNIL et CHUV[1], UNIL[2]

Abstract:

Suite au séquençage du génome, l'application de moyens d'analyse des gènes identifiés in vivo devient de plus en plus importante pour la recherche.
La plate-forme de transgénèse (TAF, Transgenic Animal Facility) de l' Université de Lausanne et des Hospices cantonaux est un service à la disposition des chercheurs de l'UNIL et du CHUV.
La plate-forme est active dans la génération de souris génétiquement modifiées transgéniques ou knock-out.
La TAF applique principalement deux techniques:
(i) la génération de souris transgéniques par micro-injection de l'ADN dans le
pronoyau des ovocytes.
(ii) la génération de souris knock-out ou conditionnelles ciblées, par recombinaison homologue dans des cellules souches embryonnaires de souris.
La TAF fonctionne également comme plate-forme interactive en ce qui concerne les questions liées à la génération et à l'analyse de ces souris.
Dès l'an prochain, une nouvelle technique sera à la disposition des chercheurs. Cela implique l'utilisation d'un laser et d'une nouvelle lignée de cellules embryonnaires, Bruce 4, issue de souris C57BL6, ce qui permettra des modifications génomiques dans cette même souche de souris.

Identification of CgPDR1 mutations involved in azole resistance among clinical Candida glabrata isolates

[1]Ferrari S., [1]Sanglard D.

Institute of Microbiology - CHUV[1]

CgPdr1p is a *C. glabrata* Zn(2)-Cys(6) transcription factor involved in the regulation of the ABC-transporter genes *CgCDR1*, *CgCDR2* and *CgSNQ2*, which mediate azole resistance. Single point mutations in *CgPDR1* have been previously shown to increase the expression of at least *CgCDR1* and *CgCDR2* and thus contribute to azole resistance of clinical isolates.
In this study, we investigated the incidence of CgPdr1p mutations in a collection of *C. glabrata* clinical isolates. *CgPDR1* was cloned and sequenced from 26 matched pairs of azole-susceptible (MIC fluconazole ≤ 16 μg/ml) and azole-resistant (MIC fluconazole ≥ 32 μg/ml) clinical isolates upregulating *CgCDR* genes. By comparison of *CgPDR1* alleles from azole-susceptible and azole-resistant matched isolates, we identified 21 distinct *CgPDR1* alleles each with a single amino acid substitution, which might confer hyperactivity to CgPdr1p in order to mediate high expression of *CgCDR1* and *CgCDR2*. Moreover, the analysis of the *CgPDR1* sequences of 56 unrelated azole-resistant clinical isolates allowed to characterize 37 additional putative gain-of-function mutations. These 58 mutations were located at 51 distinct locations along the protein, and encompassed three distinct protein domains: i) the region homologous to the inhibitory domain of *S. cerevisiae* Pdr1p ii) the central part of the protein and iii) the putative transcriptional activation domain. Disruption of *CgPDR1* in an azole-resistant isolate led to a drastic increase of azole susceptibility and to the loss of *CgCDR1* and *CgCDR2* expression, thus confirming the involvement of *CgPDR1* in azole resistance. Expression of some of the mutant *CgPDR1* alleles in the background of a *CgPDR1*-deleted strain confirmed the involvement of the identified CgPdr1p amino acid substitutions in ABC-transporter genes upregulation and thus in azole resistance. Interestingly, although *CgCDR1*, *CgCDR2* and *CgSNQ2* promoters contain binding sites for *CgPDR1*, they are not always coordinately expressed in azole-resistant isolates indicating that ABC-transporter genes might be differentially regulated. Finally, azole resistance of four isolates did not correlate with mutations in CgPdr1p. Among them, three isolates were "petite" mutants with abnormal mitochondrial functions. The mechanism(s) of *CgCDR1* and *CgCDR2* upregulation in the remaining isolate still remains to be determined.

In conclusion, this work allowed to identify new gain-of-function *CgPDR1* mutations responsible for *CgCDR* genes constitutive upregulation and for azole resistance in several clinical *C. glabrata* isolates. Our results demonstrate the high diversity of *CgPDR1* mutations potentially involved in azole resistance. Additional studies are now undertaken to understand how CgPdr1p gain-of-function mutations affect transcription of the ABC-transporter genes *CgCDR1*, *CgCDR2* and *CgSNQ2*.

Exploration of the calcineurin pathway of *Candida albicans* using a genome-wide approach: new insights in the tolerance to antifungal agents.

[1]Turner V., [1]Sanglard D.

Institute of Microbiology - CHUV[1]

Azoles antifungals possess only a fungistatic activity in *Candida albicans* and make this human pathogen tolerant to these agents. Because of their fungistatic properties, azoles increase the ability of *C. albicans* to develop drug resistance. Therefore, the conversion of azoles into fungicidal agents is of interest. In *C. albicans*, the calcineurin, which is a heterodimeric phosphatase, is essential for azole tolerance. Up to now, the only known target of calcineurin is CaCrz1p, which is a transcription factor involved in response to ionic stress. Thus, most of the components of the calcineurin pathway must be still identified in *C. albicans*. In this work, the calcineurin pathway was further investigated in order to identify fungal-specific targets that could be of interest to improve the activity of azoles.

Using a genome-wide approach with *C. albicans* microarrays, we attempted to identify the set of calcineurin-dependent genes (CDG) in this yeast species. Previous microarray experiments using stimuli such as Ca^{2+} or terbinafine (an antifungal agent targeting ergosterol biosynthesis) as calcineurin activators showed that CDG were highly dependent upon the external stimulus. In order to bypass the stimuli bias, *C. albicans* strains were designed for expressing a truncated autoactive form of the calcineurin ($Cnap^{Tr}$) in a doxycycline-dependent manner. The designed strains were applied to microarrays for transcript profile analysis and CDG were next identified. *In silico* analysis of the CDG in the Candida Genome Database (CaDB) allowed their functional classification. Our analysis showed that 30% and 18% of the CGD were involved in drug stress and cell-wall biogenesis, respectively. The microarray data therefore strongly suggest a relation between drug stress, calcineurin and cell-wall reorganisation. A second *in silico* analysis of the CGD in the CaDB and of their promoters in Yeastract (a software that allows the identification of consensus sequences recognized by *S. cerevisiae* transcription factors) allowed the identification of 22 transcription factors that are putatively regulated by calcineurin. A separate *in silico* analysis of the CDG in the CaDB and in the L2L-Database (a database containing a compilation of microarray experiments performed on *C. albicans*) revealed a putative interaction between the Cyr1p adenylate-cyclase cAPM-dependent pathway and calcineurin. To experimentally validate these *in silico* observations, 15 transcription factor mutants (out of the 22 above-mentioned factors) available from a collection of *C. albicans* mutants were screened for tolerance to the fungistatic drug terbinafine. Mutants for the transcription factors *CAS5* (involved in cell-wall integrity pathway regulation) and *UPC2* (involved in ergosterol biosynthetic pathway regulation) showed loss of tolerance upon terbinafine exposure, thus indicating that they participate in the tolerance phenomenon of *C. albicans* against antifungal agents. Interestingly, Cas5p contains a putative recognition sites (PxIxID) for phosphatase activity of calcineurin.

In conclusion, this study enabled, with the help of a genome-based approach, to identify several putative calcineurin targets. We showed that at least two transcription factors are critical for antifungal tolerance. While the interaction of these factors with calcineurin is currently being tested, the involvement of other *in silico* identified CGD in antifungal tolerance is being addressed.

Familial investigation of a rare mitochondrial myopathy

[1]Guerry F., [1]Jacquemont S., [2]Jeannet P.Y., [3] Ballhausen D.

Service de génétique médicale[1], Service de pédiatrie[2], Service de pédiatrie moléculaire[3]

The estimated prevalence of pathogenic mutations in mitochondrial DNA is 1/15000.The vast majority of mitochondrial mutations affect tRNA genes. Mutations in different tRNA genes and within the same tRNA can cause distinct clinical and biochemical phenotypes with a wide variability of expression.
We report on a family carrying a rare A3302G $tRNA^{Leu(UUR)}$ mutation. The proband developed at 2 years of age a progressive axial and limb girdle myopathy. She subsequently lost head control due to severe axial hypotonia. Biochemical analyses demonstrated a deficit in the complex I of the respiratory chain in the muscle biopsy. The deficit was borderline in the fibroblasts. Genetic analyses of the heteroplasmy ratio (proportion mutated/wild type mtDNA) showed 95 % mutant load in the muscle, 91% in the epithelial cells and 97% in the lymphocytes. The family investigation revealed that her mother, her aunt and uncle were all carriers with a mean mutant load of 40%, 5% and 20% respectively in lymphocytes and epithelial cells. These three individuals (<45 years old) are asymptomatic.
These results provide insight on genotype-phenotype correlation for children and adults younger than 45 years of age. Genetic data on older asymptomatic individuals (maternal grandmother and grand aunt – uncle) in this family will allow to estimate the heteroplasmy-threshold for later onset myopathy or exercise intolerance. This will provide useful data for adults family members seeking accurate genetic counseling.

IMI
Immunité et Infection

Low Total Plasma Concentrations (TPC) of Caspofungin (CSP) in Surgical Intensive Care Unit (ICU) Patients (Pts).

[1]Pascual A., Bolay S., Rochat B., Eggimann P., Ksontini R., Buclin T., Bille T., Calandra T., Marchetti O.

CHUV[1]

Background. CSP is a new therapy of invasive mycoses. MIC90 of CSP in *Candida* spp. is 1 mg/L. Ratios 24h-AUC TPC of CSP/MIC > 200 and peak TPC of CSP/MIC > 5 are associated with success in experimental candidiasis (Louie AAC 2005). TPC of CSP depend from drug distribution and plasma protein levels (binding >95%), which may be altered in ICU Pts.

Objective. To compare the TPC of CSP in ICU and non-ICU Pts.

Methods. CSP doses: 70 mg loading on day 1, then 50 mg/d. TPC profiles of CSP were measured by LC-MS/MS (mass spectrometry) on day 7 of therapy: 1h (peak), 4, 8, and 24 post-dose. EORTC-MSG definitions for mycoses and NCI criteria for SAE were used.

Results. 29 adult Pts: 8 ICU (87% surgical) and 21 non-ICU (95% medical). Age, sex, body weight and liver function were similar in both groups. ICU Pts (median SAPS II 41, range 29-65): 6/8 had mean blood pressure < 70 mmHg, 2/8 were on renal replacement therapy. Indications for CSP therapy i) ICU: 6/8 post-surgical prophylaxis, 2/8 invasive candidiasis, ii) non-ICU: 10/21 persistent febrile neutropenia, 9/21 invasive candidiasis, 2/21 aspergillosis. TPC profiles of CSP on day 7 were :

	ICU	Non-ICU	P
CSP dose, mg/kg/d *	0.65 (0.5-0.8)	0.7 (0.4-1.3)	NS
Days of therapy *	16 (6-32)	13 (4-31)	NS
Serum albumin, g/L *	22 (16-35)	32 (24-35)	<0.01
Peak CSP, mg/L **	4 (3.3-4.9)	5.9 (5.6-7)	<0.01
24h-AUC CSP, μg.hr.mL **	28.9 (24.9-32.9)	42.2 (35.9-48.5)	<0.01

* median (range); ** geometric mean (95% CI)

One single failure of CSP therapy was observed in a ICU patient with invasive candidiasis despite AUC/MIC > 1000 and peak/MIC > 100.
No CSP-related SAE requiring therapy discontinuation or drug interactions were identified.

Conclusions. Total blood concentrations of CSP were lower in surgical ICU than in non-ICU patients. This phenomenon is probably associated with low albumin levels and altered drug distribution. Investigations are needed to assess the clinical significance of this observation.

Renal Function-Dependent Inappropriate Imipenem (IMP) and Cefepime (CEF) Blood Concentrations (BC) in Febrile Neutropenic Cancer Patients (Pts)

[1]Lamoth F., [1]Pascual A., [1]Bolay S., [1]Vora S., [1]Calandra T., [1]Marchetti O.

Service of Infectious Diseases CHUV[1]

Background. IMP and CEF are frequently used for antibacterial therapy of febrile neutropenia. Renal clearance is determinant for their elimination. Renal function-dependent variability of BC of IMP and CEF may be associated with failure of therapy or toxicity.

Objective. To assess the influence of renal function on BC of IMP and CEF in febrile neutropenic Pts.

Method. Retrospective analysis of trough BC of IMP and CEF (HPLC) in adult febrile neutropenic cancer Pts with normal renal function (creatinine clearance ≥ 50 ml/min) vs impaired (< 50). Trough BC were classified as low [<MIC if available or <MIC_{90}, i.e. <1 mg/l (IMP), 2 mg/l (CEF)], appropriate or high (>15 mg/l). The clinical impact of low and high BC was evaluated by response to therapy or occurrence of toxicity, respectively.

Results. BC of IMP or CEF were measured 3 d (median, range 1-15) after start of therapy in 81/170 (48%) febrile episodes (38% microbiologically and 37% clinically documented, 25% fever of unknown origin). Results are shown in the table:

Creatinine clearance		< 50	≥ 50	P
IMP	Dose, g/d *	2 (0.75-2)	2 (1.5-4)	NS
	BC, mg/L *	1.5 (1.1-4.5)	0.8 (0.1-18)	0.05
	LOW	0/5 (0%)	21/46 (46%)	0.07
CEF	Dose, g/d *	6 (2-6)	6 (4-6)	NS
	BC, mg/L *	21 (2.4-38)	7.6 (2.1-36)	0.09
	HIGH	6/8 (75%)	6/22 (27%)	0.03

* Median (range)

Lack of response to IMP therapy was attributed to low BC in 6/51 (12%) episodes. Neurological toxicity related to high BC occurred in 7/30 (23%) Pts receiving CEF.

Conclusions. Low imipenem and high cefepime blood concentrations were observed in patients with normal and impaired renal function, respectively. Monitoring of blood levels may avoid failure or toxicity due to inappropriate dosing of antibiotic therapy.

Septifast PCR (SF) for Microbiological Documentation of Blood Culture (BC)-Negative Infections in Febrile Neutropenic Patients (Pts)

[1]Lamoth F., [2]Jaton-Ogay K., [2]Prod'hom G., [1]Senn L., [3]Bille J., [1]Calandra T., [1]Marchetti O.

Service of Infectious Diseases CHUV[1], Insitute of Microbiology CHUV[2], Institute of Mircobiology CHUV[3]

Background. BC are the gold standard of microbiological diagnosis in febrile neutropenic Pts. No causative agent is identified in 2/3 of febrile episodes. SF (Roche) is a new PCR test, which may detect bacterial and fungal DNA in blood of Pts with BC-negative infections.

Objective. To assess the utility of SF for the microbiological documentation in febrile neutropenic Pts.

Method. Blood samples for BC and SF were prospectively drawn in 49 adult neutropenic cancer Pts at D0 (onset of fever) and D3 (if persistent fever). Febrile episodes were classified as microbiologically (MDI) or clinically documented infection (CDI) and fever of unknown origin (FUO). Invasive fungal infections were defined according to the EORTC – MSG criteria.

Results. **186 samples were analyzed in 119 febrile episodes (38 MDI, 41 CDI, 40 FUO). BC and SF were positive in 32 (27%) and 44 (37%) episodes, respectively. The pathogens were: i) BC: G+ 54%, G- 46%; ii) SF: G+ 21%, G- 64%, fungi 15%. 32% of pathogens not detected by SF were not included in the test panel. Using BC as reference, sensitivity of SF was 50%, specificity 65%, PPV 30%, NPV 82%. Performance of BC and SF in different settings :**

	BC-positive	SF-positive	P value
No antibacterial therapy (n=74)	20 (27%)	14 (19%)	NS
Antibacterial therapy (n=112) Onset of fever, D1 (n=39) Persistent fever, D3 (n=73)	12 (11%) 8 (21%) 4 (5%)	36 (32%) 15 (38%) 21 (29%)	< 0.001 0.14 < 0.001

SF detected pathogens consistent with the site of infection in 12/41 (29%) CDI.

Using EORTC-MSG criteria as gold standard, the performance of SF for the diagnosis of invasive fungal infections was: sensitivity 71%, specificity 97%, PPV 63%, NPV 98%.

Conclusion. **Septifast PCR is a promising additional tool for the microbiological documentation of blood culture-negative febrile episodes and for the diagnosis of invasive fungal infections in neutropenic patients. Septifast may be particularly useful in patients receiving antibiotics at time of blood sampling or with persistent fever**

Caspofungin (CSP) for Prophylaxis (Px) of Intraabdominal Candidiasis (IC) in High-Risk Surgical Patients (Pts) : a Pilot Study.

[1]Senn L., [2]Eggimann P., [3]Ksontini R., [1]Pascual A., [1]Bille J., [1]Calandra T., [1]Marchetti O.

Service des maladies infectieuses, CHUV[1], Soins intensifs adultes, CHUV[2], Service de chirurgie viscérale, CHUV[3]

Background. We have previously shown that 30-40% of surgical Pts with recurrent gastrointestinal perforation/anastomotic leakage, or acute necrotizing pancreatitis develop IC (Lancet 1989, 2:1437). These Pts benefit of fluconazole Px (Crit Care Med 1999, 27:1066). A corrected *Candida* colonization index (CCI) ≥ 0.4 is a major risk factor for IC (Ann Surg 1994, 220:751). CSP, a new therapy for IC including azole-resistant *Candida* spp., may be used for Px of IC.

Objective. To conduct a non-comparative pilot study on the efficacy and safety of CSP for Px of IC in high-risk surgical Pts.

Methods. Inclusion criteria: age >18, surgery for recurrent gastrointestinal perforations/anastomotic leakage or acute pancreatitis. Exclusion criteria: documented IC, fluconazole Px. CSP Px (70 mg, then 50 mg/day) was given until resolution of the surgical condition. *Candida* colonization was monitored 1x weekly at ≥ 3 sites and the CCI calculated. Success was defined by the absence of IC during CSP Px. Occurrence of CSP-related SAE was recorded.

Results. 19 Pts were enrolled: 16/3 males/females, median age 69 (range 40-84). Underlying surgical conditions were: recurrent gastrointestinal perforation/anastomotic leakage (n=16), acute pancreatitis (n=3). At study entry, 14 (74%) Pts were in the ICU (median Simplified Acute Physiology Score II: 45, range 31-65), 19 (100%) received antibacterial therapy and 17 (89%) were colonized with *Candida (C. albicans* in 69%; CCI ≥ 0.4 in 1/17 case, 5%). Median duration of CSP Px was 16 days (range 4-46). During CSP Px, 17 (89%) Pts remained colonized (*C. albicans* in 68%), but 0/17 developed a CCI ≥ 0.4. CSP was successful for prevention of IC in 18 (95%) Pts. Among 5 deaths, none was attributed to IC. No severe CSP-related SAE requiring discontinuation of Px occurred.

Discussion. The results of this pilot study suggest that caspofungin is efficacious and safe for prophylaxis of intra-abdominal candidiasis in high-risk surgical patients.

Viral PCR in Aseptic Meningitis (AM) in Adult Patients for Reduction of the Use of Antimicrobial Therapy and the Length of Hospital Stay

CHAPUIS-TAILLARD C., JATON-OGAY K., MANUEL O., CALANDRA T., BILLE J., MEYLAN P., MARCHETTI O.,

Institute of Infectious diseases, CHUV

Background. The majority of AM are self-limited viral infections. The differentiation of these conditions from life-threatening bacterial meningitis is difficult due to overlapping clinical presentation and lack of viral diagnostic tests. This results in unnecessary antimicrobial therapy and prolonged hospitalisation. Molecular tools for documentation of a viral etiology in AM might improve clinical management.

Objectives. To assess the impact of a positive viral PCR result in AM on the use of antimicrobial therapy and the length of hospital stay.

Methods. Observational study in patients with AM (CSF pleocytosis, negative bacterial cultures). Viral PCR (Enterovirus, HSV, VZV) were performed on CSF in addition to standard tests. Demographics, clinical and laboratory data were analyzed.

Results. 43 adult patients (median age 32, 16-77) were studied: in 25/43 (58%) viral PCR was positive (enterovirus 20, HSV-2 2, VZV 3) and in 18/43 (42%) negative. The clinical presentation was similar in PCR + vs PCR - cases: headache 100 vs 100%; fever 92 vs 83%; neck stiffness 68 vs 72%. Median (range) CSF parameters in PCR + vs PCR - cases were: cells/mm^3 660 (344-2124) vs 776 (181-2170); protein 164 mg/L (17-1325) vs 162 (22-1072); ratio CSF/blood glucose 0.51 (0.4-0.6) vs 0.51 (0.4-0.6). Median days to PCR+ were 2.5 (0.5-5). The table summarizes clinical management:

	PCR + *n=25*	*PCR -* *n=18*	*P*
Empirical antibacterial therapy	*15/25 (60%)*	*12/18 (66%)*	*NS*
Median days (range)	*1 (1-3)*	*3 (1-12)*	*0.03*
Empirical acyclovir therapy	*4/25 (16%)*	*9/18 (50%)*	*0.02*
Median days hospital stay (range)	*2.5 (1-26)*	*4 (1-12)*	*0.12*

Conclusions. A positive viral PCR result in aseptic meningitis contributes to reduce the use of antimicrobial therapy and the length of hospital stay.

MECHANISMS OF ALLOGRAFT REJECTION AND TOLERANCE IN TRANSPLANTATION

[1]Golshayan D., [2]Schaefer S., [2]Abulker C., [3]Wyss J.-C., [4]Lechler R., [2]Lehr H.-A., [3]Pascual M.

Nephrology and Transplantation[1], Pathology, CHUV[2], Transplantation, CHUV[3], Nephrology and Transplantation, King's College, London[4]

The mechanisms by which CD4+CD25+Foxp3+ T cells (Treg) regulate effector T cells in a transplant setting and their in vivo homeostasis still remain to be clarified. Using a mouse adoptive transfer and skin transplant model, we analyzed the in vivo expansion, effector function and trafficking of effector T cells and donor-specific Treg, in response to an allograft. Antigen-specific Treg were generated in vitro as previously described. Fluorescent-labeled CD4+CD25-CD45RBhi T cells and Kb-specific Treg were transferred alone or co-injected into syngeneic Nude-BALB/c recipients transplanted with C57BL/6xBALB/c donor skin. Treg divided in vivo, migrated and accumulated in the allograft draining lymph nodes (drLN) and within the graft. The co-transfer of Treg didn't modify the proliferation or homing of CD4+CD25- T cells to secondary lymphoid organs. In the presence of Treg, effector T cells produced significantly less IFN-γ and IL-2, while higher amounts of IL-10 were detected in the spleen and drLN of these mice. Furthermore, time-course studies showed that Treg were recruited into the allograft at a very early stage post-transplantation and prevented infiltration by effector T cells.

Our results suggest that suppression of rejection involves the early recruitment of donor-specific Treg at the site of antigenic challenge and that Treg mainly regulate the effector arm of T cell alloresponses.

Innate Immune Responses of Macrophages and Dendritic Cells to Poxvirus

[1]Delaloye J., [1]Roger T., [2]Esteban M., [1]Steiner-Tardivel Q.-G., [1]Calandra T.

Infectious Diseases Service, Department of Medicine, CHUV, Lausanne[1], Department of Molecular and Cell Biology, Madrid, Spain[2]

Background: Attenuated NYVAC and MVA poxvirus strains are currently used for vaccine development against a broad spectrum of diseases. Whilst these vectors have been shown to be immunogenic and safe in humans, the innate immune responses they elicit remain largely unknown.

Aim: To assess the response of human THP-1 cells and mouse dendritic cells to poxviruses infection and to elucidate the role of the Toll-like-receptor (TLR) pathways in that response.

Results: MVA-stimulated THP-1 monocytes secreted large amounts of chemokines (MIP-1, MCP-1, IP-10, RANTES), but low levels of pro-inflammatory cytokines (TNF, IL-6, IL-1beta). In contrast, NYVAC induced weak production of both cytokines and chemokines in THP-1 cells. Using wild-type and TLR2, TLR4, MyD88 and TRIF deficient mouse dendritic cells, we observed that TLR2-MyD88 was essential for production of chemokines, but dispensable for IFNbeta production, after stimulation with MVA.

Conclusion: MVA triggers innate immune responses of macrophages and dendritic cells via TLR-dependent and TLR-independent pathways. Work is in progress to identify the TLR-independent pathway(s) activated by MVA.

Pilot Study on LightCycler SeptiFast® Blood Assay for the Early Diagnosis of Invasive Fungal Infections (IFI) in Neutropenic Pa

[1]Lamoth F., [2]Jaton-Ogay K., [2]Bille J., [2]Prod'hom G., [1]Senn L., [1]Marchetti O.

Service of Infectious Diseases CHUV[1], Institute of Microbiology CHUV[2]

Background. IFI are life-threatening complications in neutropenic patients with AL. Diagnosis of IFI is challenging because of the lack of specificity of clinical assessment and the poor sensitivity of cultures. This results in a large empirical use of antifungal agents. The LightCycler SeptiFast®, a new PCR-based blood assay for detection of bacterial and fungal DNA in patients with sepsis, may contribute to the early diagnosis of IFI during neutropenia.

Objective. To assess the efficiency of LightCycler SeptiFast® blood assay for the diagnosis of IFI in neutropenic patients with AL.

Method. Pilot observational prospective study. Blood samples were drawn in adult febrile neutropenic patients with AL at onset of fever and twice weekly during persistent fever. IFI were classified as proven, probable or possible according to the EORTC-MSG criteria. Efficiency of LightCycler SeptiFast® for diagnosis of IFI was compared to that of clinical assessment (persistent fever requiring empirical antifungal therapy).

Results. 81 samples were analyzed during 46 febrile episodes in 25 patients. 6 (13%) episodes were classified as probable or possible IFI (3 aspergillosis, 3 candidiasis). Empirical antifungal therapy was initiated in 13 (28%) episodes (2 probable and 3 possible IFI, 8 no IFI). No fungemia was detected by blood cultures. LightCycler SeptiFast® detected fungi in 5 febrile episodes: *A. fumigatus* in 1 patient with sinusitis (possible IFI), *C. tropicalis* (2) and *C. albicans* (2) in 4 patients with enterocolitis (3 possible IFI, 1 no IFI with GI-tract *Candida* spp. colonization). Using EORTC-MSG criteria as gold standard, efficiency of clinical assessment and LightCycler SeptiFast® for diagnosis of IFI are compared:

	Persistent fever requiring empirical antifungal therapy	LightCycler SeptiFast® blood assay
Sensitivity	83% (5/6)	67% (4/6)
Specificity	80% (32/40)	98% (39/40)
Positive predictive value	38% (5/13)	80% (4/5)
Negative predictive value	97% (32/33)	95% (39/41)
Efficiency	80%	93%

The median time interval between onset of fever and start of empirical antifungal therapy or positive LightCycler SeptiFast® was 6 days (range 2 to 7) and 4.5 days (range 0 to 19), respectively.

Conclusions. This pilot study suggests that the LightCycler SeptiFast® blood assay may be an efficient tool for the early diagnosis of invasive mycoses in neutropenic patients with acute leukemia. Excellent test's specificity and negative predictive value might contribute to targeted use of antifungal therapy.

Novel Chlamydiales isolated using amoebal co-culture

[1]Greub G., [1]Feroldi V., [1]Aeby S., [1]Greub G.

Inst of Microbiology[1]

Introduction
In the last years, amoebae have emerged as natural hosts of an increasing number of novel *Chlamydiales*. Some of them are emerging pathogens of humans. Members of the family *Parachlamydiaceae* are implicated in opportunistic respiratory infections. Culture-independent PCR-based studies indicated a higher diversity within the *Chlamydiales*, which may suggest the existence of yet unknown pathogens. Since amoebae play a key role as natural reservoir for these bacteria, we searched for the presence of chlamydiae in water treatment systems, which are an ideal niche for a large variety of protists.

Methods
We used *Acanthamoeba* co-culture to isolate chlamydiae from water treatment plant. Water samples (1 L) were filtered through a 0.2-µm polycarbonate membrane, and the filter was resuspended in 50 mL of water. Then, 200 µL of the suspension were inoculated onto 24-well plates seeded with axenic *Acanthamoeba* cells (strain ATCC 30010). Searching for chlamydiae was performed by applying modified Giemsa stain and pan-chlamydia 16S rDNA PCR plus sequencing.

Results
Using *Acanthamoeba* co-culture on 127 samples, 10 chlamydial strains (7.8 %) were recovered, mainly from raw-surface waters (n=4) and biofilm/sediment from reservoirs (n=5). Only one chlamydial strain was recoverd from a treated water sample. Nearly full 16S rDNA sequences of all these strains were obtained and analysed. BLAST analysis and sequence idendity (ID) revealed that five strains belonged to the *Parachlamydiaceae*, two strains exhibited as closest relative *Criblamydia sequanensis*, two strains showed some similarities with *Rhabdochlamydia* spp., and one strain had no close cultured relatives. Phylogenetic analyses confirmed these genetic affiliations with high bootstrap values. As expected, *Parachlamydiaceae* are the most abundant (5/10 recovered strains), and fall into three sublineages : *Protochlamydia* (3 strains, 95-99 % ID), *Neochlamydia* (1 strain, 96-98 % ID), and the UWE1 endosymbiont (1 strain, 95 % ID). The two strains related to *Criblamydia sequanensis* (>92 % ID) very likely represent new members of that family. One of these strains exhibits a star-shaped elementary body, characteristic of *Criblamydia*. The two strains related to *Rhabdochlamydia* spp. (89-91 % ID) emerge as distinct lineages, more related to some environmental clones. Finally the latter strain emerges within a deep lineage including only environmental clones (ca. 90 % ID), and could be the first cultured strain of a novel chlamydial lineage.

Conclusion
This study confirm the high diversity of the *Chlamydiales* in the environment. The *Acanthamoeba* co-culture is a usefulness tool to isolate new chlamydial species from complex samples, that are further investigated for their human pathogenicity.

Hemophagocytic syndrome after HAART initiation: a life-threatening event related to immune restauration inflammatory syndrome (IRIS) ?

[1]Cavassini M., [1]Cuttelod M., [1]Pascual A., [2]Duchosal M., [3]Baur A., [1]Osih R., [1]Alain C.

MIN, CHUV[1], Hematology, CHUV[2], Pathology, CHUV[3]

Background: The hemophagocytic syndrome (HS) is a life-threatening condition and may be primary or secondary related to various infections, autoimmune diseases or malignancies. HS has been described among HIV patients during primary infection or opportunistic infections. HS is known to be a rare complication of Hodgkin's lymphoma (HL).
Cases reports: We describe two severe cases of HS with HL shortly after HAART initiation
Discussion: Both patients presented a history of weight loss and fatigue attributed to HIV disease. CD4 counts before HAART initiation were below 100 cell/mm^3. Within a week after HAART initiation patients developed high fever and the biological features were consistent with HS : ferritin > 10'000 µg/l, pancytopenia, acute renal failure and cholestasis. A CT-scan showed a hepatosplenomegaly and a lymphadenopathy. Bone marrow biopsies confirmed HS and revealed HL in both patients. Steroids and chemotherapy (adriamycin, bleomycin, vinblastine and dacarbazine) were administrated respectively 23 and 6 days after HAART initiation. Outcome was fatal for the patient in whom diagnose and therapy was delayed.
Conclusion: These two cases of HS suggest an IRIS related event in two HIV patients with an underlying HL. Unlike most of the described IRIS related events, these cases do not suffer any delay in diagnose and may resolve under specific and intensive clinical management.

Waddlia chondrophila enters and multiplies within human macrophages

[1]Goy G., [1]Croxatto A., [1]Greub G.

Institute of Microbiology - CHUV[1]

Background:
Waddlia chondrophila is an obligate intracellular bacterium, which belongs to the *Chlamydiales* order. It was isolated twice from aborted bovine fœtuses, first in 1990 in the United States and then in 2002 in Germany. A serological study supported the abortigenic role of *Waddlia* in bovine species and inoculation of a pregnant cow with this intracellular bacteria was associated with foetal death within 2 weeks. Recently, we observed a strong association between the presence of anti-*Waddlia* antibodies and human miscarriage. To further investigate the pathogenic potential of *W. chondrophila* in humans, we studied the entry and the multiplication of this obligate intracellular bacteria in human macrophages.

Methods:
Monocyte-derived macrophages were incubated with living or heat-inactivated bacteria for 15 min at 37°C after a centrifugation step. Cells were then washed and further incubated for different periods at 37°C. Entry was assessed by confocal microscopy and bacterial growth was assessed using immunofluorescence with home-made mice anti-*Waddlia* antibodies and real-time PCR.

Results:
Confocal microscopy confirmed that *W. chondrophila* is able to enter into human monocyte-derived macrophages. *W. chondrophila* organisms were shown to multiply readily within macrophages. The proportion of infected macrophages increased from 13% at day 0 to 96% at day 4, and the mean number of bacteria per macrophage increased of 3 log in 24 hours. This growth was confirmed by real-time PCR and was associated with a decrease in the number of macrophages. As expected, the heat-inactivated bacteria, which also entered into the macrophages, did not increase over time and exhibited no cytopathic effect.

Conclusion:
This study shows that *W. chondrophila* enters passively into and multiplies logarithmically within human macrophages suggesting its human pathogenicity.

Escherichia coli Up-Regulates MIF Gene Expression by Innate Immune Cells in a MEK1/2-, Sp1-Dependent Manner

[1]Roger T., Ding X., Chanson A.-L., Renner P., KnaupReymond M., Calandra T.

Infectious diseases, CHUV[1]

Background: Macrophage migration inhibitory factor (MIF) is an important regulator of innate immunity, inflammation and oncogenesis. Polymorphisms within the MIF promoter have been associated with susceptibility to and/or severity of inflammatory and autoimmune diseases. We have previously shown that the binding of Sp1 transcription factor is a critical positive regulator of human *MIF* gene expression at baseline and that microbial products up-regulate MIF mRNA expresison.

Objective: To elucidate the molecular mechanisms involved in the up-regulation of *MIF* gene expression after stimulation of cells of the monocytic/macrophage lineage with bacterial pathogens.

Methods: Experiments were performed with human PBMCs and THP-1 monocytic cells pretreated for 1 h with or without U0126 and SB203580 and exposed to heat-killed *Escherichia coli* (*E. coli*). MIF mRNA, protein and promoter activities were assessed by Northern blotting, Western blotting and luciferase reporter assay, respectively. Transcription factor binding activity was assessed by EMSA, supershift and chromatin immunoprecipitation (ChIP). MEK1/2 (ERK kinases) and p38.

Results: Stimulation of THP-1 cells with *E. coli* up-regulated MIF mRNA levels, MIF promoter activity and Sp1-DNA binding activity. Whereas ChIP analyses showed that *E. coli* did not modify Sp1 binding to the endogenous MIF promoter, Western blot experiments revealed a strong increase of phosphorylated Sp1 nuclear content. *E. coli*-induced MIF promoter activity, Sp1-DNA binding activity and MIF mRNA expression were inhibited by pretreatment of THP-1 cells with the Sp1 inhibitor mythramycin A and the MEK1/2 inhibitor SB203580 but not with the p38 inhibitor U0126. These observations were in line with recent reports showing that stimulus-induced phosphorylation of Sp1 mediated by MEK1/2 may increase its transactivation activity without any change in its DNA-binding activity. Recapitulating the results obtained in THP-1 cells, stimulation of PBMCs with *E. coli* increased phosphorylated Sp1 nuclear levels, Sp1 DNA binding activity and MIF mRNA expression.

Conclusions: Our results strongly argue in favor of a central role of the MEK1/2 signaling pathway in the phosphorylation of Sp1 and MIF expression upon exposure of innate immune cells to *E. coli*. Taken together with previous observations of an important role for MIF in pro-inflammatory macrophage responses, these present findings suggest a key role for Sp1 in transcriptional regulation of *MIF* gene expression and MIF-dependent host antimicrobial innate immune defenses.

Anti-Toll-like Receptor 4 (TLR4) Antibody Protects from Gram-negative Septic Shock

[1]Roger T., [1]LeRoy D., [1]Froidevaux C., [1]KnaupReymond M., [1]Chanson A.-L., [2]Mauri D., [3]Akira S., [4]Tschopp J., [1]Calandra T.

Infectious diseases, CHUV[1], Apotech Biochemicals[2], Osaka University[3], Department of Biochemistry[4]

Background: TLR4, an essential signalling component of the LPS receptor complex, plays a critical role in innate immune defenses against Gram-negative (GN) bacteria, suggesting that it might be a candidate target for therapeutic interventions in patients with GN septic shock. To test this hypothesis, we have generated anti-TLR4 IgG that were shown to protect mice from lethal endotoxemia.

Objective: To explore the molecular mechanisms by which anti-TLR4 IgG interfere with LPS sensing and to investigate the effects of these antibodies in murine models of GN septic shock.

Methods: RAW 264.7 macrophages and bone marrow-derived macrophages (BMDMs) were exposed to LPS, Pam3CSK4 and CpG ODN. The phosphorylation of ERK1/2 and p38 MAPKs was analyzed by Western blotting. NF-kB transcriptional activity was measured in RAW 264.7 cells transfected with a multimeric-kB site luciferase reporter vector. Peritonitis was initiated by i.p. injection of 10^9 CFU of *Escherichia coli* (*E. coli*) O18 into mice. Mice were injected with antibiotics (ceftriaxone and gentamicin i.p.) 15 min or 1 h after infection and, in selected experiments, treated prophylactically (-4 h and -30 min and +4 h) or therapeutically (+1 h and +4 h) with control or anti-TLR4 IgG (160 mg/kg i.p). Survival was followed daily. Blood samples were collected to quantify the levels of TNF and IL-6.

Results: Anti-TLR4 IgG inhibited LPS-induced NF-kB-dependent luciferase reporter activity, phosphorylation of the ERK-1/2 and p38 and cytokine release by macrophages. MyD88-/- and TLR4-/- mice, but not wild-type and TLR2-/- mice, were protected from *E. coli*-induced lethal sepsis (n=7; p=0.0001), indicating that the MyD88-dependent TLR4 pathway played an essential role in mediating the deleterious effects of acute *E. coli* sepsis. In line with this observation, prophylactic and therapeutical application of anti-TLR4 IgG significantly reduced cytokine blood levels and morbidity parameters and enhanced the survival (n=10, $p<0.0001$ and $p=0.02$ for prophylactic and therapeutic treatment, respectively) of wild-type mice subjected to lethal *E. coli* peritonitis.

Conclusions: Anti-TLR4 IgG interfered with LPS-induced intracellular signaling and cytokine release by innate immune cell, providing a molecular explanation for their powerful protective effect against lethal endotoxemia. Most importantly, both therapeutical and prophylactic application of anti-TLR4 IgG protected from lethal *E. coli* peritonitis. Collectively, these results support the proof of principle that antibodies interfering with TLR4-mediated LPS sensing may protect from GN sepsis and could be a useful adjunctive therapy for the treatment of sepsis.

Characterization of highly differentiated viral-specific T cells in multiple sclerosis using quantitative real-time PCR

[1]Jaquiéry E., [2]Jilek S., [2]Garcia M., [3]LeGoff G., [3]Schluep M., [2]Pantaleo G., [4]DuPasquier R.

Immunology and allergy - CHUV[1], Division of Immunology - CHUV[2], Division of Neurology - CHUV[3], Divisions of Immunology and Neurology - CHUV[4]

We have previously shown that there was an enrichment in highly differentiated (CCR7-) CD8+ T cells in the cerebrospinal fluid of patients with early multiple sclerosis (MS). We have also found that these patients had a high Epstein-Barr virus (EBV)-specific CD8+ T cell response in the blood, confirming results from others showing that there is an association between EBV and MS.

Quantitative real-time PCR was performed on EBV stimulated highly differentiated CD4+ and CD8+ T cells of ten MS patients and eleven healthy controls (HC). Gene transcripts of interest were pro-inflammatory (IFN-gamma, IL-1beta, IL-2) and anti-inflammatory (IL-4, TGF-beta1, FOXP3) cytokines.

Under basal conditions, mRNAs coding for the pro-inflammatory cytokine IFN-gamma and the anti-inflammatory cytokine FOXP3 were increased in CD8+ T cells of MS patients as compared with HC. TGF-beta1 mRNA was also found to be increased in unstimulated CD4+ T cells of MS patients. After EBV stimulation, CD8+CCR7- T cells of MS patients harbored more IFN-gamma mRNA than HC.

These results suggest that CD8+ T cells of MS patients are more activated than CD8+ T cells of HC without stimulation. However, anti-inflammatory cytokines are also elevated in MS patients, suggesting that there are mechanisms of endogenous immunomodulation. Further reinforcing the link between EBV and MS, we found that IFN-gamma gene expression is increased in CD8+CCR7- T cells of MS patients after EBV stimulation.

Increased numbers of circulating polyfunctional Th17 memory cells in patients with seronegative spondyloarthropathies

[1]Jandus C., [2]Bioley G., [3]Rivals J.-P., [4]Dudler J., [5]Speiser D., [6]Romero P.

Ludwig Institute for Cancer Research, Division of Clinical Onco-Immunology; National Center for Competence in Research, Molecular Oncology, Epalinges,[1], Laboratory of Cancer Vaccinotherapy, INSERM U601, CLCC René Gauducheau, Bd Jacques Mono, F-44800 Saint-Herblaind[2], Service of Otorhinolaryngology and Head and Neck Surgery, University Hospital (CHUV), Lausanne, Switzerland[3], Service of Rheumatology, Department of Medicine, University Hospital (CHUV), Lausanne, Switzerland[4], Division of Clinical Onco-Immunology, Ludwig Institute for Cancer Research, Lausanne Branch, University Hospital (CHUV), Lausanne, Switzerland; Nation[5], 1Division of Clinical Onco-Immunology, Ludwig Institute for Cancer Research, Lausanne Branch, University Hospital (CHUV), Lausanne, Switzerland; Natio[6]

Reassessment of autoimmune inflammatory disorders in mouse models has suggested that among the major factors involved in their pathogenesis the IL-23/IL-17 axis, rather than the previously postulated IL-12/IFNγ axis plays a fundamental role. Indeed, the presence of IL-17 producing $CD4^+$ T cells (Th17 cells) has been shown to be necessary for the induction of different autoimmune diseases in mouse models. However, the implication of this newly identified $CD4^+$ T cell population in mediating autoimmune pathologies in humans has not yet been demonstrated. In this study we measured the levels of circulating Th17 cells in several human autoimmune pathologies, as compared to healthy donors. We document elevated levels of circulating Th17 cells in psoriatic arthritis as well as ankylosing spondylarthritis patients, but not in peripheral blood of rheumatoid arthritis, vitiligo and melanoma patients. In addition, a more pronounced differentiation state and poly functionality of Th17 was observed exclusively in arthritis patients. Unexpectedly, we found a population of $CCR6^-$ Th17 cells in psoriatic arthritis as well as ankylosing spondylarthritis patients, while this subset was absent in HDs and rheumatoid arthritis patients, suggesting a possible implication in disease establishment. Finally, the increase in Th17 cells did not correlate with a decrease neither in frequencies, nor in function and suppressive activity of circulating regulatory T cells. Together, these observations suggest a possible role for Th17 cells in the pathogenesis in the seronegative subset of inflammatory arthropathies.

Strong EBV-specific CD8+ T cell Response in Patients with Early Multiple Sclerosis

[1]Jilek S., [2]Schluep M., [2]Vingerhoets F., [1]Guignard L., [2]Kleeberg J., [2]LeGoff G., [1]Pantaleo G., [3]DuPasquier R.

Division of Immunology and Allergy - CHUV[1], Division of Neurology - CHUV[2], Division of Immunology and Allergy and division of Neurology - CHUV[3]

Epstein-Barr virus (EBV), in contrast to cytomegalovirus (CMV) has been repeatedly associated with a higher relative risk of developing MS. Here, we studied the EBV- and CMV-specific T cell response in patients with multiple sclerosis (MS), other neurological diseases (OND) as well as in healthy subjects (HC).

We enrolled patients with inflammatory MS, chronic MS, OND and HC and analysed the EBV- and CMV-specific T cell responses by ELISPOT (IFN-gamma secretion).

The EBV-specific CD4+ T cell responses were similar between the groups, however we found that EBV-specific CD8+ T cells in inflammatory MS patients secreted a higher amount of IFN-gamma than all other categories, including chronic MS patients. Interestingly, we found that the shorter the interval between MS onset and the assay, the higher the intensity of IFN-gamma secreting EBV-specific CD8+ T cells. However, the disease activity played no role as we did not find differences between MS patients in relapse or in remission.
By contrast, CMV-specific CD4+ T cell responses were moderately enhanced in patients with inflammatory and chronic MS as compared to OND and Hc subjects. No difference was found in the CMV-specific CD8+ T cell responses and there was no correlation with the time elapsed since MS onset.

Our data suggest that EBV, more than CMV, might be involved in the onset of MS and that this effect might be mediated by CD8+ T cells.

A Novel Population of Human Melanoma-Specific CD8 T Cells Recognizes Melan-AMART-1 Immunodominant Nonapeptide but Not the Corresponding Decapeptide.

[1]Derré L., [2]Ferber Mathias., [1]Touvrey C., [1]Devévre E., [3]Zoete V., [3]Leimbruger A., [1]Romero P., [3]Michielin O., [1]Levy F., [1] Speiser D.

Ludwig Institute for Cancer Research[1], Swiss Institute of Bioinformatics,[2], Swiss Institute of Bioinformatics[3]

HLA-A2-restricted cytolytic T cells specific for the immunodominant human tumor Ag Melan-A^{MART-1} can kill most HLA matched melanoma cells, through recognition of two naturally occurring antigenic variants, i.e., Melan-A nonamer AAGIGILTV and decamer EAAGIGILTV peptides. Several previous studies have suggested a high degree of TCR cross-reactivity to the two peptides. In this study, we describe for the first time that some T cell clones are exclusively nonamer specific, because they are not labeled by A2/decamer-tetramers and do not recognize the decamer when presented endogenously. Functional assays with peptides gave misleading results, possibly because decamers were cleaved by exopeptidases. Interestingly, nonapeptide-specific T cell clones were rarely Vα2.1 positive (only 1 of 19 clones), in contrast to the known strong bias for Vα2.1-positive TCRs found in decamer-specific clones (59 of 69 clones). Molecular modeling revealed that nonapeptide-specific TCRs formed unfavorable interactions with the decapeptide, whereas decapeptide-specific TCRs productively created a hydrogen bond between CDR1α and glutamic acid (E) of the decapeptide. Ex vivo analysis of T cells from melanoma metastases demonstrated that both nonamer and decamer-specific T cells were enriched to substantial frequencies in vivo, and representative clones showed efficient tumor cell recognition and killing. We conclude that the two peptides should be regarded as distinct epitopes when analyzing tumor immunity and developing immunotherapy against melanoma.

E7-specific CD8 T cell immune responses in the genital mucosa of mice vaccinated against HPV-16 and cervical cancer

[1]Decrausaz L., [1]Duc M., [1]Bobst M., [1]Zosso N., [1]Nardelli-Haefliger D.

Institute of Microbiology[1]

Cervical cancer, the second leading cause of cancer mortality in women worldwide results from infection with a sub-set of human papillomavirus (HPV), HPV-16 being the most prevalent type. The available prophylactic vaccines are an effective strategy to prevent this cancer but decades will be needed before it may be eradicated. Therapeutic vaccines are necessary to eliminate infected cells and associated lesions in women who have no benefit from prophylactic vaccination. Until now, therapeutic vaccines only showed poor clinical results, possibly linked to inefficient targeting of protective immune responses in the genital mucosa. Here we evaluated by IFN-γ ELISPOT combinations of different adjuvants with a synthetic HPV16 $E7_{1-98}$ polypeptide vaccine for inducing E7-specific CD8 T cell responses in the genital mucosa of mice. Parenteral vaccination with CpG and HLT adjuvants induced high E7-specific responses in blood, whereas combination of Resiquimod, HLT and CpG was the best combination after aerosol immunization, although this response was 5-fold lower than after parenteral vaccination. The amplitude and kinetics of E7-responses were also measured in draining lymph nodes and genital mucosa. Despite the lower E7-specific response in the periphery after aerosol immunization, similar responses were measured in the genital mucosa after both types of vaccination. There was no correlation between the responses measured in the periphery with those measured in the genital mucosal, highlighting the necessity to determine the immune responses in the mucosa where the tumor reside. Our results suggest that the adjuvanted $E7_{1-98}$ peptide could be a potent therapeutic vaccine against cervical cancer.

Dysregulation of channel activating protease 1 in the epidermis of the mouse

[1]Frateschi S., [2]Membrez M., [1]Charles R., [3]Breiden B., [3]Sandhoff K., [4]Beermann F., [5]Stehle J., [1]Rotman S., [1]Porret A., [1]Hummlér E.

UNIL[1], Nestlé[2], Kekulé Institut für Organische Chemie und Biochemie[3], ISREC[4], Département de Phatologie, Lausanne[5]

Background Mutations or alterations in the expression of several serine proteases (SP) and SP inhibitors can lead to skin diseases. In the epidermis the channel activating protease 1 (CAP1, also known as Prostasin and Prss8) is a serine protease expressed in the stratum granulosum and in the upper part of the stratum spinosum. The aim of this study is to investigate the importance of balanced CAP1 expression in the epidermis by addressing the CAP 1 transgenic expression to the stratum basale.

Materials and Methods Transgenic mice harboring the coding sequence of CAP 1 under the control of the keratin 14 (K14) promoter have been generated by micro-injection into fertilized mouse oocytes. The genotypes and phenotypes of the transgenic mice were assessed using standard molecular, cellular, histological means. The epidermal permeability barrier integrity was evaluated by measuring the trans epidermal water loss (TEWL).

Results CAP1 transgenic mice show a skin phenotype characterized by red, scaly skin with itch. These transgenic animals exhibit also lower body weight, higher TEWL, thicker and hyperkeratotic epidermis, dermis infiltrated by cells of the immunity system and increased postnatal mortality.

Conclusions Mice with an altered CAP 1 expression in the skin present impaired epidermal barrier function and skin inflammation. This study shows that regulated CAP 1 expression in the epidermis is important for the skin physiology. CAP1 transgenic mice can be used as a model for atopic dermatitis disease.

Peroxynitrite exerts complex and opposite effects on nuclear factor kappa B in vitro, revealing novel redox-based mechanisms controlling cell signal t

[1]Levrand S., [1]Rolli J., [2]Feihl F., [2]Waeber B., [1]Liaudet L.

Service de Médecine Intensive Adulte-CHUV[1], Division de Physiopathologie Clinique-CHUV[2]

Background. Redox signaling refers to the ability of oxidants to modulate the activity of proteins involved in signal transduction. Redox-based mechanisms control critical functions, including apoptosis and the regulation of inflammation. A master regulator of apoptosis and inflammation is the transcription factor nuclear factor kappa B (NF-kB). NF-kB is classically activated by inflammatory mediators, but it is also suspected to be redox sensitive. However, the modes of interactions between oxidative stress and NF-kB are poorly defined. Here, we investigate the redox mechanisms controlling NF-kB activity in vitro. Method. NF-kB activation was evaluated in the lung epithelial cell line A549. Cells were stimulated with the classical NF-kB activator TNFalpha (TNFa), or with the potent oxidant peroxynitrite. NF-kB was assessed by the activation of the upstream kinase IKK, the phosphorylation and degradation of IkappaBalpha (IkBa), the nuclear translocation of NF-kB p65 subunit, the DNA binding activity of NF-kB, and the NF-kB-dependent transcription of a luciferase reporter gene. Results. TNFalpha activated NF-kB through the classical pathway of IKK activation followed by IkBa phosphorylation and degradation. Peroxynitrite also activated NF-kB, but did so independently from IKK activation. When cells were pretreated with peroxynitrite before TNFa, NF-kB activation was abrogated, due to the abolition of IKK activation. In contrast, when peroxynitrite was added after TNFa, a long lasting hyperactivation of NF-kB was noted, dependent on a robust activation of IKK, followed by a durable degradation of IkBa. Similar conclusions were reached in other cell systems, including renal 293T cells and cardiac H9C2 cardiac cells. Conclusion. Oxidative stress exerts complex and opposite effects on NF-kB, depending on the condition. These preliminary observations provide new insights into the redox regulation of this critical transcription factor.

Bacterial flagellin triggers myocardial innate immune responses and acute contractile failure.

[1]Rolli J., [1]Levrand S., [2]Waeber B., [2]Feihl F., [1]Chioléro R., [1]Liaudet L.

Service de Médecine Intensive Adulte-CHUV[1], Division de Physiopathologie Clinique-CHUV[2]

Background. Septic shock is associated with severe cardiac dysfunction, whose mechanisms remain partly undefined. Recent data suggested that it might be triggered by the direct action of microorganisms and their products on the heart itself. We previously showed that flagellin, the protein monomer from bacterial flagella, is a potent activator of NF-κB-dependent pro-inflammatory signaling in cultured cardiomyocytes. In the present study, we investigated whether flagellin might induce such an inflammation in the heart in vivo and contribute to cardiac dysfunction.
Methods. Mice were injected intravenously with 1μg flagellin (30 min to 4h). The effects of flagellin were evaluated by its ability to activate NF-κB and downstream signaling. Expression of the flagellin receptor TLR5 was also investigated. Cardiac function was evaluated after 4h using a microtip pressure-volume (PV) catheter inserted into the left ventricle (LV).
Results. Flagellin activated NF-κB in cardiomyocytes in vitro and in vivo, and upregulated the transcription of TNFα and MIP-2. Flagellin also increased cardiac neutrophils recruitment. Flagellin induced significant increases in end-systolic and end-diastolic LV volumes, indicating cardiac dilation, and a significant reduction of the load-independent indices of LV systolic function (end-systolic PV relationship, ESPVR, and maximal elastance, Emax), indicating significant LV systolic dysfunction. In contrast, no change in the slope of the end-diastolic PV relationship (EDPVR) was noted.
Conclusion. Bacterial flagellin induces a prototypical inflammatory response in cardiomyocytes in vitro and in the myocardium in vivo. These effects are associated with a profound alteration of the LV systolic function in vivo, suggesting that flagellin may represent a critical mediator of cardiac dysfunction in septic shock.

EX VIVO CYTOTOXIC FUNCTION BY INFLUENZA SPECIFIC CD8 EFFECTOR T CELLS FROM HEALTHY HUMANS IN MEMORY PHASE

[1]Touvrey C., [1]Derré L., [2]Rufer N., [1]Romero P., [1]Speiser D.

Ludwig Institute for Cancer Research[1], CEPO[2]

The majority of influenza specific CD8 T cells in healthy adults are memory cells with strong proliferative capacity, and expression of the IL-7 receptor CD127 and the costimulatory molecules CD28 and CD27. However, other subsets of influenza specific T cells have different phenotypes and unknown functions. Here we show that up to ~20% of HLA-A*0201 / influenza matrix protein$_{58-66}$ specific T cells from healthy donors did not express CD127 and/or CD28. Granzyme B and perforin were frequently expressed by CD28$^-$ cells, suggesting that they may be effector cells. With a FACS based cytotoxicity assay we show that these cells are indeed capable to lyse target cells directly ex vivo without prior stimulation. Sequencing of TCR chains revealed that the response to this epitope was dominated by ~1-3 T cell clonotypes. Interestingly, identical clonotypes were found as memory and effector cells, demonstrating for the first time that T cell memory is maintained by clonotypes that persist simultaneously in multiple differentiation stages. The data suggest that efficient secondary responses against influenza virus may depend on both, rapid expansion of memory cells and immediate function by long term persisting cytotoxic effector cells.

Analysis of HIV-1 CA Residues under Positive Selective Pressure

[1]Ciuffi A., [1]Zhang K., [1]Martinez R., [1]Munoz M., [1]Telenti A.

Institute of Microbiology, CHUV[1]

Background. HIV-1 CA contains 231 amino acids defining two domain structures that are conserved across retroviruses: a N-terminal and a C-terminal domain connected by a flexible linker. Several CA functions and functional surfaces have been characterized by mutagenesis. The aim of the current study is to complete the characterization of CA by applying evolutionary genetics tools to identify amino acids under positive selection. This approach may identify key residues interacting with cellular partners or targeted by the immune system.

Methods. We analyzed 377 HIV CA sequences (125 from subtype B, 172 from subtype C and 80 from other subtypes). Maximum likelihood trees were built for each subtype using the HKY85 substitution model, and implemented in PHYML v2.4.4. with estimated ts/tv ratio and p-invar. Data were also analyzed using a star tree for comparison. Bayes Empirical Bayes analysis applied the M2a model to identify amino acids under positive selection. Residues under positive selective pressure were mutated, and the infectivity of the resulting viruses was tested in single-round assays.

Results. CA is under strong purifying selection (Ka/Ks=~0.03). However, 12 of 231 (5%) CA amino acids are under positive selection: I6 (β hairpin); L83, H87, and I91 (CypA loop); A14 and T148 (inter β hairpin-helix 1, and interdomain linker, possibly targeted by CTL); N120 and I124 (between helix 6 and 7); T171 (helix 8); N183 and T210 (helix9/turn, CA-CA interaction); G225 (CA/SP1 cleavage/fitness). We mutated each residue for the minor natural variant or an alanine residue. All viruses were infectious; viral infectivity varied from 0.74 to 1.71 fold the VSV-G pseudotyped HIVNL4-3 infectivity. Alanine mutagenesis resulted in lower infectiousness of viral particles than that of minor variant mutants, mean fold MFI (SD) 0.98 (0.19) and 1.34 (0.22), respectively, p=0.0025.

Conclusions. CA is a highly conserved protein under purifying selection. There are, however, a minority of variable amino acids that identify sites under selective pressure. Mutation at these sites leads to changes in viral fitness. Their delineation should serve to explore the interaction of CA with the host intrinsic, innate and acquired immunity.

Genome sequencing of Protochlamydia naegleriophila strain KNIC, a potential new agent of pneumonia.

[1]Bertelli C., [1]Collyn F., [1]Greub G.

Institute of Microbiology, CHUV[1]

Background and Objectives
Protochlamydia naegleriophila strain KNIC is a newly identified *Chlamydia*-related bacterium which role in pneumonia is supported by a recent case documented by real-time PCR and direct immunofluorescence. As no classical genetic manipulations can be performed on this obligate intracellular bacterium, genome sequencing is essential to identify virulence genes and better understand the biology and evolution of this emerging human pathogen.

Methods
Genome sequencing of *P. naegleriophila* strain KNIC was completed by two runs of Genome Sequencer 20 (GS20) at 454 Life Science Sequencing Center (Branford, USA). Assembly was then achieved with the GS *De Novo* Assembler. Finally, scaffolding for gap closure was initiated by using nucleotide (Mauve) and protein (BLAST) homology searches relying on the colinearity between *P. naegleriophila* strain KNIC and the published genome of Candidatus *Protochlamydia amoebophila* UWE25, its closest known relative.

Results and Discussion
Using the GS20 pyrosequencing approach, we obtained over 711'000 reads corresponding to 75 million bases that were assembled in 148 contigs containing almost the entire genome; 2'957'535 bp for an expected size of 3'000'000 bp. The accuracy exceeded 99.99% for nearly all bases (99.7%) whereas the overall coverage surpassed 25X, indicating a high quality assembly. Scaffolding strategy enabled to solve sixty gaps.
A preliminary annotation of the contigs revealed the presence of two systems critical for bacterial virulence: a type IV secretion system encoded by the *tra* operon and several genes encoding type III secretion system proteins. Many other virulence genes present along the genome of *P. amoebophila* strain KNIC further support its possible pathogenic role. We also identified genes encoding energy parasitism, i.e. exchanging ATP from the host cell with ADP from bacterial metabolism.
After completing the gap closure, genome evolution will be further investigated by identifying putative genomic islands and horizontal gene transfers. Moreover, complete reconstruction of metabolic pathways will be of major importance to understand the determinants of the strict intracellular lifestyle of this bacterium.

Peroxynitrite exerts complex and opposite effects on nuclear factor kappa B: a novel redox-based mechanism controlling cell signal transduction.

[1]Liaudet L., [1]Levrand S., [1]Rolli J., [2]Feihl F., [2]Waeber B.,

Service de Médecine Intensive Adulte-CHUV[1], Division de Physiopathologie Clinique-CHUV[2]

Background. Redox signaling refers to the ability of oxidants to modulate the activity of proteins involved in signal transduction. Redox-based mechanisms control critical functions, including apoptosis and the regulation of inflammation. A master regulator of apoptosis and inflammation is the transcription factor nuclear factor kappa B (NF-kB). NF-kB is classically activated by inflammatory mediators, but it is also suspected to be redox sensitive. However, the modes of interactions between oxidative stress and NF-kB are poorly defined. Here, we investigate the redox mechanisms controlling NF-kB activity in vitro. Method. NF-kB activation was evaluated in the lung epithelial cell line A549. Cells were stimulated with the classical NF-kB activator TNFalpha (TNFa), or with the potent oxidant peroxynitrite. NF-kB was assessed by the activation of the upstream kinase IKK, the phosphorylation and degradation of IkappaBalpha (IkBa), the nuclear translocation of NF-kB p65 subunit, the DNA binding activity of NF-kB, and the NF-kB-dependent transcription of a luciferase reporter gene. Results. TNFalpha activated NF-kB through the classical pathway of IKK activation followed by IkBa phosphorylation and degradation. Peroxynitrite also activated NF-kB, but did so independently from IKK activation. When cells were pretreated with peroxynitrite before TNFa, NF-kB activation was abrogated, due to the abolition of IKK activation. In contrast, when peroxynitrite was added after TNFa, a long lasting hyperactivation of NF-kB was noted, dependent on a robust activation of IKK, followed by a durable degradation of IkBa. Similar conclusions were reached in other cell systems, including renal 293T cells and cardiac H9C2 cardiac cells. Conclusion. Oxidative stress exerts complex and opposite effects on NF-kB, depending on the condition. These preliminary observations provide new insights into the redox regulation of this critical transcription factor.

Epidemiology of Severe Sepsis and Septic Shock in Lausanne

[1]Que Y.-A., [1]Oddo M., [2]Schaller M.-D., [1]Eggimann P., [1]Revelly J.-P., [1]Berger M., [1]Chioléro R., [1]Liaudet L.

Service de Médecine Intensive Adulte-CHUV[1], Service de Médecine Intensive Adulte-CHUVService de Médecine Intensive Adulte-CHUV[2]

Background. Despite recent improvements in its management, sepsis remains a major health issue, with a dismal prognosis. The incidence of sepsis is continually rising, implying an inexorable increase in the consumption of health care resources. **Objective.** Characterization of severe sepsis and septic shock epidemiology in Lausanne. **Design.** 4 year retrospective study (1st January 2001 to 31st December 2004). Patients transferred from and to primary hospitals were excluded. **Setting.** 14-bed medical intensive care unit. **Results.** From 2001 to 2004, a total of 322 patients (mean age 62.5 +/- 15.4, 66% male) were treated, 114 for severe sepsis (35%, mean age 58.2 +/- 16.1, 70% male) and 208 for septic shock (65%, mean age 63 +/- 14.9, 64% male). 44% of the infections were from pulmonary, 16% from abdominal, and 11% from urinary tract origin. Severity of infections varies among subgroups, with APACHE II scores ranging from 17.5 +/- 6.7 to 24 +/- 8.7 for patients with severe sepsis and septic shock respectively. In comparison with published studies, 28d mortality in Lausanne was rather low : 5.2% for severe sepsis and 33% for septic shock. During the 4y period, we observed a decrease in 28d mortality for all subgroups of patients, particularly among patients admitted for septic shock and APACHE II score > 25 (n= 112, 28d global mortality 42.8%, decreasing from 51.9% in 2001 to 31.2% in 2004). Interestingly, 35-40% of infection were due to gram-positive bacteria, Gram-negative bacteria being responsible for only 25-30% of infection. **Conclusion**. In Lausanne, mortality of severe sepsis patient is very low, whereas mortality of septic shock is lower than reported in the literature. Reasons for the decrease in the observed mortality is unknown and probably multi-factorial : implementation of early goal directed therapy, protective ventilation, uses of supra-physiologic doses of steroids and introduction of a closed unit. On the basis of these observations, we have launch a large scale prospective cohort study to better characterize the epidemiology of sepsis in our population and to improve our understanding of its pathophysiological mechanisms.

Outcomes of second line therapy after NNRTI failure for the treatment of HIV: The Swiss HIV Cohort Study

[1]Osih R., [2]Furrer H., [3]Bernasconi E., [4]Opravil M., [5]Battegay M., [6]Schmid P., [1]Cavassini M.

CHUV Service des Maladies Infectieuses[1], InselSpital Bern[2], Ospedal Civico Lugano[3], UniversitätsSpital Zürich[4], UniversitätsSpital Basel[5] , KantonsSpital St.Gallen[6],

BACKGROUND: Non-nucleoside reverse transcriptase inhibitors (NNRTI) have been used as first line agents in the treatment of HIV for the past 7 years, however, very few data exist on outcomes after failure of NNRTI-based regimens.

OBJECTIVES: to investigate the outcomes in patients registered in the Swiss HIV Cohort Study (SHCS) from 1998-2006 who were started on a new regimen after NNRTI failure .

METHODS: All patients who had received an NNRTI – based regimen as first line therapy and were reported to have failed as defined by specific codes recorded or a viral load (VL)>400 at the time of the change were reviewed. Demographic information, laboratory data and treatment history were collected. Outcomes of interest were VL<400 copies/ml at 24 and 48 weeks after starting a new regimen, and number of subsequent regimen switches over 2 years.

RESULTS: 951 patients started an NNRTI based first line regimen among which 47 (4.9%) had treatment failure (59.6% male, 61.7% Caucasian, 57.5% heterosexual acquisition of HIV). 34 of 40(85%) patients who had data available at 24 weeks and 27of 29(93.1%) at 48 weeks were suppressed. Of the 47 patients, 44(93.6%) patients received at least 1 PI, 33 (70.6%) received a boosted PI (BPI) and 11(23.4%) patients switched to a dual boosted PI regimen (DBPI), however, the choice of new regimen was not predictive of suppression (p=0.3 for both DBPI and BPI). 12 (27.9%) patients had switched therapy for any reason at 24 weeks but only one of them was on a DBPI at the time (p=0.4).

CONCLUSIONS: Change to a DBPI after failing an NNRTI-based regimen may be associated with fewer future regimen changes. This result warrants further studies with larger sample sizes to determine the impact of DBPI regimens in salvage therapy.

Outcomes of the use of Dual-boosted Protease Inhibitors in the Swiss HIV Cohort Study (SHCS)

[1]Osih R., [2]Gayet-Ageron A., [3]Battegay M., [4]Fux C., [5]Opravil M, [6]Bernasconi E., [1]Cavassini M., Swiss HIV Cohort Study

Centre Hospitalier Universitaire Vaudois et Université de Lausanne, Service des Maladies Infectieuses, Lausanne[1], Hopital Cantonal et Universitaire de Genève, Service des Maladies Infectieuses, Geneva[2], University of Basel, Medicine, Division of Infectious Diseases, Basel[3], Universitätsspital Bern, Klinik und Poliklinik für Infektiologie, Bern[4], University of Zürich, Department of Medicine, Division of Infectious Diseases, Zürich[5], Ospedale Civico, Department of Medicine, Division of Infectious Diseases, Lugano[6]

Introduction : Dual-boosted protease inhibitor regimens (DBPI) are often used in salvage therapy for HIV, despite not being recommended by treatment guidelines.
Objectives: To characterize patients who receive DBPI within the SHCS and evaluate treatment outcomes of these regimens.
Methods: Patients who received ritonavir with 2 other protease inhibitors within the SHCS from January 1996 to March 2007 were included. Demographic information, laboratory values, and treatment regimens used were extracted from a database. Logistic regression was used to study the likelihood of suppression (HIV RNA <400 copies/mL) within 6 months and Kaplan-Meier estimates were used for median time to suppression.
Results: 407 patients were identified, 295 (72.5%) were on DBPI for at least 6 months and 50.3% were still receiving DBPI at the most recent follow-up. Median duration of therapy was 2.2 [IQR, 1.2-3.9] years.. 239 (81%) were ever suppressed while on DBPI and 208 (70.5%) were suppressed within 24 weeks. The median time to suppression was 101 days (95% confidence interval 90-125) and the median number of past regimens was 6 [IQR, 3-8]. The main reasons for discontinuing the regimen were provider/patient preference (48.3%) and treatment failure (22.5%). Toxicity accounted for 15.8% of the treatment changes. Intravenous drug use and lopinavir in combination with amprenavir, saquinavir, atazanavir as well as atazanavir-saquinavir were associated with an increased likelihood of suppression within 6 months. In contrast, starting the DBPI regimen before the year 2000, higher RNA at cohort entry and at start of DBPI treatment were associated with a decreased likelihood of suppression.
Conclusion: Viral suppression within 6 months for patients on DBPI regimens is high and median time to suppression comparable to other regimens. There may be a place for DBPI regimens in the treatment of HIV, particularly in resource-poor settings where more expensive alternates are not available.

synovial inflammasome expression in rheumatoid arthritis and osteoarthritis is not linked to IL1 activation

Kolly L., Chobaz V., Busso N., So A.

Service of rheumatology - CHUV

Background: The inflammasome is a multiprotein complex that is responsible for the activation of caspases-1 and -5, leading to the processing and secretion of the pro-inflammatory cytokines IL-1β and IL-18. It has been implicated in numerous inflammatory diseases. In rheumatic diseases, its role in gout has recently been demonstrated, but its participation in rheumatoid arthritis (RA), a chronic auto-inflammatory disease, is unknown.

Objectives: To determine the expression of the known inflammasome components in synovial membranes from RA and from osteoarthritis (OA), a non-inflammatory rheumatic disease. To investigate the relationship between caspase-1 activation and IL-1β production. To assess this relationship in primary cultures of RA synoviocytes

Methods: Synovial biopsies from RA (n=9) and OA (n=11) patients were obtained from the patients undergoing joint surgery. In addition, RA synoviocytes from 3 different RA patients were purified. Synovial RNA was extracted for RT-PCR using NALP1-14 primers. Protein extracts were analyzed by western blot using NALP1, 3 and 12, ASC and caspase-1 antibodies. The levels of synovial caspase-1 and IL-1β were measured by ELISA. NALP3 immunohistochemistry was performed on selected RA and OA samples.

Results: At the mRNA level, the expression of NALPs was similar between RA and OA synovial tissues. This was confirmed at the protein level by western blotting of NALP1, NALP3, NALP12 and ASC. No difference in NALP-3 staining was observed by histochemistry between RA and OA. Caspase-1 levels (by ELISA) were significantly increased in RA versus OA samples ($p<0.04$) but active IL-1β levels were similar in RA compared to OA samples. Finally, no correlation was found between active caspase-1 and active IL-1β levels.

Conclusion: In RA, there is increased active caspase-1 in the synovium compared to OA. However, we did not find any differences in expression of the known inflammasome components (NALP1,3,12 and ASC) between RA versus OA. Finally, there was no correlation between active caspase-1 and active IL-1β levels. These findings suggest that caspase-1 is not responsible for activation of IL-1β in RA and that the inflammasome is not implicated in synovial IL-1β activation.

Growth Arrest-Specific Gene 6 product modulates innate immunity in sepsis

[1]Burnier L., [1]Sugamele R., [2]LeRoy D., [2]Roger T., [3]Fumeaux T., [4]Chanson M., [5]Rignault S., [6]Carmeliet P., [3]Pugin J., [5]Feihl F., [7]Borgel D., [8]Liaudet L., [8]Chioléro R., [1]Schapira M., [2]Calandra T., [1]Angelillo-Scherrer A.

Laboratoire central d'Hématologie, CHUV[1], Infectious Diseases Service, CHUV[2], Division of Medical Intensive Care, HUG, Genena[3], Laboratory of Clinical Investigation III, Department of Pediatrics, HUG, Geneva[4], Division of Clinical Physiopathology and Medical Teaching, CHUV[5], The Center for Transgene Technology & Gene Therapy, Flanders Interuniversity Institute for Biotechnology, Leuven, Belgium[6], Laboratoire d'Hématologie, Faculté de Pharmacie, Chatenay Malabry, France[7], Department of Intensive Care Medicine, CHUV[8]

Background: *Growth Arrest-Specific Gene 6* product (Gas6) is, like anticoagulant protein C, a vitamin K-dependent protein. Our aim was to determine whether Gas6 plays a role in sepsis.
Materials and Methods: We submitted mice lacking Gas6 ($Gas6^{-/-}$) or one of its receptors ($Axl^{-/-}$, $Tyro3^{-/-}$ or $Mertk^{-/-}$) to LPS-induced endotoxemia and peritonitis (cecal ligation and puncture (CLP) and inoculation of *E. coli*). In addition, we measured Gas6 or its soluble receptors in plasma of 8 volunteers that received LPS, 13 healthy subjects, 28 patients with severe sepsis, and 18 patients with non-infectious inflammatory diseases.
Results: Gas6 and its soluble receptor sAxl raised in mice models and TNF-α was more elevated in $Gas6^{-/-}$ mice than in wild-type (WT). Blood pressure and heart rate was lower in $Gas6^{-/-}$ mice compared to WT after LPS injection but not at baseline. Protein array showed that before and after LPS injection, titers of 62 cytokines were more elevated in plasma of $Gas6^{-/-}$ than WT mice. Endotoxemia-induced mortality was higher in $Gas6^{-/-}$, $Axl^{-/-}$, $Tyro3^{-/-}$ and $Mertk^{-/-}$ compared to WT mice and mortality subsequent to CLP was amplified in $Gas6^{-/-}$ mice. LPS-stimulated $Gas6^{-/-}$ macrophages produced more cytokines than WT macrophages. This production was dampened by recombinant Gas6. Phosphorylation of Akt in $Gas6^{-/-}$ macrophages was reduced, but p38 phosphorylation and NF-κB translocation were increased.
In human, Gas6 raised in plasma after LPS (2ng/kg). Gas6 and sAxl were higher in patients with severe sepsis than in healthy subjects or control patients, and there was a non-significant trend for higher Gas6 in the survival group. Gas6 level correlated with C-reactive protein levels.
Conclusions: Our data point to Gas6 as a major modulator of innate immunity and provide thereby novel insights into the mechanism of sepsis. Thus Gas6 and its receptors might constitute potential therapeutic targets for the development of new immunomodulating drugs.

Exploiting lymphatic transport and complement activation in nanoparticle vaccines

[1]Reddy S., [1]VanderVlies A., [1]Simeoni E., [1]O'neil C., [1]Kourtis I., [1]Swartz M., [1]Hubbell J.

Institute of Bioengineering - EPFL[1]

The development of vaccine technologies has emerged as a forefront healthcare initiative, especially technologies for use in developing countries, posing severe economic and logistic constraints. One must develop antigen targeting[1-5] and adjuvant schemes[6,7] that respectively facilitate delivery of antigen to dendritic cells (DCs) and elicit their activation. Here we engineered antigen-bearing nanoparticle vaccines with two novel features: lymph node-targeting and *in situ* complement activation. Following intradermal injection, interstitial flow transported our ultra-small nanoparticles (25 nm) highly efficiently into lymphatic capillaries and their draining lymph nodes, targeting half of the DCs there, whereas nanoparticles even 100 nm large were only 10% as efficient. Furthermore, the surface chemistry of our nanoparticles activated the complement cascade, which spontaneously generated a danger signal *in situ* and potently activated DCs. With the model antigen ovalbumin conjugated to the nanoparticles, we demonstrated humoral and cellular immunity in mice in a highly size-dependent and complement-dependent manner.

Effects of viral vaccine vectors on macrophage migration inhibitory factor (MIF) expression by myeloid cells

[1]Delaloye J., [1]Roger T., [1]KNAUPREYMOND M., [2]ESTEBAN M., [1]CALANDRA T.

Service des Maladies Infectieuses, CHUV[1], Centro Nacional de Biotecnología, CSIC, Ciudad Universitaria Cantoblanco, Madrid, Spain[2]

Background: MIF is constitutively expressed by immune cells and rapidly released after exposure to bacterial products. Once released MIF exerts powerful pro-inflammatory properties. In agreement, MIF has emerged to be an important effector molecule of innate immune host responses to bacterial and parasitic infections. Yet, the role of MIF in viral infections remains scarcely studied. Whilst poxviruses (

Attenuated Modified Ankara virus (MVA) poxvirus strain) and adenoviruses (Ad) are currently used for vaccine development against a broad spectrum of diseases, to which extent these viruses modulate innate immune responses remains largely unknown. The cytokine macrophage migration inhibitory factor (MIF) has emerged to be an important effector molecule of innate immune responses in some bacterial and parasitic infections. However, the role of MIF in viral infections, notably in vaccine vectors, remains largely uncharacterized.

Aim: To assess To assess the impact of poxvirus vectors on the host responses, we studied the role of MIF in host response to impact of MVA poxvirus (MVA and NYVAC) and adenovirusAd vaccine vectors on MIF expression byin human innate response elicited byimmuneTHP-1monocytic cells (PBMCs and THP-1 cells) and mouse bone marrow-derived dendritic cells dendritic cells(BMDCs) cells and in human THP-1 monocytic cells by measuring cytokines and chemokines in cell supernatantsto . We also analysedelucidate the role of the Toll-like-receptor (TLR) pathways in that response.

Method:

The human monocytic cell line THP-1 was differentiated or not with phorbol myristate acetate for 24h. BMDCs obtained from wild-type, TLR2 and MyD88 knock-out mice were produced from the bone-marrow precursors using granulocyte monocyte colony-stimulating factor. Undifferentiated and PMA-differentiated THP-1 cells and wild-type, MyD88-/- and TLR2-/- cells and BMDCs were infected with increasing doses (Multiplicity of infection (MOI) 1, 5, 20) of either MVA or and, or adenovirusAd (MOI 250, MOI 1000). MIF mRNA, MIF protein and MIF promoter activity were analyzed by real-time PCR (RT-PCR), ELISA, Western blot and transient transfection, respectively. For Apoptosis and necrosisapoptosis analysis of, THP-1 cells were analyzed by stained by Annexin V-FITC and propidium iodide staining and flow cytometry.6h and 24h after poxvirus stimulation and analyzed using a FACS Calibur.

The use of recombinant vaccinia viruses, such as the attenuated NYVAC and MVA poxvirus strains, for vaccine development against a broad spectrum of diseases, is promising. Whilst these vectors have been shown to be immunogenic and safe in humans, the nature of the innate immune responses triggered by these vectors in human cells remain largely unknown.

Results: Ad and

MVA , but not NYVAC, inducesd MIF release in a time- and dose-dependent manner in PMA-differentiated andby non-differentiated THP-1 cells. In THP-1 cells, MVA up-regulated Following MVA stimulation, MIF promoter activity and MIF mRNA levels and MIF promoter activity were upregulated by 12.5 to 21.5 fold, suggesting that MVA increased *MIF* gene transcription, suggesting that an active process involving transcription caused the production of MIF by THP-1 cells. However, Concomitantly, MVA induced an important death rate, particularly in differentiated THP-1 cells. Finally, MVA stimulated MIF release and up-regulated MIF mRNA expression by wild-type BMDCs, but not by TLR2-/- and MyD88-/- BMDCs.

analyse of cell survival demonstrated that MVA induced a greater amount of cell death (apoptosis and necrosis) than NYVAC, which might also contribute to MIF release.

Using , TLR2 and MyD88 deficient 2 and TLR4 to MVAobservedthat TLR2-MyD88 was essential for production of MIF after MVA stimulation, as is the case for cytokine production. Finally, we demonstrated that adenovirus vector induced MIF release in THP-1 cells and in BMDCs.

In mouse BMDCs, we observed that TLR2-MyD88 was essential for production of MIF after MVA stimulation, as is the case for cytokine production. Finally, we demonstrated that adenovirus vector also induced MIF release in THP-1 cells and in BMDCs.

wild-type, TLR2 and deficient TLR-2 and TLR4 knockout mouse dendritic cells to MVA stimulation to MVA, we further demonstrate that TLR2-MyD88 was essential for production of MIF after MVA stimulation, as is the case for cytokine production.

in poxvirus infection using KO murine strains

Conclusion: In THP-1 cells, MVA-induced MIF release may result from both MIF discharge from dying cells and an active process involving the up-regulation of *MIF* gene expression. In line with this hypothesis, sensing of MVA through the MyD88-TLR2 pathway was absolutely required to mediate MIF release by BMDCs. Altogether, our data indicate that MVA and Ad viral vaccine vectors induce MIF release by human and mouse innate immune cells, which may contribute to the development of immune responses against vaccines.

CD8 T cell differentiation and TCR repertoire dynamics in Epstein-Barr and Cytomegalovirus infected individuals

[1]Iancu E., [2]Bruyninx M., [1]Corthesy P., [2]Baumgaertner P., [2]Devevre E., [2]Romero P., [2]Speiser D., [1]Rufer N.

Division of Experimental Oncology, Multidisciplinary Oncology Center (CePO)[1], Division of Clinical Onco-Immunology, Ludwig Institute for Cancer Research, Lausanne Branch[2]

Protective immune responses against viral infections involve the selection and generation of differentiated antigen-specific CD8 T lymphocytes with potent effector functions, restricted clonal diversity and increased avidity of their T cell receptors (TCR). Since cytolytic T lymphocytes are generated against both persistent viral antigens and tumor antigens, our objective is to determine and compare the mechanisms by which the immune responses to chronic EBV and CMV infections can provide life long protection in healthy individuals, while immune responses against tumors like melanoma are spontaneously induced and enhanced by vaccination, but remain largely inefficient. We found that EBV-specific CD8 T lymphocytes consist primarily of early-differentiated effector memory cells (EM/CD28+), while CMV-specific T lymphocytes are mostly composed of differentiated effector cells (EMRA/CD28-). Although the proportions of these distinct T cell subsets are different among EBV- and CMV-specific T cells, ex-vivo analysis of several functionally relevant proteins (CD27, CD57, CD127, granzyme B and perforin) revealed that they follow the same pathway of T cell differentiation; from EM/CD28+ to EMRA/CD28-. Detailed TCR repertoire analysis of EBV and CMV-specific T cells revealed an initial restriction in the TCR diversity within the EM/CD28+ compartment with only limited restriction towards the highly differentiated EMRA/CD28- T cell subset. This is in contrast to the tumor antigen-specific T cells against Melan-A, in which TCR repertoire restriction occurs from the EM/CD28+ to the EM/CD28- compartment. Detailed ex-vivo TCR repertoire analysis showed that the EBV specific responses are dominated by several T cell clonotypes bearing the BV2 and BV4 chains. In contrast CMV specific responses are found to be highly restricted to two or three different TCR clonotypes, but with Vbeta chains that can vary from donor to donor (BV13, BV14, BV15). In order to determine the frequency of each clonotype and study the dynamics of dominance along the pathway of differentiation, we generated EBV and CMV specific T cell clones from the least differentiated (EM/CD28+) and from the most differentiated subsets (EMRA/CD28-). TCR repertoire analysis of in vitro generated clones showed differences in dominance patters between various TCR clonotypes. Specifically, while certain clonotypes were selected towards differentiation as their frequencies increased in the most differentiated subset, other clonotypes were lost with differentiation and were most dominant in the early differentiated compartment. We are currently investigating factors such as TCR affinity that may be involved in the selection of particular clonotypes towards differentiation, as well as whether these dominant clonotypes are found to persist over time during chronic infection. Altogether, combined analysis of T cell differentiation and TCR repertoire provide novel insights in the dynamics of T cell responses. Identifying the parameters associated with response generation and maintenance will reveal differences between viral- and tumor-specific immune responses. Ultimately, this will lead to the identification of correlates of immune protection in humans, which is crucial for the development of therapeutic vaccination against cancer.
Supported by the National Center of Competence in Research (NCCR) Molecular Oncology and the Swiss National Science Foundation grant (3100A0-105929).

PAR2 Signalling Promotes Myeloid Dendritic Cell Differentiation and Maturation

[1]Karababa M., [2]Miconnet I., [1]So A., [1]Busso N.

Laboratoire de rhumatologie-CHUV[1], IAL-CHUV[2]

Background: Protease activated receptor-2 (PAR2) belongs to the family of G-protein-coupled, seven-transmembrane-domain receptors that are activated by proteolytic cleavage of their N-terminus. Our recent data showed that PAR2 deficient mice have reduced severity of antigen induced arthritis and reduced immune response to BSA (1). Moreover, recent experiments have shown that PAR-2 activation is linked to dendritic cell (DC) development (2-3).

Aim: We therefore investigated the role of PAR2 in the differentiation and maturation steps of human monocyte- derived DC (DC) and the contribution of CCL19, a chemokine known to modulate DC activation, to these steps.

Methods/Results: The function of PAR2 was then investigated in human DC and showed that PAR2 signalling acts in the differentiation and maturation of human myeloid DCs. 1/ Inhibition of PAR2 activation blocked DCs differentiation from monocytes. 2/ PAR2 activation increased specific surface markers expression (CD80, CD86), markers of dendritic cell maturaton. 3/ T cell proliferation assayed in a mixed lymphocyte reaction using DCs activated via PAR2 activation was comparable to that obtained after CD40L treatment. 4/ Inhibition of PAR2 activation during CD40L treatment did not alter T cell proliferation in the MLR. 5/ Activation of PAR2 induced CCL19 up-regulation in human DC. 6/ CCL19 inhibition did not inhibit DC differentiation but induced the loss of PAR2-activated DC maturation.

Conclusion: The results of the current study suggest that PAR2 signalling regulates DC maturation independently of CD40L signalling, and that PAR2 plays a key role in the differentiation process of DCs from monocytes. CCL19 expression is PAR2-dependent and its inhibiton blocks DC maturation. The understanding of the mechanisms which mediate these effects may lead to the development of novel therapeutic targets in human immuno-inflammatory diseases.

Ref.:
(1) Busso et al., Arthritis Rheum., 2007.
(2) Fields et al., Am. J. Pathol., 2003.
(3) Csernok et al., Blood, 2006.

Crucial role of ASC in murine antigen-induced arthritis

[1]KARABABA M., [1]Kolly L., [2]Salvi R., [1]Dudler J., [3]DeSmedt T., [1]So A., [1]Busso N.

Laboratoire de rhumatologie-CHUV[1], , Laboratoire endocrinologie, diabétologie et métabolisme-CHUV[2], TopoTarget[3]

Background :
ASC (Apoptosis-associated Speck-like protein containing a CARD) is a bipartite protein that contains a pyrin domain belonging to the death domain members and a CARD (caspase-recruitement domain) which allows homotypic interaction with protein containing a CARD. ASC is involved in 3 main cellular processes : apoptosis, tumorigenesis and inflammation. For the latter, ASC has been shown to be a crucial component of a multiprotein complex involved in the activation of pro-inflammatory cytokines such as IL-1β, IL-18 and IL-33. This multiprotein complex called inflammasome is composed on a signal sensing component NLR for Nod-Like Receptor, in which NALPs (such as NALP3 and IPAF, two well investigated members) represent the major sub-family, the common adaptor ASC and a effector component such as caspase-1, an inflammatory caspase.

Purpose :
IL-1β is a crucial pro-inflammatory cytokine implicated in human and experimental arthritis. As the murine Antigen-Induced Arthritis (AIA) model is IL-1β dependent we wondered whether individual deficiencies for genes encoding inflammasome components can affect the onset and the severity of AIA.

Methods :
8-10 weeks old ASC-, IPAF- and NALP3-deficient mice in a C57/Bl6 background and their corresponding +/+ and/or +/- littermates were used in the AIA model. In AIA model, arthritis is induced by i.a. injection of mBSA in previously immunized mice. The severity of arthritis was assessed by technetium uptake measurement in knee, histological analysis of joints and dosage of an acute phase protein in the serum ; serum amyloid A (SAA) by ELISA. In protein extracts from the inflamed arthritic joint, the levels of active IL-1β, IL-6 and TNFα were measured by ELISA and active caspase-1 was determined by Western blotting. The effect of ASC deficiency was assessed on humoral and cell-mediated immune responses and on the levels of some Th1 and Th2 cytokines.

Results :
ASC deficiency induces the reduction of inflammation in the murine model of arthritis whereas NALP3 and IPAF KO mice do not. The reduction of inflammation is based on the significant reduction of 1/ technetium uptake ratio 2/ the level of SAA 3/ histological scoring of inflammation. The reduction of inflammation in ASC KO mice correlates with the significant reduction of active IL-1β levels, with no alteration of caspase-1 activation in inflamed joints. Moreover ASC deficiency does not alter humoral immune response as anti-mBSA antibodies levels are similar in both WT and KO sera. However, ASC-deficient T cells activation is altered as measured by thymidine incorporation and correlates with a reduction of Th1 cytokines production.

Conclusion :
ASC is important for the severity of the disease in the AIA murine model of arthritis an dis linked to IL-1β activation in a caspase-1 independent manner. ASC is also crucial for T cell activation and Th1 cytokine production.

MCV
Métabolisme et Cardiovasculaire

Diabetes and pre-diabetes are associated with cardiovascular risk factors and carotid/femoral intima-media thickness independently of markers of insul

[1]Faeh D., [1]Bovet P.

IUMSP[1]

Background
Impaired glucose regulation (IGR) is associated with detrimental cardiovascular outcomes such as cardiovascular disease risk factors (CVD risk factors) or intima-media thickness (IMT). Our aim was to examine whether these associations are mediated by body mass index (BMI), waist circumference (waist) or fasting serum insulin (insulin) in a population in the African region.

Methods
Major CVD risk factors (systolic blood pressure, smoking, LDL-cholesterol, HDL-cholesterol,) were measured in a random sample of adults aged 25-64 in the Seychelles (n=1255, participation rate: 80.2%). According to the criteria of the American Diabetes Association, IGR was divided in four ordered categories: 1) normal fasting glucose (NFG), 2) impaired fasting glucose (IFG) and normal glucose tolerance (IFG/NGT), 3) IFG and impaired glucose tolerance (IFG/IGT), and 4) diabetes mellitus (DM). Carotid and femoral IMT was assessed by ultrasound (n=496).

Results
Age-adjusted levels of the major CVD risk factors worsened gradually across IGR categories (NFG < IFG/NGT < IFG/IGT < DM), particularly HDL-cholesterol and blood pressure (p for trend <0.001). These relationships were marginally attenuated upon further adjustment for waist, BMI or insulin (whether considered alone or combined) and most of these relationships remained significant. With regards to IMT, the association was null with IFG/NGT, weak with IFG/IGT and stronger with DM (all more markedly at femoral than carotid levels). The associations between IMT and IFG/IGT or DM (adjusted by age and major CVD risk factors) decreased only marginally upon further adjustment for BMI, waist or insulin. Further adjustment for family history of diabetes did not alter the results.

Conclusions
We found graded relationships between IGR categories and both major CVD risk factors and carotid/femoral IMT. These relationships were only partly accounted for by BMI, waist and insulin. This suggests that increased CVD-risk associated with IGR is also mediated by factors other than the considered markers of adiposity and insulin resistance. The results also imply that IGR and associated major CVD risk factors should be systematically screened and appropriately managed.

Blood microparticles in erythrocyte concentrates

[1]Rubin O., [1]Crettaz D., [1]Tissot J.-D.

Service Régional de Transfusion Sanguine[1]

Among several components, circulating blood contains small phospholipids vesicles of less than 1 micrometer in size called microparticles (MPs). Those MPs are released from different cells such as red and white blood cells or platelets. MPs are heterogeneous, and vary in size, phospholipids and protein composition. MPs are involved in a broad spectrum of biological activities such as hemostasis. Furthermore, an elevated level of MPs in plasma has been demonstrated in numerous diseases.

Despite their implication in numerous physiopathological processes, only few studies are available on MPs in blood products. The aim of our studies was to have a better comprehension of MPs. Therefore, quantitative and qualitative experiments using either flow cytometry, electronic microscopy or proteomics were performed on erythrocytes concentrates (EC) during storage from day 0 to day 42.

Shortly, preliminary results revealed an increase of MPs in erythrocyte concentrates during storage at 4°C. The number of MPs in the supernatants of EC of less than 10 days was 333 /μL $\pm$ 168 (mean $\pm$ SD), whereas the number after 42 days was 2186 / μL $\pm$ 1924. Small differences of protein profiles between samples of MPs and erythrocytes were observed. Moreover, blood group system was shown to be present on erythrocyte microparticles membrane.

These observation are of particular interest for transfusion medicine.

Ral GTPases as potential regulators of insulin secretion

[1]Ljubicic S., [1]Bezzi P., [1]Regazzi R.

Department of Cellular Biology and Morphology, UNIL[1]

Background and Aims: RalA and RalB form a special branch within the Ras monomeric GTPase family and have been implicated in the modulation of a variety of cellular processes including exocytosis and endocytosis. The main goal of this project was to investigate the possible role of Ral GTPases in the control of insulin release from pancreatic beta cells.

Material and Methods: The experiments were performed in the insulin-secreting cell lines INS1E and MIN6B1. Expression of Ral GTPases was measured by RT-PCR and Western Blotting analysis. Activation of Ral GTPases in living cells was assessed by Fluorescence Resonance Energy Transfer (FRET) using a construct including a YFP-labeled RalA and a CFP-labeled Ral effector. The role of Ral GTPases in insulin exocytosis was assessed by reducing the endogenous levels of each of these GTPases by RNA interference.

Results: We found that INS1E and MIN6 cells express both RalA and RalB. Incubation of these cells with 30 mM potassium or 20 mM glucose, 0.01 mM Forskolin and 0.1 mM IBMX led to a rapid activation of Ral GTPases. This activation was prevented by the addition of the Ca2+ channel blocker nifedipine (10 μM) suggesting that it is probably a consequence of the increase in cytoplasmic free Ca2+ concentration following depolarization of beta cell membrane. Reduction of the endogenous level of RalA or RalB by RNA interference resulted in a significant decrease in secretagogue-induced insulin release, indicating that these small GTPases are required for beta cell exocytosis. However, excessive amounts of Ral GTPases were also deleterious for insulin secretion. In fact, overexpression of wild type or constitutively active mutants of Ral GTPases led to a reduction in insulin exocytosis. This suggests that the level of Ral GTPases has to be maintained in a narrow range to insure an optimal secretory response.

Conclusion: Ral GTPases are activated by insulin secretagogues and participate in the control of insulin exocytosis. Future experiments will need to elucidate the mechanisms leading to the activation of these GTPases and to precisely define their mode of action.

Alteration in microRNA expression contributes to cytokine-induced pancreatic b-cell dysfunction

Roggli E., Regazzi R.

Dpt de Biologie Cellulaire et Morphologie

In Type I diabetes mellitus pancreatic β-cells are the target of an autoimmune reaction and are exposed to proinflammatory cytokines such as IL-1β, TNFα and IFNγ released by activated macrophages and T cells. Chronic exposure to cytokines has a detrimental impact on pancreatic β-cell functions leading to reduction in insulin content, defects in insulin secretion and sensitization toward apoptosis. In this study, we investigated the possible involvement in this phenomenon of microRNAs, a recently discovered class of non-coding RNAs that regulate gene expression by sequence-specific inhibition of target mRNA translation. Global expression profiling of microRNAs in the mouse insulin-secreting cell line MIN6 exposed to IL-1β or to a mixture of cytokines including IL-1β, TNFα and IFNγ for 24 hours revealed a selective alteration in the level of a group of microRNAs. These changes in microRNA expression were confirmed by quantitative Real time-PCR measurements both in the insulin-producing cell lines MIN6 and INS-1E and in isolated rat and human pancreatic islets. Changes in microRNA expression that mimic the effect of IL-1β were found to reproduce the defects in insulin synthesis, insulin secretion and apoptosis observed in β-cells chronically exposed to the cytokines. Taken together, our findings suggest that at least part of the deleterious effects of cytokines on β-cell functions may be attributed to alterations in the level of specific microRNAs.

The stem cell antigen-1 (Sca-1) preserves cardiac integrity by modulating the number of cardiac resident Nkx2.5+ cells.

[1]Rosenblatt-Velin N., [1]Ogay S., [1]Felley A., [1]Pedrazzini T.

Department of medecine-CHUV[1]

Sca-1 (Ly 6a) is a glycosyl phosphatidylinositol (GPI)-anchored protein expressed on hematopoietic precurseurs as well as on differentiated cells. In the neonatal and adult mouse hearts, high number of Sca-1$^+$ cells was detected. We showed also that cardiac precursor cells (CPCs) expressed during their differentiation into cardiomyocytes Sca-1. Despite the characterisation of the cardiac Sca-1$^+$ cells, the real function of Sca-1 in the heart remains unknown. Using mice lacking stem cell antigen-1 (Sca-1) protein expression, we investigated the role of Sca-1 in maintaining cardiac integrity.

Sca-1-deficient mice develop with ageing a dilated cardiomyopathy, characterized 4 weeks after birth by a decrease of the left ventricular thickness and 18 weeks after birth by an enlargement of the left ventricular diameter. The fractions of shortening and of ejection of the Sca-1 deficient hearts were significantly decreased compared to values measured in control hearts at the same age. No fibrosis was detected in the Sca-1 deficient dilated hearts. Using Taqman analysis, we detected no upregulation of genes involved in hypertrophy (ANF, beta MHC).

These results showed that cardiac function was significantly affected in Sca-1 knockouts suggesting that Sca-1 is required for normal cardiac function. Thus, we hypothetized that Sca-1 is involved into heart regeneration after birth via regulation of CPC number or/and cardiomyocyte differentiation. Non-myocyte cells (NMCs), previously shown to contain CPCs able to differentiate into cardiomyocytes, were isolated from Sca-1 deficient hearts. Sca-1 deficient NMCs showed the same capacity than control NMCs to differentiate into cardiomyocytes. The number of CPCs was evaluated *in vivo* by determining the number of **Nkx2.5$^+$ α-actinin$^-$** cells. The number of **Nkx2.5$^+$ α-actinin$^-$** cells is decreased in neonatal Sca-1 deficient hearts compared to control hearts. This is also the case for the number of non-myocyte cells which were isolated from the hearts of 4 week-old Sca-1 deficient mice (3 time less cells compared to the number isolated from the hearts of control mice). Thus, we investigated whether the decreased number of Sca-1 NMCs is due to a deficient cell proliferation. Using thymidine incorporation, we observed an increased cell proliferation in neonatal Sca-1 deficient NMCs compared to this measured in control hearts.

Finally, our results showed that the function of Sca-1 in the heart is essential to preserve cardiac integrity. Sca-1 seems not to be involved in the differentiation of CPCs into cardiomyocytes. However, the absence of Sca-1 expression leads to a reduced number of **Nkx2.5$^+$ α-actinin$^-$** cells. Whether, this is due to accelerated differentiation of CPCs into cardiomyocytes or to increased apoptosis of cardiomyocytes remains to be determined.

Acute renal failure : can renal function outcome be predicted by I-123-hippuran (OIH) renography ?

[1]Boubaker A., [1]Allenbach G., [2]Berwert L., [3]Venetz J.-P., [1]BischofDelaloye A.

Dpt of Nuclear Medicine[1], Dpt of Nephrology[2], CTO[3]

Objective : To determine if renal function measured during I-123-OIH renography can predict renal function recovery in patients with acute renal failure (ARF).
Material and Methods : We retrospectively reviewed the results of I-123-OIH renography in 31 patients (6 F, 66 M) aged 34-82 y (63±15 y) addressed for evaluation of the potential of renal function recovery. ARF was due to post-surgical complications (n=7), septic shock (n=8), heart failure (n=9), renal vascular disease (n=2), and tubulointerstitial disorders (n=5). One patient was examined twice. Individual renal function was measured during I-123-OIH renography by an accumulation index (AI) defined as the percentage of injected activity extracted from 30 to 90 sec after heart peak activity. Global AI was obtained by adding left and right AI. Effective renal plasma flow (ERPF) was obtained using the single blood sample method at 44min pi according to Tauxe.
Results : Among 31 patients, 11 recovered from ARF (9 normal, 2 reduced renal function) and 20 did not recover (4 deaths, 16 end-stage renal failure). Age and serum creatinine at the time of examination were comparable in both groups. Global AI and ERPF were higher in patients who recovered when compared to patients who developed progressive renal failure ($p<0.001$, and $p=0.002$ respectively).

	Renal function recovery		***End-stage renal failure***	
	n=11		***n=20***	
Global AI	11.1±2.5	7.7-16.9	4.8±2.6	1.2-10.2
ERPF	185±54	120-258	115±50	21-228
Serum creatinine	434±230	170-905	451±191	146-858
Age	65±17	32-84	62±15	34-82

Conclusions : In patients with acute renal failure, we observed that renal function measured during I-123-OIH renography was significantly higher in patients who recovered when compared to those who developed progressive renal failure. It is a simple method that may provide valuable information for further patient management.

Activation of the Signal Transducer and Activator of Transcription 3 within the embryonic heart in response to anoxia and reoxygenation

[1]PEDRETTI S., [1]GARDIER S., [1]RADDATZ E.

Department of Physiology[1]

Background: Involvement of the *Signal Transducer and Activator of Transcription 3* (STAT3) in the response of the embryonic/fetal heart to oxygen deprivation and reoxygenation remains unknown. We sought to assess STAT3 phosphorylation in atria (A), ventricle (V) and outflow tract (OT) under basal conditions, anoxia-reoxygenation and after a severe oxidative stress.
Materials and methods: Total and phosphorylated forms of STAT3 were determined in A, V and OT of hearts isolated from 4-day-old chick embryos using western immunoblotting. This was done under basal conditions, anoxia (30min)-reoxygenation (60min) and after exposure to H_2O_2 (1mM, 1h). Beating rate of A, V and OT was also measured.
Results: Under basal conditions, although total STAT3 was twofold higher in OT than in A and V, level of STAT3 phosphorylation was the highest in A (twofold). In V, STAT3 phosphorylation increased upon reoxygenation and peaked fourfold after 60min. Exposure to H_2O_2 increased STAT3 phosphorylation in V (twofold) but had no effect in A and OT. After exposure to H_2O_2 atrial activity persisted in 50% of the hearts whereas atrioventricular propagation was preserved in 25% only.
Conclusion: These findings indicate that in the developing heart, STAT3 is inhomogeneously distributed and activated in response to anoxia-reoxygenation and severe oxidant stress. The tolerance of the atrial pacemaker to oxidative stress might be associated with the high level of STAT3 phosphorylation.
Supported by the SNSF n°3100A0-105901

Spleen derived vascular progenitor cell transfer restores metabolic and vascular insulin sensitivity in high-fat diet insulin resistant mice

[1]Bloch J., [1]Schwab M., [1]Duplain H., [1]Dessen P., [1]Mathieu C., [1]Monney A., [1]Nicod P., [1]Sartori C., [1]Scherrer U.

Département de médecine interne-CHUV[1]

BACKGROUND
Type 2 diabetes and insulin resistance are reaching epidemic proportions worldwide. Despite much progress in the field, the underlying mechanisms of insulin resistance remain incompletely understood. There is increasing evidence that endothelial dysfunction (related to defective nitric oxide synthesis/bioavailability) not only contributes to the cardiovascular complications associated with insulin resistance, but also contributes to metabolic insulin resistance, because it leads to impaired insulin stimulation of blood flow and substrate delivery to skeletal muscle tissue.
Circulating endothelial progenitor cells (EPC) play a role in endothelial repair and function. A decreased EPC number and/or function are a marker of endothelial dysfunction, a defect that can be restored by administration of functional EPC. Diabetes and insulin resistance are associated with a decreased number and dysfunctional EPC, but it is not clear whether this is a cause or merely a consequence of the disease.

HYPOTHESIS
We hypothesized that transfer of functional EPC's improves metabolic and vascular insulin sensitivity in insulin resistant high-fat diet fed mice.

METHODS
Six weeks old C57/Bl6 mice were put on a high-fat diet (UAR, France) for 8 weeks. 4 and 6 weeks after the start of the diet, mice received an i.v. injection of 200 Mio vascular progenitor cells in 500 microL normal saline, or vehicle. The cells were prepared by extracting the monocytic fraction from spleens of 6 weeks old C57/Bl6 mice. 2 weeks after the second injection, we assessed insulin sensitivity (intraperitoneal insulin injection, 0.5U/kg). To gain insigth into underlying mechanisms, in separate groups of mice, we measured insulin stimulation of muscle blood flow during euglycemic hyperinsulinemic clamp studies, and we studied basal and insulin-stimulated glucose uptake in skeletal muscle in vitro.

RESULTS :
The major new findings were that vascular progenitor cell transfer markedly improved both metabolic and vascular insulin sensitivity in insulin-resistant high-fat diet fed mice. The insulin-induced decrease in glycemia was more than twice as large in EPC-treated than in vehicle treated high-fat diet fed mice (decrease from basal glycemia 15 min after insulin injection, -26.1±3.0% vs -10.8±4.2%, P=0.012). During the hyperinsulinemic clamp studies, the insulin-induced stimulation of skeletal muscle blood flow was more than 4 times larger in the EPC-treated than in the vehicle treated high fat diet fed mice (95.4±22.1% vs 22.4±9.7% P>0.01). The basal and insulin stimulated glucose uptake in isolated muscle in vitro was similar in the two groups (P= 0.97).

CONCLUSION
Here we show that heterologous transfer of circulating vascular progenitor cells markedly improves insulin sensitivity in insulin resistant mice. This favorable metabolic effect appears to be related, at least in part, to restoration of the endothelium-dependent vasodilation and substrate delivery in skeletal muscle tissue. These data provide the first evidence that vascular progenitor cell transfer has favorable effects on glucose homeostasis.

Therapeutic Non Adherence Is The First Precipitating Factor For Acute Hyperglycemic Crises

[1]Nguyen S., [2]Waeber G., [3]Schaller M.-D., [4]Trueb L., [1]Ruiz J.

Dept. of Endocrinology, Diabetology and Metabolism, CHUV[1], Dept. of Internal Medicine, CHUV[2], Dept. of Intensive care, CHUV[3], Dept. of Emergency Medicine[4]

Introduction: Diabetes mellitus affects about 8% of the adult population. Diabetic keto-acidosis (DKA) and the hyperglycemic hyperosmolar state (HHS) are the most serious acute complications of diabetes. They are frequent within the diabetic population and tend to increase with the growing diabetes pandemia. These acute complications remain associated with a high mortality rate (<5% for DKA and 15% for HHS) despite an optimal care. The aim of the study was to analyze the precipitating factors, complications, treatment, length of stay (LOS) and mortality of these hyperglycemic crises in the university hospital of Lausanne.

Methods: This study describes a retrospective analysis of 101 patients admitted for DKA, HHS or both in the department of Internal Medicine (Emergency Room, Intensive Care Unit, Ward) between 1995 and 2006. The following parameters were assessed: precipitating factors, complications, length of stay, treatment, mortality. The acute hyperglycemic crises were defined according to the 2004 ADA criteria, i.e. **DKA** as a plasma glucose ≥ 14 mmol/L, an arterial pH≤7,30 with the presence of either blood or urine ketones; **HHS** as a plasma glucose ≥ 33,3 mmol/L together with an effective serum osmolality ≥ 320mOsm/kg. We defined **mixed DKA–HHS crises** as the combination of both.

Results: Mean age of the study population was 54 (37,5–76,5) years, 53% were males. Sixty-two percent of cases presented DKA, 22% HHS and 16% had a mixed (DKA and HHS) at the admission. The main precipitating factors were non adherence (42%), infections (26%), inaugural diabetes (18%), idiopathic (9%) and cardiovascular (7%). Non compliant patients had more DKA than other type of hyperglycemic crises (29.7% vs. 11.9%, OR=1.71, p=0.038), as did type 1 diabetics (38.1% vs. 6%, OR=4.49, p=0.001). The median LOS was 9 (6-14) days, type 2 diabetic patients staying longer on the ward than type 1 diabetics (9 vs. 3 days, p<0.0001) and in hospital (12 vs.7 days, p<0.0001). DKA patients had a shorter median hospital LOS than other patients (7 vs. 10 days, p=0.037). In summer, patients presented a higher frequency of HHS compared to DKA (OR=2.81, p<0.000). In-hospital mortality was the highest in mixed DKA-HHS (12.5%), followed by DKA (8.1%) and HHS (4.6%). Older age was a predictive factor for mortality (77 vs. 53, p=0.011). Consultation by a diabetes team was associated with much lower mortality rates (4.5% vs. 66.7%, OR=0.09, p<0.0001). Multivariate analyses show that consultation by a diabetes team reduces significantly mortality rate (p<0.0001). Older age remained predictive of mortality on multivariate analyses (p<0.0001).

Conclusions: Patient's non adherence with their diabetes treatment is the major precipitating factor for DKA, HHS and mixed DKA-HHS crises, which was never previously described in HHS and mixed DKA-HHS crises. We can observe a shift in the distribution of the precipitating factors, which were previously outclassed by infections. Mortality was highest in the mixed DKA-HHS crises group, a situation that can be accounted for by the greater metabolic unbalance in this group. We also highlight that a consultation by a diabetes team highly decreases these mortality rates. Thus, we suggest that diabetic patients' education be reinforced and should also be screened at the admission in order to help prevent diabetic hyperglycemic crises.

Immunohistological analysis of Notch signaling in the heart

[1]Lepore M., [1]Nemir M., [1]Pedrazzini T.

CHUV[1]

The Notch signaling is important for development of most organs in metazoans. In adult organisms, it plays a crucial role in the activation of stem cells in tissue regeneration. In mammals, Notch signaling is mediated by four Notch receptors (Notch1-4) and five ligands (Jagged1,2, Delta-like1, 3 and 4). Both ligands and receptors are single-pass transmembrane proteins. Ligand-receptor interaction on adjacent cells leads to proteolytic cleavage of the receptor, which releases the intracellular domain (NIC) that enters the nucleus and activates transcription of target genes.
In our laboratory, we found that Notch1 regulates cardiomyocyte differentiation and cardiac remodeling in vivo (see poster by Nemir et al.). To further understand Notch1 signaling in the heart, we performed immunofluorescence staining using anti-NIC antibody to detect Notch1 activation in cardiac tissue and in cultured cardiac cells. In the heart, Notch1 is activated predominantly in non-myocyte cells (NMCs). NIC-positive NMCs express GATA4 or NKx2.5 suggesting that Notch1 activation occurs in cells that represent cardiac precursor cells (CPCs). Jagged1 is the major ligand of Notch1 in the adult heart. Cardiomyocytes express Jagged1 on the plasma membrane supporting the idea that activation of Notch1 in NMCs may be mediated by a direct interaction with adjacent Jagged1-expressing cardiomyocytes.
In vitro, when cultured in proliferation conditions, most NMCs displayed intense NIC staining and the number of NIC-positive cells expressing Nkx2.5 increased with time. When cultures were shifted to differentiation conditions, we observed a decrease in the number of NIC-positive cells. Differentiated alfa-sarcomeric actinin-positive cardiomyocytes showed very low levels of or no NIC staining.
In conclusion: Notch1 signaling pathway is activated in cardiac cells both in vitro and in vivo. Notch1 activation occurs predominantly in undifferentiated cells and is reduced in mature cells. These results are consistent with the idea that Notch1 plays a role in proliferation and maintenance of the CPCs population.

Adrenal Gland Stimulation in Cyclists After Injection of Synthetic ACTH (Synacthen®). Effects on Hormones Profile, Physical Performance and Perceived

[1]Baume N., [2]Steel G., [3]Edwards T., [4]Thorstensen E., [5]Miller B.

Laboratoire suisse d'Analyse du Dopage[1], Drug Free Sport New Zealand[2], Adidas Sports Medicine Centre, Auckland[3], The Liggins Institute, University of Auckland[4], Department of Health and Exercise Science, Colorado State University[5]

The effect of a single intramuscular (IM) dose of synthetic ACTH (Synacthen®) on performance and perceived exertion was studied in 8 healthy trained cyclists. Plasma and urine hormones were quantified to investigate potential profiles alterations after treatment. All subjects completed 2 exercise sessions of 2 consecutive days; one with Synacthen® (TX) and the other with a placebo (PLA) injection on the first day of the sessions. Performance was assessed throughout a 20 km time trial (TT) after a 90-min fatigue period on day 1 and without fatigue on day 2. Plasma cortisol, dehydroepiandrosterone (DHEA), androstenedione (Adione), free testosterone and ACTH concentrations were measured during the course of the exercise bouts as well as the rate of perceived exertion (RPE). Basal plasma hormones did not differ significantly between PLA and TX groups before and 24 hours after the IM injection ($p>0.05$). After TX injection, ACTH peaked at 30min and hormone profiles were significantly different compared to the PLA trial ($p<0.001$). RPE increased significantly in both groups as the exercise sessions progressed ($p<0.001$) but was not influenced by treatment. The time to completion of the TT was not affected on both days by Synacthen® treatment. These results suggest that a single IM injection of synthetic ACTH might not be considered as an effective doping agent to improve either acute or subsequent cycling performance, or to decrease perceived exertion. In addition, glucocorticoids and androgens quantified in urine did not show a typical profile reinforcing the difficulty for ATCH abuse detection.

Dietary Potassium Supplementation Normalizes the Impaired Endothelium-Dependent Vasodilatation Independently of Blood Pressure in DOCA/Salt Mice

[1]Schäfer S.C. †, [2]Wang Q. †, [1]Abulker C. †, [2]Wyss J.C., [2]Golshayan D., [2]Burnier M., [2]Lehr HA.
(† equal contribution)

Instituts de Pathologie[1] et Institut de Nephrologie[2], CHUV, Lausanne

Background: We reported previously that one-renin gene mice receiving deoxycorticosterone acetate (DOCA) and salt develop hypokalemia, cardiac and renal hypertrophy, perivascular fibrosis, and cardiac dysfunction in the absence of hypertension. Correction of hypokalemia prevents DOCA/salt induced cardiac and renal hypertrophy and cardiac dysfunction. In this study, we assessed the impact of DOCA /salt and hypokalemia on endothelium function.

Methods: DOCA was administered subcutaneously in uninephrectomized C57BL6/J mice together with 1% NaCl in the drinking water. Five weeks later, one group of DOCA/salt mice received 0.4%KCl in drinking fluid for 3 weeks. Control animals were uninephrectomized and received tap water. Eight weeks later, endothelial-dependent and –independent vasodilatation in response to acetylcholine (ACh, 10^{-7} to 10^{-5} mM, EC-dependent) and to S-nitroso-N-acetyl-D,L-penicillamine (SNAP, 10^{-5} mM, EC-independent) were measured in precapillary arterioles (20-60µm internal diameter) of striated dorsal skin muscle using dorsal skin fold chamber technique in awake animals. Blood pressure (BP) and heart rate (HR) were recorded intra-arterially in conscious mice.

Results:

Group (n)	Basal diameter (mm)	ACh 10^{-5} M (%)	SNAP 10^{-5} M (%)	Fraction ACh to $SNAP_{max}$ (%)	MBP (mmHg)	Serum K^+ (mM)
Tap (4)	37 ± 4	13 ± 3	14 ± 3	92 ± 8	116 ± 3	4.4 ± 0.2
DOCA/salt (7)	43 ± 4	4 ± 2 *	7 ± 1*	34 ± 29*	110 ± 4	3.3 ± 0.1**
DOCA/salt+KCl(4)	36 ± 1	10 ± 2	11 ± 3	104 ± 17	110 ± 5	4.4 ± 0.2

Data are mean ± SEM, * $p<0.05$ and ** $p<0.01$ DOCA/salt vs DOCA/salt + KCl group and tap.

Conclusions: An excess of mineralocorticoids and salt impairs endothelial-dependent vasodilatation in mice without hypertension. In this model, correction of hypokalemia normalizes the endothelial dysfunction suggesting that hypokalemia may mediate the mineralocorticoid/salt-induced impaired endothelial dysfunction. This provides additional evidence for a favourable effect of potassium in cardiovascular prevention.

PREVALENCE, AWARENESS, TREATMENT AND CONTROL OF HYPERTENSION IN A SWISS GENERAL POPULATION: THE COLAUS STUDY

[1]Danon-Hersch N., [2]Marques-Vidal P., [1]Bovet P., [1]Chiolero A., [1]Paccaud F., [3]Pécoud A., [4]Hayoz D., [5]Mooser V., [6]Waeber G., [6]Vollenweider P.

Institute of Social and Preventive Medicine (IUMSP)[1], Institute of Social and Preventive Medicine (IUMSP) and Cardiomet, University Hospital (CHUV)[2], Medical Outpatient Clinic, University of Lausanne[3], Department of Medicine, Vascular Medicine, University Hospital (CHUV)[4], Medical Genetics, GlaxoSmithKline, Philadelphia, Pennsylvania, USA[5], Department of Medicine, University Hospital (CHUV)[6]

Objective: To assess the prevalence levels of awareness, treatment and control of hypertension and associated factors in Switzerland.

Methods: Population-based cross-sectional study of 6,182 subjects (52.5% women) aged 35-75 years living in Lausanne, Switzerland. Hypertension was defined as blood pressure ≥140/90 mm Hg or current antihypertensive medication.

Results: The overall prevalence of hypertension was 36% (95% CI: 35-38%). Among hypertensive participants, 63% were aware of having hypertension. Among aware hypertensives, 78% were treated, and among treated hypertensives 48% were controlled (BP <140/90 mmHg). In multivariate analysis, prevalence of hypertension was associated with older age, male gender, low educational level, high alcohol intake, awareness of diabetes, awareness of dyslipidaemia, obesity and parental history of myocardial infarction (MI). Awareness of hypertension was associated with older age, female gender, awareness of diabetes, awareness of dyslipidaemia, obesity and parental history of MI. Control was associated with younger age, higher educational level and no alcohol intake. Alone or in combination, sartans were the most often prescribed antihypertensive medication category (41%), followed by diuretics, beta-blockers, ACE inhibitors and calcium channel blockers. Only 31% of treated hypertensives were taking ≥2 antihypertensive medications.

Conclusion: Although more than half of the participants with hypertension were aware of being hypertensive and more than three quarters of them received a pharmacological treatment, less than half of those treated were adequately controlled. Treated hypertensive subjects should be followed up more closely.

Flexible, Intensive Insulin Therapy in Patients with Type 1 Diabetes: Longterm Effects on Metabolic Control, Quality of Life, Locus of Control and Dia

[1]Puder J., [2]Falconnier C., [2]Keller U., [2]Moriconi N., [2]Gessler A., [1]Ruiz J.

Department of Diabetes, Endocrinology and Metabolism, University Hospital of Lausanne, Switzerland[1], Division of Endocrinology, Diabetes and, Clinical Nutrition, University Hospital of Basel[2]

Background/Introduction
Few longterm data exist on the metabolic and psychological effects of flexible intensive insulin therapy (FIT) in unselected populations of type 1 diabetic patients.

Methods:
Between April 2002 and April 2004 we prospectively included 45 of a total of 47 participants (96%) of 5 consecutive FIT group courses performed at the Divison of Diabetes, Endocrinology and Clinical Nutrition at the University Hospital of Basel. Outcome measures included HbA1c, frequency of severe hypoglycemia, quality of life (Diabetes quality of life questionnaire, DQoL), locus of control (IPC-9 questionnaire) and diabetes knowledge (Diabetes-Knowledge Test Type 1, DWT) and were tested before and 1, 6 and 18 months after completion of the FIT course.

Results:
All participants were type 1 diabetic patients, 21 (47%) were females. Their age ranged between 18-74 years (median 41 yrs) and their diabetes duration between 1-49 years (median 10 yrs). Their BMI was 23 ± 3.5. kg/m^2. At the beginning of the course, the large majority used insulin glargine or NPH insulin in combination with insulin lispro or aspart and needed a total daily insulin dose of 0.6 ± 0.3 U/d that remained unchanged.

	Baseline	After 1 month	After 6 months	After 18 months	Overall p
HbA1C (%)	7.2 ± 1.1 (5.3-10.0)	7.0 ± 0.9 (5.2-9.4)	7.1 ± 0.9 (5.8-10.6)	7.1 ± 0.8 (5.6-9.1)	NS
Severe hypoglycaemic episodes/6 months[1]	0.33 (0-3.25)	N/A	0.1 (0-0.75)	0.03 (0-0.75)	<0.05
Quality of Life (DQoL), (lower scores indicate an increase in QoL)	91.8 ± 22.5 (53-162)	N/A	85.7 ± 21.2 (51-164)	85.6 ± 20.0 (60-151)	<0.001
Locus of Control (IPC-9) (lower scores indicate an increase in self control)	69.4 ± 22.3 (38-125)	N/A	60.1 ± 21.2 (28-118)	62.4 ± 20.7 (35-124)	<0.001
Diabetes knowledge (DWT)	24.2 ± 8.7 (9-41)	27.1 ± 7.0* (11-42)	27.0 ± 6.5* (11-41)	28.2 ± 6.2* (11-39)	<0.001

Data are shown as mean ± SD (range), N/A denotes not applicable, NS denotes not significant
[1] Data were log-transformed for analyses

Overall glycemic control was already good and did not change over the test period of 18 months. The frequency of severe hypoglycemic events was low, but decreased even further after the FIT course. Quality of life, self control and diabetes knowledge all improved. Despite this, most parameters showed a high intra-class correlation, i.e. a high variation between individuals, while the variation within individual (intra-individual variation) was low. This was especially the case for psychological parameters (between subject variance 81-86 % of total variance).

Conclusion:
In an unselected population of relatively well controlled type 1 diabetic patients, flexible, intensive insulin therapy is able to decrease the frequency of severe hypoglycemia, improve quality of life, self control and diabetes knowledge and maintain a stable metabolic control in type 1 diabetics. However, metabolic and psychological changes showed a large inter-individual variation.

Discrimination of insulin-treated diabetic subjects at the workplace and by insurances

[1]Nebiker-Pedrotti P., [1]Keller U., [2]Iselin H.U., [3]Ruiz J., [4]Pärli K., [5]Caplazi A., [3]Puder J.

[1]Division of Endocrinology, Diabetes and Clinical Nutrition, University Hospital of Basel, [2]Division of Internal Medicine, Spital Rheinfelden, [3]Division of Endocrinology, Diabetes and Metabolism, Centre Hospitalier Vaudois, Lausanne, [4]Center for Labor Law and Social Security, University of Applied Sciences Zurich, [5]University of Applied Sciences Northwestern Switzerland, School of Social Work, Institute for Integration und Participation, Olten

Background/Introduction:

Patients in the diabetes consultation often report of problems at the workplace or when contracting insurances because of their diabetes. Despite this, we did not find any data regarding discrimination of diabetic patients in Switzerland. The aim of this study was to analyse the frequency of work- and insurance-related discrimination in insulin-treated Type 1 and Type 2 diabetes and to detect socio-demographic and diabetes-related factors which are associated with increased discrimination.

Methods:

297 type 1 and 205 insulin treated type 2 diabetic patients, consecutively recruited from hospitals, generalist and specialist practices of the north-western part of Switzerland, filled out a self report questionnaire which included questions concerning discrimination at work (asked about diabetes during the application, not employed or loosing their jobs because of diabetes) and insurance-related (being refused or having a proviso for daily allowance resp. by providence insurance) as well as socio-demographic datas.

Results

Overall 11% of patients were asked in application interviews if they had diabetes, although employers are not allowed by law to ask about health status of their employee if it doesn't influence the current ability to work in order to fulfil the relevant job requirements. 10% of patients didn't get a job because of diabetes and 5% lost their job because of diabetes. Six percent and 4% of patients were refused by daily allowance insurance or by providence insurance, respectively, while 13% and 15% of patients had a proviso in the mentioned insurances. The analysis of socio-demographic factors revealed no differences related to gender or origin (Swiss vs non-Swiss). Unemployed patients reported five times more often that they didn't get a job because of diabetes compared to currently employed patients ($p<0.0001$). Patients with higher educational level (over 9th grade) were asked significantly more often questions about their health by daily allowance insurances ($p<0.01$). After adjusting for age, there was no difference in occupational status between type 1 and type 2 diabetic patients. However, patients with type 1 diabetes reported thrice as frequently to be asked about their diabetes during their application and to have provisos in providence insurance compared to type 2 diabetic patients, even after adjusting for age ($p<0.05$). Patients with more than 1 severe hypoglycaemic event/year reported around 4 times more often to be asked about their diabetes during their application or not to be hired due to their diabetes and 7 times more often to have lost their job due to their diabetes, independent of age and diabetes type (all $p<0.005$). After adjusting for age and diabetes type, overweight and obese diabetic patients were twice as often asked about their diabetes during their application and reported 2-4 times as often to be refused or the have a proviso both for their daily allowance and for providence insurance compared with normal weight patients (all $p<0.05$). Presence or absence of diabetes-related complications and level of self-control were not associated with any measures of discrimination in this population.

Conclusion:

These data demonstrate that the presence of type 1 diabetes and of severe hypoglycaemic episodes as well as overweight and obese weight status were independently associated with significantly more discrimination at work and/or by insurances. Further studies should delineate if these associations can be confirmed by objective measures.

Clinical study: criteria setting for the misuse of glucocorticosteroids

[1]Avois L., [2]Bailloux I., [1]Desmarchelier A., [2]Lahaussois A., [2]Méchin N., [2]deCeaurriz J., [1]Saugy M.

Institute of Legal Medicine, CHUV[1], French Anti-Doping Laboratory, AFLD[2]

Synthetic glucocorticosteroids are widely used by athletes in various sports, as indicated by the annual statistics regarding the requests for therapeutic use exemption (TUE). Glucocorticosteroids are known as very potent anti-inflammatory products. They are not only used in the treatment of chronic asthmatic symptoms, but are also currently applied in sport medicine for tendonitis, articular sprains, pain, injuries and overuse syndromes. Unfortunately, their systemic use is often associated with significant side effects, as Cushing syndrome.

To prevent their misuse, corticosteroids appear on the prohibited list of substances issued by the World Anti-Doping Agency (WADA). Consequently, the use of corticosteroids is controlled and restricted by WADA and sport federations: topical preparations are not prohibited, systemic use is forbidden and requires a standard TUE when medically necessary, whereas local applications and intra-articular injections are allowed under medical supervision and require an abbreviated TUE.

Elsewhere, there is no update agreement about effectiveness of corticosteroids, information in the literature is not sufficient and clinical guidelines are poor. Optimal timing, dosage and injection volume, remain answered. Comparison of efficacy with other treatments are not well established. Finally, at the present time, it is not possible to characterize the type of application (intra-muscular or intra-articular injections, local or oral application, nasal or pulmonary inhalations,…) in relation with measured urinary concentrations.

In order to clearly evaluate and establish some criteria in relation with glucocorticosteroids administration, WADA accepted to support a research project over two years, involving 3 anti-doping laboratories.

Table: Administration trial of synthetic glucocorticosteroids (Paris □, Lausanne ▭ Sydney ▨ not available X)

	Administration modes			
Substances	**Oral**	**Intra-muscular injection**	**Nasal and pulmonary inhalation**	**Intra- and peri-articular injection**
Triamcinolone acetonide	XXXXXXXXXXXX		Azmacort®	Triamcort Depot®
Methylprednisolone			XXXXXXXXXXXXXXXXXXXXX	Depot Medrol®
Prednisolone		Prednisolone Streuli®		
Dexamethasone		Chronocorte®		Fortecortin®
Betamethasone	Celestone®	Diprophos®		
Budesonide	Budenofalk®	XXXXXXXXXXXXXX	Pulmicort®	XXXXXXXXXXXXXXXXX
Triamcinolone	Kenacort®		XXXXXXXXXXXXXXXXXXXXX	
Prednisone		XXXXXXXXXXXXXX	XXXXXXXXXXXXXXXXXXXXX	

After acceptance of Ethical Committee, synthetic glucocorticosteroids currently administered were tested on numerous volunteers. For each compound, existing administration modes were applied (single and multiple applications) and urinary concentrations, excretion kinetics and patterns, were established. Moreover, endogenous profiles were evaluated in order to assess the influence of glucocorticosteroids administration on the metabolism. Analyses were performed by LC-MS^n.

This poster presents the results obtained by the Swiss Anti-Doping Laboratory. Obtained results are convincing and it could be possible from then to establish some criteria to prevent the misuse of glucocorticosteroids in the sport field.

***Acknowledgements**: Research project granted by WADA (over years 2006 and 2007).*

The MRL mouse does not regenerate cardiac muscle after injury

[1]Vassalli G., [1]Meinhardt A., [2]Lehr H.-A., [3]Kappenberger L., [4]Barrandon Y., [1]Vassalli G.

Department of Cardiology - CHUV[1], Department of Pathology - CHUV[2], Cardiomet - CHUV[3], Department of Surgical Research - CHUV, and Laboratory of Stem Cell Dynamics -EPFL[4]

Objective: The MRL mouse strain shows extraordinary wound healing capacities. Some years ago, Leferovich et al. (Proc Natl Acad Sci 14 U. S. A. 2001;98:9830–35) have reported the absence of scar formation after cryogenically-induced right ventricular myocardial infarcts in adult MRL mice. An independent group (Cardiovasc. Pathol. 2004;13:203–6) found that MRL mice repair left ventricular ischemic infarcts after coronary artery ligation with regular scar formation. Given the divergent outcomes in infarct healing in MRL mice reported by those two studies, we have investigated whether MRL mice heal myocardial infarcts without scar both in the cryoinjury and in the coronary ligation model.
Methods and Results: Four different protocols of cryogenically induced right and left ventricular injury, as well as permanent ligation of the left anterior descending coronary artery, were tested in adult MRL and control C57Bl/6 mice. At 60 days after experimental infarction, MRL mice showed pronounced scarring of the affected right and left ventricular areas, with no significant differences in infarct size and thickness between MRL and C57Bl/6 mice using any of the five experimental protocols. Analysis of cell proliferation by 5-bromo-deoxyuridine (BrdU) incorporation into the DNA did not show any difference between the two strains of mice after infarction. Histological analysis of infarct areas using picrosirius red staining did not show differences in extent of collagen and distribution between the two mouse strains. Conclusions: MRL mice heal myocardial infarcts with scar formation in response to ischemic as well as to cryogenic injuries.

Cardiovascular Assessment Facility

[1]Felley A., [1]Berthonneche C., [1]Pedrazzini T.

Cardiomet - CHUV[1]

The number of rodent genetic models of human disease has increased dramatically over the past several years. Studying the complex phenotypes of these rodent models requires standardized, state-of-the-art investigative techniques, and often calls for the development of new tools. The Cardiovascular Assessment Facility (CAF) was recently established to fulfill the demands of cardiovascular research in both humans and rodents. The center aims at providing researchers with the tools necessary to characterize a wide range of rodent models of cardiovascular and metabolic disorders.

More specifically the center will:
•**Provide phenotyping services** to Lemanic, Swiss, and European Academic researchers on a « fee for service » basis
•**Develop new interdisciplinary investigative techniques** in partnership with laboratories at Vaud University Hospital (CHUV), Lausanne University (UniL), and Lausanne School of Technology (EPFL)
•**Provide courses** to Academic partners
•**Foster joint projects** in clinical and basic research

Tests and services provided by the center include : high resolution echocardiography, microsurgery, blood pressure and heart rate measurements, and ECG monitoring.

Immunophenotypical analysis of putative cardiac progenitor cells isolated based on high ALDH activity from adult mouse and human hearts

[1]Roehrich M.-E., [1]Spicher A., [1]Meinhardt A., [1]Vassalli G.

Department of Cardiology - CHUV[1]

Background:
Myocardial perfusion is currently investigated by means of SPECT acquisitions with Tc-99m-MIBI. PET myocardial perfusion using either generator produced radioisotopes like Rb-82 is becoming attractive. Thus, to optimize imaging protocols, it is necessary to assess the exactness of data acquisition and treatment. The goal of this work was to compare measured ejection fraction (EF) by mean of a dynamic cardiac phantom with SPECT and PET.

Methods:
We imaged a cardiac dynamic phantom (BSI, Lübbecke, Germany) filled with 15 MBq F-18 and 30 MBq Tc-99m in the inner membrane chamber and fixed in a water filled torso-antropomorphic phantom for different heart beat frequencies. The PET/CT Discovery LS (GE MS) in 2D mode and the SPECT camera ECAM (Siemens MS) were used for gated acquisitions. Attenuation correction were performed with a CT attenuation map for PET and a standard Chang approach for SPECT. To obtain the actual EF CT of diastolic and systolic volumes were acquired. Special dedicated medical cardiac tool (ECtoolbox and 4DM) were used to calculate the EF.

Results:
Averaged measured volumes and EF are summarized in the table 1. SPECT and PET acquisitions systematically underestimate systolic (SPECT: -31.6%, PET: -17.9%) and diastolic (SPECT: -30.7%, PET:-30.7%) volumes. CT alone leads to an EF of 66.1%. Averaged SPECT and PET calculated EF were respectively 66.6% (error: 1.0%) and 59.9% (9.3%).

Table 1 : Measured systolic and diastolic volume and EF.

	Systolic volume (ml)	Diastolic volume (ml)	EF (%)
CT	38.4	113.4	66.1
SPECT	26.3	78.6	66.6
PET	31.5	78.6	59.9

Conclusion:
Despite the fact that PET have better resolution and quantification performances than SPECT, EF calculated from SPECT seems better. This can be explain by the fact that SPECT underestimates systolic and diastolic with a comparable error. On the contrary, for the PET images the systolic volume estimation is better because of less partial volume effects.

Genetic Selection System Allowing Monitoring of Myofibrillogenesis in Living Cardiomyocytes Derived from Mouse Embryonic Stem Cells

[1]Bougorski R., [2]Perriard J.-C., [3]Vassalli G.

Department of Cardiology - CHUV, ETH Zürich[1], ETH Zürich[2], Department of Cardiology - CHUV[3]

Embryonic stem (ES) cell-derived cardiomyocytes recapitulate cardiomyogenesis *in vitro* and are a potential source of cells for cardiac repair. This requires enrichment of mixed populations of differentiating ES cells into cardiomyocytes. Toward this goal, we have generated bicistronic vectors that express both the blasticidin S deaminase (*bsd*) gene and a fusion protein consisting of either myosin light chain (MLC)-3f or human α-actinin 2A and enhanced green fluorescent protein (EGFP) under the transcriptional control of the α-cardiac myosin heavy chain (α-MHC) promoter. Insertion of the DNase I-hypersensitive site (HS)-2 element from the β-globin Locus Control Region (LCR), which has been shown to reduce transgene silencing in other cell systems, upstream of the transgene promoter enhanced MLC3f-EGFP gene expression levels in mouse ES cell lines. The α-MHC-α-actinin-EGFP, but not the α-MHC-MLC3f-EGFP, construct resulted in the correct incorporation of the newly synthesized fusion protein at the Z-band of the sarcomeres in ES cell-derived cardiomyocytes. Exposure of embryoid bodies to blasticidin S selected for a relatively pure population of cardiomyocytes within 3 days. Myofibrillogenesis could be monitored by fluorescence microscopy in living cells due to sarcomeric epitope tagging. Therefore, this genetic system permits the rapid selection of a highly purified cardiomyocytes from a mixed population of differentiating ES cells, while simultaneously allowing monitoring of myofibrillogenesis in selected cardiomyocytes.

N-cadherin is essential for retinoic acid mediated cardiomyogenic differentiation in mouse embryonic stem cells

[1]Bougorski R., [2]Perriard J.-C., [3]Vassalli G.

Department of Cardiology - CHUV and ETH Zürich[1], ETH Zürich[2], Department of Cardiology - CHUV[3]

Contraction forces developed by cardiomyocytes are transmitted across the plasma membrane through end-to-end connections between the myocytes, called intercalated disks, which enable the coordinated contraction of heart muscle.
A component of the intercalated disk, the adherens junction, consists of the cell adhesion molecule, N-cadherin. Embryos lacking N-cadherin die at mid-gestation from cardiovascular abnormalities. We have evaluated the role of Ncadherin in cardiomyogenesis using *N-cadherin*-null mouse embryonic stem (ES) cells grown as embryoid bodies (EBs) *in vitro*.
Myofibrillogenesis, the spatial orientation of myofibers, and intercellular contacts including desmosomes were normal in *N-cadherin*-null ES cell-derived cardiomyocytes.
The effect of retinoic acid (RA), a stage and dosedependent cardiogenic factor, was assessed in differentiating ES cells. all-trans (at) RA increased the number of ES cell-derived cardiomyocytes by ≈3-fold (at $3 \cdot 10^{-9}$ M) in wt EBs. However, this effect was lost in *N-cadherin*-null EBs.
In the presence of supplemented *at*-RA, the emergence of spontaneously beating cardiomyocytes appeared to be delayed and slightly less efficient in *N-cadherin*-null compared with wt and heterozygous EBs (frequencies of EBs with beating activity at 5 days: 54±18% vs. 96±0.5%, and 93±7%, respectively; peak frequencies of EBs with beating activity: 83±8% vs. 96±0.5% and 100%, respectively).

In conclusion, cardiomyoyctes differentiating from *N-cadherin*null ES cells *in vitro* show normal myofibrillogenesis and intercellular contacts, but impaired responses to early cardiogenic effects mediated by *at*-RA. These results suggest that N-cadherin may be essential for RA-induced cardiomyogenesis in mouse ES cells *in vitro*.

GENERATION OF A MOUSE INDUCIBLE MODEL OF FRAGMENT N EXPRESSION IN PANCREATIC BETA CELLS

[1]Bulat N., [1]Widmann C.

Physiology institute - UNIL[1]

RasGAP is a GTPase-activating protein specific for Ras. RasGAP is also a substrate of the caspase family of proteases. Under mild stress conditions RasGAP is cleaved by caspases into two fragments, fragment C (C-terminal part) and fragment N (N-terminal part). Fragment N expressed in cells, including insulinoma cell lines, induces potent survival signals that depend on the activation of Akt and the repression of NF*k*B. Transgenic mice expressing fragment N under the control of the rat insulin promoter (RIP-N mice) are more resistant to streptozotocin-induced diabetes. Islet cells isolated from this transgenic mouse are also more resistant to a series of pro-apoptotic stimuli, including inflammatory cytokines, palmitate, hypoxia and high glucose concentrations. The RIP-N mice however constitutively express fragment N. An inducible model of fragment N expression in beta cells would represent a better system to assess the therapeutical potential of fragment N at the onset of diabetes. Generation of such a model requires that a targeting DNA sequence allowing a tight and specific regulation of fragment N expression in beta cells be constructed. We first attempted to use the classical Tet-on system based on the reverse tetracycline-controlled trans-activator (rtTA) to bind tetracycline-response elements (TREs). This system however proved to be leaky and poorly inducible in our hands. We therefore developed an alternative strategy based on the ability of a fusion protein (called tTRKRAB) between KRAB (Krüppel-associated box protein) and the tetracycline repressor to block gene expression. Upon addition of tetracycline (or the doxycycline analogue), the fusion protein detaches from TREs allowing transcription to resume. We have constructed a targeting vector containing fragment N, RIP, tTRKRAB, and TRE sequences that allows specific expression in beta cells upon doxycycline addition *in vitro*. This vector will now be used to generate mice that can be turned on and off at will for the expression of fragment N specifically in pancreatic beta cells.

Kinetics and membrane incorporation of omega-3 polyunsaturated fatty acids administrated as a 1 hour fast infusion or one week oral supplementation

[1]Rohrer M., [1]Chioléro R., [1]Soguel-Alexander L., [2]Voirol P., [3]Henry H., [4]Tappy L., [5]Carpentier Y., [1]Berger M.

Plateforme de recherche biomédicale et Service de Médecine Intensive Adulte - CHUV[1], Pharmacie - CHUV[2], Laboratoire de Chimie clinique - CHUV[3], Institut de Physiologie - UNIL[4], Labo. de Chirurgie expérimentale - Université Libre Bruxelles[5]

Background: Omega-3 polyunsaturated fatty acids (n-3PUFA) have many beneficial effects. Their anti-arrhythmic properties as well as their ability to blunt the inflammatory responses give them an important therapeutic potential in acute cardiac conditions. The study aimed at investigating the pharmacology of a 1-hour infusion and of 5 days of oral supplementation.
Methods : 8 volunteers received both treatments: first an infusion of 0.2g/kg in 1 hour of a fish oil–based emulsion rich in omega-3 (Omegaven ®, Fresenius Kabi) and after a washout period, 0.1g/kg/day of fish oil capsules (Omega 3 Gisand ®) during 5 days. Plasmatic triglyceride concentration and the fatty acid composition of platelet membrane phospholipids were analysed, and clinical tolerance evaluated. PUFA incorporation is expressed in molar %.
Results : The subjects, aged 42±9 years, weighting 69±8 kg, did not present any side effect. The 1 hour infusion was clinically well tolerated and safe : the triglyceride concentration transitorily rose during the infusion above the fasting normal threshold to peak at the end of the infusion at 5.2±1.2 mmol/L, and were back at their basal values 5 hours later. The platelet membrane enrichment in total n-3 PUFA, EPA and DHA was significant already at 1 hour and continued to rise the 5 following hours. After oral administration the composition of cell membranes was modified already in 2 days, and enrichment continued during the 3 next days.
Conclusions : The study showed that a significant incorporation of n-3PUFA in platelets membranes occurred already after 1 hour of infusion, as well as after 2 days of oral supplementation. The administration was safe and well tolerated. These results open important therapeutic perspectives, in particular in cardiac pre-conditioning.

Neuroprotection for coma after cardiac arrest: clinical criteria to identify patients who benefit from therapeutic hypothermia.

[1]Oddo M., [1]Ribordy V., [2]Feihl F., [3]Rossetti A., [1]Schaller M.-D., [1]Eggimann P., [1]Revelly J.-P., [1]Que Y.-A., [1]Berger M., [1]Liaudet L.

Service de Médecine Intensive Adulte-CHUV[1], Division de Physiopathologie Clinique-CHUV[2], Service de Neurologie-CHUV[3]

Background. Despite recent demonstration of its efficacy, therapeutic hypothermia (TH) is used only in a minority of comatose survivors of cardiac arrest, i.e. in patients without asystole, pulseless electrical activity, and circulatory shock. Studies are needed to better define the indications of TH in this setting. Objective: To define predictors of outcome in comatose survivors of cardiac arrest from all causes, following application of therapeutic hypothermia. Design: Cohort study carried out from December 2004 to October 2006. Setting: Medical intensive care unit (ICU) in a large teaching Swiss hospital. Patients: All patients aged < 80 years admitted to the ICU for coma after cardiac arrest during the study period. TH was systematically applied (33°C for 24 hours). whatever the cause of arrest. 74 patients were included. Main outcome measures: Duration of cardiac arrest, initial arrest rhythm, presence of post-resuscitation circulatory shock, hospital survival and neurological recovery at hospital discharge were recorded prospectively. Results: 51/74 patients (69%) did not meet current indications for TH due to non-ventricular fibrillation (VF) rhythm (17 patients), shock (15), or both (19). The median duration of cardiac arrest was 25 minutes. 65.7% of patients with arrest duration ≤ 25 minutes survived, and 57.9% had good neurological recovery. By contrast, almost none (3.1%) of those with arrest > 25 minutes survived, and none survived with good neurological recovery. With multivariable logistic regression, the duration of cardiac arrest was the single most important determinant of hospital survival (odds ratio in favour of survival: 0.80 for each additional minute of arrest, 95% confidence interval 0.71-0.90, $p<0.0001$), while non-VF rhythm and post-resuscitation shock were all rejected as independent predictors ($p>0.2$). Conclusion: In patients admitted for coma following cardiac arrest of short duration, therapeutic hypothermia should be used irrespective of initial arrest rhythm and presence of post-resuscitation shock.

Haemodynamic effects of hydroxyl-ethyl-starch 130/0,4 (VoluvenR) in patients suffering from symptomatic vasospasm after subarachnoid haemorrhage

[1]van Tulder L., [1]Chioléro R., [1]Oddo M., [1]Eggimann P., [2]Regli L., [1]Revelly J.-P.

Service de Médecine Intensive Adulte-CHUV[1], Service de Neurochirurgie-CHUV[2]

Introduction. Patients suffering from symptomatic cerebral artery vasospasm (CAV) after subarachnoid haemorrhage (SAH) develop alterations in sodium and fluid homeostasis. Their fluid management is controversial, and the effects of fluid infusion are uncertain. We assessed the effect of a single colloid infusion on global haemodynamics. **Methods.** In a prospective interventional study, 500 ml of 130/4 hydroxyl-ethyl-starch (HES) was administered over 30 minutes to 20 patients with CAV after SAH. Mean arterial pressure (MAP), central venous pressure (CVP), fluid balance, cardiac index (CI), intra-thoracic blood volume (ITBV,), and extra-vascular lung water (EVLW) were measured immediately before, and 60, 120, 180 and 360 min after HES by transpulmonary thermodilution (PiCCO, Pulsion). Comparisons between time-points were performed with one-way ANOVA for the entire group. Patients increasing CI by more than 10% were considered as responders. Comparisons between responders (R) and non-responders (NR) at different time points were performed by 2-ways ANOVA ($p<0.05$ significant, mean$\pm$SD). **Results.** After HES infusion CI changed from minus 14% to plus 62%. Considering the entire group, CI increased at time 60 min, (4.3 ± 0.7 vs 4.8 ± 0.9 l/m^2/min, $p<0.05$) but returned to baseline value at time 120 min (4.6 ± 0.9 l/m^2/min) and thereafter. There was no difference in MAP, CVP, ITBV and EPLW over time. 10 patients were R and 10 NR. Baseline MAP, CVP, CI, ITBV and EPLW were not different between R and NR. Norepinephrine infusion rate was higher in NR than in R (18.4 + 12.5 vs 5.8 + 8.8 mcg/min, $p<0.05$). CI increased in R from time 60 min to time 180 minute, and returned to baseline at 360 min (4.0 ± 0.6; 5.2 ± 1.1; 4.9 ± 1.1; 4.8 ± 1.0; 4.2 ± 1.1; l/m^2/min respectively). The evolution of fluid balance was different between R and NR: It remained unchanged in R, while it was negative at time 360 min in NR (-0.60 ± 0.87 vs -0.04 ± 0.47l, $p<0.05$). MAP, CVP, ITBV and EPLW were not different between R and NR throughout. **Conclusions.** Besides cardiac index, transpulmonary thermodilution provided serial data on ITBV and EVLW at the bedside. The haemodynamic effects of a short HES infusion were variable and unpredictable. In responders, the increase in cardiac output lasted 3 hours. In non-responders, fluid infusion may even be deleterious, since it seems to be associated with a negative fluid balance, likely due to cerebral salt wasting. Our data suggest that fluid therapy should be closely monitored in this population of patients with altered homeostasis.

Kinetics and membrane incorporation of intravenous n-3 polyunsaturated fatty acids administrated as a 1 hour fast infusion or one week oral supplement

[1]Rohrer M., [1]Chioléro R., [1]Soguel L., [2]Voirol P., [3]Henry H., [4]Tappy L., [5]Carpentier Y., [1]Berger M.

Service de Médecine Intensive Adulte-CHUV[1], Pharmacie-CHUV[2], Laboratoire Central de Chimie Clinique-CHUV[3], Institut de Physiologie-UNIL-CHUV[4], Labo. de Chirurgie Expérimentale, Université Libre, Bruxelles, Belgique[5]

Background: Omega-3 polyunsaturated fatty acids (n-3PUFA) have many beneficial effects. Their anti-arrhythmic properties as well as their ability to blunt the inflammatory responses give them an important therapeutic potential in acute cardiac conditions. The study aimed at investigating the pharmacology of a 1-hour infusion and of a 5 days of oral supplements. Methods: 18 volunteers received both treatments: first an infusion of 0.2g/kg in 1 hour of a fish oil–based emulsion rich in omega-3 (Omegaven ®, Fresenius Kabi) and after a washout period, 0.1g/kg/day of fish oil capsules (Omega 3 Gisand ®) during 5 days. Plasmatic triglyceride concentration and the platelet membranes fatty acid composition of phospholipids were analysed, and clinical tolerance evaluated. PUFA incorporation is expressed in molar %. Results: The subjects, aged 42±9 years, weighting 69±8 kg, did not present any side effect. The 1 hour infusion was clinically well tolerated and safe: the triglyceride concentration transitorily rose during the infusion above the fasting normal threshold to peak at the end of the infusion at 5.2±1.2 mmol/L, and were back at their basal values 5 hours later. The platelet membrane enrichment in all n-3 PUFA, EPA and DHA was significant already at 1 hour and continued to rise the 5 following hours. After oral administration the composition of cell membranes was modified already in 2 days, and enrichment continued during the 3 next days. Conclusions: The study showed that a significant incorporation of n-3PUFA in platelets membranes occurred already after 1 hour of infusion, as well as after 2 days of oral supplementation. The administration was safe and well tolerated. These results open important therapeutic perspectives, in particular in cardiac pre-conditioning.

Isolation of cardiac precursor cells from the human fetal heart

[1]Gonzales C., [1]Pedrazzini T.

CHUV[1]

Cardiovascular diseases, in particular heart failure, are major health problems in developed countries. Weakening of cardiac function is essentially due to a loss of contractile units in the damaged heart. In this context, cell replacement therapies to induce myocardial regeneration represent attractive alternatives to classical drug approaches. In many adult organs, pluripotent progenitors with self-renewal capacity and an ability to differentiate into a variety of cell types have been identified. In the present study, we establish the conditions to isolate cardiac precursors from human fetal hearts. Heart tissues were collected from donation following voluntary pregnancy termination at 12 weeks of gestation (approved by the Hospital Ethics Committee). Atria and ventricles were separated and cells were isolated after different rounds of digestions (collagenase/pancreatin) based on their capacity to adhere or not to plastic (differential plating). The adherent population consists in non-myocyte cells containing, among other cell types, cardiac precursor cells whereas the non-adherent fraction contains mostly myocytes. Each cell population was expanded in DMEM containing 10%HS and 5% FCS, and their capacity to produce differentiated cardiomyocytes was tested in two differentiation media, specifically: mediumA (MEM-Alpha, 0%FCS, 1µM dexamethasone, 50µg/ml ascorbic acid, 10mM β-glycerophosphate); mediumB (KO-DMEM, 10%KOSR). Evidence of differentiation was obtained by immunostaining for cardiac α-actinin and by measuring cardiac-specific gene expression using real-time PCR (cardiac-troponin-I, α-MHC, β-MHC, GATA4, Nkx2.5). Expression of the stem cell marker (Isl-1) was also measured. Results demonstrate that both differentiation media promote cardiogenic differentiation as shown by the dramatic increase in cardiac α-actinin positive cells after induction of differentiation. Expression of cardiac markers, more specifically α-MHC and β-MHC, as well as the stem cell marker Isl-1, was also significantly increased in most of the cell populations. To conclude, our work demonstrates that cardiac precursors can be isolated from the human fetal heart, and can be differentiated into cardiomyocytes in vitro. Further experiments are needed to assess the capacity of these cells to produce functional cardiomyocytes in vivo.

Optimization of Injected Dose Based on Noise Equivalent Count Measurement for 2D and 3D Cardiac PET/CT imaging

[1]Modolo L., [1]Dupuis P., [2]Prior J., [1]Bolard G., [2]BischofDelaloye A., [1]Verdun F.

Institute for Radiation Physics - CHUV[1], Department of nuclear medicine - CHUV[2]

Background:
To investigate whether PET characterization according to NEMA NU 2-2001 guidelines may be used to optimize acquisition protocols for cardiac PET studies or whether a dedicated heart torso phantom is needed.

Methods:
A PET/CT unit (D-LS, GEMS) was first characterized according to NEMA NU 2-2001 guidelines using the complete set of standard NEMA test objects (PTW, Freiburg, Germany) and F-18 in a wide range of activities (0 to 3300 MBq) in 2D and 3D acquisition modes. The characterization parameters obtained (NEC, correction for count losses and randoms events) were compared to corresponding parameters measured in the dedicated heart torso phantom with F-18 filled heart walls (PTW, Freiburg, Germany) that better render clinical conditions.

Results:
The accuracy of correction for count losses and random events assessed with the set of NEMA test objects is within 7% for activities well above the NEC1R peak in 2D and 3D mode (error < 6.5% for activity < 3134 MBq in 2D and < 4.4% for activity < 637 MBq in 3D). Significant differences in NEC results were obtained between data measured unsing NEMA test objects and the hear torso phantom (2D: NEC1R maximal activity is 2358 MBq and 636 MBq for the NEMA and heart torso phantom, respectively; 3D: NEC1R maximal activity is 224 MBq and 163 MBq for the NEMA and heart torso phantom, respectively).

Conclusion:
Although the NEMA guidelines apply to PET systems used for oncological studies, they cannot readily be used to optimize activity and acquisition parameters for cardiac PET, especially when working with very high activities as needed to quantify myocardial blood flow with short-lived radioisotopes.

Intramyocellular lipid quantification in human lumbar muscle by means of 3T NMR spectroscopy: a feasibility study

[1]Modolo L., [1]Monnin P., [1]Verdun F., [2]Meuli R., [2]Theumann N.

Institute for Radiation Physics - CHUV[1], Department of Radiologie - CHUV[2]

Background:
Measurement of intramyocellular lipids (IMCL) in muscles with proton nuclear magnetic resonance spectroscopy allows to perform metabolic studies. Most of these studies focus on the tibialis anterior muscle because of its simple geometry. It is also of interest to study the feasibility of such measurements in more complex muscle geometries such as in lumbar muscles in order to acquire data that might be used for the diagnostic and rehabilitation of patient suffering from chronic low back pain.

Methods:
Measurements were performed in lumbar paraspinal muscles on ten volunteers using a 3T MRI unit. After optimization of the protocol, well-resolved spectra were acquired in the lumbar muscles of all volunteers. Absolute quantification of intramyocellular lipid content was determined for each case. The results have been then compared with data acquired in tibialis anterior.

Results:
Averaged IMCL concentrations of 2.1 and 4.8 mmol/kg wet weight were measured respectively in the calf muscle and in the low back muscle. Variability of 10.6% in the calf muscle and of 11.4% in the low back muscle was obtained.

Conclusion:
The results of this study show that IMCL absolute quantification in lumbar muscles is feasible at 3T. Commercially available NMR units enables reliable and accurate measurements of IMCL content.

High Density Lipoproteins Protect Pancreatic Beta-cells by Targeting 4E-BP1

[1]Petremand J., [1]Butty A.-C., [1]Yang J.-Y., [2]Bulat N., [2]Poussin C., [2]Thorens B., [2]Widmann C., [3]Waeber G.

UNIL CHUV[1], UNIL[2], CHUV[3]

Low level of HDL cholesterol is one of the lipid phenotype observed in diabetic patients. HDLs exert numerous protective effects on endothelial cells such as prevention of LDL oxidation, endothelial dysfunction and apoptosis. In the case of pancreatic beta cells, HDLs have been shown to protect against apoptosis elicited by various stress stimulus such as serum starvation, cytokines, or oxidized LDL. However, the molecular mechanisms of HDL-induced beta cells protection are not entirely identified.

Affymetrix gene chip technology was used in stress or normal conditions to identify the target genes by which HDL exert their anti-apoptotic activities in insulin-secreting cells. One interesting target identified was the translational repressor 4E-binding protein (4E-BP1). This small protein regulates protein synthesis by sequestering eIF4E which is necessary for initiation of translation. Mammalian target of rapamycin (mTOR) is able to regulate 4E-BP1 by phosphorylation on multiple sites and therefore decreasing its affinity to eIF4E. 4E-BP1 expression is induced by starvation or hypoxia and has been demonstrated to induce apoptosis.

In this study, stresses such as serum starvation induced 4E-BP1 expression in two types of insulin-secreting beta cell lines. The induction of 4E-BP1 expression was significantly reduced by HDL, and this effect was correlated with prevention of apoptosis. Moreover, 4E-BP1 overexpression in beta cells induced apoptosis, mimicking the starvation effect. Finally, 4E-BP1 silencing reduced the apoptotic response showing that there is a direct link between 4E-BP1 and apoptosis in beta cells.

These data indicate that HDL block stress-induced expression of 4E-BP1 and prevent beta cell apoptosis, showing that 4E-BP1 is a possible target to prevent development of diabetes.

Integrated chip-based microsystem with rapid fluidic exchange to perform electrophysiological studies on Xenopus laevis oocytes

[1]Bize V., [2]Dahan E., [2]Lehnert T., [2]Gijs M., [1]Horisberger J.D.

Department of Pharmacology and Toxicology - University of Lausanne[1], Institute of Microelectronics and Microsystems, Ecole Polytechnique Fédérale de Lausanne, Lausanne[2]

To improve the throughput of the traditional Two-Electrode Voltage-Clamp (TEVC) on *Xenopus* oocytes, we developed a novel non-invasive chip-based technique. An interdisciplinary research effort in biology and microtechnologies permitted to design an integrated and automated voltage-clamp microsystem.
The cell is immobilized by suction on a conical hole. No puncturing with microelectrodes is required any more, since the upper part of the cell membrane is permeabilized by means of a ionophore (nystatine). The lower part of the cell membrane extends into a microchannel through which reagents can be dispensed. Only small-volumes of solution (< 1 mL) are required. A rapid and cost effective fabrication is made possible thanks to the use of a moulded elastomer (poly-dimethylsiloxane). These characteristics render this microsystem suitable for high throughput screening.
Promising results have been obtained: measurements of sodium benzamil- and amiloride-sensitive currents in oocytes expressing the human Epithelial Sodium Channel (hENaC), recordings of benzamil-sensitive I-V curves for potentials between -100 and +50 mV (with a large signal to noise ratio), comparable to measurements performed with the classical TEVC system.
It was then possible to characterize the fast solution exchange system. We obtain exchange times smaller than 50 ms and effective exchange times (90% of the maximum current measured on hENaC-expressing oocytes) of 80 and 250 ms in case of respectively an increase of the extracellular sodium concentration and a washout of the channel blocker amiloride. These properties of the system enable us to improve measurements and analysis on fast kinetics phenomena (e.g. self-inhibition of hENaC).

Long-Term Benefits of Functional Insulin Therapy (FIT) in Type 1 Diabetic Patients –the CHUV- FIT Cohort Study

Meister R., Nguyen S. , Puder J., Comte-Perret S., Ruiz J. [1]

Department of Endocrinology, Diabetology and Metabolism, Centre Hospitalier Universitaire Vaudois, Lausanne, Switzerland.

Introduction : A high level of self-management is necessary in patients with type 1 diabetes mellitus to have a good glycemic in order to prevent micro- and macro-vascular complications and to reduce the risk of severe hypoglycemic events. Functional insulin therapy (FIT) is a therapeutic education program allowing patients to develop skills and self efficacy perception by teaching them a self-care method. Its aim is to transfer the decisional process and the management of insulin treatment to the patient, adjusting to the various acts of everyday life and particularly to nutritional intake. FIT has been recognized to improve short-term metabolic control, but no long term data exist. The aim of this study is to investigate the long-term impact of these educational courses and the factors associated with a good metabolic control.

Methods : We report the preliminary results of a cohort of 100 type 1 diabetic patients who attended FIT courses between 1996 and 2005 in the diabetes unit at the CHUV. The current report is based on the data of the first 80 patients. The following parameters were assessed before and after the course: HbA1c, frequency of severe hypoglycemia, type of insulin treatment: multiple injections versus insulin-pump. Severe hypoglycemia was defined as a hypoglycemia requiring treatment by a third person. We defined the change in metabolic control according to absolute differences in the HbA1c levels before the FIT course compared to the levels at the last patient's interview: 1° stable when the difference in HbA1c was less than 0,3%, 2° improved when it dropped more than 0,3% and 3° worse when it increased more than 0,3%.

Results : The median (interquartile range) age of the study population was 40 (35-48) years and 46% were males. Median diabetes duration was 16 (10-24) years, patient's follow up after FIT was 6 (3-9) years. 19% percent of the patients were treated with an insulin-pump before the course and 58% after ($p<0.001$). Mean ($\pm$SD) HbA1c prior to FIT was 8.06% ($\pm$%), while the mean HbA1c at the last interview was 7,67% ($\pm$%) with mean HbA1c reduction of 0,38% ($p= 0,004$). At the last interview, insulin-pump treated patients had a better metabolic control when compared to those treated with a basal-bolus insulin (HbA1c 7,47% vs. 7,87%, $p= 0,033$). Fifty percent of the patients had an improvement in metabolic control, 24% were stable and in 26% the metabolic control worsened. Patients with a stable or improved glycemic control had a longer duration of diabetes before FIT compared to the ones whose glycemic control worsened (11 vs. 4 years, $p=0,006$). We observe a reduction of hypoglycemia's frenquency in the last 3 years of follow-up (14%) in comparison to before the FIT (31%), (OR=0.68 ; $p=0.003$). In multivariate analyses, the higher HbA1c level before the FIT course adjusted for age , sex, pump-wearing and diabetes duration, is a predictive factor for an improved or stable metabolic control 6 years later ($p=0.004$).

Conclusions : FIT courses allow a significant sustained long term improvement in metabolic control, after 6 years follow-up, a situation we would not have fully expected according to the DCCT/EDIC studies. Patients with a longer diabetes duration, with pump therapy as well as with higher HbA1c levels prior to course seemed to best profit from the FIT. This can be explained by a greater gain in experience in diabetes management and a more accurate and physiologic treatment with insulin pumps respectively. Furthermore, this improvement in metabolic control was achieved with a decreased risk of severe hypoglycemia for the last three years of follow up.
A further FIT course may be necessary 2 years after the initial course in order to maintain and improve benefits.

Human oxidized low density lipoprotein-particles cause a loss of insulin secretion by inducing the transcriptional repressor ICER

[1]FAVRE D., [1]NIEDERHAUSER G., [1]ALLAGNAT F., [1]HAEFLIGER J.-A., [2]PLAISANCE V., [2]REGAZZI R., [1]WAEBER G., [1]ABDERRAHMANI A.

Service of Internal medicine[1], Department of Cellular Biology and Morphology[2]

Patients with type 2 diabetes and metabolic syndrome have elevated circulating concentrations in oxidized LDL-cholesterol particles (oxLDL) and low levels in high density lipoproteins (HDL). Several lines of evidence support the hypothesis that modified and inappropriate levels of these lipoproteins may adversely favour pancreatic β-cell dysfunction, thereby contributing to development of diabetes and its related complication. In *vitro* chronic exposure of β-cells to 2 mM human oxLDL-cholesterol increases the rate of apoptosis and reduces the capacity of β-cells to produce insulin. In line with their protective role, HDL efficiently antagonised the harmful effects of oxLDL, suggesting that low levels of HDL would be inefficient to protect β-cells against oxLDL attack in patients. Prolonged incubation of β-cells with high glucose or free fatty acids concentration leads to similar defects. These are in part attributed to induction of the inducible cAMP early repressor (ICER), a transcriptional repressor that inhibits expression of genes containing cAMP response elements. In this study, we hypothesize that oxLDL could mediate β-cell dysfunction by inducing the transcriptional repressor ICER. Exposure of the mouse insulin-secreting MIN6 cells or isolated rat islets to 2 mM oxLDL led to progressive elevation in ICER expression and its repressor activity. Induction of ICER was efficiently blocked in cells incubated with the pharmacological inhibitor of the protein kinase A H89, indicating that oxLDL stimulate the expression of ICER in PKA-dependent manner. Because ICER is also involved in the control of insulin secretion by modulating the expression of connexin 36 and some genes of the secretory apparatus such as Rab3a, Noc2, Granuphilin and Rab27a, we investigate the possibility that oxLDL might also alter insulin exocytosis. As expected, the rise in the ICER activity was followed by a reduction in the endogenous expression of its target genes and impairment in insulin secretion in response to several secretagogues. Finally, we found that co-incubation of the cells with 1mM HDL-cholesterol efficiently prevented induction of ICER and its target gene elicited by oxLDL. In conclusion, these data pinpoint the involvement of ICER in the deleterious effects exerted by the modified LDL and emphasize the efficiency of HDL to antagonise the outcomes of oxLDL.

Intercellular mechanical coupling coordinates myofibroblast contraction

[1]Follonier L., [2]Schaub S., [1]Meister J.-J., [1]Hinz B.

Laboratory of Cell Biophysics - EPFL[1], CNRS UMR 6543 - Université de Nice[2]

Neo-formation of intercellular adherens junctions (AJs) accompanies the differentiation of fibroblasts into smooth muscle cell-like contractile myofibroblasts, which is a key event during development of fibrosis and wound healing. We have previously shown that intercellular coupling of stress fibers at sites of AJs improves contraction of collagen gels by myofibroblast populations. By assessing spontaneous variations in the intracellular Ca^{2+} concentration, we here test whether AJs mechanically coordinate contraction between myofibroblasts. We show that both, cultured fibroblasts and myofibroblasts exhibit periodic intracellular Ca^{2+} oscillations which are synchronized between contacting myofibroblasts. Myofibroblasts but not fibroblasts become desynchronized upon inhibition of 1) AJ formation with specific cadherin function-blocking peptides, 2) contraction using myosin inhibitors and 3) mechanosensitive ion channels using Gd^{3+}. In contrast, uncoupling of gap junctions with palmitoleic acid is without effect on myofibroblast coordination but desynchronizes contacting fibroblasts that have been pre-selected for exhibiting synchronous Ca^{2+} oscillations. Moreover, Ca^{2+} waves, evoked by local stimulation of single cells, propagate intercellularly with a delay of ~6 seconds between myofibroblasts; passage of Ca^{2+} between fibroblasts is 3-times faster. Together our results suggest that mechanical AJ coupling coordinates Ca^{2+} oscillations between myofibroblasts whereas fibroblasts are coupled electrochemically. We propose that myofibroblast communication improves remodeling of cell-dense tissue: single myofibroblast contraction is transmitted via AJs to adjacent cells, there leading to opening of stretch-activated ion channels, Ca^{2+} influx and contraction that feeds back to the first cell.

MYOFIBROBLAST CONTRACTION ACTIVATES TGFbeta1 FROM THE EXTRACELLULAR MATRIX

[1]Wipff P.-J., [2]Rifkin D., [3]Meister J.-J., [3]Hinz B.

EPFL-LCB[1], New York University School of Medicine, New York, USA[2], EPFL - LCB[3]

The conjunct presence of mechanical stress and active TGF□1 is essential to convert fibroblasts into contractile myofibroblasts, causing tissue contractures in fibrotic diseases. Using cultured myofibroblasts and conditions in which the tension on the ECM can be modulated, we have established that myofibroblast contraction serves as a novel mechanism to directly activate TGFβ1 from self-generated stores in the ECM. Contraction of myofibroblasts and of myofibroblast cytoskeletons prepared with Triton-X-100 releases active TGFβ1 from the ECM. This process is inhibited either by antagonizing integrins or by reducing ECM compliance and is independent from protease activity. Stretching myofibroblast-derived ECM in the presence of mechanically apposing stress fibers immediately activates latent TGFβ1. In myofibroblast-populated wounds, activation of the downstream targets of TGFβ1 signaling, Smad2/3, is higher in stressed compared to relaxed tissues despite similar levels of total TGFβ1and its receptor. We propose activation of TGFβ1 via integrin-mediated myofibroblast contraction as a potential checkpoint in the progression of fibrosis, restricting autocrine generation of myofibroblasts to a stiffened ECM.

Reproducibility of Myocardial Blood Flow Quantitation with Rubidium-82 Cardiac PET

[1]Allenbach G., [1]Prior J., [2]Modolo L., [2]Kosinski M., [1]Malterre J., Verdun F., BischofDelaloye A.

Nuclear Medicine - CHUV[1], Institute for Radiation Physics[2]

Aim: Generator-produced rubidium-82 (^{82}Rb) is of interest for centers lacking access to a cylotron. Quantitation of myocardial blood flow (MBF) has been performed with ^{82}Rb using compartment-based models. However, reproducibility of such MBF quantitation with ^{82}Rb is not known precisely.

Material and Methods: Fourteen individuals (mean age 47±19y range 21–75y; 4W, 10M; including 10 volunteers and 4 patients with angiographically proved CAD) underwent dynamic PET imaging studies (21 frames) at rest and during adenosine stress (0.14mg/kg/min for 6 min) after injection of 1100MBq of ^{82}Rb (Discovery LS, GEMS). After waiting period of ≥30min, the rest-adenosine stress sequence was repeated. MBF was determined using a 1-compartment model including a correction for flow-dependent extraction fraction of ^{82}Rb (PMOD 2.80 analysis software, www.pmod.ch). Myocardial flow reserve (MFR) was defined by the ratio of stress/rest MBF. For comparison, paired *t*-test and Bland-Altman plots were used.

Results: There was no difference in hemodynamic parameters between baseline and repeat measurements (rate-pressure product: 7.42E3±0.20E3 vs. 7.34E3±0.17E3 mmHg/min, p=0.70). One volunteer refused to undergo adenosine stress because of side effects. There was no significant difference between baseline and repeat studies regarding MBF at rest (0.84±0.18 vs. 0.87±0.19 ml/min/ml, p=0.45), during adenosine stress (2.50±0.84 vs. 2.43±0.99 ml/min/ml, p=0.49) or in MFR (3.07±0.79 vs. 2.80±0.81, p=0.14). The correlations between baseline and repeat studies were also excellent (rest: r^2=0.97 y=1.02·x; adenosine: r^2=0.98 y=0.98·x; MFR: r^2=0.96 y=0.90·x). Finally, overall agreement was very good on Bland-Altman plots with 26 out of 27 measurement pairs (96%) being within reference range for difference, without any systematic difference (p=0.72).

Conclusion: These results demonstrate an excellent reproducibility of myocardial blood flow measurements with ^{82}Rb at rest and under adenosine challenge.

Myocardial Blood Flow Quantitation using Rubidium-82 Cardiac PET: Direct Comparison with Oxygen-15 Water in Volunteers and Patients

[1]Prior J., [2]Modolo L., [2]Kosinski M., [1]Allenbach G., [3]Valenta I., [3]Hoefflinghaus T., [3]Burger C., [2]Verdun F., [3]Kaufmann P., [1]BischofDelaloye A.

Nuclear Medicine - CHUV[1], Institute for Radiation Physics[2], Nuclear Medicine - University Hospital Zurich[3]

Aim: Generator-produced rubidium-82 (^{82}Rb) has been used for myocardial perfusion imaging as an attractive alternative to ^{15}O-H_2O or ^{13}N-ammonia. Quantitation of myocardial blood flow (MBF) has been performed with ^{82}Rb using compartment-based models. We aimed to directly compare MBF in the same individual with ^{82}Rb vs. ^{15}O-H_2O.

Material and Methods: In 14 individuals (mean age 47±19y range 21–75y, 4W, 10M), including 10 healthy volunteers and 4 patients with angiographically documented CAD we performed dynamic PET imaging studies at rest and during adenosine stress (0.14mg/kg/min for 6 min) with ^{82}Rb (1100MBq, 21 frames) and ^{15}O-H_2O (500–700Mq, 24 frames) within 1 week (Discovery LS and ST, GEMS). MBF was determined using 1-compartment models, including a correction for flow-dependent extraction fraction of ^{82}Rb using commercially available analysis software (PMOD 2.80, www.pmod.ch). Myocardial flow reserve (MFR) was computed as the ratio of stress/rest MBF.

Results: There was no difference in hemodynamic parameters between ^{82}Rb and ^{15}O-H_2O studies (rate-pressure product 7.42E3±0.20E3 vs. 7.33E3±0.21E3 mmHg/min, p=0.75). One volunteer refused to repeat adenosine stress with ^{82}Rb. Correlation between MBF obtained by ^{15}O-H_2O and ^{82}Rb was good (r^2=0.965, $MBF[^{82}Rb]=0.855*MBF[^{15}O\text{-}H_2O]$, range 0.74–3.88 ml/min/ml), as was the agreement between both methods (93% of all 27 measurement pairs were within reference range on the Bland-Altman plot), with a systematically lower MBF as determined with ^{82}Rb (mean difference 0.26 ml/min/ml, 95%CI 0.10–0.43). There was no significant difference in MFR (^{82}Rb: 3.07±0.79 vs. ^{15}O-H_2O: 3.24±0.77, p=0.39) with a good correlation (r^2=0.957, $MBF[^{82}Rb] = 0.930*MBF[^{15}O\text{-}H_2O]$) and no systematic difference.
Compared to the volunteers, the patients with CAD had significantly lower MBF at stress (^{82}Rb: 1.61±0.27 vs. 2.89±0.68 ml/min/ml, p=0.005; ^{15}O-H_2O: 2.11±0.27 vs. 3.28±0.47 ml/min/ml, p=0.0006), as well as a lower MFR (^{82}Rb: 2.27±0.72 vs. 3.42 0.53, p=0.007; ^{15}O-H_2O: 2.44±0.52 vs. 3.52±0.60, p=0.009), without significant difference in resting MBF (^{82}Rb: 0.73±0.10 vs. 0.88±0.19, p=0.17; ^{15}O-H_2O: 0.88±0.14 vs. 0.94±0.19, p=0.43).

Conclusion: This comparison suggests that myocardial blood flow quantitation can be performed with available generator-based ^{82}Rb and PET compartmental analysis allowing quantifying MBF and MFR in patients with macrovascular CAD.

Engineering the intestinal microenvironment for optimizing nanoparticle drug delivery

[1]Dixon B., [1]Raghunathan S., [1]Swartz M.

EPFL[1]

The lymphatic vasculature in the gut exists primarily to transport lipid from the absorptive epithelial cells of the small intestine to the collecting lymphatic ducts, where it is then emptied into the bloodstream, allowing absorbed lipid to bypass the liver in its first pass through the circulation. Drug bioavailability would be greatly increased if one were to develop a delivery method that would follow a similar pathway of absorption to that of lipid. We describe here the first in vitro model system that incorporates both enterocytes and lymphatics into a 3D tissue construct for studying the absorption and transport of a nanoparticle drug delivery system into lymphatics. Such a model will be useful in quantifying the efficacy of various nanoparticle delivery systems, as well as provide valuable information that will feedback into the design process. With this system we have the capability to measure transport at various time intervals and to image nanoparticle transport using confocal microscopy. Here we compare the efficacy of several nanoparticle systems, in addition to the effects of co-delivery with oleic acid and taurochloric acid, precursors known to induce chylomicron formation.

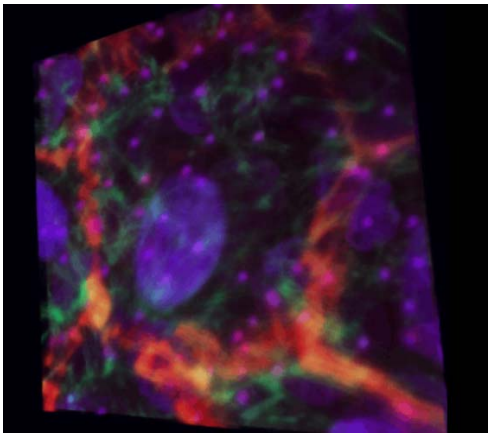

Figure 1: Lymphatic endothelial cells (top) and differentiated Caco-2 cells (on bottom) cultured together in a transwell system stained with: DAPI (blue), Phalloidin (green), and VE-Cadherin (red).

A Novel Culture Device Expands Mesenchymal Stem Cell Cultures By Preserving The Proliferative Naïve Stem Cell Phenotype

[1]Majd H., [2]Quinn T., [1]Hinz B.

Laboratory of Cell Biophysics - EPFL[1], Cytomec GmbH, Spietz, Switzerland[2]

Mesenchymal stem cells (MSC), used to repair bone, cartilage, vascular and neuronal tissue, generally lose their stem cell features within ~8 passages in standard culture. With further passaging they reduce the proliferative potential and differentiate into fibrogenic myofibroblasts. To improve MSC culture we here develop a new culture method consisting of a motorized device that gradually expands a highly elastic novel culture surface by up to 10-times. After functionalization, MSC exhibit similar rates of attachment and proliferation to the static surface compared with control tissue culture plastic. Dynamically enlarging the surface by 8-times over 20 days yields ~2-times higher cell numbers compared with the corresponding surface gain after three standard trypsin passages. After three passages on the device, MSC exhibit unchanged proliferation; cell numbers are ~10-times higher than that of MSC in standard culture, which are growth arrested at the corresponding passage 15. In contrast to standard culture, dynamic MSC culture expansion preserves expression of naïve MSC markers as assessed by flow cytometry and qRT-PCR as well as a non-fibrogenic cell character, appreciated from the absence of α-smooth muscle actin expression. These MSC are still inducible to differentiate into chondrogenic, osteogenic, myogenic, and neurogenic lineages. In conclusion, our novel culture expansion device reduces MSC passaging and dramatically increases cell yield by simultaneously preserving the naïve MSC character and suppressing generation of fibrotic cells.

Prevalence of the metabolic syndrome in the Seychelles according to different definitions, contribution of components, and agreement between different defi

[1]KELLINY C., [2]Gabriel A., [1]Paccaud F., [1]Bovet P.

Institut Universitaire de Médecine Sociale et Préventive, Lausanne[1], Ministère de la Santé, République des Seychelles[2]

Background: The metabolic syndrome (MS) represents a cluster of metabolic disorders that predicts diabetes and cardiovascular disease. Several definitions exist and further descriptive and prospective data are needed to compare these definitions and their significance in different populations.

Objective: We examined, in a country of the African region, i) the prevalence of MS according to three major definitions (ATP, IDF, WHO); ii) the contribution of individual MS components; and iii) the agreement between the three considered definitions. We also examined the prevalence among diabetics and non-diabetics.

Methods: We conducted an examination survey in a sample representative of the general population aged 25-64 of the Seychelles (Indian Ocean, African region), attended by 1255 persons (participation rate of 80.2%).

Results: The prevalence of MS was similar with either definition of MS in men (24%-25%) but differed in women (WHO: 25%, ATP: 32%; IDF: 35%). Upon exclusion of diabetic persons, the prevalence was 5-10% lower for all three MS definitions: most diabetic persons had MS although a substantial proportion of diabetic men aged 45-64 did not have MS. The following components were found most often among persons with MS: 90% had high blood pressure (HBP) and 78% had obesity (ATP); 95% had obesity and 84% had HBP (WHO), and 89% had HBP and 75% had impaired glucose regulation (IDF) -not considering impaired glucose regulation and obesity that are compulsory components of the WHO and IDF definitions, respectively. Among persons with MS based on either of the three definitions (37% of total population), less than 80% met both ATP and IDF criteria, 67% both WHO and IDF criteria, 54% both WHO and ATP criteria and only 37% met all three definitions.

Conclusions. We found a fairly high prevalence of MS in an African population. However, because there was only poor agreement between the 3 MS definitions, the fairly similar proportions of MS based on ATP, IDF or WHO definitions identified, to a substantial extent, different subjects as having MS.

Risk factors of stroke mortality in the African region: a cohort study

[1]BOVET P., [2]Didon J., [2]Gabriel A., [3]Michel P., [1]Paccaud F.

Institut Universitaire de Médecine Sociale et Préventive, Lausanne[1], Ministère de la Santé, Seychelles[2], Service de Neurologie, CHUV[3]

Background: Population-based cohort studies of risk factors of stroke are scarce in developing countries and none has been done in the African region. We conducted a longitudinal study in the Seychelles (Indian Ocean, east of Kenya), a middle-income island state where the majority of the population is of African descent. Such data in Africa are important for international comparison and for advocacy in the region.

Methods: Three examination surveys of cardiovascular risk factors were performed in independent samples representative of the general population aged 25-64 in 1989, 1994 and 2004 (n=1081, 1067, and 1255, respectively). Baseline risk factors data were linked with cause-specific mortality from vital statistics up to May 2007 (all deaths are medically certified in the Seychelles and kept in an electronic database). We considered stroke (any type) as a cause of death if the diagnosis was reported in any of the 4 fields in the death certificates for underlying and concomitant causes of death.

Results. Among the 2479 persons aged 35-64 at baseline, 280 died including 56 with stroke during follow up (maximum: 18.2 years; mean: 10.2 years). In this age range, age-adjusted mortality rates (/100'000/year) were 969 for all cause and 187 for stroke; age-adjusted prevalence of high blood pressure (≥140/90 mmHg) was 48%. In multivariate Cox survival time regression, stroke mortality was increased by 18% and 35% for a 10-mmHg increase in systolic, respectively diastolic BP ($p<0.001$). Stroke mortality was also associated with age, smoking ≥5 cigarettes vs. no smoking (HR: 2.4; 95% CI: 1.2-4.8) and diabetes (HR: 1.9; 1.02-3.6) but not with sex, LDL-cholesterol intake, alcohol intake and professional occupation.

Conclusion. This first population-based cohort study in the African region demonstrates high mortality rates from stroke in middle-aged adults and confirms associations with high BP and other risk factors. This emphasizes the importance of reducing BP and other modifiable risk factors in high risk individuals and in the general population as a main strategy to reduce the burden of stroke.

OBESITY-RELATED PHENOTYPES ARE ASSOCIATED TO PARENTAL LONGEVITY IN A SWISS POPULATION-BASED STUDY

[1]Jaunin J., [1]Bochud M., [1]Marques-Vidal P., [2]Vollenweider P., [2]Waeber G., [3]Mooser V., [1]Paccaud F.

University Institute of Social and Preventive Medicine (IUMSP), University of Lausanne, Switzerland[1], Department of Medicine, Internal Medicine, CHUV, Lausanne, Switzerland[2], Medical Genetics, GlaxoSmithKline, Philadelphia, Pennsylvania, U.S.A.[3]

PURPOSE. Longevity has been attributed to decreased cardiovascular mortality. Subjects with long-lived parents may represent a valuable group to study cardiovascular risk factors (CVRF) associated with longevity, possibly leading to new ways of preventing cardiovascular disease.

METHODS. We analyzed data from a population-based sample of 2561 participants (1163 men and 1398 women) aged 55-75 years from the city of Lausanne, Switzerland (CoLaus study). Participants were stratified by the number of parents (0, 1, 2) who survived to 85 years or more. Trend across these strata was assessed using a non-parametric k-mean test. The associations of parental age (independent covariate used as a proxy for longevity) with fasting blood glucose, blood pressures, blood lipids, body mass index (BMI), weight, height or liver enzymes (continuous dependent variables) were analyzed using multiple linear regressions. Models were adjusted for age, sex, alcohol consumption, smoking and educational level, and BMI for liver enzymes.

RESULTS. For subjects with 0 (N = 1298), 1 (N = 991) and 2 (N = 272) long-lived parents, median BMI (interquartile range) was 25.4 (6.5), 24.9 (6.1) and 23.7 (4.8) kg/m^2 in women (P <0.001), and 27.3 (4.8), 27.0 (4.5) and 25.9 (4.9) kg/m^2 in men (P = 0.04), respectively; median weight was 66.5 (16.1), 65.0 (16.4) and 63.4 (13.7) kg in women (P = 0.003), and 81.5 (17.0), 81.4 (16.4) and 80.3 (17.1) kg in men (P = 0.36). Median height was 161 (8), 162 (9) and 163 (8) cm in women (P = 0.005) and 173 (9), 174 (9) and 174 (11) cm in men (P = 0.09). The corresponding medians for AST (Aspartate Aminotransferase) were 31 (13), 29 (11) and 28 (10) U/L (P = 0.002), and 28 (17), 27 (14) and 26 (19) U/L for ALT (Alanin Aminotransferase, P = 0.053) in men. In multivariable analyses, greater parental longevity was associated with lower BMI, lower weight and taller stature in women (P < 0.01) and lower AST in men (P = 0.011). No significant associations were observed for the other variables analyzed. Sensitivity analyses restricted to subjects whose parents were dead (N = 1844) led to similar results, with even stronger associations of parental longevity with liver enzymes in men.

CONCLUSIONS. In women, increased parental longevity was associated with smaller BMI, attributable to lower weight and taller stature. In men, the association of increased parental longevity with lower liver enzymes, independently of BMI, suggests that parental longevity may be associated with decreased nonalcoholic fatty liver disease.

NOTCH SIGNALLING: A POTENTIAL REGULATOR OF CARDIAC RESPONSE TO HYPERTROPHIC STIMULI

[1]Nemir M, [1]Croquelois A., [1]Domenighetti A., [1]Lepore M., [1]Pedrazzini T.

University of Lausanne, Switzerland, Department of Medicine, CHUV, Lausanne, Switzerland[1]

Notch signalling controls cell differentiation and fate decisions in several developmental processes. We have previously shown that Notch inhibits cardiomyocyte differentiation from embryonic stem cells by repressing the cardiac gene program. Here, we analyzed whether Notch controls response of the adult heart to acute and chronic hypertrophic stimuli.
We have used the one kidney-one clip model to induce cardiac hypertrophy and found that at 4 days post-clipping, the expression of Notch1, Jagged1 and Hes1 is upregulated 3-5 fold relative to sham-operated mice and that Notch1 is activated in the cardiomyocytes. We also found that expression of Notch ligands and receptors is upregulated in our Tg1306 mice which express AngII in the heart and which gradually develop cardiac hypertrophy. Chemical inhibition of Notch in these mice accelerates and exacerbates cardiac hypertrophy. In addition, the cardiac response in 1K1C model, as measured by the expression level of cardiac hypertrophy genes is 2-4 times more elevated in mice lacking Notch1 than in wild type counterparts.
Quantitative analysis of cardiac gene expression and α-actinin/NIC immunostaining revealed that cultured Notch1-deficient cardiac myocytes express 4-10-fold more cardiac-specific genes, are generally larger and display a more elaborate myofibrillar apparatus than wild-type counterparts. Our results suggest that Notch modulates cardiac response to stress by controlling cardiac gene expression program.

Ejection fraction measurement with a dynamic cardiac phantom : a SPECT and PET comparision

[1]Modolo L., [2]Allenbach G., [2]Maillard D., [2]Flaction L., [2]BischofDelaloye A., [2]Prior J., [1]Verdun F.

Institute for Radiation Physics - CHUV[1], Department of nuclear medicine - CHUV[2]

Background:
Myocardial perfusion is currently investigated by means of SPECT acquisitions with Tc-99m-MIBI. PET myocardial perfusion using either generator produced radioisotopes like Rb-82 is becoming attractive. Thus, to optimize imaging protocols, it is necessary to assess the exactness of data acquisition and treatment. The goal of this work was to compare measured ejection fraction (EF) by mean of a dynamic cardiac phantom with SPECT and PET.

Methods:
We imaged a cardiac dynamic phantom (BSI, Lübbecke, Germany) filled with 15 MBq F-18 and 30 MBq Tc-99m in the inner membrane chamber and fixed in a water filled torso-antropomorphic phantom for different heart beat frequencies. The PET/CT Discovery LS (GE MS) in 2D mode and the SPECT camera ECAM (Siemens MS) were used for gated acquisitions. Attenuation correction were performed with a CT attenuation map for PET and a standard Chang approach for SPECT. To obtain the actual EF CT of diastolic and systolic volumes were acquired. Special dedicated medical cardiac tool (ECtoolbox and 4DM) were used to calculate the EF.

Results:
Averaged measured volumes and EF are summarized in the table 1. SPECT and PET acquisitions systematically underestimate systolic (SPECT: -31.6%, PET: -17.9%) and diastolic (SPECT: -30.7%, PET:-30.7%) volumes. CT alone leads to an EF of 66.1%. Averaged SPECT and PET calculated EF were respectively 66.6% (error: 1.0%) and 59.9% (9.3%).

Table 1 : Measured systolic and diastolic volume and EF.

	Systolic volume (ml)	Diastolic volume (ml)	EF (%)
CT	38.4	113.4	66.1
SPECT	26.3	78.6	66.6
PET	31.5	78.6	59.9

Conclusion:
Despite the fact that PET have better resolution and quantification performances than SPECT, EF calculated from SPECT seems better. This can be explain by the fact that SPECT underestimates systolic and diastolic with a comparable error. On the contrary, for the PET images the systolic volume estimation is better because of less partial volume effects.

NEU
Neurosciences et Psyché

Phosphorylation of neurofilament subunit NF-M is regulated by NMDA receptors and modulates cytoskeleton stability and neuronal shape.

[1]Fiumelli H., [2]Martin J.-L., [3]Riederer I., [4]Riederer B.

DP, UNIL[1], DP, UNIL & CNP, CHUV[2], CNP, CHUV[3], DBCM, UNIL & CNP, CHUV[4]

The cytoskeleton is essential for the structural organization of neurons and is influenced during development by excitatory stimuli such as activation of glutamate receptors. In particular, activation of the NMDA subtype of glutamate receptors is known to modulate the function of several cytoskeletal proteins and to control cell morphology. However, the cellular and molecular mechanisms underlying these effects remain unclear. In this study, we investigated the effects of NMDA receptor antagonists on NF-M, a neurofilament subunit that contributes to filament assembly. Our data revealed that chronic treatment of cultured cortical neurons with NMDA receptor antagonists MK-801 or AP5 upregulated the expression of NF-M and increased the molecular weight of this neurofilament subunit. Phosphatase assays showed that the enhanced molecular weight of NF-M after chronic exposure to NMDA receptor antagonists resulted from an increased phosphorylation of this neurofilament subunit. Consistent with these data, neurons treated with cyclosporin, an inhibitor of the Ca2+-dependent phosphatase calcineurin, exhibited increased levels of phosphorylated NF-M. Interestingly, analysis of neurofilament stability revealed that the increased phosphorylation of NF-M enhanced the solubility of NF-M. Finally, cortical neurons cultured in the presence of MK801 or AP5 grew longer neurites. Together, these data indicate that blockade of NMDA receptors during development of cortical neurons causes an increased phosphorylation and solubility of NF-M, and thereby favors neurite outgrowth.

3R in schizophrenia research: proteomic changes in fibroblast cultures allow an investigation of metabolic changes in relation to the disease

[1]Gysin R., [2]Riederer I., [3]Riederer B., [2]Do K.

CNP,CHUV[1], CNP, CHUV[2], DBCM, UNIL & CNP, CHUV[3]

The goals of 3R are to refine, to reduce or to replace animal experiments. We report on a novel test that fulfils these criteria. A significant association between schizophrenia and a GAG trinucleotide repeat (TNR) polymorphism in the glutathione (GSH) key synthesizing gene, glutamate cysteine ligase (GCL) catalytic subunit (GCLC) was reported (Gysin &al 2007). The "high risk" TNR genotype (HR: 7/8, 8/8, 8/9, 9/9) is correlated with a decrease in skin biopsy derived fibroblasts cultures of GCLC protein expression, GCL activity and GSH levels when compared with the "low risk" genotype (LR: 7/7, 7/9) . We thus compared proteome changes in fibroblast cells from three HR schizophrenia patients with that of three LR control subjects in oxidative stress conditions induced by tert-butylhydroquinone (t-BHQ). Following analysis by two-dimensional gel electrophoresis (2-DE), proteomic results revealed ten spots that were specifically upregulated in patients following t-BHQ treatment, but not in controls. Nine of these proteins could be identified using MALDI TOF mass spectrometry: they were involved in various cellular functions, including energy metabolism, oxidative stress response, cytoskeletal reorganization, and regulation of protein expression. Three of the identified proteins have previously been associated with schizophrenia. The present study corroborates that an impaired capacity to synthesize GSH plays a role in schizophrenia and offers new insights in consequences of GSH-related vulnerability. Therefore, fibroblast cultures from patients offer a direct means to study the dysregulation ofGSH metabolism in schizophrenia and therefore may replace or reduce the number of animals otherwise used to study the underlying mechanisms.

Differential gel electrophoresis of oxidized and non-oxidized proteins in Alzheimer's disease

[1]Riederer I., [1]Leuba G., [2]Riederer B.

CNP, CHUV[1], DBCM, UNIL & CNP, CHUV[2]

Protein oxidation is closely related to protein damage and a loss of specific protein function. Oxidative Stress is also involved in the aging process and in the pathogenesis of Alzheimer's disease. Among the protein backbone, a variety of amino acids are especially vulnerable to oxidation, such as cysteines. We have developed a sensitive protein labeling procedure with infrared fluorescent dyes that allow a detection of proteins in the femto-gramme range. This technique has been further elaborated for serial labeling of first, all cysteines that are present in reduced form, followed by a reduction of oxidized cysteines and subsequent fluorescent labeling with a second dye of different emission wavelength. This mixture of proteins was then separated by two-dimensional gel electrophoresis. In that way, on the same gel oxidized and non-oxidized proteins were present and easily distinguished by their difference in light emission. This novel staining method allows now to distinguish between oxidized and non-oxidized portions of the same protein and it will be interesting to correlate these data with the age of individuals or with the severity of the disease. We currently identify differences in disease- and age-related protein oxidation. It is foreseen to identify mechanisms that are involved in the pathogenesis of Alzheimer’s disease.

Differential changes in synaptic proteins in the frontal cortex of Alzheimer patients

[1]Leuba G., [2]Savioz A., [1]Vernay A., [1]Carnal B., [3]Kraftsik R., [4]Tardif E., [1]Riederer I., [5]Riederer B.

CNP, CHUV[1], Dep.Psychiatry, HUG[2], DBCM, UNIL[3], IP, UNIL[4], DBCM, UNIL & CNP, CHUV[5]

Here we investigated dendritic and synaptic plasticity in the neurodegeneration process of the human frontal cortex. Pre- and postsynaptic proteins of area 9 from patients with Alzheimer's disease (AD) and age-matched controls were quantified by immunohistochemical methods and by Western blots. The main finding was a significant increase in the postsynaptic density protein PSD-95 in AD brains, revealed both on sections and immunoblots, together with an increase in MAP2, a somatodendritic microtubule protein, while spinophilin associated to spines, remained unchanged. Presynaptic protein alpha-synuclein was equally significantly increased in AD, without formation of Lewy bodies, while another presynaptic protein linking to small synaptic vesicles, synaptophysin, was unchanged. Other AD markers such as ß amyloid protein, phosphorylated protein tau and phosphorylated neurofilament proteins were all increased in AD. These data indicate an involvement of the frontal cortex in the disease pointing to a damaged function due to beta amyloid deposits and abnormal phosphorylation of cytoskeletal proteins, but suggest also some attempt to synaptic reorganization. In particular the significant increase in PSD-95 suggests a change in NMDA trafficking and may represent a novel marker for the disease.

Postsynaptic density protein PSD-95, a marker for cognitive failure? A behavioural and proteomic analysis.

[1]Preissmann D., [2]Leuba G., [1]Schenk F., [3]Riederer B.

Inst.Psychol., DP, UNIL, & CNP, CHUV[1], CNP, CHUV[2], DBCM, UNIL & CNP, CHUV[3]

Aging is well known to impair memory processes but it does not affect everyone to the same extent. Here we assessed and classified individual performance in cognitive tests (place learning, retention and working memory) of senescent rats. Two subgroups were established, one severely impaired across all tests and the opposed group being unimpaired. Samples of frontal cortex tissue of never impaired and always impaired rats were separated on a gradient electrophoresis gel (4%-15% SDS-PAGE), either stained with Coomassie blue or transferred to nitrocellulose and immunostained with antibodies for MAP2, neurofilament subunits (SMI31), PSD-95, tau protein, tubulin, GFAP and SNAP25. Immunoreactivity was quantified by densitometry and used for correlation with behavioural studies. Among these proteins, the PSD-95 protein level was significantly correlated with memory performance. It is suspected that the PSD-95 level may influence glutamate receptors and cognitive functions. Proteomic changes were also investigated by two-dimensional gel electrophoresis. Coomassie blue stained 2D gels were analysed with the computer software Image master for differences in the protein composition between the two groups. This analysis points to a variety of protein changes that may be related to the performance of animals and is still work in progress.

Mechanism of action of kisspeptin / GPR54 system in GnRH neurons

Gamba M., Mansuy V., Gaillard R., Pralong F.

Service of Endocrinology, Diabetology and Metabolism and Center for CardioVascular and Metabolic Diseases, University Hospital, 1011 Lausanne

Background/Introduction:

Kisspeptins are the products of the metastasis suppressor gene Kiss-1 and they represent the natural ligands for the G-protein coupled receptor GPR54. It has been demonstrated that at the hypothalamic level, kisspeptins stimulate GnRH secretion. Consequently, gonadotropins are synthesized and released by pituitary gonadotrope cells.
Despite a putative key role of the hypothalamic kisspeptin system in the regulation of the gonadotrope axis, little is known about its mechanism of action. However, it has been shown in COS cells and in hippocampal dentate granulate cells that kisspeptins can activate the MAP kinase pathway.

Methods:

In this work, we examined the mechanism of action of kisspeptin in the regulation of GnRH expression in two GnRH-expressing cell lines: Gnv-3 cells (obtained by conditional immortalization of adult neurons) and GT1-7 cells (derived from a mouse hypothalamic).
The presence of GPR54 in Gnv-3 cells was assessed by RT PCR and immunohistochemistry. The expression levels of GnRH were evaluated by the measurement of GnRH mRNA levels, using real time RT-PCR (LightCycler®). Finally, activation of the MAP kinase Erk1 /2 intracellular signaling pathway was assessed by Western Blot experiments.

Results:

We could demonstrate the expression of GPR54 in both *in vitro* models. We found that stimulation of cells with kisspeptin-10 (1μM) could induce a rapid and significant activation of the MAPK Erk1/2 pathway. Furthermore, GnRH mRNA levels were also increased following stimulation with the same concentration of kisspeptin-10.

Conclusion:

The presence of GPR54 in two different models of GnRH neurons strongly suggests that kisspeptins activate the neuroendocrine gonadotrope axis directly at the level of these neurons. Furthermore, our data suggest that this effect involves the MAP kinase intracellular signaling pathway and the regulation of GnRH expression. Taken together, these results represent the first data regarding the mode of action of kisspeptins on hypothalamic GnRH neurons, the key activators of the reproductive axis.

Molecular mechanisms involved in ammonia-induced cell death in reaggregated developing brain cell cultures.

[1]Cagnon L., [2]Honegger P., [1]Braissant O.

Clinical Chemistry Laboratory, CHUV[1], Department of Physiology, UNIIL[2]

Hyperammonemia in neonates and infants is mainly due to urea cycle enzymes defects and induces irreversible damages on the developing CNS such as cortical atrophy, ventricular enlargement and demyelination. Recently the use of alternative-pathway therapies detoxifying ammonia clearly improved the survival of patients but was correlated with a worsening of the neurological and cognitive outcome in survivors. Thus, development of neuroprotective therapeutics is crucial for the patients. For this purpose, unraveling the precise molecular mechanisms triggering ammonia-induced cell death in the developing brain is necessary.

We used reaggregated primary cell cultures of fetal rat telencephalon treated with ammonium chloride as an experimental model for the developing brain exposed to hyperammonemia. We provide evidence that apoptosis is strongly induced in our model. We also show that ammonia exposure triggers caspases and calpain activation, as well as the cleavage of the regulatory subunit of cyclin-dependent kinase 5 (cdk5), p35, to p25. Roscovitine, an inhibitor of cdk5, protected brain cell cultures from cell death as well as the expression of the neurofilament M.

Molecular consequence of aging in the mouse peripheral nervous system

[1]Verdier V., [1]Chrast R.

DGM - UNIL[1]

The peripheral nervous system (PNS) is involved in many age-dependent neurological deficits that are common in the elderly and account for approximately 50% of disability after age 65. Although morphometric studies of mammalian models have provided valuable information on structural changes associated with PNS aging, less is known about the precise identity of age-regulated molecular changes in either neuronal or glial compartments of the nerve.

To unravel molecular pathways affected by aging in the PNS, our approach is to conduct a genome-wide analysis of aging-related gene expression changes in the mouse sciatic nerve, using 17 developmental stages from day of birth (P0) until senescence (28 month-old). Expression in Schwann cells-containing endoneurium and sensory neurons-containing Dorsal Root Ganglia (DRG) is being analyzed using Illumina Bead Chips.

Our preliminary analysis of the array data (i) reproduced the previously described expression pattern of known myelin genes serving as an internal control for our experiment and (ii) revealed substantial differences in the dynamic changes in gene expression between the two compartments (endoneurium versus DRGs). Clustering analysis is underway to identify age-regulated PNS-specific molecular mechanisms that should provide insight into the age-related neuropathies.

Transcriptional and phenotypic characterization of the onset of diabetic peripheral neuropathy (DPN) in a model of type I diabetes, the Akita mice

[1]de Preux Charles A.-S., [1]Verdier V., [1]Médard J.-J., [2]Kuntzer T., [1]Chrast R.

Department of Medical Genetics - UNIL[1], Neurology Service - CHUV[2]

Even though the pathological and morphological changes underlying diabetic peripheral neuropathy (DPN) are relatively well described, the implicated molecular mechanisms remain poorly understood. Akita$^{Ins2/+}$ mice are a model of spontaneous early-onset type I diabetes mellitus. These mice express a mutated non-functional isoform of insulin, leading to a reduced number of pancreatic beta cells and thereby to hypoinsulinemia and hyperglycaemia. To determine the onset of DPN, weight, blood glucose and motor nerve conduction velocity (MNCV) were measured in Akita$^{Ins2/+}$ mice during the first three months of life. We observed that a decrease in MNCV was present already one week after the onset of hyperglycaemia. To explore the molecular changes associated with the development of DPN, we performed gene expression profiling using sciatic nerve endoneurium and dorsal root ganglia (DRG) isolated from pre-diabetic and early diabetic male Akita$^{Ins2/+}$ mice and sex-matched littermate controls. These experiments should allow us to determine to which extent the two compartments of the nerve (the DRG composed mostly of neurons and the endoneurium containing mostly Schwann cells) are affected by diabetes, to analyze the possibility of a chronological order in alterations observed in these compartments and to correlate phenotypic changes observed in Akita$^{Ins2/+}$ mice with underlying transcriptional alterations.

ANALYSIS OF SOLVENT ACCESSIBILITY OF THE EXTRACELLULAR LOOP OF ACID-SENSING ION CHANNEL 1A (ASIC1A)

[1]Bargeton B., [2]Hovius R., [3]Kellenberger S.

Department of Pharmacology and Toxycology - UNIL[1], Laboratory of Physical Chemistry of Polymers and Membranes, Institute of Biomolecular Sciences, EPFL[2], Department of Pharmacology and Toxycology, UNIL[3]

ASICs are non-voltage-gated neuronal sodium channels activated by protons. They belong to the Epithelium Sodium channel/Degenerin family of ion channels. ASICs likely contribute to long term potentiation, the expression of fear, nociception and neuronal death after ischemia. These functions make ASICs potential drug targets.
Functional ASICs are assemblies of three homologous subunits. Each subunit has two transmembrane domains and a large extracellular loop, the N- and C-termini being cytoplasmic. The extracellular loop (ECL) is the sensor of the surrounding acidity and the target of several activity modulators. The crystal structure of the ECL of the desensitized channel has recently been solved.
We introduced cysteine residues by site-directed mutagenesis at selected sites of the ECL of ASIC1a with the aim to identify and study the accessible sites/domains of the channel protein. The mutant proteins were expressed in *Xenopus* oocytes. Western blot analysis was used to detect site-selective modification of the protein by a biotin linked to a cysteine-reactive group. To determine the functional relevance of the sites mutated we incubated *Xenopus* oocytes expressing ASIC1a with sulfhydryl reagents and analyzed the changes in the ASIC function by Two-Electrode Voltage-Clamp.
These analyses indicate whether a chosen site in the closed channel is accessible from the extracellular solution. The results of this screening, and their implication for our understanding of the function of ASICs will be discussed.

Structural and morphometric alterations in the diaphragm neuromuscular junctions and phrenic nerve in myotonic dystrophy transgenic mice

[1]Panaite P., [1]Gantelet E., [1]Caria-Dekhissi S., [2]Kraftsik R., [3]Gourdon G., [1]Kuntzer T., [1]Barakat-Walter I.

(2)de Recherche Neurologique - CHUV[1], Département de biologie cellulaire et de morphologie, UNIL[2], 3INSERM U383, Hôpital Necker, Paris, France[3]

Myotonic dystrophy (DM) is caused by abnormal expansion of a polymorphic (CTG)n repeat, located in the DM protein kinase gene. Respiratory problems have long been recognized to be a major feature of patients with advanced DM1 disease and are probably the major factors contributing to mortality. Since several pulmonary impairments are associated with phrenic nerve and diaphragm dysfunction, the present study was designed to determine if there are structural alterations in diaphragm and neural network in transgenic mice displaying the human DM1 phenotype. The morphological and morphometric analysis of numerous adjacent diaphragm muscle sections labeled with rhodamine α-bungarotoxin and neurofilament antibody revealed that the size and the shape complexity of endplates as well as the density of ACh receptors on postsynaptic membrane were significantly reduced in DM1 transgenic mice than in controls. The analysis of both semi-thin and thin phrenic nerve sections demonstrated there is no loss in the number of myelinated fibers in DM1 mice, however, there is a severe and significant reduction in the number of unmyelinated fibers. The examination of the medullary respiratory centers or cervical phrenic motor neurons did not show any pathological signs or loss of neuronal cells.
Since the involvement of neuromuscular junction in respiratory drive and the role of afferent phrenic unmyelinated fibers in the control of inspiratory activity are well documented, our results suggest that the respiratory impairment associated with myotonic dystrophy disease may be due, at least partially, to the pathological alterations in diaphragmatic neuromuscular junctions and phrenic nerves (NFRS102175/12003)

Role of disease activity for decision making ability in early multiple sclerosis

[1]Simioni S., [2]Ruffieux C., [1]Kleeberg J., [1]Bruggimann L., [1]Annoni J.-M., [1]Schluep M.

Neurology - CHUV[1], Social and Preventive Medicine - CHUV[2]

Background and purpose: Decision making (DM) has been defined as the process through which a person forms preferences, selects and executes actions, and evaluates the outcome related to a selected choice. This ability represents an important factor for adequate behaviour in everyday life. DM impairment in multiple sclerosis (MS) has been previously reported. The purpose of the present study was to assess DM in patients with MS at the earliest clinically detectable time point of the disease.

Methods: Patients with definite (n=109) or possible (clinically isolated syndrome, CIS; n=56) MS, a short disease duration (mean 2.3 years) and a minor neurological disability (mean EDSS 1.8) were compared to 50 healthy controls aged 18 to 60 years (mean age 32.2) using the Iowa Gambling Task (IGT). Subjects had to select a card from any of 4 decks (A/B [disadvantageous]; C/D [advantageous]). The game consisted of 100 trials then grouped in blocks of 20 cards for data analysis. Skill in DM was assessed by means of a learning index (LI) defined as the difference between the averaged last three block indexes and first two block indexes (LI=[(BI-3+BI-4+BI-5)/3-(BI-1+B2)/2]). Non parametric tests were used for statistical analysis.

Results: LI was higher in the control group (0.24, SD 0.44) than in the MS group (0.21, SD 0.38), however without reaching statistical significance (p=0.7). Interesting differences were detected when MS patients were grouped according to phenotype. A trend to a difference between MS subgroups and controls was observed for LI (p=0.06), which became significant between MS subgroups (p=0.03). CIS patients who confirmed MS diagnosis by presenting a second relapse after study entry showed a dysfunction in the IGT in comparison to the other CIS (p=0.01) and definite MS (p=0.04) patients. In the opposite, CIS patients characterised by not entirely fulfilled McDonald criteria at inclusion and absence of relapse during the study showed an normal learning pattern on the IGT. Finally, comparing MS patients who developed relapses after study entry, those who remained clinically stable and controls, we observed impaired performances only in relapsing patients in comparison to stable patients (p=0.008) and controls (p=0.03).

Discussion: These results raise the assumption of a sustained role for both MS relapsing activity and disease heterogeneity (i.e. infra-clinical severity or activity of MS) in the impaired process of decision making.

High prevalence of cognitive disorders in HIV+ patients with undetectable viremia

[1]Simioni S., [2]Annoni J.-M., [3]Cavassini M., [4]RimbaultAbraham A., [4]Schiffer V., [5]Chave J.P., [6]Giacobini E., [7]Hirschel B., [2]DuPasquier R.

Neurology - CHUV[1], Neurologie - CHUV[2], Maladies infectieuses - CHUV[3], Neurologie - HUG[4], Hôpital La Source[5], Réhabilitation et Gériatrie - HUG[6], Maladies infectieuses - HUG[7]

OBJECTIVE : 1) To determine the prevalence of cognitive disorders in a cohort of aviremic HIV+ patients. 2) To assess the accuracy of the HIV Dementia scale (HDS) and the International HDS (IHDS) for the detection of mild cognitive deficits.

BACKGROUND : 1) In the HAART era, the prevalence of HIV-associated mild cognitive disorders seems to have increased. However, the relationship between HIV viremia, immune status and cognitive disorders remains unclear. 2) The relevance of HDS and IHDS to diagnose HIV-associated minor cognitive disorders is unknown.

DESIGN/METHODS : Fifty aviremic HIV+ patients (98% on HAART) with subjective cognitive complaints completed the HDS, the IHDS, and a battery of neuropsychological tests assessing the sub-cortical functions. Cognitive impairment was defined as $\geq$2 tasks below 2 Z-scores. Major opportunistic infection in the past two years, active drug use and major depression were exclusion criteria. Non parametric tests were used for statistics.

RESULTS : The median and IQR for age, CD4+ T cells count and duration of undetectable HIV viremia before testing were 45+/-12 years, 523+/-332/mcl, and 36+/-40 months, respectively. Thirty-one HIV+ patients (62%) displayed cognitive deficits, showing mainly executive dysfunction and mental slowing. There were no significant differences between cognitively impaired and not impaired patients in terms of age, CD4+ T cells count, duration of undetectable HIV viremia, HCV serostatus, or mood disorders. A cut-off of $\leq$13 on the HDS and of $\leq$10 points on the IHDS were found to have a sensitivity of 77.4% (p=0.01) and 82.1% (p=0.03), respectively, for the diagnosis of mild cognitive deficits.

CONCLUSIONS/RELEVANCE : Our results show that 1) the prevalence of mild cognitive disorders is high in aviremic, immunocompetent HIV+ patients and 2) the HDS and IHDS are useful not only to detect full-blown HIV-associated dementia but also milder cognitive disorders.

Funding: Swiss HIV Cohort Study.

Lipin1-regulated lipid metabolism is essential for Schwann cell myelination

[1]Nadra K., [1]DePreuxCharles A.-S., [1]Médard J.-J., [2]Han G.-S., [3]Grès S., [2]Carman G., [3]Saulnier-Blache J.-S., [1]Chrast R.

Department of Medical Genetics, University of Lausanne, Switzerland [1], Graduate Program in Neurosciences, University of Lausanne, Switzerland.[2], Department of Food Science, Cook College, New Jersey Agricultural Experiment Station,U.S.A.[3], Inserm, U586, Unite de Recherches sur les Obesites, Toulouse,France.[4]

Lipin1 knockout animals ($Lpin1^{fld/fld}$) are characterized by a reduced adipose tissue mass (lipodystrophy), insulin resistance, and a progressive peripheral neuropathy. Sciatic nerve analyses in these mice revealed severe demyelination, poorly compacted myelin sheaths, active myelin breakdown, and hypertrophic Schwann cells.

We have previously found that the lipodystrophy in adult Lipin1 knockout animals extends to the epineurium of the sciatic nerve, which contains a reduced amount of fat deposits. Our current data demonstrates that in addition to epineurial lipodystrophy, there is an accumulation of lipid debris in the perineurial and endoneurial compartment of the peripheral nerve, which goes along with the development of peripheral neuropathy. In order to study the role of Lipin1 in the development and maintenance of the peripheral nervous system, we have used a conditional knockout approach to inactivate its function selectively in Schwann cells. We have generated mice in which the coding region of Lipin1 is flanked by loxP sites ($Lipin1^{floxEx2\text{-}3/floxEx2\text{-}3}$) and crossed it with the myelin protein zero-Cre transgenic mice (Mpz-Cre). While epineurial fat deposits are not affected in $Lipin1^{\Delta Ex2\text{-}3/\Delta Ex2\text{-}3}$/Mpz-Cre mice, the endoneurial compartment shows a demyelinating phenotype and an accumulation of lipid debris similar to the complete Lipin1 knockout mice. In addition, we have observed a significant decrease of Mg^{2+}-dependent phosphatidate phosphatase (PAP1) activity in endoneurium of both complete and Schwann cell specific Lipin1 knockout mice, consistent with the recently suggested function of Lipin1 as PAP1 in liver, WAT and kidney. These results demonstrate that the pronounced peripheral neuropathy evident in the mutants is a direct consequence of the absence of Lipin1 within Schwann cells and strongly suggests that during peripheral nerve myelination, the Lipin1 mediated PAP1 activity plays a crucial role in the in situ production of diacylglycerol needed for the synthesis of triacylglycerol and phospholipids by the Schwann cells.

Une étude de cas pragmatique d'une psychothérapie psychodynamique brève d'un patient hospitalisés.

[1]Gay C., [1]Ambresin G., [1]De Rothen Y., [1]De Coulon N., [1]Despland J.N.

Centre de Recherche en Psychothérapie, Institut Universitaire de Psychothérapie (IUP), Département de Psychiatrie, Université de Lausanne[1]

L'efficacité de la psychothérapie ambulatoire de patients souffrant de dépression, seule ou combinée à la psychopharmacologie pour les cas les plus graves, a été démontrée. En comparaison, les résultats de recherche sur la psychothérapie hospitalière sont rares. Une étude récente a montré la supériorité d'un programme hospitalier pour patients déprimés intégrant une psychothérapie brève et intensive et la pharmacothérapie par rapport au traitement habituel (Schramm, 2007).

L'admission à l'hôpital est une des manifestations de la rupture de l'équilibre intra-psychique et/ou interpersonnel du patient. Ce moment de crise est potentiellement fécond (de Coulon, 1999). Débuter le travail psychothérapique au cours de l'hospitalisation apporte plus de bénéfices aux patients déprimés, lorsqu'on les compare à un groupe de patients dont le travail a débuté après l'hospitalisation (Miller, 1989). Dans le cadre du DP CHUV, en collaboration entre l'Institut Universitaire de Psychothérapie et la section Karl Jaspers (Troubles de l'humeur), les patients hospitalisés pour un trouble dépressif participent à une étude sur l'efficacité d'une psychothérapie psychodynamique en 12 séances. Dans cette présentation, les auteurs étudient un cas en comparant le raisonnement clinique (autour des enjeux dynamiques des symptômes dépressifs) avec un instrument de recherche (The Psychotherapy Process Q-set, PQS) qui permet à un juge externe d'observer le processus d'une séance et de le comparer avec des prototypes idéaux construits par des experts.

Delayed priming promotes CNS regeneration post-rhizotomy in Neurocan and Brevican-deficient mice

[1]Zurn A., [1]Quaglia X.

CHUV[1]

Reactive tissue at the site of CNS injury is rich in chondroitin sulfate proteoglycans which may contribute to the non-permissive nature of the CNS. We have demonstrated that the proteoglycans Neurocan and Brevican are differentially expressed in the spinal cord dorsal root entry zone (DREZ) following dorsal root lesion (rhizotomy). However, direct evidence for a growth-inhibitory role of these proteoglycans *in vivo* is still lacking. Rhizotomy in mice deficient in both Neurocan and Brevican resulted in no significant increase in the number of fibers regenerating through the DREZ compared to controls. Likewise, a conditioning peripheral nerve lesion prior to rhizotomy enhanced growth to the same extent in transgenic and control mice. In contrast, when priming of the median nerve was performed 7 weeks post-lesion, axonal growth was facilitated in knockout, but not in control animals. This demonstrates that Neurocan and Brevican contribute to the non-permissive environment of the DREZ and that delayed peripheral nerve priming can facilitate regeneration across the DREZ, provided its growth-inhibitory properties are attenuated. Post-injury enhancement of the growth capacity of sensory neurons combined with removal of inhibitory proteoglycans may therefore help to restore sensory function and attenuate pain following human brachial plexus injury.

Molecular analysis of proteoglycan expression in two spinal cord regions with distinct growth-inhibitory properties using LCM and real-time PCR

[1]Waselle L., Quaglia X., Amarante J., Zurn A.

Chirurgie Expérimentale-CHUV[1]

Chondroitin Sulfate Proteoglycans (CSPGs) are a family of extracellular matrix glycoproteins with inhibitory properties whose expression is increased following CNS lesion. We have shown recently that different CSPGs are expressed by distinct reactive glial cells in the dorsal root entry zone (DREZ) following dorsal root lesion, indicating that they may contribute to its growth-inhibitory environment. In the dorsal root lesion model, sensory axons regenerate through the peripheral dorsal root but stop growing once they reach the DREZ. This lesion leads to a glial reaction in the DREZ and dorsal column of the spinal cord and to Wallerian degeneration. Recent studies in the rat indicate that the dorsal column is less inhibitory to axonal growth than the DREZ. We used LCM to harvest the DREZ and the dorsal column post-lesion and compared temporal and quantitative changes in CSPG gene expression in these two regions by real-time PCR. Our preliminary results show that genes for glial markers and Neurocan are increased 1, 3, and 5 days post-lesion in both regions, whereas Brevican, Versican V1 and V2 gene expression is increased only in the DREZ. This indicates that these proteoglycans may contribute to shaping the distinct inhibitory properties of these two areas.

Experimental neuropathic pain: transcriptional characterization of tetrahydrobiopterin pathway in injured and non-injured primary neurons

[1]Huguenin-Elie A., [1]Berta T., [1]Pertin M., [1]Decosterd I.

Anesthesiology (CHUV) & DBCM (UNIL)[1]

BACKGROUND: Peripheral nerve injury may lead to neuropathic pain that is characterized by changes in gene expression in both injured and adjacent non-injured dorsal root ganglia (DRG) neurons. Among those changes, the synthesis of tetrahydrobiopterin (BH4) via GTP cyclohydrolase (GCH1) is augmented. Our goal here was to further characterize transcriptional variations of key elements of BH4 pathway in injured and non-injured nociceptors.
METHODS: One week after spared nerve injury (SNI n=4) - or sham (n=4) surgery- we analyzed transcriptional profile of BH4-related enzymes by real-time RT-PCR. We selected nociceptors and injured versus non-injured neurons from DRG tissue sections by laser capture microdissection (LCM). In addition, *in situ* hybridization was performed on tissue sections from animals previously injected with retrograde tracers in the specific territories of injured and non-injured nerves.
RESULTS: We observed a significant increase ($p<0.05$) of BH4-related enzymes (GCH1, sepiapterin reductase and quinoid dihydropteridine reductase) after SNI. Refined transcriptional analyses showed an upregulation of mRNA for all transcripts, with predominant changes in the injured neurons population.
CONCLUSION: We demonstrated that the gene expression for the whole BH4 pathway is altered, this in specific population of sensory neurons. Taking into account that in human, the presence of a particular GCH1 haplotype with a potential loss of function is pain-protective; our results provide new information for the hyperalgesic state following nerve injury.

Expression profiling of genes regulated by the depolarizing activity of GABA during the development of cortical neurons in vivo

[1]Fiumelli H., [1]Martin J.-L.

Department of Physiology, UNIL[1]

Although GABA is the main inhibitory neurotransmitter in the adult brain, it depolarizes immature neurons and serves trophic functions during neuronal development. Overexpression of the K^+/Cl^- cotransporter KCC2 in developing neurons prematurely shifts the reversal potential for chloride ions and converts early GABA action from excitation to inhibition. Using this approach, we have demonstrated that the depolarizing action of GABA is essential for the morphological maturation of cortical neurons *in vivo*. However, the cellular and molecular mechanisms underlying perinatal trophic actions of GABA are unknown. We propose to identify genes pertaining to the excitatory action of GABA during development of cortical neurons by comparing the gene expression profile of normal developing cortical neurons to that of cortical neurons in which the action of GABA is prematurely converted to inhibition. In this study, we perform *in utero* electroporation of ventricular progenitors giving rise to layer II/III cortical neurons with GFP or KCC2/GFP-expressing plasmids to yield GFP-labeled populations of control neurons or of neurons in which excitatory GABA-mediated responses are eliminated, respectively. These populations of GFP- and KCC2/GFP-expressing cortical neurons are then purified postnatally by fluorescence-activated cell sorting and RNA isolated. Genes whose expression levels are different between these populations will be identified by microarray analysis. This study may lead to the identification of genes that are essential for cortical development and that may represent novel targets for the treatment of cortical development disorders.

Bmi1 deletion delays photoreceptor degeneration in Rd1 mice independently of the ink4a/arf locus

[1]Zencak D., [1]Crippa S., [1]Tekaya M., [1]Wanner D., [2]Tanger E., [2]vanLohuizen M., [3]Arsenijevic Y.

Jules Gonin Eye Hospital[1], Netherlands Cancer Institute[2], Jules GOnin Eye Hospital[3]

Rd1 mice are a well-known model of retinitis pigmentosa, characterized by a mutation in the Pde6b gene. They display a very rapid degeneration of rod photoreceptors (PRs) starting at 2 weeks of age, followed by a progressive loss of cones. Bmi1 is a polycomb family member impotant in CNS development and known to repress the p16ink4a and p19arf tumor suppressors encoded by the ink4a/arf locus. Here, we characterized the progression of the disease in Rd1 versus Rd1;Bmi1-/- mice by comparing the histology at different stages between P12 and P34 and tested retinal function by electroretinogram (ERG) recording. At P34, Rd1;Bmi1-/- retinas harboured 5-10 rows of rhodopsin and recoverin-positive PRs in the central retina compared to 1 scattered row in Rd1 mice. ERG recording in scotopic conditions showed that the photoreceptors preserved in Rd1;Bmi1-/- were functional. To test whether the Bmi1-related rescue occurred via the ink4a/arf locus, we analyzed Rd1;Bmi1-/-;Ink4a/Arf-/- eyes and observed no difference compared to Rd1;Bmi1-/- littermates. Thus, Bmi1 deletion delays degeneration in Bmi1 in an ink4a/Arf-independent manner. We are currently investigating the mechanisms underlying this rescue.

THE DISSOCIATED EXPRESSION OF AGAT, GAMT AND CT1 IN CNS SUGGESTS THE TRANSPORT OF GUANIDINOACETATE BETWEEN BRAIN CELLS FOR CREATINE SYNTHESIS TO OCCUR.

[1]Braissant O., [1]Henry H.

Clinical Chemistry Laboratory, CHUV[1]

The lack of creatine transporter (CT1) in astrocytes makes the import of creatine from blood inefficient in CNS, which relies more on endogenous creatine synthesis through AGAT and GAMT expression. This seems contradictory with CT1 deficiency, which, despite AGAT and GAMT expression, leads to creatine lack in CNS. To elucidate this, our aim was to finely dissect the cell-to-cell (co-)expression of AGAT, GAMT and CT1 in CNS.
AGAT, GAMT and CT1 (co-)expression was analyzed by combining in situ hybridization and immunohistochemistry. The proportions of cells expressing AGAT, GAMT, CT1, AGAT+GAMT, AGAT+CT1, GAMT+CT1, AGAT+GAMT+CT1, or none, were calculated in various regions of the rat brain (cortex, caudate putamen, hippocampus, hypothalamus, inferior colliculus, pons, cerebellum).
In most structures, cells co-expressing AGAT+GAMT, equipped to self-synthesize creatine, were <20%. Cells co-expressing GAMT+CT1 were also <20%. In whole CNS, 30-50% of cells did not express AGAT nor GAMT, and only 2-15% express CT1 alone. In cortex and caudate putamen, very few cells seemed able of their own creatine synthesis, in agreement with the creatine lack observed by MRS in CT1-deficient patients.
Our work suggests that to allow CNS synthesis of creatine, guanidinoacetate must be transported from AGAT- to GAMT-expressing cells possibly through CT1, thus explaining why CT1-deficient patients lack creatine in CNS. Moreover, high proportion of cells with no expression of AGAT, GAMT and CT1, and low proportion of cells expressing CT1 alone, suggest that brain cells express AGAT, GAMT and CT1 on demand to timely adapt their creatine needs.

Supported by the Swiss National Science Foundation (grants 3100A0-100778 & 3100A0-116859)

Combined liver-kidney transplantation in methylmalonic acidemia : autonomous methylmalonate synthesis in the brain necessitates peri-operative and long ter

[1]BALLHAUSEN D., [2]BOULAT O., [3]KERN I., [4]GIRARDIN E., [4]PARVEX P., [5]CHARDOT C., [6]BELLI D., [7]HABRE W., [7]MAMIE C., [8]BIANCHI N., [1]PITTET V., [1]MITTAZ-CRETTOL L., [2]BRAISSANT O., [1]BONAFE L.

Molecular Pediatrics, CHUV[1], Clinical Chemistry Laboratory, CHUV[2], Inborn Errors of Metabolism, HUG[3], Pediatric Nephrology, HUG[4], Pediatric Surgery, HUG[5], Pediatric Gastroenterology and Hepatic Transplantation, HUG[6], Pediatric Anesthesia, HUG[7], Unit for Clinical Nutrition, CHUV[8]

In methylmalonic acidemia, methylmalonate (MMA) and propionate (PA) are mainly produced in the liver from Isoleucine, Leucine, Threonine, and odd-chain fatty acids. Catabolic states (infections, fasting, major surgery) mobilize branched-chain amino acids from muscle and odd-chain fatty acids from adipose tissue, resulting in life-threatening accumulation of PA and MMA. MMA and PA toxicity occurs during acute phases of metabolic decompensation but also leads to chronic renal failure necessitating kidney transplantation. However, in these patients the life-span of the transplanted organ is shortened due to ongoing MMA toxicity. The rational of combined liver-kidney transplantation is to reduce MMA production to protect the kidney from further intoxication as well as to "cure" the metabolic disease and discontinue the low-protein diet. The experience of liver-kidney transplantation is limited to a small number of cases and shows a high incidence of peri-/post-operative brain damage, despite strong reduction of plasma MMA after transplantation.

We present a new approach to liver-kidney transplantation in a patient with methylmalonic acidemia based on the assumption that brain damage may occur during or after transplantation because of autonomous synthesis of MMA in brain. The peri-operative management consisted in maximal anti-catabolic treatment, adapted anesthesia protocole, and careful tuning of plasma amino acid concentrations by nutritional intervention. While plasma MMA levels after transplantation reduced enormously (-90%), the decrease of CSF MMA was less important (-36%), suggesting that MMA synthesis takes place autonomously in brain. The low-protein diet was maintained as neuroprotective measure. Follow-up at 6 months shows good liver and kidney function, no metabolic decompensation, and no neurological deterioration.

Autonomous synthesis of MMA in brain tissue is hypothesized but not demonstrated to date. Our preliminary data on methylmalonyl-CoA mutase expression in the rat brain seem to confirm this hypothesis.

Activation of c-Jun in the nuclei of neurons of the CA-1 in thrombin preconditioning

[1]Hirt L., [2]Jerome B., [1]Hirt L.

Neurology, CHUV[1], Neurosurgery, CHUV[2]

Recently it has been shown that the c-Jun N-terminal kinase (JNK) plays a role in thrombin preconditioning (TPC) in vivo and in vitro.
To further investigate the pathways involved in TPC we performed an immunohistochemical study in hippocampal slice cultures. Here we show that the major target of JNK, the AP-1 transcription factor c-Jun is activated by phosphorylation in the nuclei of neurons of the CA1 region using phospho-specific antibodies against the two JNK phosphorylation sites. The activation is early and transient, peaking at 90 minutes and not present by three hours after low dose thrombin administration (0.01U/mL). Interestingly, if we use high doses of thrombin (10U/mL) which are not toxic and do not induce neuroprotection, activation of c-Jun is also observed in the nuclei of neurons in the CA1 but after 6hours, with stronger labelling and still activated at 24hours.
Using an antibody against the Ser 73 phosphorylation site of c-Jun we identify additional immunoreactive proteins on Western blots which we show, by immunohistochemistry analysis, are under the control of thrombin at preconditioning doses activating the JNK pathway.
Identification of these proteins may provide important clues to targets involved in establishing tolerance to ischemia in thrombin preconditioning.

Psychotherapeutic Case Conceptualization using Plan Analysis for Bipolar Affective Disorder

[1]Kramer U., [2]Berger T., [2]Caspar F.

Insitut Universitaire de Psychothérapie[1], Université de Berne[2]

Valid individualized case conceptualization methodologies, such as Plan Analysis, are rarely used for the psychotherapeutic treatment conceptualization and planning of Bipolar Affective Disorder (BD), even if data do exist showing that psychotherapy interventions might be enhanced by applying such analyses for treatment planning for several groups of patients. We applied Plan Analysis as a research tool (Caspar, 1995) to *N* = 30 inpatients presenting Bipolar Affective Disorder, who were interviewed twice. Our study aimed at producing a prototypical Plan structure encompassing the most relevant data from the 30 individual case conceptualizations. Special focus was given to links with emotions and coping Plans. Inter-rater reliability of these Plan Analyses was considered sufficient. Results suggest the presence of two subtypes based on plananalytic principles: emotion control and relationship control, along with a mixed form. These subtypes are discussed with regard to inherent plananalytic conflicts, specific emotions and coping Plans, as well as symptom level and type. Finally, conclusions are drawn for enhancing psychotherapeutic practice with BD patients, based on the motive-oriented therapeutic relationship.

Enhancement of autophagy in a rat model of neonatal cerebral hypoxia-ischemia

[1]GINET V., [2]PUYAL J., [3]MAGNIN G., [2]CLARKE P., [4]TRUTTMANN A.

Departement of Neonatology-CHUV[1], DBCM[2], DBCM-CHUV[3], CHUV[4]

Understanding the cell death mechanisms involved in hypoxia-ischemia (HI) insult in neonatal models is essential to design new therapeutic strategies for perinatal asphyxia. In fact, the dichotomy of apoptosis and necrosis is changing now to a more complex view of the cell death types involved since there is evidence for a third morphological cell death type: autophagic cell death. (Macro)autophagy is a mechanism consisting in sequestering organelles and part of the cytosol in double-membrane vesicles (autophagosomes) inside the cell followed by their fusion with lysosomes for degradation (autolysosomes). Moderate autophagy occurs in healthy cells to maintain cellular homeostasis, but in some stress conditions such as excitotoxicity, excessive autophagy is involved in mediating neuronal death. In the present study we investigated if neonatal cerebral HI (permanent occlusion of the right common carotid artery followed by 2h hypoxia in P7 male rats) enhances autophagic mechanisms.

Western blot analysis against LC3 showed a significant increase in the LC3-II form (a specific marker of autophagosomes) in the damaged hemisphere from 6h after HI. Immunohistochemistry showed that LC3 was mainly expressed by neurons and electron microscopy confirmed the presence of enhanced autophagy in some dying neurons displaying numerous autophagosomes and autolysosomes. Moreover we also demonstrated that lysosomal activities were significantly increased in the lesion as shown by the strong labelling for cathepsin D in neurons and by the increase in acid phosphatase and β-hexosaminidase activities.

In conclusion, our results show for the first time that cerebral HI strongly enhances autophagic mechanisms in the neonatal rat brain. In the future we will investigate the functional significance of the autophagy in mediating neuronal death and its relationship with the other cell death pathways.

DEMYELINATION IN EARLY ALZHEIMER'S DISEASE: A MAGNETIZATION TRANSFER IMAGING STUDY AT 3T.

[1]Fornari E., [2]Knyazeva M., [1]Meuli R., [3]Ghika J., [3]Brioschi A., [3]Bourquin I., [1]Maeder P.

Department of Radiology, Centre Hospitalier Universitaire Vaudois and University of Lausanne[1], Department of Radiology and Department of Neurology, Centre Hospitalier Universitaire Vaudois and University of Lausanne[2], Department of Neurology, Centre Hospitalier Universitaire Vaudois and University of Lausanne[3]

BACKGROUND
AD is a neurodegenerative disorder manifested by progressive cognitive deterioration. Since higher cognitive functions are based on distributed neural networks, AD-associated cognitive impairment is expected to result from compromised cortical connectivity. Recently, the breakdown of myelination has been suggested to be an essential factor in AD development (Bartzokis 2004). The aim of this study is to estimate regional myelination in newly diagnosed AD patients.
METHODS
Ten patients (mean age 68.8 yrs, CDR:0.5-1, FAST:3-4) and 9 age-matched controls were successfully scanned on a 3 Tesla Philips scanner. The protocol included a sagittal T1-weighted 3D gradient-echo sequence (MPRAGE, 160 slices, 1mm isotropic voxels) and a gradient-echo MTI (FA 30, TE 15, matrix size 256*256, pixel size 1*1 mm, 36 slices, 3mm thick, MT pulse duration: 7.68 ms, FA 500, Frequency offset 1.5kHz). MT images were coregistered to the T1 acquisition. The MTR for every intracranial voxel was calculated as follows:
$MTR = (M0 - Ms)/M0 * 100\%$
where Ms represents the intensity of voxels with saturation, and M0 that without saturation. Subsequently, the T1 images were segmented, producing probability maps for the grey matter (GM), white matter (WM), and CSF for each subject in its native space. A mask was defined by thresholding the WM probability map at $p>0.95$. In order to exclude the contribution of GM and CSF, the mask was applied to the MTR coregistered images. Only voxels with MTR>10% were included in the following calculations. For parcellation of the entire brain, we used the MNI template and Brodmann Atlas. Each area of interest was denormalized according to the subject's morphology and applied separately to the individual MTR maps. We chose mean regional MTR values as an estimator of myelination. Differences in mean MTR values between AD patients and controls were tested with the Two-sample T-test.

RESULTS
We found a decrease (t-test, $p<0.05$) in the mean regional MTR values in the frontal and temporal lobes of the left hemisphere (Fig. 1a) and a tendency for similar changes in the symmetrical lobes of the right hemisphere ($p<0.07$), as well as in occipital lobes ($p<0.07$) in AD patients compared to controls. No region revealed the opposite trend. To test the fine-scale performance of MT-MRI, we selected Brodmann's areas 22, 44-45, and 46, where cortical damage has been reported early in AD (Bozzali 2006). We found significant area-specific demyelination (Fig. 1b) in the left hemisphere.
CONCLUSION
The preliminary data confirm that the MT-MRI protocol is sufficiently sensitive both for a meso-scale and for a fine-scale quantification even when applied to a small sample of AD patients.

Bozzali et al. "The contribution of voxel-based morphometry in staging patients with mild cognitive impairment." Neurology. 2006
Bartzokis G et al. "Quantifying age-related myelin breakdown with MRI: novel therapeutic targets for preventing cognitive decline and Alzheimer's disease." J Alzheimers Dis. 2004

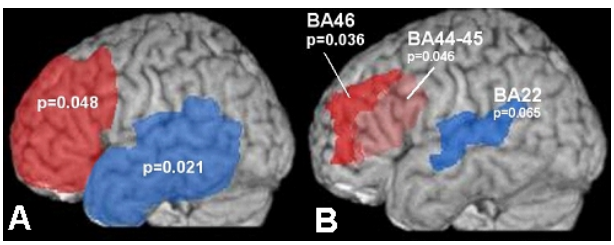

Comparison of CT-Based vs. Source-Based Attenuation Correction in Striatal F-18-DOPA Uptake

[1]Prior J., [1]Allenbach G., [1]Castaldo S., [1]Malterre J., [1]BischofDelaloye A., [2]Vingerhoets F.

Nuclear Medicine - CHUV[1], Neurology department - CHUV[2]

Aim:

F-18-DOPA PET is a well-established method to image dopamine transporter system in human brain. In PET/CT scanners, AC is performed with a CT-based method (CT-AC) as compared to Ge-68/Ga-68 source transmission scan (S-AC) of PET only scanners. The influence of CT-AC on the determination of the influx constant (Ki) to measure dopamine transporter expression is unknown.

Methods:

Ten volunteers and Parkinson disease patients (55±15y) underwent a 38-frame 120-min or 25-frame 96-min acquisition after the injection of 120MBq of F-18-FDOPA, performed after AC acquisitions (CT-AC: 140keV, 80mA; S-AC: 10-min transmission scan; Discovery LS, GE). Striatal and occipital ROIs were drawn and time-activity curves (TAC) were generated summing the 5 central slices encompassing the striatum. Ki was computed using the occipital cortex TAC as input function. Differences in striatal and occipital TAC were characterized, and differences in Ki derived using voxel-based kinetic analysis (PMOD software). Comparisons were performed with Pearson's correlation and Bland-Altman plots.

Results:

Absolute differences in striatal and occipital TAC between CT-AC and S-AC were <0.3kBq/mL (7%) in all studies (mean –0.01±0.16kBq/mL [–1±4%]). Absolute difference in Ki was <0.7E-3/min (7.7%) in any striatal voxel (mean –0.03E-3±0.3E-3/min [0.2±3.6%]). Correlation of Ki between both AC methods was excellent (y=0.9990 x+0.0, r=0.9947, p<0.0001) without systematic error (p>0.8). All measurement pairs were within Bland-Altman's reference range (–1E-3 to +1E-3/min). The largest variations were observed around the skull's outline and at the interface between air and bone, in relation to differences in AC maps resolution or minor patient motion (n=1).

Conclusion:

CT-based AC introduces a difference <7% in TAC and <8% in voxel-based striatal Ki estimates as compared to source AC. Average differences of 1±4%, an excellent correlation between AC methods and absence of systematic differences allows using both AC method or norms interchangeably when comparing patient groups. However, in follow-up studies aiming at assessing individual disease progression or response to treatment, the same AC method should be used to avoid introducing additional variability.

Induction of aquaporin 4 expression in ischemic mouse brain after thrombin preconditioning: correlation with the reduction in oedema

[1]Badaut J., [2]Price M., [2]Wiegler K., [1]Mastour N., [1]Brunet J.-F., [2]Hirt L.

Neurosurgerical Research Group[1], Neurology[2]

Background :

Our recent studies have shown that the water channel aquaporin-4 (AQP4) is induced 1h after stroke onset. AQP4 has a dual function in the evolution of oedema; the absence of AQP4 in KO-mice reduces the early cytotoxic oedema formation and in contrast aggravates the later vasogenic oedema. A second aquaporin, AQP9, is induced at a later time-point after stroke onset, and the function of AQP9 is predicted to be in relation with brain energy metabolism.

Thrombin at high doses is known to induce oedema while preconditioning is induced by a single injection of a low dose of thrombin (TPC). TPC attenuates lesion size and oedema after middle cerebral artery occlusion (MCAo). TPC is a useful model to understand endogenous mechanisms of protection after brain ischemia and increase our knowledge of the roles of aquaporins in oedema development. We studied the expression of AQPs in ischemic mouse brains after TPC in correlation with the reduction in oedema formation.

Methods :

For TPC, mice were injected ICV with 0.01U of mouse thrombin, or with and equal volume of saline (controls), followed 24 hours later by 30mins of transient MCAo. Expression of AQP4 and AQP9 was evaluated by RT-PCR and immunohistochemistry 1h and 48h after ischemia and correlated with oedema.

Results :

In TPC animals, oedema formation assessed by measurement of the hemispheric enlargement is significantly reduced at 1h (4.5 ± 2% vs 11.0 ± 5% in controls, $p<0.05$, $n=8$) and confirmed by the wet-weight/dry-weight ratio. Correlating with the reduction in oedema, there was a 1.5 fold increase in AQP4 levels compared to controls localised in the ischemic striatum. The AQP4-M1 mRNA isoform was induced at 1h in the ischemic hemisphere. The oedema is also significantly decreased at 48h after stroke in TPC mice, and the level of expression for AQP4 is still higher, but the difference is no longer significant.

At 1h, the number of AQP9 positive astrocytes is also 2 fold higher in TPC animals than in controls (1089 ± 260 vs 480 ± 280 positive cells in CTL) throughout the brain. At 48h, there is no difference in AQP9 positive cells between controls and TPC mice.

Discussion :

The correlation between the early induction of AQP4 and the decrease in oedema formation in TPC mice suggests that the induction of AQP4 prevents the development of the oedema. In ischemic hemisphere, the isoform AQP4-M1 is preferentially induced and could contribute to the disorganization of orthogonal arrays in astrocyte endfeet. AQP9 was also induced in TPC mice, throughout the brain and may also participate in tissue protection but the mechanisms need future investigations.

Neurobiology of addiction : role of the transcriptional regulators CREB, CBP, and C/EBPbeta ?

[1]Guidi R., [1]Steimann M., [1]Boutrel B., [2]Magistretti P., [3]Halfon O., [1]Cardinaux J.-R.

CNP-CHUV[1], CNP-CHUV, BMI-EPFL[2], SUPEA-CHUV[3]

Drug addiction is a chronic, relapsing psychiatric disorder that results from adaptations of the brain in response to excessive drug stimulation. The substrates of persistent compulsive drug use are hypothesized to be molecular and cellular mechanisms that underlie long-term associative memories in several forebrain circuits. In this context, the transcription factor CREB was shown to be critical. When CREB is phosphorylated, it recruits the CBP coactivator, and activates the expression of a set of genes that modifies the properties of certain neurons in the reward pathway. We postulated that the transcription factor C/EBPbeta, as a CREB target gene, could be involved in the drug-induced molecular adaptation of the reward pathway, and that the preventing CREB:CBP interaction would decrease CREB transcriptional activity, and thus C/EBPbeta expression. We are developing different strategies to selectively block CREB-mediated transcription in vivo either by interfering with the binding of CBP to CREB, or by blocking CBP HAT activity. Furthermore, several transgenic mice lines expressing eGFP under the control of 5 C/EBP-binding sites have been developed to determine C/EBP-dependent gene expression. Our aim is to use a conditioned place preference paradigm to better define the role of CREB, CBP, and C/EBPbeta in reward-related learning and memory.

Bioengineering artificial neural stem cell niches

[1]Cordey M., [1]Limacher M., [1]Lutolf M.

Institute of Bioengineering - EPFL[1]

In humans and rodents, newborn neurons arise from neural stem/progenitor cells (NSCs) in the subgranular zone of the dentate gyrus in the hippocampus, and in the subventricular zone of the lateral ventricule wall. The regionally restricted nature of adult neurogenesis indicates that extracellular cues specific to neurogenic regions, termed *niches*, induce neuronal competence in NSCs. In order to harness the tremendous potential of neural stem cells for clinical use, a better molecular understanding of the soluble and insoluble factors that control NSC maintenance, self-renewal and differentiation is crucial. To meet this need we are developing versatile microengineered platforms that allow fate decisions of individual NSCs to be monitored under well-controlled conditions. A microwell array system is presented that consists of polyethylene glycol (PEG) hydrogel substrates, micropatterned and selectively functionalized with relevant signaling proteins to reconstruct desired biochemical aspects of the NSC niche in vitro. Propagation of single NSCs to neurospheres within microwells was tracked by time-lapse video microscopy. Trapping of single stem cells on the array surface thus allowed *i)* to prevent “fusion” events that are likely in conventional neurosphere suspension cultures (Singec *et al*, Nature Methods, 2006), thereby unequivocally attributing sphere formation to an individual cell, and *ii)* to quantitatively assess the heterogeneity in neurosphere-forming capability of the entire population.

Effects of albumin treatment on the AQP4 expression in a rat model of neonatal stroke

[1]Badaut J., [2]Ashwal S., [3]Obenaus A.

Neurosurgery Research Group[1], Deaprtment Pediatrics, Loma Linda University[2], Department of Radiation Medicine, Loma Linda University[3]

Serum albumin treatment has been shown to be a potential therapy in adult rodent stroke models. Neuroprotective effects of albumin have been attributed to hemodilution of blood. Albumin also can have other effects including reducing activity, improving tissue perfusion, reducing brain edema and maintaining normal astrocytic function. In a previous study, we have shown that albumin is ineffective in reducing infarct volume in a neonatal 10d-old rat pup transient filament middle cerebral artery occlusion (tfMCAO) model (Wang A et al., Pediatric Res. 2007). However, serum albumin therapy reduced the blood-barrier permeability (BBB).

Because aquaporin 4 expression in astrocytes is related to BBB maintenance and involved in edema evolution after stroke, we investigated whether albumin treatment in neonatal stroke alters AQP4 expression in 10 day rat pups treated with 0.25% albumin or saline 1 hour after reperfusion. Magnetic resonance imaging (MRI) measurements and AQP4 immunohistochemistry at 3were performed after tfMCAO.

Quantitative MR analysis at 3 days after tfMCAO demonstrated increased T2-values (60%) while ADC values were decreased in the ischemic compared to the contralateral tissues in both saline and albumin treated pups. These MR values modifications are correlated with a decrease of the AQP4-labelling (73%) in the ischemic compared to contralateral hemispheres. However at 28 days ADC values were significantly higher (139%) in the albumin-ischemic hemisphere than the contralateral hemisphere and saline group. The intensity of the AQP4 staining was also significantly higher (150%) in ischemic part than the contralateral part at 28 days. Double immunolabelling with GFAP showed that the increased of the AQP4 staining was observed in glial cells.

Interestingly, albumin treatment in rat pups results in a long term modification of the level of AQP4 expression that correlated to a significant increase in MR-signals (T2 and ADC) at 28 days after stroke onset. This increase of the AQP4 can facilitate the water movement between injured tissues through the glial cells that can be monitored by MRI.

Metabolism and neuroprotection in focal cerebral ischemia

[1]Berthet C., [2]Lei H., [2]Gruetter R., [3]Gruetter R., [4]Magistretti P., [5]Magistretti P., [6]Hirt L.

Chuv, neurologie[1], CIBM, EPFL[2], radiologie, unil[3], neurosciences psychiatriques, chuv[4], brain and mind institute, EPFL[5], Neurologie, chuv[6]

Cerebral ischemia results in a lack of oxygen and nutrient supply to the affected area, leading to lactate accumulation as an end product of anaerobic glycolysis, due to oxygen deprivation. High levels of lactate are known to be toxic and extent of lactate accumulation correlates with lesion size. On the other hand, lactate can be used as an energy substrate by neurons and has also been shown to protect against excitotoxic damage to the brain. Indeed, in the prensence of oxygen, lactate can be converted directly to pyruvate which can then produce 17 ATPs per oxydized molecule. In an attempt to understand the exact role of lactate in ischemia, we tested if lactate administration directly after ischemia could be neuroprotective.
In an in vitro model of oxygen and glucose deprivation (OGD) on rat organotypic hippocampal slices, addition of lactate to the medium at a final concentration of 4mM, directly after OGD, protected against neuronal death, whereas a higher dose of 20mM was toxic. In vivo, in a model of middle cerebral artery occlusion, intra-cerebroventricular injection of 2µl of 100mM lactate (corresponding to 4mM final concentration) after reperfusion, lead to a decrease in lesion size.
We also tested the feasibility of establishing a neurochemical profile of the ischemic region by ^{1}H NMR sperctroscopy at 14.1T. Preliminary results of ^{1}H NMR spectroscopy confirmed the strong increase in lactate observed by others.
Our first results with lactate injection show a neuroprotective effect of lactate directly after ischemia. Further data on the therapeutic window and the mode of administration will tell us if lactate could be given as a neuroprotectant to stroke patients in the future. The neurochemical profile obtained at different timepoints after ischemia will help us to understand better the role of lactate and other metabolites in ischemia.

ODE
Oncologie et Développement

Oncologie et Développement/ODE-1

Human observer template in mammography

[1]Castella C., [2]Abbey C., [2]Eckstein M., [1]Verdun F., [3]Kinkel K., [4]Bochud F.

Institut Universitaire de Radiophysique AppliquÃ©e - CHUV[1], University of California, Santa Barbara, USA[2], Clinique des Grangettes, ChÃªne-Bougerie[3], Institut Universitaire de Radiophysique Appliquée - CHUV[4]

In this study we estimated human observer linear templates underlying the detection of a realistic, spherical mass signal with mammographic backgrounds. Five trained naïve observers participated in two-alternative forced-choice (2-AFC) detection experiments with the signal superimposed on synthetic, clustered lumpy backgrounds (CLB) in one condition, and on nonstationary real mammographic backgrounds in another. Human observer linear templates were estimated using a genetic algorithm. A variety of common model observers templates were computed and their shapes and associated performances were compared to the human observers'.

The estimated linear templates are not significantly different for stationary CLB and real mammographic backgrounds. The estimated performance of the linear template compared with the human observers is within 5% in terms of percent correct (Pc) for the 2-AFC task. Channelized Hotelling models can fit human performance, but the templates differ considerably from the human linear template. Due to different local statistics, detection efficiency is significantly higher on nonstationary real backgrounds than on globally stationary synthetic CLB. This finding emphasizes that nonstationary backgrounds need to be described by their local statistics.

Transmembrane domains of the Latent membrane protein 1 of Epstein-Barr virus play a critical role in beta-TrCP binding

[1]Zuercher E., [1]Butticaz C., [1]Wyniger J., [2]Baur A., [1]Telenti A., [1]Rothenberger S.

Institute of Microbiology- CHUV[1], Institute of Pathology-CHUV[2]

Background:
The B lymphotropic human herpes virus Epstein-Barr (EBV) latently infects > 90% of the population and is associated with several types of malignancies. Latent membrane protein 1 (LMP1) is predominant among the proteins that contribute to cell transformation. LMP1, a transmembrane protein with a short N-terminus, six transmembrane segments (TM1-6) and a long C-terminus, activates Nuclear Factor-κB (NF-κB) constitutively. In this study we mapped the interaction site between LMP1 and Beta-transducing repeats-containing proteins (β-TrCPs). β-TrCP1 and 2 are two homologous F-box proteins that function as the substrate recognition subunit of the E3 ubiquitin ligase $SCF^{\beta\text{-}TrCP}$, a complex which mediates the ubiquitination and degradation of many proteins involved in the regulation of the cell cycle and signal transduction, such as the NF-κB inhibitor IκBα.

Materials & Methods:
LMP1 with deletions or point mutations were constructed by PCR and verified by sequencing. Expression vectors for LMP1, LMP1 mutants and β-TrCP were transfected into HEK 293 T cells and protein expression verified 24 hours post-transfection by western blotting. Interaction between LMP1 and β-TrCP was assessed by co-immunoprecipitation. The activation of NF-κB was measured 24 hours after transfection in 24 well plates using dual luciferase Promega kit and a Berthold luminometer.

Results:
LMP1 with mutations in a putative β-TrCP binding motif DSGXXS located in the C-terminal domain behave as the wild-type LMP1, with respect to β-TrCP binding and NF-κB activation. LMP1 constructs with deletions of either the N-terminal domain (a.a. 1-24) or the C-terminal domain (a.a 187-386) bind β-TrCP as the full length form, indicating that these two domains are dispensable for the interaction. To evaluate the contribution of individual transmembrane segments pairs to β-TrCP binding we generated LMP1 mutants lacking various combinations of TMs. In parallel, we measured NF-κB activation levels and the binding to Tumor necrosis factor receptor-associated factor 3 (TRAF3). Taken together our results reveal a critical role of TM 3 and 4 and the intracellular loop L4 that link TM4 to TM5 for β-TrCP1 and β-TrCP2 binding. In particular, point mutations in L4 were associated with a decrease in β-TrCPs and TRAF3 binding, and an increase in NF-κB activation levels.

Conclusions:
We demonstrate that LMP1 transmembrane segments and the loops that link them are not only important for membrane insertion but play a determinant role in protein-protein interaction and regulation of signalling properties.

Activated wnt/beta-catenin pathway cooperates with MDR1 in multi-drug resistant neuroblastoma cells

[1]Flahaut M., [1]Muhlethaler A., [2]Niggli F., [1]Meier R., [1]Coulon A., [1]Joseph J.-M., [1]Gross N.

Paediatrics Oncology-DMCP-CHUV[1], University Children Hospital, Zürich, Switzerland[2]

Neuroblastoma (NB) is an extremely heterogeneous neural crest-derived embryonic childhood neoplasm. Despite the most recent advances in combined therapies, the development of multi-drug resistance (MDR) represents a major obstacle of successful therapy.

To address the mechanisms involved in the development of multi-drug resistance, two doxorubicin-resistant (DoxR) NB cell lines (IGRN-91R and LAN-1R) were generated. These cells were shown to overexpress the *MDR1* gene-encoded P-glycoprotein, and were cross-resistant to other MDR1 and non-MDR1 substrate drugs. As the P-gp inhibitor verapamil was not able to restore 100% of drug sensitivity, the identification of other potentially MDR-related deregulated molecules was investigated. Microarray expression profiles of resistant versus sensitive parental cell lines only showed a limited number of differentially expressed genes in IGRN-91-DoxR cells. Not surprisingly the *MDR1* gene was included in the list of the 16 upregulated transcripts, while the highest overexpressed transcript was the Wnt1 receptor, frizzled-1 (*FZD1)* gene, belonging to the wnt/β-catenin pathway. FZD1 overexpression in DoxR cells was confirmed at the mRNA and protein level and functional analyses indicate that FZD1 overexpression is associated with a sustained activation of the wnt/β-catenin pathway. It is known that in some tumors activation of the wnt/β-catenin pathway may occur in the absence of β-catenin gene mutations.
To investigate the functional role of the FZD1 receptor in resistant NB cells, the microRNA-adapted small hairpin RNA (shRNAmir) method was used to specifically silence the *FZD1* gene in the two DoxR cell lines. In parallel, FZD1 was overexpressed in the two sensitive parental cell lines. Preliminary functional analyses indicate that specific FZD1 knock-down in the LAN-1R cells is associated with a sensitisation of the cells to the chemotherapeutic drugs such as doxorubicin, taxol and etoposide. Interestingly, it appears that the shRNA-mediated-FZD1 silencing effect and the verapamil-induced MDR1 inactivation effect are additive, indicating that the two mechanisms are distinct and partially implicated in the drug-resistant phenotype.
This report represents the first implication of pathological activation of the wnt/β-catenin pathway in the aggressive and drug-resistant behaviour of NB. In addition to provide new insights into the mechanisms of drug resistance and tumorigenesis, these findings could lead to the identification of specific targets to treat aggressive and resistant NB.

Functional evaluation of monoclonal antibodies against chronic lymphocytic B-cell leukaemia

[1]Andre P.-A., [1]BischofDelaloye A., [1]Kosinski M., [1]Viertl D., [2]Mach J.-P., [1]Buchegger F.

Service de Medecine Nucleaire - CHUV[1], Institute of Biochemistry - UNIL[2]

New monoclonal antibodies (mAb) against different antigens expressed by B-CLL, developed within a European program, were evaluated.
Binding and internalisation assays were performed with ^{125}I-radiolabelled antibodies on various cell lines including the original and the CD5-transfected leukaemia cell line JOK1 and JOK1-5.3, respectively. mAb mediated cell proliferation inhibition was tested with a radiolabelled-thymidine analogue and FACS analysis. Anti-tumour efficacy was tested in an intra-peritoneal (i.p.) JOK1-5.3 B-CLL model in SCID mice using early and delayed (1 and 7 days, respectively) antibody treatment initiation. Mice were sacrificed at appearance of significant disease.
Radiolabelled mAbs against CD5, CD32, CD71 and anti-HLA-DR showed specific direct bindings of ~45-70% on target cells and induced variable internalisation effects. Anti-HLA-DR strongly inhibited cellular proliferation of all cell lines tested and directly induced apoptosis. Anti-CD71 inhibited the proliferation of most cell lines with an accumulation of cells in early S-phase, but had no effect on JOK1-5.3 cell growth. No proliferation inhibition was observed with anti-CD5 or anti-CD32 mAbs. JOK1-5.3 tumour mice treated with anti-CD71 or anti-HLA-DR showed a prolonged survival of about 20 days compared with untreated or isotype matched irrelevant mAb treated controls. Similar results were observed after treatment with anti-CD5 as compared to untreated controls or sham-treated JOK1 tumour grafted mice ($CD5^-$).
In conclusion, all mAbs inhibited JOK1-5.3 leukemia development while showing variable *in vitro* effects. The broader *in vivo* efficacy of certain mAbs might be explained by their IgG_2 subclass, allowing recruitment of effector functions, but the *in vivo* efficacy of the anti-CD71 mAb, of mouse IgG_1 subclass, and having no effect on JOK1 5.3 *in vitro*, remains currently unexplained.

FDG PET/CT IN PEDIATRIC ONCOLOGY: EVALUATION OF OUR EXPERIENCE IN 15 CASES.

[1]Orcurto M.-V., [2]Garcia R.-E., [2]Beck-Popovic M., [3]AlamoMaestre L., [3]Gudinchet F., [1]BischofDelaloye A., [1]Boubaker A.

Dpt of Nuclear Medicine[1], Dpt of Pediatry[2], Dpt of Radiology[3]

Background: the aim of our study was to evaluate the impact of FDG PET or PETCT in pediatric oncology cases, and to compare the results with the conventional imaging modalities (CIM) at diagnosis and follow-up.
Methods: Between November 2003 and December 2006, 54 studies were performed in 19 patients aged 4-17 years. Four children with lymphoma were examined after initiation of chemotherapy and were excluded from the present study. We reviewed 42 studies (5 PET, 37 PETCT) performed in 15 children. Indication for PET/PETCT was: initial staging (n=9), evaluation of response to treatment (n=29) and suspicion of recurrence (n=4). Children were fasting for at least 4 hrs. Acquisition was started 45-60 min after injection 5 MBq/Kg of F18-FDG in 5-7 bed position of 3-4 minute (GE Discovery LS). A low-dose CT-scan was obtained without contrast injection.
Results: Among 15 children, 9 had lymphoma: 6 Hodgkin's disease (HD) stage II (n=1), III (n=3) and IV (n=2), and 3 stage III non-Hodgkin lymphoma (NHL), Burkitt lymphoma (n=2) and T-cell lymphoma (n=1). All had PET/PETCT performed at diagnosis. In 3 of 9 children, PET/PETCT detected more lesions than CIM, but staging was modified from stage II to III only in one child. During follow-up 20 PET/PETCT were obtained in 8 children: based on FDG uptake, complete remission was assessed after 2 courses of chemotherapy in 4 children, and after 3 to 7 cycles in 4, whereas CIM showed residual masses in 7 children. Four children had soft tissue sarcoma (2 embryonal rhabdomyosarcoma, 1 embryonal sarcoma of the liver, and 1 undifferentiated sarcoma), and two germ cell tumors (1 immature teratoma, 1 mixed germ cell tumor). PETCT allowed to detect (n=2) or confirm (n=2) recurrence in 4 of 6 children. Follow-up examinations were obtained in these 4 children: progressive disease was observed in 3 children with sarcoma, and was stable in one.
Conclusions: In children with lymphoma, FDG-PET/PETCT performed at diagnosis modified staging in one child (upstaging from II to III), and was able to evaluate early response to treatment and assess complete remission before CIM. In children with sarcoma and germ cell tumors, FDG-PET/PETCT allowed to detect or confirm recurrence, and was helpful in the evaluation of tumor progression or stability.

Title: Imatinib metabolite profiling in parallel to imatinib quantification in plasma of treated patients using Liquid chromatography - mass spectrome

[1]Rochat b., [2]Fayet a., [2]Widmer n., [1]Lahrichi s., [1]Pesse b., [2]Decosterd l., [2]Biollaz J.

qMSF - CHUV - UNIL[1], PCL - CHUV[2]

Besides affecting the systemic bioavailability of the parent drug, drug metabolizing enzymes may produce bioactive and/or toxic metabolites of clinical interest. We have investigated the capability to analyze simultaneously the parent drug and newly identified metabolites in patients' plasma by liquid chromatography coupled to tandem mass spectrometry (LC-MS/MS).

The anti-cancer drug, imatinib, was chosen as a model drug because it has opened a new area in cancer therapy and is given orally and chronically. In addition, resistance and rare but sometimes severe side effects have been reported with this therapy.

The quantification of imatinib and the profiling of its metabolites in plasma were established following 3 steps: 1. set-up of a generic sample extraction and LC-MS/MS conditions ; 2. metabolite identification by LC-MS/MS using either *in vitro* incubations performed with human liver microsomes or patient plasma samples ; 3. the simultaneous determination of plasma levels of imatinib and 14 metabolites in 38 patient plasma samples.

Partial or cross method validation has been done and revealed that precise determinations of metabolite levels can be performed whereas pure standards are not available.

Preliminary results indicate that the disposition of imatinib and its metabolites is related to interindividual variables and that outlier metabolite profiles can be revealed.

This article underscores that, in addition to usual therapeutic drug monitoring (TDM), LC-MS/MS methods can record simultaneously a complete drug metabolic profile enabling various correlation studies of clinical interest.

Journal of Mass Spectrometry ; *in press*

The t(3;5)(q21~27;q31~35) translocation in AML/MDS: a further three case reports and review of the literature

[1]PORTER S., [1]MÜHLEMATTER D., [1]BOUGEON S., [1]GOGNIAT C., [1]MERCANTON N., [1]RUCHET M.-C., [1]BEYER V., [1]PARLIER V., [2]ARBER C., [2]TICHELLI A., [3]STALDER M., [1]JOTTERAND M.

Medical Genetics - CHUV[1], Hämatologische Abteilung, KS Basel[2], Laboratoire Consilia, Sion[3]

The t(3;5) translocation and its variant, ins(3;5), is a infrequent non-random abnormality that has been documented both in AML and MDS and which results in an NPM1/MLF1 gene fusion in many, but not all, reported cases. The breakpoints described in the literature vary considerably and range from 3q21~27 and 5q31~35. Other authors have already addressed the question of true molecular heterogeneity versus variability of interpretation of the breakpoints by conventional cytogenetics and have elucidated the nature of the resulting genetic rearrangements in some of the more recently described cases. We report a further three cases of t(3;5) as a sole abnormality at disease presentation (in a 50-year-old male patient diagnosed with AML-M2, a 35-year-old female patient with AML-M2 and a 52-year-old female patient with RAEB-T). The results obtained both by G-banded chromosome analysis and fluorescence *in situ* hybridisation are presented, together with an overview of the literature to date, thus reviewing the evidence for this translocation representing a clinically distinct subtype of AML/MDS as previously suggested.

INCREASED CHROMOSOMAL ABERRATIONS AND TRANSFORMATION OF ADULT MOUSE RETINAL STEM CELLS

[1]Djojosubroto M., [1]Tekaya M., [1]Wanner D., [2]Wirapati P., [3]Radtke F., [1]Arsenijevic Y.

Jules Gonin Eye Hospital & Dept. Ophthalmology, UNIL[1], Swiss Institute of Bioinformatics (SIB)[2], Swiss Institute for Experimental Cancer Research (ISREC)[3]

The potential of stem cell degenerative diseases therapy such as retinal degeneration is recognized. Generation of high numbers of retinal stem cells (RSCs) in vitro would thus be beneficial for retina transplantation. However, cells in cultivation might be unstable and thus have higher risk of transformation.

In this study, we analyzed retinal stem cells isolated from retinas of neonatal and from epithelium of ciliary margin zone of adult mouse eyes. Both cells types are highly proliferative. Most neonatal RSCs (83%) at passage 9 retain normal chromosome number, nevertheless only 73% have normal karyotype by chromosomal painting analysis. At passage 36, 33% retain normal chromosomal number, however all cells have translocation of chromosome 16 to 9. Surprisingly, adult mouse RSCs show more chromosomal aberrations even at early passage. The chromosome number highly varies, with large proportion of cells being aneuploid.

To check for transformation possibility, we performed telomerase activity assay, anchorage-dependent cell proliferation, and subcutaneously transplanted these cells into nude mice. We found that adult RSCs formed tumors within 4-8 weeks, but no tumor was formed by neonatal RSCs after 4 months. Our data indicate that neonatal and adult RSCs have different level of chromosomal stability, and adult RSCs may have higher chance of spontaneous transformation in vitro.

PSGL-1 is not the only one

Lambelet M.

division of Hematology-CHUV

P-selectin glycoprotein ligand-1 (PSGL-1) is a major selectin ligand, which plays a critical role in mediating leukocyte rolling along inflamed vascular endothelium and malignant cell metastasis. Blocking adhesion studies with the anti-PSGL-1 mAb KPL1, showed that this mAb only partially inhibits blast cell rolling on P-selectin (11/22 cases) or L-selectin (3/9 cases) whereas it abrogates neutrophil rolling. E-selectin-dependent rolling was not affected by KPL1 mAb, suggesting that additional ligands are involved. The ability of myeloblasts, isolated from a patient with acute leukemia (#32), to roll on L- and P-selectin was only partially inhibited by KPL1 mAb (~60% inhibition). Using these cells, we examined whether additional ligands cooperate with PSGL-1 in supporting blast rolling on selectins. The expression of the selectin carbohydrate ligand CLA by blast cells from this patient was examined by western-blot analysis, which revealed five CLA+ bands migrating with molecular weights of 85,100,130,170 and 210. The ability of these potential selectin ligands to support selectin-dependent rolling was examined by performing rolling assays on western blot membranes. CHO-P-, K562-E- and 300.19L-selectin cells efficiently rolled on ~85 kDa, ~100 kDa, ~130 kDa and 210 kDa bands. An additional band of ~150-170 kDa supported E-selectin-dependent rolling. Western-blotting indicated that these bands may correspond to known potential selectin ligands CD44, CD43 and PSGL-1, which respectively migrate with a MW of ~85 kDa, 130 kDa and ~210 kDa. Immunodepletion of blast cell lysate with anti-PSGL-1, anti-CD44 or anti-CD43 supported this hypothesis. Blast cell rolling strongly decreased on the 210 kDa band after depletion of cell lysate in PSGL-1, on the 130 kDa band after depletion in CD43 and on the 85-100 kDa band after depletion in CD44. Rolling adhesion assays performed on immunoadsorbed CD43, CD44 and PSGL-1 directly demonstrated their capacity to interact with L-, P- and E-selectin. Ligands migrating as ~85 and 150-170 kDa band remain to be identified. In conclusions, our results indicate that PSGL-1, CD43 and CD44 cooperate in supporting leukemic blast cell rolling on selectins. Additional ligands migrating with as ~85 and 150-170 kDa bands remain to be identified.

Fenretinide-Induced Caspase-8 Activation and Apoptosis in Metastatic Neuroblasts

[1]RAGUENEZ G., [2]MUHLETHALER-MOTTET A., [2]MEIER R., [3]BENARD J., [2]GROSS N.

CMRS UMR 8126-IGR[1], DMPC-CHUV[2], CNRS UMR 8126- IGR[3]

Metastatic neuroblastoma (NB) is particularly resistant to cytotoxic therapy and thus raises a major therapeutic challenge in paediatric oncology. Recent studies demonstrated that NB metastasis is enhanced by the simultaneous loss of caspase-8 and $\alpha 3\beta 1$-integrin preventing Integrin-Mediated Death (IMD) to occur (Stupack *et al.,* 2006). As the role of caspase-8 appears critical in preventing metastasis, we proposed to study the effect of an antiproliferative and apoptotic inducer, the synthetic retinoid fenretinide (4-HPR), in NB. The human *MYCN*-amplified NB experimental model, - the IGR-N-91 model derived from an involved bone marrow of an high-risk NB patient (HR-NB, stage 4) – is able to disseminate *in vivo* from the primary nude mouse tumor xenograft (PTX) into myocardium (Myoc) and bone marrow (BM) of the animal. Using such model, we observed that metastatic BM and Myoc neuroblasts downregulate caspase-8 expression in contrast with a notable expression in PTX cells. This caspase-8 loss parallels a concomitant decrease of $\alpha 3$- and $\beta 1$-integrins while caspase -3, –9, -10, Bcl-2 or Bax expressions were unchanged. Data show that increasing doses of 4-HPR up-regulates caspase-8 expression in BM metastatic neuroblasts that parallels an higher sensitivity to apoptotic cell death in BM compared to PTX cells. No change was noted in the $\beta 1$-integrin or caspase-3, -9, -10 and Bcl-2 expressions. Stable caspase-8-silenced SH-EP cells appear more resistant to 4-HPR-induced cell death compared to control or caspase-10-silenced SH-EP cells. Our study thus corroborates the synergistic effect of 4-HPR with drugs, since apoptosis is restored in the VP16-resistant BM metastatic neuroblasts. This study demonstrates that 4-HPR up-regulates caspase-8 expression and induces apoptosis in metastatic neuroblasts through caspase-8 activation. These data confirm the interest to use fenretinide in clinical treatment of HR-NB patients, the performance of which currently remaining very poor despite intensive high-dose chemotherapy.

Dose optimization in pediatric Computed Tomography with a visual discrimination model

[1]Gutierrez D., [2]Gudinchet F., [2]AlamoMaestre L., [1]Bochud F., [1]Verdun F.

Institut de Radiophysique Appliquée - CHUV[1], Département de Radiologie - CHUV[2]

Technological developments of computed tomography (CT) have led to a drastic increase of its clinical utilization, creating concerns about patient exposure. To better control dose to patients, we propose a methodology to find an objective compromise between dose and image quality by means of a visual discrimination model.

A GE LightSpeed-Ultra scanner was used to perform the acquisitions. A QRM 3D low contrast resolution phantom (QRM – Germany) was scanned using $CTDI_{vol}$ values in the range of 1.7 to 103 mGy. Raw data obtained with the highest $CTDI_{vol}$ were afterwards processed to simulate dose reductions. Noise realism of the simulations was verified with normalized noise power spectra (NNPS) and standard deviation measurements.

Patient images were acquired according to Diagnostic Reference Levels (DRL) proposed in Switzerland. Noise reduction was then simulated as for the QRM phantom, to obtain five different $CTDI_{vol}$ levels, down to 3.0 mGy.

Image quality of phantom images was assessed with the Sarnoff JNDmetrix visual discrimination model and compared to an assessment made by means of ROC methodology, taken as a reference. For patient images a similar approach was taken but using as reference the Visual Grading Analysis (VGA) method.

A relationship between Sarnoff JNDmetrix and ROC results was established for low contrast detection in phantom images, demonstrating that the Sarnoff JNDmetrix can be used for qualification of images with highly correlated noise. Patient image qualification showed a threshold of conspicuity loss only for children over 35 kg.

Keywords: Computed Tomography, pediatric dose optimization, image quality, visual discrimination model

Preclinical evaluation of APO866, a novel anti-tumor agent in treatment of hematological malignancies

[1]Nahimana A., [1]Aubry D., [2]Attinger A., [2]Ireson C., [2]Greaney P., [2]Dawson K., [2]Butcher S., [2]Dupuis M., [1]Duchosal M.

Service d'hématologie[1], TopoTarget S.A.[2]

Treatment of cancers is currently under intense development. Despite the progress achieved, cancer drug resistance still a major problem in chemotherapy. Apoptosis resistance is one of the central hallmarks by which cancer cells survive. Targeting cell death by new pathways would be an attractive approach in cancer treatment. In this context, efforts were deployed to develop anticancer agents that induce cell death by manipulating the cellular energy stores through nicotinamide and adenosine triphosphate (ATP). Intracellular depletion of nicotinamide adenine dinucleotide (NAD) and ATP was reported to have a strong cytolytic effects. Recently, a novel antitumor agent, APO866, has been reported to induce apoptosis by reducing cellular NAD^+ content. APO866 is a novel antitumor agent of a new class that elicits a potent growth-inhibitory response in many solid tumors by inhibiting Nicotinamide Phosphoribosyltransferase (NAmPRTase), a key enzyme in the regulation of NAD^+ biosynthesis from the natural precursor nicotinamide.

To identify hematological indications that could potentially benefit from APO866 treatment, we evaluated the *in-vitro* and *in-vivo* anti-tumor effects of APO866 on cell lines (n= 42) and primary cells (n= 31) representing various hematological malignancies. APO866 exhibits a potent anti-growth and tremendous killing effect in various hematological malignant cells with acute myeloid leukemia, acute lymphoblastic leukemia, chronic lymphocytic leukaemia, mantle cell lymphoma, and T-lymphoma primary cells being the most sensitive. Treatment with APO866 induced a rapid decrease in intracellular NAD, which was followed by that of ATP. The decrease in intracellular ATP correlated with detection of cell death. Further, the *in-vivo* administration of APO866 as single agent prevents and abrogates tumor growth in animal models of different human hematological malignancies.

The results provide evidence for the potential use of APO866 as a therapeutic agent in various hematological malignancies.

MOLECULAR MECHANISMS OF HDAC INHIBITORS-INDUCED CELL DEATH IN NEUROBLASTOMA CELLS

[1]Mühlethaler-Mottet A., [2]Flahaut ., [2]BalmasBourloud K., [2]Nardou K., [3]Joseph J.-M., [2]Gross N.

Recherche en oncologie pédiatrique DMCP[1], Recherche en oncologie pédiatrique, DMCP[2], Chirurgie pédiatrique, DMCP[3]

Histone deacetylase inhibitors (HDACi) are a new class of promising anti-tumour agent inhibiting cell proliferation and survival in tumour cells with very low toxicity toward normal cells. Neuroblastoma (NB) is the second most common solid tumour in children and cause 15 % of death from neoplasia in children, thus NB strongly require novel treatment modalities. We show that the HDACi Sodium Butyrate (NaB), suberoylanilide hydroxamic acid (SAHA) and Trichostatin A (TSA) strongly reduce NB cells viability. The anti-tumour activity of these HDACi involved the induction of cell cycle arrest in the G2/M phase, followed by the activation of the intrinsic apoptotic pathway, via the activation of the caspases cascade. Moreover, HDACi mediated the activation the pro-apoptotic proteins Bid and Bim_{EL} and the inactivation of the anti-apoptotic proteins XIAP, Bcl-x, RIP and survivin, that further enhanced the apoptotic signal. Interestingly, the activity of these apoptosis regulators were modulated by different mechanisms, either by caspases dependent proteolytic cleavage or by degradation via the proteasome pathway. In addition, SAHA reduced the constitutive and hypoxia-induced secretion of VEGF by IMR32 cells.

HDACi are therefore interesting new anti-tumour agents for targeting highly malignant tumours such as neuroblastoma, as these agents display a strong toxicity toward aggressive NB cells and they may possibly reduce angiogenesis by decreasing VEGF secretion by NB cells.

PERFORMANCE OF PET/CT AND MRI IN LIVER METASTASES FROM UVEAL MELANOMA

[1]victoria o., [2]Denys A., [3]Voelter V., [2]Artemisia S., [3]Leyvraz S., [4]Prior J., [4]BischofDelaloye A., [4]Malterre J.

Nuclear Medicine- CHUV[1], radiology[2], oncology[3], nuclear medicine[4]

Aim: PET has been found to be very sensitive and accurate for diagnosing metastases within lymph nodes and viscera from cutaneous melanoma, but it was found inferior to CT for lung and liver metastases. Uveal melanoma presents a specific tropism to metastasize to liver in the first place. With the advent of newer chemotherapy regimen for liver metastases from uveal melanoma, there is a need for early assessment of the effect of therapy. We aimed at determining the diagnostic value of PET/CT and MRI in the same patient with liver metastases from uveal melanoma and its possible use for follow-up of therapeutic response.

Methods: From 2004–2006, a total 9 patients (6W/3M, aged 58±19y [range 30–76]) with biopsy-proven liver metastases from uveal melanoma had both a pretherapeutic whole-body unenhanced PET/CT and liver MRI within 2 weeks. PET/CT was acquired 50–60min after injection of F-18-FDG (5MBq/kg) and standardized uptake values (SUV) were computed for each visible liver lesion. A 1.5T MRI was performed using HASTE 3-mm slice thickness, T2 Fast Spin echo 6-mm slice thickness and in/out of phase dynamic gradient echo sequences after administration of gadolinium. Both PET/CT and MRI were evaluated blindly and then compared to determine the correspondence of each lesion on each modality. Lesion size on MRI was compared to SUV uptake measured by PET when lesions were visible with both modalities.

Results: In total, 71 suspicious liver lesions were seen, 26 (40%) on both PET/CT and MRI, 4 (6%) by PET/CT alone and 35 (54%) by MRI alone. For lesions detected by both modalities, there was a strong correlation between PET SUV and MRI lesion size (SUV=1.34*$size$+2.83, r=0.81, p<0.0001). Of note, there were 8 subcentimetric lesions detected by PET with significantly increased SUV above liver background (4.6±1.1g/mL vs. 3.2±0.4g/mL, p=0.002). MRI lesions without PET/CT correspondence had significantly lower size (0.6±0.2cm vs. 1.8±1.2cm, p<0.0001). For lesions ≥1cm on MRI, PET/CT correspondence existed for 18 out of 20 (90%), while it did only for 8 out of 41 (20%) subcentimetric lesions. PET lesions without MRI correspondence presented significantly elevated SUV as compared to liver background (4.0±0.5g/mL vs. 3.2±0.4g/mL, p=0.004). On a per patient basis, each patient presented at least with 1 (range 1–11) liver lesions seen on both modalities.

Conclusion: PET/CT performance was strongly dependent on lesion size. As compared to MRI, PET/CT detected known liver metastases in all patients (100% sensitivity on a per patient basis). On a per lesion basis, PET/CT missed 10% of the lesions ≥1cm in size (90% sensitivity); for liver lesions <1cm, PET/CT detected only 20% of MRI lesions due to known partial volume effect and patient or breathing movements. Importantly, these results make possible the use of PET/CT for follow-up of therapeutic response in patients with liver lesions ≥1cm in size, which were initially detected on a baseline PET.

PERNTINENCE ET FREQUENCE DES TEST D'HOMOGENEITE DES GAMMA CAMERAS: COMPARAISON ENTRE DEUX SYSTEMES

[1]Maillard D., [2]Dupuis P., [2]Francis V., [1]Allenbach G., [1]Prior J., [1]BischofDelaloye A.

Service de Médecine Nucléaire - CHUV[1], Institut Universitaire de Radiophysique appliquée - IRA[2]

Introduction

Selon la directive fédérale suisse L-09-04, le contrôle d'homogénéité fait partie des trois contrôles obligatoires permettant de vérifier la stabilité des gamma caméras. Cette directive définit les fréquences minimales des contrôles de qualité. Les valeurs limites doivent être définies par le fournisseur et sont établies pour l'homogénéité intrinsèque uniquement. Par conséquent, la procédure et les valeurs limites sont spécifiques à chaque gamma caméra. Ce travail a pour but de comparer les contrôles réalisés sur deux gamma caméras différentes (Millenium GE, une tête; e.cam Siemens, deux têtes) en vérifiant la pertinence des valeurs limites et de la fréquence des contrôles.

Méthode

L'étude s'est portée sur deux gamma caméras (Millenium GE ; e.cam, Siemens MS). Les paramètres étudiés sont l'homogénéité intrinsèque et l'homogénéité extrinsèque. Le contrôle de l'homogénéité intrinsèque est effectué de façon quotidienne sur la gamma caméra e.cam et de façon hebdomadaire sur la Millenium. Sur la Millenium, c'est le contrôle extrinsèque qui sert de contrôle journalier, alors qu'il n'est effectué sur l'e.cam que de façon mensuelle. Nous avons analysé les résultats de nos contrôles de stabilité sur une période de cinq mois, de janvier à mai 2007, et calculé la valeur moyenne et l'écart type de l'uniformité intégrale. Nous avons aussi analysé les contrôles hors normes des douze mois précédents.

Résultats

Homogénéité intrinsèque

Pour la Millenium, les valeurs de l'uniformité intégrale varient peu (de 1.5 à 4%) et sont toutes nettement en dessous de la limite du contrôle intrinsèque fixée par le fournisseur à 8 %.
Pour l'e.cam, les valeurs de l'uniformité intégrale varient peu (de 1.4 à 2.8%), hormis une valeur qui se situe en dessus de la norme. Un contrôle, dont la valeur d'uniformité intégrale se situe dans les normes indiquées par le fournisseur, mais d'aspect fort hétérogène de l'image, a pu être observé. En effet, on a remarqué des régions photopéniques correspondant à l'emplacement des photomultiplicateurs.
Malgré le temps nécessaire au retrait des collimateurs, le contrôle de l'homogénéité intrinsèque n'est pas nécessairement plus long à effectuer qu'un contrôle extrinsèque. En outre, la mise en place de ce dispositif de mesure permet également d'effectuer un contrôle de la position du pic photoélectrique.

Homogénéité extrinsèque

Les fournisseurs ne recommandent pas l'homogénéité extrinsèque comme contrôle journalier. Pourtant, le collimateur est un acteur essentiel à la formation de l'image, et il est fragile.
Pour la Millenium, les valeurs de l'uniformité intégrale sont toutes en dessous de la limite du contrôle intrinsèque, aucune valeur n'est très éloignée de la valeur moyenne.

Conclusion

Bien que sur la période test nous n'ayons observé qu'un seul contrôle de qualité hors norme, un contrôle régulier de l'homogénéité nous paraît indispensable. L'utilisation de paramètres objectifs comme l'uniformité intégrale semble à première vue idéale pour s'assurer de l'homogénéité du système d'acquisition. Elle n'est toutefois pas suffisante, car malgré une image clairement inhomogène, le résultat peut se trouver dans les normes indiquées par le fournisseur. Il est donc primordial que le technicien, en plus du suivi de l'évolution des paramètres objectifs, observe attentivement les images pour garantir l'absence d'artefact. Sur la Millenium, la valeur limite de l'homogénéité intrinsèque fixée par le constructeur est nettement plus élevée que la moyenne des mesures réalisées et pourrait être abaissée, ce qui améliorerait la sensibilité du test. En ce qui concerne l'e.cam, les normes semblent appropriées. Toutefois, la recommandation de ne mesurer qu'une fois par mois l'homogénéité extrinsèque qui permet de détecter une anomalie de collimateur, nous semble insuffisante.

Aspartic acid 681 in CYLD is required for the cleavage of K63-linked polyubiquitin chains

[1]Almeida S., [1]Maillard C., [1]Hohl D., [1]Huber M.

Service of Dermatology and Venereology, CHUV[1]

The ubiquitin-specific protease (UBP) CYLD is a tumor suppressor which specifically removes K63-linked polyubiquitin chains from Bcl-3, TRAF2, TRAF6, NEMO and Lck. CYLD regulates negatively NF-κB and JNK signaling and positively T-cell receptor signaling. We investigated the novel missense mutation D681G found in the germline of a family in which 11 out of 12 tumors isolated from different body sites of 3 members were trichoepitheliomas, benign tumors of skin appendages. Aspartic acid 681 is highly conserved in CYLD homologues and other members of the UBP family but does not belong to the Cys and His boxes providing the CYLD catalytic triad (Cys_{601}, His_{871}, Asp_{889}). CYLD-D681G and CYLD-C601A (active-site mutant) had a strongly reduced ability to inhibit TRAF2- and TRAF6-mediated NF-κB activation and TNFalpha-induced JNK signaling in 293T cells. Unlike wild- type protein, CYLD mutants were unable to deubiquitinate polyubiquitinated TRAF2 in 293T cells. CYLD-D681G was coimmunoprecipitated by TRAF2 to the same extent as wild type enzyme showing that the D681G mutation did not affect TRAF2 binding. In contrast, immunopurified CYLD-D681G could not cleave K63-linked polyubiquitin chains *in vitro*. These findings support the notion that aspartic acid 681 is required for binding and/or enzymatic reaction of CYLD with K63-linked polyubiquitin chains.

Identification of neuroblastoma progenitors gene expression profile by micro-array time-course analysis of neurospheres

[1]Coulon A., [1]Mühlethaler-Mottet A., [1]Flahaut M., [1]Meier R., [2]Fuchs S., [2]Sommer L., [1]Gross N.

Pediatrics - CHUV[1], Institute of Anatomy - University of Zurich[2]

Solid tumors are believed to arise from a minor population of tumor-initiating cells with typical stem cell (SC) markers and properties. The so-called cancer stem cells (CSCs) would possess the exclusive ability to initiate and maintain the tumour. Rare populations of undifferentiated cells with SC characteristics have been identified in several malignancies. The identification of CSC therefore establishes a new putative cellular target for more effective therapies in aggressive cancers.

Neuroblastoma (NB), the most common extracranial childhood solid tumor originates from neural crest-derived malignant sympathoadrenal cells. We have identified cells within primary NB tissue and cell lines that express neural crest SC markers. Moreover, NB primary tumors were shown to include differentiated cell types normally generated from neural crest cells, leading us to postulate the existence of CSCs in NB tumor (NBSC) that recapitulate the properties of sympathetic precursor cells.

As reliable and specific cell surface markers to isolate CSCs are not available for solid tumours, functional assays such as ability of SC to grow as spheres in non-adherent conditions have been developed to reliably detect and quantify CSCs. By serial passages of neurospheres generated from a dissociated stage 4 NB tumour, a subset of cells was gradually selected and its specific gene expression profile identified by micro-array time-course analysis. GeneOntology analysis revealed in the set of differentially expressed genes from neurospheres, an enrichment in genes implicated in development, including the known CD133 and NOTCH CSCs markers. We compared these results with genes enriched in neural crest and other SC types by overlap. Interestingly, these markers were found to be highly expressed by NB primary tumor cells propagated in a serum-free medium preventing cell differentiation. This preliminary study uncovers putatively relevant markers for the isolation and further investigation of the *in vitro* and *in vivo* tumourigenic potential of NBCSs in tumours.

Analysis of naturally acquired CD4+ T cell responses to MAGE-A3 and MAGE-A4 cancer/testis antigens in patients with resected head and neck squamous ce

[1]Cesson V., [2]Escher A., [2]Piotet E., [2]Rivals J.-P., [1]Speiser D., [2]Bron L., [1]Romero P.

Ludwig Institute for Cancer Research[1], ORL department, CHUV[2]

Despite tremendous advance in the medical and surgical treatment of Head and Neck (HN) squamous cell (HNSCC), long term survival remain unchanged in the last 20 years. The obvious limitations of traditional therapeutic options strongly urge the development of novel therapeutic approaches. The molecular cloning of tumor antigens recognized by T lymphocytes in recent years has provided targets for specific immunotherapy. In this regard, frequent expression of Cancer Testis Antigens (CTA) has been repeatedly observed among HN tumors. We analyzed CTA expression in HNSCC 46 patients and found that MAGE-A3 and/or -A4 CTA were positive in over 70%, regardless of the anatomical site of primary tumors in the upper aerodigestive tract. However, immune responses against these CTA in HNSCC patients have not yet been investigated in detail. In this study we assessed the responsiveness of HNSCC patient's lymphocytes against overlapping peptides spanning the entire MAGE-A3 and -A4 proteins. After depletion of $CD4^+CD25^+$ regulatory T cells, and following three rounds of *in vitro* stimulation with pools of overlapping peptides, peripheral blood mononuclear cells (PBMCs) of HNSCC patients were screened by IFN-γ and TNF-α intracellular cytokine staining for reactivity against MAGE-A3 or -A4 derived peptides. Cytokine secreting $CD4^+$ T cells, specific for several peptides, were detected in 7/7 patients. In contrast, only 2/5 PBMC from healthy donors showed weak T cell responses against 2 peptides. $CD4^+$ T cells specific for one epitope MAGE-$A3_{(281-295)}$, previously described as an HLA-DR11 restricted epitope naturally processed and presented by dendritic cells and tumor cells, were detected in two patients. MAGE-$A3_{(161-175)}$ specific $CD4^+$ T cells were found in one patient. Six MAGE-A3 and -A4 new epitopes are being characterized. Together, these data suggest that naturally acquired $CD4^+$ T cell responses against CT antigens occur *in vivo* in HNSCC patients, providing a rationale basis for immunotherapy targeting MAGE-A3 and –A4 in those patients.

Targeted Disruption of GAS6-Mertk Pathway Leads to Defects in Physiological Clearance of Expelled Nuclei from Erythroblasts by Bone Marrow Macrophages

Linda Kadi[1], Laurent Burnier[1], Rocco Sugamele[1], Peter Carmeliet[2], Greg Lemke[3], H. Shelton Earp[4], Glenn K. Matsushima[5], Marc Schapira[1],Anne Angelillo-Scherrer[1].

Service and Central Laboratory of Hematology, CHUV - University Hospital Center, Lausanne[1], The Center for Transgene Technology & Gene Therapy, Flanders Interuniversity Institute for Biotechnology, Leuven, Belgium[2]; Salk Institute for Biological Studies, La Jolla, CA, United States[3]; Lineberger Comprehensive Cancer Center, University of North Carolina at Chapel Hill, United States[4], UNC Neuroscience Center, University of North Carolina at Chapel Hill, United States. [5]

Body: Late in erythropoiesis, nuclei are expelled from erythroblasts and engulfed by macrophages located in the blood island. Expelled nuclei expose phosphatidylserine (PS) on their surface, which is used as a signal for their engulfment by macrophages. PS opsonins milk-fat-globule EGF8 (MFG-E8) and *Growth arrest-specific gene 6* product (GAS6) together with their respective receptors a_vb_5 (and a_vb_3) and Axl/Mertk/Tyro3, are involved in the phagocytosis of apoptotic cells. Because fetal liver and bone marrow macrophages do not express MFG-E8, GAS6-Mertk pathway might constitute a major pathway for the engulfment of nuclei expelled from erythroblasts.

To test this hypothesis, we isolated nuclei from late-stage erythroblasts from the spleens of phlebotomized mice (500 µl), and tested the capacity of bone marrow-derived macrophages (BMDM) from mice deficient either in *GAS6* (*GAS6*$^{-/-}$), *Axl* (*Axl*$^{-/-}$), *Mertk* (*mertk*^{kd}) or *Tyro3* (*Tyro3*$^{-/-}$) to internalize these nuclei. Spleen erythroblasts were isolated 4 days after phlebotomy and cultured for 5 hours. Nuclei were obtained after disconnection from reticulocytes by mechanical shaking. Released nuclei were then identified by flow cytometry according to their size and their positive staining for the erythroid lineage marker Ter119 and Annexin V for PS labelling. Purity of the preparation was double-checked by morphological examination of cytospin preparations. Primary BMDM isolated from wild-type (WT) controls and *GAS6*$^{-/-}$, *Axl*$^{-/-}$, *Mertk*^{kd}, *Tyro3*$^{-/-}$, *Axl/Tyro3*$^{-/-}$, *Axl*$^{-/-}$*/Mertk*^{kd} mice were incubated with nuclear preparation for 3 hours. BMDM were then washed to remove un-engulfed nuclei, analyzed in bright field and stained with May-Grünwald-Giemsa. Phagocytosis was determined by counting the number of BMDM with ingested nuclei and the phagocytosis index indicated the number of engulfed nuclei per macrophage. We found that *GAS6*$^{-/-}$ BMDM cleared 30% less nuclei than WT BMDM ($p<0.01$). We observed a slight decrease of internalization capacity for *Axl*$^{-/-}$ BMDM, whereas *Tyro3*$^{-/-}$ BMDM engulfed the nuclei as efficiently as WT BMDM. In contrast, Mertk deficiency nearly abolished the nuclei phagocytosis ($p<0.001$). *Axl/Tyro3*$^{-/-}$ and *Axl*$^{-/-}$*/Mertk*^{kd} BMDM were tested in comparison with WT BMDM and single knockouts, and did not show any cumulative effects when compared to single knockouts. Thus, Mertk was critical for the phagocytosis of nuclei from erythroblasts whereas the role of Axl and Tyro3 appeared to be negligible.

In conclusion, we have shown that GAS6 and its receptor Mertk were involved in late erythropoiesis when nuclei are expelled from the erythroblasts and engulfed by BMDM in the blood island. Indeed, GAS6 binding to nuclei exposing PS on their surface might form a bridge between PS and Mertk receptor on BMDM, allowing their efficient clearance.

3D in vivo dosimetry in tomotherapy: preliminary results

[1]schombourg k., [1]bochud f., [1]moeckli r.

institut universitaire de radiophysique-CHUV[1]

Introduction:

Tomotherapy is a new machine for the treatment of tumors. The tomotherapy unit delivers dose by intensity modulated beams. During the whole irradiation the gantry is rotating around the patient, with 72 gantry positions per rotation, while the table is moving.
A detector composed of 738 ion chambers filled with Xenon is integrated in the unit, thus an MV CT image can be performed for patient positioning. The aim of this study is to use this detector for 3D in-vivo dosimetry. A method is being developed to reconstruct the dose delivered to the patient during an irradiation. The only data needed for the reconstruction process is the transmitted dose. The reconstructed dose can be compared with the dose given by the treatment planning system in order to detect some possible dosimetric differences. The dose delivery in the next fractions can afterward be re-planned in order to take these differences into account. In this study, the dose reconstruction method is tested on a linear accelerator.

Method:

Delivered dose calculations are done on an extended phantom composed of the patient CT, the air gap between the patient and the detector, and the detector itself [1]. The MV CT performed by the tomotherapy imaging beam (3.47 MV) can be used as well as the dedicated kV CT to represent the patient [2].

During the dose delivery, transmitted dose is recorded at each gantry position. The measured transmitted dose has a primary and a scatter component [1]. For the reconstruction it is first needed to estimate the primary fraction. Then the primary transmitted energy fluence is calculated. In order to know the energy fluence at the entrance of the phantom, the primary transmitted fluence is back-projected through the whole phantom thickness by taking the inverse square low and the exponential attenuation into account. A convolution between the primary energy fluence and the dose kernels finally gives the total dose delivered to the phantom.
The dose reconstruction model is being tested on a solid water phantom, and a phantom containing a lung simulator. These phantoms are irradiated by single beams. The algorithm has also been tested on non-trivial transmitted dose profiles.

Results:

The algorithm developed in this study for the dose reconstruction converges well in all the tested cases. The dose distribution has been reconstructed and is in good agreement with the dose calculated independently by the treatment planning system.

Discussion:

In this method the only input for dose reconstruction is the transmitted dose recorded at each gantry angle. Thus all the treatment delivery is verified independently. The 3-D in-vivo dosimetry makes possible a direct verification of the dose delivered to the target and organs at risk for each fraction and adaptive radiotherapy can be done.

References:

[1] McNutt et al., 1996, Med. Phys. 23 (8) : 1381-92
[2] McNutt et al., 1997, Med. Phys. 24 (9) : 1465-1476

Fluorodeoxyuridine induced S-phase synchronization and increased incorporation of 125I-iododeoxyuridine in vitro and in vivo A promising approach for Auge

[1]Viertl D., [2]Perillo F., [1]BischofDelaloye A., [1]Kosinski M., [1]Buchegger F.

Institute of Nuclear Medecine[1], Institute of Radio Oncology[2]

Introduction

Radio-iododeoxyuridine (IdUrd), a thymidine (dThd) analogue, has been proposed as a therapeutic agent for human cancer treatment. IdUrd is stably incorporated into DNA of proliferating cells and can be labelled with Auger electron emitter radio-iodines which is able to break double strand DNA. However, IdUrd DNA-incorporation rate is limited, mainly due to the endogenous dThd competition. Fluorodeoxyuridine (FdUrd), an other dThd analogue, depletes the cellular dTTP pool by inhibiting the dThd synthesis, and blocks cells in S-phase. Therefore, FdUrd favours DNA incorporation of exogenous radio-IdUrd. Our objectives are to study *in vitro* and *in vivo* cellular cycling, radio-IdUrd DNA incorporation after different delays post FdUrd pre-treatment and to correlate this enhanced incorporation with an increased therapeutic efficacy.

Material and methods

For incorporation assays, two human glioblastoma (LN229, U251) and two lymphoma (BL60.2, Daudi) cell lines, were pre-treated with 1 μM FdUrd for 1 hour. After different times delay (0 to 72 hours), cells were incubated with ^{125}I-IdUrd. Radio-IdUrd DNA incorporation was then measured with a γ counter. Using the same delays, cell cycle FACS analyses were performed based on propidium iodide and FITC double staining. Radio-sensitivity was evaluated by colony forming assay, 16 hours post FdUrd pre-treatment, after irradiation with 0.8 to 8 Gy. *In vivo*, cell cycle FACS analysis were achieved on SCID mice bearing subcutaneous (SC) BL60.2 tumour. Mice were pre-treated with 0.5 mg FdUrd and treated with 1 mg IdUrd, both injected intraperitoneally. Moreover, 20 kBq of ^{125}I-IdUrd were intra-tumourly injected, in SC Daudi tumour, at different time after FdUrd pre-treatment. Biodistribution of ^{125}I-IdUrd was then measured 5 hours after the radio-IdUrd injection.

In vitro results

For the different cell lines tested an enhanced radio-IdUrd incorporation was observed post FdUrd pre-treatment. The highest incorporation rate was reached after a delay of 16 to 24 hours between FdUrd and IdUrd treatments.

The FACS results showed that the FdUrd pre-treatment induced an accumulation of cells undergoing the S-phase and that the largest population of S-phase cells was obtained after a delay of 16 hours. For the two glioblastoma cell lines the increased incorporation of radio-FdUrd and the accumulation of cells in S-phase enhanced the cytotoxicity of the treatment as revealed by the colony forming assays.

First *in vivo* results

Biodistribution experiments showed that FdUrd pre-treatment followed by a delay of 10 hours increased up to 4 times the incorporation of radio-IdUrd compared to the untreated samples. Moreover, incorporation was mainly due to the tumour cells, whereas other organs were showing a weak incorporation. As observed *in vitro*, the *in vivo* FdUrd pre-treatment led also to an accumulation of cells in S-phase but the maximum was reached after a delay of 4 hours between the pre-treatment and the treatment.

Conclusion

These results indicated that the maximal percentage of S-phase cells was timely correlated with the highest radio-IdUrd DNA incorporation, suggesting that they are functionally linked. *In vitro*, the increased incorporation was related with an improved cytotoxic effect. So far, we have been able to reproduce the *in vitro* results in a murine model with lymphoma tumour. These results might allow the rational design of an Auger radiation therapy targeting a maximal percentage of cells in S-phase after FdUrd pre-treatment.

Assessment of immune suppressive circuits in the tumor microenvironment of human head and neck squamous cell carcinoma (HNSCC)

[1]Rivals J.-P., [2]Cesson V., [2]Rimoldi D., [3]Seelentag W., [2]Speiser D., [2]Romero P., [1]Monnier P., [1]Bron L.

Service of Head and Neck surgery-CHUV[1], Division of Clinical OncoImmunology, Ludwig Institute for Cancer Research, Lausanne Branch, University Hopital (CHUV), Switzerland[2], Institut of Pathology-CHUV[3]

The presence of tumor infiltrating lymphocytes (TILs), notably $CD8^+$ T cells, in several types of tumors, has been correlated with good prognosis. Moreover, some T cells among TILs have been shown to kill tumor cells in vitro through a tumor-associated antigen recognition mechanism. In contrast, accumulation of another subset of T cells, regulatory CD4 T cells ($FoxP3^+$), may correlate with poor prognosis. In general, most tumors progress despite naturally acquired immune responses. Reasons for failure of adaptive anti-tumor immunity may be the usually weak immunogenicity of tumor cells and antigens, and a large variety of immunosuppressive mechanisms present in the tumor microenvironment.

Despite advances in the diagnosis and treatment of HN cancer, survival rates for this disease have not improved over recent years. New therapeutic strategies, including immunotherapy, are potentially useful approaches. In this regard, a better understanding of the cellular and molecular interactions taking place at tumor sites is required for the rational development of therapeutic interventions. Such insight would allow identifying novel immune modulators, which could be used to enhance vaccine specific immunity and increase both specific T cell responses and clinical response.

Our analysis of 46 HNSCC demonstrated that MAGE-A3/-A4 cancer testis antigens were expressed in over 70% of samples, indicating that these antigens are suitable targets for immunotherapy. Immunohistological studies showed that over 50% of tumors had a moderate to strong infiltration for $CD3^+$, $CD8^+$ and $S\text{-}100^+$ cells. We further evaluated the distribution of $BDCA\text{-}2^+$, $CD11^+$, $CD56^+$ and $FOXP3^+$ cells in the same cohort of patients. The expression of IDO, iNOS, Arginase, Bcl-2 and Cox-2 was also evaluated by immuno-histochemistry, and assessed for correlation with clinical data. $BDCA2^+$ and $FOXP3^+$ cells were observed in all tumor samples, both in cancer stroma and within cancer epithelium. The median counts of stromal $BDCA\text{-}2^+$ and $FOXP3^+$ were 36 cells/mm^2 (range 0-243 cells/mm^2) and 132 cells/mm^2 (range 7-551 cells/mm^2), respectively. The median counts of intratumoral $BDCA\text{-}2^+$ and $FOXP3^+$ were 5 cells/mm^2 (range 0-200 cells/mm^2) and 27 cells/mm^2 (range 1-115 cells/mm^2), respectively. $CD11^+$ and $CD56^+$ cells were poorly present and no significant difference was observed between stroma and epithelium. Analysis of expression of IDO, iNOS, Arginase, Bcl-2 and Cox-2 are currently ongoing.

Together, our data reveal the presence of immune regulatory cells. The relatively easy accessibility of Head and Neck tumors provides an essential basis for further exploration, and a more precise characterization of immunosuppressive mechanisms revealed by ex vivo analysis of human cancer tissue.

Elucidating the role of CXCL12 receptors in the growth/survival of neuroblastoma

[1]Liberman J., [1]Meier R., [1]Coulon A., [2]Sengstag T., [3]Joseph J.-M., [1]Gross N.

Pediatric Oncology Research Unit -CHUV[1], ISREC and Swiss Institute of Bioinformatics (SIB) Bioinformatics Core Facility (BCF), Epalinges[2], Paediatric Surgery Unit - CHUV[3]

Neuroblastoma (NB) is the most frequent extracranial childhood tumour. For patients suffering from advanced stage NB, no efficient treatment can currently be offered. The chemokine CXCL12 and its receptors CXCR4 and CXCR7, seem to play a particular role in cancer. *In vivo* growth assessment in an orthotopic NB mouse model revealed that CXCR4 overexpression in defined NB cell lines strongly increased growth of primary tumours and liver metastases. High levels of CXCL12 were detected at the primary tumour site, as in the liver, suggesting a role for CXCL12 in the increased primary NB tumour and metastatic growth. Moreover, CXCR4 overexpression in NB cells was shown to increase resistance to serum deprivation. These observations strengthen a pivotal and tumour microenvironment-related role for CXCR4 in the growth and survival of NB tumours. However, the particular pathways involved in such CXCR4-mediated growth and environmental factors responsible for the activation or regulation of the CXCR4/CXCL12 axis still need to be identified. Furthermore, CXCR7, a novel CXCL12 receptor may also confer specific properties to cancer cells.

Using a genome-wide approach by microarray expression profiling, we propose to identify genes and gene networks regulated by CXCR4/CXCR7 expression in NB cells with manipulated levels of CXCR4/CXCR7 expression. Further *in vitro* and *in vivo* functional analyses will be performed to validate particular differentially regulated genes. In addition, a large number of patient samples will be screened for expression of CXCL12 and its receptors on a tissue microarray. Assessing the expression of these proteins and further elucidating their role in NB tumour progression may provide additional NB risk group markers as well as new therapeutic targets.

PET/CT and endobronchial ultrasound-guided fine-needle aspiration (EBUS) for mediastinal staging of known or suspected lung cancer

[1]Nicod Lalonde M., [1]Prior J., [2]Egger B., [1]Orcurto M.-V., [3]Letovanec I., [2]Aubert J.-D., [2]Favre L., [1]BischofDelaloye A.

Nuclear Medicine - CHUV[1], Pneumology Department - CHUV[2], Pathology Department - CHUV[3]

Objectives:

Accurate mediastinal staging is essential for optimizing treatment lung cancer patients. PET/CT is more accurate than CT for staging mediastinal lymph nodes (LNs), but is limited by false positive results requiring histopathological examination. EBUS is an emerging attractive, less invasive alternative to mediastinoscopy. We evaluated PET/CT and EBUS performances in lung cancer patients with mediastinal involvement.

Methods:

Nineteen patients (61±9y) with known (n=9) or suspected (n=10) lung cancer and enlarged LNs on ceCT underwent F-18-FDG PET/CT before (n=13) or after (n=6) EBUS. EBUS used a real-time ultrasonography-guided 22-gauge needle to obtain tissue specimen. Final diagnosis was established by cytology, mediastinoscopy/surgery or radiological follow-up.

Results:

Twenty-seven LNs were sampled without complication. Final diagnosis showed 16 tumoral and 11 non-tumoral LNs. EBUS correctly detected 12/16 tumoral LNs (10 NSCLC/2 SCLC) and 8 negative LNs, however with a 26% rate of inconclusive cytology (7 unsampled LNs, among which 4 were tumoral). PET/CT correctly identified 15/16 (95%) tumoral LNs, but only 5/11 (45%) non-tumoral LN (SUV 7.2±3.1 vs. 4.0±1.2g/mL, p=0.004). With respect to correct LNs staging, sensitivity, specificity, PPV and NPV were 94%, 46%, 71%, 83% for PET/CT and 75%, 100%, 100%, 73% for EBUS. In all 21 PET-positive LNs, EBUS confirmed a tumor in 12 (57%), a non-tumoral origin in 6 (29%), and was inconclusive in 3 (14%). Whether PET/CT was performed before or after EBUS played no role, nor whether lung cancer was known or only suspected. SUV and LN size were associated in tumoral LNs (p=0.002), but not in non-tumoral LNs. EBUS avoided mediastinoscopy in 9 (47%) patients with tumoral-positive cytology.

Conclusions:

About 30% of PET positive LNs were negative by EBUS, emphasizing the need of pathologic confirmation of PET-positive findings. Considering the 26% rate of inconclusive EBUS tissue sampling, PET/CT had better sensitivity and NPV. EBUS is a safe procedure, offering an opportunity to avoid mediastinoscopy in about half of patients with known or suspected lung tumor.

Value of PET/CT for Evaluating Malignant Origin of Pleural Effusions in Patients with Known Cancer

[1]Allenbach G., [1]Prior J., [1]Orcurto M.-V., [1]NicodLalonde M., [1]Gremion I., [2]Mihaescu A., [1]BischofDelaloye A., [2]Letovanek I.

Nuclear Medicine - CHUV[1], Pathology Department - CHUV[2]

Aim: We aimed at determining the utility of PET/CT to differentiate malignant from benign pleural effusions in patients with known cancer.

Material and Methods: We examined 55 ^{18}F-FDG PET/CT performed in 52 patients (31M, 20W, 60±16y) with known cancer (25 non-small cell lung carcinomas [NSCLC], 7 lymphomas, 6 breast cancers, 4 head & neck cancers, 3 mesotheliomas, 3 GIST, 2 melanomas, 1 malignant teratoma, 1 colon cancer) for ^{18}F-FDG uptake in pleural effusions using the maximal standardized uptake value normalized for body weight [$SUV_{bw\ max}$]. This was correlated to the results of cytopathological analysis of thoracentesis performed within a median interval of 9 days (interquartile range –3 to 38 days), which included the pH, relative distribution (macrophages, neutrophiles, eosinophiles, basophiles, lymphocytes, plasmocytes), as well as absolute cell count (10^9/L, available in *n*=35 effusions) and presence of malignant cells. Using Receiver Operating Characteristics (ROC) curves, we determined the ability of PET/CT to detect the presence of malignant cells in the pleural effusion, and the corresponding sensitivity, specificity, negative and positive predictive value for a determined SUV threshold.

Results: Cytopathological examination revealed malignant cells in 19 pleural effusions (25%) (11 carcinoma, 5 lymphoma, 2 mesothelioma, 1 melanoma), whose corresponding SUV were significantly higher than benign pleural effusions (3.8 g/mL 95%CI 2.1–5.6 vs. 1.7 g/mL 95%CI 1.5–1.9, *p*=0.001), with a significant correlation between malignant pleural effusion and SUV (Spearman correlation ρ=0.55, p<0.0001). There was no other significant correlation between SUV and cytopathological or radiological parameters, including absolute cell count or relative distribution, pH, volume of thoracentesis or estimate of pleural effusion volume on CT. The area under the curve of the ROC analysis was 0.83±0.06. Using a SUV threshold of 2.2 g/mL, 13 PET/CT studies were considered positive and 36 were negative. This led to sensitivity, specificity, positive and negative predictive values for detecting malignant pleural effusion of 53%, 92%, 77% and 79%, respectively. When limiting the analysis to NSCLC (*n*=26 studies in 25 patients), ROC area was 0.95±0.04. Using the same SUV threshold of 2.2 g/mL, 6 PET/CT studies were positive and 20 were negative with sensitivity, specificity, positive and negative predictive values of 67%, 90%, 67% and 90%, respectively.

Conclusion: We can conclude that PET/CT may be helpful determining the malignant or benign nature of pleural effusions in patients with known cancer or with NSCLC.

A new, automated, four-colour interphase FISH approach for the simultaneous detection of specific aneuploidies of diagnostic and prognostic significance in

[1]Talamo Blandin A., [1]Muehlematter D., [1]Bougeon S., [1]Gogniat C., [1]Porter S., [1]Beyer V., [1]Parlier V., [2]Beckmann J., [3]Van Melle G., [1]Jotterand M.

Unité de cytogénétique du cancer, Service de génétique médicale, CHUV-UNIL, Lausanne.[1], Service et Département de génétique médicale, CHUV-UNIL, Lausanne.[2], Institut universitaire de médecine sociale et préventive, Lausanne.[3]

In hyperdiploid acute lymphoblastic leukaemia (ALL), the simultaneous occurrence of specific aneuploidies confers a more favourable outcome than hyperdiploidy alone. Interphase (I) FISH complements conventional cytogenetics (CC) through its sensitivity and ability to detect chromosome aberrations in non-dividing cells. To overcome the limits of manual I-FISH, we developed an automated four-colour I-FISH approach and assessed its ability to detect concurrent aneuploidies in ALL.

I-FISH was performed using centromeric probes for chromosomes 4, 6, 10 and 17. Parameters established for automatic nucleus selection and signal detection were evaluated (3 controls). Cut-off values were determined (10 controls, 1000 nuclei/case). Combinations of aneuploidies were considered relevant when each aneuploidy was individually significant. Results obtained in 10 ALL patients (1500 nuclei/patient) were compared with those by CC.

Various combinations of aneuploidies were identified. All clones detected by CC were observed by I-FISH. I-FISH revealed numerous additional abnormal clones, ranging between 0.1 % and 31.6%, based on the large number of nuclei evaluated.

Four-colour automated I-FISH permits the identification of concurrent aneuploidies of prognostic significance in hyperdiploid ALL. Large numbers of cells can be analysed rapidly by this method. Owing to its high sensitivity, the method provides a powerful tool for the detection of small abnormal clones at diagnosis and during follow up. Compared to CC, it generates a more detailed cytogenetic picture, the biological and clinical significance of which merits further evaluation. Once optimised for a given set of probes, the system can be easily adapted for other probe combinations.

Mimicking interstitial microenvironments for lymphatic capillary tissue engineering

[1]Overney J., [1]Foretay D. [2]Swartz M.A.

Mechanobiology and Morphogenesis Laboratory, EPFL[1], Institute of Bioengineering – EPFL[2]

Lymphangiogenesis depends mainly on three factors: interstitial flow, the extracellular matrix, and the matrix environment (chemical and physical factors). We have previously shown in vivo as well as in vitro that the organization of lymphatic endothelial cells (LEC) is guided by slow interstitial flow. Additionally, it is known that vascular endothelial growth factor (VEGF)-C is important for lymphatic proliferation and migration via signaling through its receptor VEGFR-3. We have engineered a VEGF-C protein that can covalently bind to fibrin such that it can be liberated by cellular proteolytic activity. Using a novel 3D radial flow chamber developed in our lab, we studied the effects of subtle flow on cells cultured in this VEGF-C linked matrix. These studies showed that liberation of the bound VEGF-C protein from the fibrin gel synergizes with slow flow to promote the formation of small capillary networks, presumably by preferentially cleaving VEGF-C in the direction of flow thereby biasing the free morphogen gradient and inducing subsequent morphogenesis. We also show that fibroblasts co-cultured with LECs strongly promote lymphangiogenesis and give them more relevant morphologies and possibly stabilize them. These new models of the lymphatic microenvironment can thus be used both to better understand the biology governing lymphangiogenesis as well as provide engineering design criteria for creating functional lymphatic vessels in vitro and for regenerative medicine.

Change in oncology clinician's defense mechanisms after training: A controlled study

[1]Bernard M., [2]Favre N., [3]DeRoten Y., [3]Despland J.-N., [2]Stiefel F.

Psychiatrie de Liaison et Centre de Recherche en Psychothérapie[1], Psychiatrie de Liaison[2], Centre de Recherche en Psychothérapie[3]

Background. We have adapted the Defense Mechanism Rating Scales (Perry, 1990) to study clinician's defenses during highly emotional sessions of oncology consultation. Our aim is to evaluate the impact of communication skills training (CST) on the clinician's use of defense mechanisms.
Method. The sample included 113 clinicians (57 in training, 56 controls). Each clinician conducted two interviews with simulated patients in a 6 months interval, before and after the training. Four raters coded the 226 sessions with the Defense Mechanism Rating Scales for Clinicians (DMRS-C; Despland et al., 2006).
Results. The number of defenses per session ranged from 5 to 35 (M = 18; SD = 6). The most frequent ones were displacement (20%), rationalization (19%) and intellectualization (12%). When controlling for the pre-scores, comparison between trained and control clinicians showed:

- A tendency for a higher level of Overall Defensive Functioning after training (4.57 vs. 4.41, F = 3.33 , p = .07, d = 0.33).
- A higher proportion of obsessional defenses after training (22.4% vs. 17%, F = 5.74 , p = .02, d = 0.49).
- A lower proportion of disavowal defenses after training (25 vs. 30, F = 3.86 , p = .05, d = 0.39).

Discussion. These results are discussed in the context of defensive improvement after communication skills training and the possible inclusion of this topic during the training. The study of defense mechanisms represents a promising way of taking into consideration the clinician's characteristics.

Keywords: Communication Skills Training; Defense mechanisms; Clinician attitude

THE
Procédures Thérapeutiques

Computer assisted navigation in Total Knee Arthroplasty (TKA) : Comparison with the conventional method.

[1]Locherbach C., [2]Conrad C., Berthet S.

Orthopedic Hospital Lausanne[1], Department of traumatology, University of Lausanne[2]

The aim of this retrospective study was to compare the clinical and radiographic results after TKA (LCS, DePuy), performed either by computer assisted navigation (Brainlab, Johnson&Johnson) or by conventional means.
Material and Methods: Between May and December 2006 we reviewed 32 conventional TKA performed between 2000 and 2004 (group A) and 36 navigated TKA performed between 2004 and 2005 (group B) by the same experienced surgeon. The mean age in group A was 74 (range 60-87) years and 73 (range 38-86) in group B with a similar age distribution. Patients with a previous tibial osteotomy or revision arthroplasty were excluded from the study. The preoperative mechanical axes were –25° (varus) to +15° (valgus) in group A and –24° to +13° in group B. Examination was done by an experienced orthopedic resident independent of the surgeon. All patients had pre- and postoperative long standing radiographs. The IKSS and the WOMAC were utilized to determine the clinical outcome. Patient's degree of satisfaction was assessed on a visual analogous scale (VAS).
Results: The postoperative mechanical axis in group A ranged between –12° to +3° (mean –2.33°, SD 4.34), in contrast the mechanical axis in group B was on average closer to the neutral axis (–6° to +4°, mean –1.65°, SD 2.21). This difference in variation of the mechanical axis between both groupes was pronounced in patients with large initial deformities, however it didn't reach statistical significance. Both groups showed a significant postoperative improvement of their mean IKSS-values (group A: 103 preoperative to 182 postoperative, group B 106 to 181) without a significant difference between the two groups. Neither the WOMAC nor the patient's degree of satisfaction -as assessed by VAS- showed significant differences. Operation time was significantly higher in group B (mean 124.65 min.) than in group A (mean 94.70min., $p<0.001$).
Conclusion: Computer assisted navigation in TKA seems to yield reproducible results superior to conventional TKA concerning the postoperative alignment especially in patients with large preoperative deformities. The relevance for clinical outcome and lifetime of TKA remains to be prooved in long term studies to justifie the longer operation time.
References:
1)Stulberg SD Clin Orth Rel Res 2003 Nov;(416):177-84
2)Chauhan SK JBJS Br. 2004 Apr ;86(3) :372-7 3)Bäthis H et al. Orthopäde 2006 Oct;35(10):1056-65

Measurement of free plasma levels of antiretroviral drugs using a new ultrafiltration method circumventing the loss by adsorption reveals high interin

[1]FAYET A., [1]BUCLIN T., [2]TELENTI A., [1]BIOLLAZ J., [1]DECOSTERD L.A.

Division of Clinical Pharmacology - CHUV[1], Institute of Microbiology - CHUV[2]

Background: Total plasma levels are used for TDM of antiretroviral drugs, whereas unbound concentrations are expected to exert antiviral activity. The determination of free drug levels in plasma can be performed by ultrafiltration, a technique flawed however by the irreversible adsorption of many drugs onto the membrane filters and plastic components. This results in spuriously low levels and underestimated free fractions. We report a new procedure for the accurate measurement of unbound plasma levels of antiretroviral drugs by ultrafiltration.
Methods: During *in vitro* experiments, plasma spiked with antiretroviral drugs were placed in pre-washed Centrifree® ultrafiltration tubes, and centrifuged at 2000g. The ultrafiltrate was collected in four fractions (0-8, 8-16, 16-24 and 24-30 minutes), diluted 1:1 with MeOH without delay, and analysed by LC-MS/MS.
Results: Free drug levels in the early 0-8 min ultrafiltrate fraction were very low and highly variable, and gave free fractions substantially lower than the mean value in the late three fractions (8-16,16-24 and 24-30 minutes) for LPV (mean: 0.89 vs 2.01%, $p<0.01$), NFV (0.091 vs 0.52%, $p<0.01$), SQV (0.98 vs 2.73%, $p<0.01$), TPV (0.014 vs 0.072%, $p<0.01$) and EFV (0.28 vs 1.17%, $p<0.01$). In the two last fractions, the ultrafiltrate levels remained constant, indicating a saturable initial drug adsorption without further influence on the accuracy of free drug level determination beyond 16 min of ultrafiltration. The adsorption phenomenon was modest for IDV, APV and RTV and unnoticeable for ATV and NVP. Applied to patients' plasma, the procedure reveals a substantial inter-individual variability in the free fraction for many HIV drugs.
Conclusions: The change in procedure for the determination of free antiretroviral drug levels enables to circumvent drug loss due to early adsorption on ultrafiltration membrane. Measurement of free drug levels is thus made easier in special situations (pregnancy, haemodilution, protein level changes, liver/kidney insufficiency etc.).

Development and validation of analytical methods by LC-MS/MS for antimalarials combination in plasma

[2]Zanolari B., [1]Hodel EM., [2]Mercier T., [1]Keiser J., [1]Beck HP., [1]Genton B., [1]Decosterd L.,

Swiss Tropical Institute, CH-4002 Basel, Switzerland[1]
Laboratory of Division of Clinical Pharmacology, BH18-218, CHUV, University Hospital, Lausanne, Switzerland [2]

Both efficacy and safety of antimalarial drug combinations strongly depend on the achievement of appropriate drug concentrations during treatment. As part of an ongoing multicentre field study on the influence of pharmacogenetics on overall treatment efficacy of antimalarial drugs, we have developed a sensitive and accurate liquid chromatography-tandem mass spectrometric (LC-MS/MS) method for the simultaneous determination of 13 antimalarial drugs and metabolites (artemether, artesunate, dihydroartemisinine, lumefantrine, desbutyllumefantrine, amodiaquine, desethylamodiaquine, piperaquine, mefloquine, chloroquine, quinine, pyrimethamine, and sulfadoxine) in a small volume of plasma (200 µl).
Plasma sample is purified by a combination of protein precipitation, evaporation and reconstitution in MeOH/ammonium acetate 20 mM 50:50. Chromatographic separation of antimalarial drugs is performed with a 2.1 x 50 mm Atlantis^{TM} dC18 3 µm column equipped with a 2.1 x 10 mm guard column at 25°C using 20 mM ammonium acetate pH 4.1 with formic acid (solvent A) and acetonitrile with 1% formic acid (solvent B) distributed according to a linear gradient elution program: 10% of B at 0 min, → 100 % of B at 15 min. This is followed by an intensive rinsing and re-equilibration step to the initial solvent composition up to 20 min. Analyte quantification, using matrix-matched calibration samples is performed by electro-spray ionisation–triple quadripole mass spectrometry by selected reaction monitoring (SRM) detection using the positive mode. The method validation is based on recommendations of the US Food & Drug Administration. The lower limit of quantification ranges between 0.25 ng/ml (pyrimethamine) to 5 ng/ml (artermisine derivatives).
This analytical method is sensitive, precise and accurate, uses small sample material only, and can be conveniently used in clinical studies and pre-clinical research for which the measurement of plasma concentrations of antimalarial drugs is necessary. Further developments of the LC-MS/MS assay in whole blood and red blood cells (at the site of pharmacological action) are currently underway.

Oral hygiene intervention as motivational tool in tobacco smoking cessation: a pilot study.

[1]Gonseth S., [2]Abarca M., [2]Madrid C., [2]Bouferrache K., [1]Cornuz J.

Department of Ambulatory Care and Community Medicine, PMU[1], Department of Oral Surgery, Oral Medicine and Dental Care, PMU[2]

In Switzerland the prevalence of tobacco smoking is high (31%). At any period of life stopping nicotine consumption generates beneficial effects on health. The development of new strategies to increase the rate of stopping the tobacco consumption is of great interest. The professionals of oral medicine detained a considerable potential of effectiveness in this field. Fried describes that the discovery of periodontal lesions (*gum disease*), induced by tobacco smoking, has been a *teachable moment* to encourage the decision of stop smoking.

The objective of this pilot study is to evaluate the assumption that an oral hygiene treatment at the time of stopping the tobacco consummation helps in the smoking cessation, and brings an extra benefit on oral health reinforcing the motivation of the subject which starts the tobacco smoking cessation therapy.

This open clinical study will evaluate the impact of an additional oral care intervention in 40 patients, from 18 to 70 years, following tobacco smoking cessation therapy by a team of tabacology and smoking cessation specialists, as well as a treatment using nicotine substitutes.

The oral intervention consists of an oral clinical examination (oral status), by a dentist specialist in periodontology, having as aim to detect particular oral diseases. A standardized explanation on the risks of the tobacco smoking in oral health (periodontitis, bad breath, cancer etc.) is given by the dentist during the first visit. After an interval of 7 ± 2 days, the subject will receive an oral hygiene treatment.

During the tabacology follow-up each subject profits of professional counseling for tobacco smoking cessation during 4 visits within two months, and therapy of nicotine substitutes according to existing guidelines. The nicotine status is evaluated after 2 months by means of a personal interview and expiratory CO, and after 6 months by a personal interview (telephone contact). All the participants receive a written documentation *"I want to stop smoking"* according to Swiss recommendations.

Primate adult brain cell autotransplantation for brain repair: study in a MPTP low-dose parkinsonian model.

[1]Brunet J.-F., [2]Redmond D., [1]Bloch J.

Service of Neurosurgery - CHUV[1], Yale Medicale School - New Haven CT - USA[2]

Restoring function of the central nervous system is a challenging task. The large fetal transplantation experience mainly acquired in the context of neurodegenerative diseases, has offered promising results. Despite the great enthusiasm, ethical controversies and lack of fetal donors remain a major problem. Therefore, adult brain cell autotransplantation represents an attractive restoration alternative.

Primocultures were obtained from cortical biopsy. One week after biopsy, monkeys were treated with MPTP leading to an asymptomatic dopamine-depleted parkinsonian model. Cells were grown *in vitro*, fluorescently labeled and reimplanted in the right caudate nucleus. All the animals (4 MPTP-reimplanted, 2 MPTP- and 2 normalcontrols) were sacrified at five months. Cryosections were immunostained for tyrosine-hydroxylase.

Autotransplanted cells survived and still expressed nestin. Migration through corpus callosum was also observed to the controlateral caudate nucleus. Compared to the MPTP control monkeys that exhibit a decrease of 50% of TH-neurons, all the reimplanted MPTP monkeys had a normal count of TH-neurons in the substantia nigra. Adult brain cells can easily be kept in culture, reimplanted in the donor and survive *in vivo*. The long-term impact of autotransplantation has to be evaluated in a symptomatic MPTP model. These attractive results open new perspectives in the field of brain repair.

Primate adult brain cell autotransplantation, a new tool for brain repair? Jean-François Brunet, Eric Rouiller, Thierry Wannier, Jean-Guy Villemure and Jocelyne Bloch. *Experimental Neurology* 2005;196(1):195-198.

A novel method for *in vitro* production of human glial-like cells from neurosurgical resection tissue. Jean-François Brunet, Luc Pellerin, Yvan Arsenijevic, Pierre Magistretti and Jean-Guy Villemure. *Laboratory Investigation* 82 (2002) : 809-812.

Cryopreservation of human brain tissue allowing timely production of viable adult human brain cells for autologous transplantation. Jean-François Brunet, Luc Pellerin, Pierre Magistretti and Jean-Guy Villemure. *Cryobiology* 47:2 (2003) : 179-183.

Neurosurgery Research Group,
CHUV-UNIL,
Beaumont Pavillon 3 - 1011 Lausanne, Switzerland

Ruthenium-Porphyrin Conjugates for Photodynamic Therapy of Cancer

[1]Schmitt F., [2]Govindaswamy P., [2]Suss-fink G., [3]Ang W., [3]Dyson P., [1]Juillerat-jeanneret I., [2]Therrien B.

Pathology Institute, CHUV[1], Chemistry Institute, UniNe[2], ISIC, EPFL[3]

Five new porphyrin-ruthenium conjugates were prepared, characterized and tested for the photodynamic therapy of cancer. The porphyrin moiety (5,10,15,20-tetra(4-pyridyl)porphyrin) provides photosensitizing properties and the ruthenium-arene center provides antineoplastic properties similar to platinum. Osmium and rhodium analogues were also synthesized for comparative studies. The biological effects of all these derivatives were assessed on human melanoma tumor cells, and their cellular uptake and intracellular localization were determined. All molecules, except the rhodium complex which was not cytotoxic, demonstrated comparable cytotoxicity in the absence of laser irradiation. The ruthenium complexes exhibited good phototoxicities to melanoma cells when exposed to laser light at 652 nm. Cellular uptake and localization fluorescence microscopy studies of conjugates revealed that they accumulated in the melanoma cell cytoplasm in granular structures different from lysosomes. The fluorescent porphyrin moiety and the metal component of the complexes localized in similar structures in the cells. Thus, porphyrin-ruthenium derivatives represent promising new organometallic photosensitizers, able to combine chemotherapeutic activity with photodynamic therapeutic treatment of cancer.

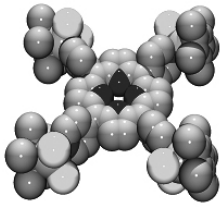

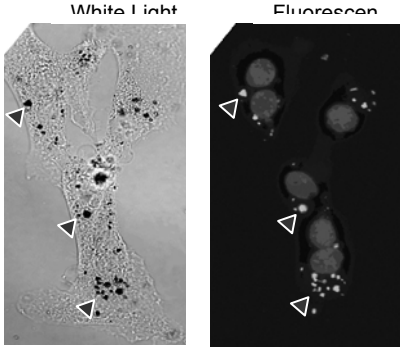

Formation à l'entretien motivationnel chez des cliniciens en toxicodépendance: quels effets sur leurs compétences relationnelles?

[1]Carruzzo E., [1,2]Zimmermann G., [3]Zufferey C., [4]Rougemont Buecking A., [4]Monnat M., [4]Besson J., [1]Despland J.N.

Institute for Psychotherapy, CHUV, University of Lausanne[1], Departement of psychology, University of Fribourg ++[2], Institute for Psychotherapy, University of Lausanne[3], Toxicodependance's Unit, department of psychiatry, CHUV, University of Lausanne[4]

Introduction : L'entretien motivationnel (EM) est un style thérapeutique centré sur le client et directif qui vise à développer la motivation au changement par l'exploration et la résolution de l'ambivalence. De nombreux travaux empiriques mettent en évidence l'efficacité et l'efficience de l'EM dans le traitement des dépendances, sans toutefois, examiner les mécanismes sous-jacents expliquant ce succès thérapeutique. Dans la recherche en psychothérapie, le rôle joué par les facteurs processuels (en particulier alliance et empathie) a été abondamment souligné. Pour l'EM, les études centrées sur les variables processuelles et sur les travaux centrés sur les qualités du thérapeute sont rares. **Objectifs :** Cette étude propose d'examiner le lien entre l'adhérence à l'EM, les caractéristiques des cliniciens en toxicodépendance, l'alliance thérapeutique et l'évolution des patients en cours de la prise en charge. **Design :** Etude naturaliste avec comparaison des pratiques avant (pratique thérapeutique habituelle) et après formation à l'EM. Dans un premier temps, le processus thérapeutique sera examiné pendant 12 séances où le thérapeute utilisera sa pratique thérapeutique habituelle. Puis la formation à l'EM leur sera donnée. Enfin, le processus thérapeutique sera à nouveau examiné pendant 12 séances alors que le thérapeute aura été formé à l'EM. Nous allons en particulier nous intéresser à l'alliance (WAI), à l'empathie (BLRI) et aux réactions émotionnelles (REACT) du thérapeute, à son adhérence à l'EM (MITI) en relation avec les résultats thérapeutiques. **Conclusion :** Cette étude centrée sur le thérapeute permettra de mieux comprendre les variables liées au succès thérapeutique avec une population toxicodépendante.

MAR-enhanced gene expression stability in mesoangioblast stem cells: towards a cell therapy for Duchenne's muscular dystrophy.

[1]vanZwieten R., [1]Puttini S., [1]Saugy D., [1]Mermod N.

Laboratory of Molecular Biotechnology UNIL[1]

Cell therapy is a promising approach to the treatment of Duchenne's muscular dystrophy. For instance, transplantation of normal stem cells in animal models has been shown to improve muscular function and to yield a therapeutic benefit. The potential of mesoangioblast adult stem cells has recently been shown in a Duchenne's muscular dystrophy dog model that was transplanted with wild type stem cells. However, attempts to use virally transduced mesoangioblasts for transplantation were met with modest success. This may be explained by unstable transgene expression after cell differentiation and/or reduced biological activity of the mini-dystrophin gene accomodated in the viral vector. In the current project, we address these issues by stabilizing expression of the transfected full-length dystrophin gene in murine mesoangioblasts by using a human MAR element. We show that usage of the MAR element facilitates clone isolation and gene expression level. Furthermore, eGFP expression in monoclonal mesoangioblasts was found to be stable for weeks without selection pressure and it is sustained during differentiation *in vitro*. We demonstrate that the transfection procedure does not impair differentiation into muscle fibers when transplanted in mice muscle. These data illustrate the potential of the MAR driven dystrophin expression, and the use of transfected stem cells for cell therapy.

Surface Functionalization of Nanoparticles for Cell-Targeted Drug Delivery

[1]Cengelli F., [2]Grzyb J., [3]Tschudi-Monnet F., [4]Montet X., [1]Montoro A., [5]Hofmann H., [2]Hanessian S., [1]Juillerat-Jeanneret L.

Institute of Pathology, CHUV[1], University of Montreal, Montreal (Canada)[2], Institute of Physiology, CHUV[3], University of Geneva[4], EPFL[5]

INTRODUCTION: SuperParamagnetic Iron Oxide Nanoparticles (SPIONs) with a core size of 9-10 nm diameter and a polymer coating such as polyvinyl alcohols (PVA) [1] may be useful both for selective disease detection by MRI and targeted drug delivery provided that their polymer surface is functionalized with therapeutic drugs and/or cell-targeting molecules. Our objectives are to develop surface-functionalized-SPIONs and to evaluate their biocompatibility, uptake by specific cells and cellular localization in cells and organs, and their therapeutic efficacy.

METHODS: The cell uptake of surface-functionalized-SPIONs was evaluated using either 2-dimensional cell cultures or 3-dimensional tumor cell spheroids or brain cell aggregates. SPIONs were injected i.v. in normal mice and organs were examined for their SPIONs content. To evaluate the cell and tissue uptake of SPIONs we combined detection of their fluorescent coating by confocal microscopy and of the iron oxide core by prussian blue detection and transmission electron microscopy. To determine their biocompatibility and their potential for chemotherapy, we evaluated cell survival by measuring metabolic activity and DNA synthesis.

RESULTS & DISCUSSION: Using 2-dimensional cell cultures the presence of amino groups on the SPIONs coating was shown to be mandatory for cell uptake, and this uptake did not modify cell proliferation. SPIONs uptake by cells was increased in the presence of an external magnetic field. The polymer coating and the iron oxide core of SPIONs were internalized by cells *in vitro* (Fig. 1) [2]. In 3-dimensional cell culture models SPIONs were found associated with cells, being able to invade tumor spheroids [3] but not differentiated brain aggregates [2]. *In vivo* amino-functionalized-SPIONs were found in the spleen and the liver but not the brain and kidneys [3]. SPIONs functionalized by therapeutic drugs such as 5-fluorouridine, displayed anti-tumor activity [4].

CONCLUSIONS: These approaches gave a proof of concept of the feasibility of using drug functionalized-SPIONs in biological systems for targeted cell-delivery of therapeutic agents and of their potential to be selectively taken up by living cells in 3-dimensional structures.

REFERENCES: [1] Petri-Fink A, Chastellain M, Juillerat-Jeanneret L, *et al* (2005) *Biomaterials* **26**:2685-2694 ; [**2**] Cengelli F, D. Maysinger D, Tschudi-Monnet F, *et al* (2006) *JPET* **318**:108-116 ; [**3**] Cengelli F, *et al*. ; [**4**] Hanessian S, *et al*., *submitted*

ACKNOWLEDGMENTS: This work was supported by the Swiss National Scientific Research Foundation (Grant 3152A0-105705) and the Swiss Society for Multiple Sclerosis.

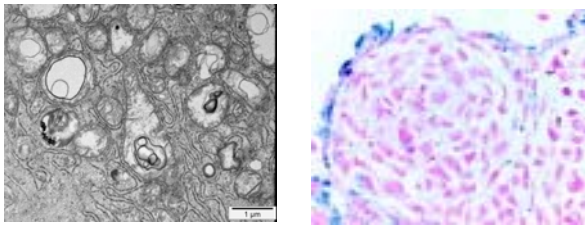

Fig. 1: *Transmission electron and light microscopy of functionalized-SPIONs (arrow) in human melanoma cells and in human melanoma cell spheroids [3].*

In vivo evaluation of human fetal cells as allogenic cell source for tissue engineering

[1]Pioletti D., [1]Montjovent M.-O., [2]Zambelli P.-Y., [3]Scaletta C., [4]Bourban P.-E., [3]Applegate L.,

LBO EPFL-HOSR[1], HOSR[2], Orthopedic Cell Therapy Unit, CHUV[3], LTC, EPFL[4]

Introduction: Recently, human fetal bone cells were characterized in vitro to investigate their potential use for tissue engineering (1). They were shown to be able to proliferate and differentiate into mature osteoblasts in vitro when seeded on poly(L-lactic acid)/5 %wt β-tricalcium phosphate (PLA/TCP) scaffolds (2). In the present study, we describe the combination of fetal bone cells with PLA/TCP implants for cortical and trabecular bone repair. Fetal bone cells were used in their proliferating phase without induction of differentiation to evaluate their osteogenic potential in vivo. Cortical and trabecular bone regeneration were assessed in rat cranial defect, respectively in metaphyseal trabecular network of rat femoral condyle with PLA/TCP implants with and without human fetal bone cells.

Materials and Methods: Human fetal bone cells were obtained from our cell bank comprising eight donors at the end of April 2007 (1). Biocomposite scafold made of PLA reinforced by ceramic particles were used in this study (2). Scaffolds were placed in 24-well plates and cells were seeded by direct pipetting at a density of $2x10^6$ cells/scaffold. Wistar rats (females, 84-92 days old, 275-300 g) were used for the femoral condyle models. At sacrificied (2 months; n = 6 in each group) femoral sections were obtained. Sections were stained with toluidine blue enabling the distinction between the non-mineralized osteoid and the mineralized bone matrix.

Results: Histology of femoral samples. 1. PLA/TCP: implants were surrounded by new bone, formed either by prolongations of the cortical shell or by expansions of the metaphysiseal trabecular lattice, confirming the osteoconductivity of these structures. Infiltrations of newly synthesized bone were strong at the periphery of the scaffolds and remained reduced in the center (Fig 1A). 2. PLA/TCP seeded with fetal bone cells: implants were also well anchored into the neighboring bone. Notable stronger infiltrations of new bone were assessed in the volume of the scaffolds when compared with PLA/TCP alone (Fig. 1B).

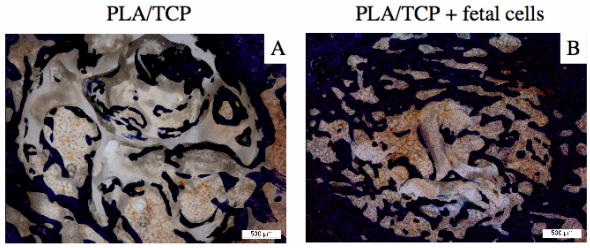

Fig. 1 Representative photomicrographs of histological femoral sections 2 months after implantation. A) PLA 5% β-TCP alone and B) PLA 5% β -TCP seeded with fetal bone cells.

Discussion: The aim of this study was to test the association of fetal bone cells with ceramic reinforced PLA scaffolds for tissue engineering. As animal models, the craniotomy and the femoral condyle approaches in rats were chosen to follow cortical and trabecular bone repair processes. Key findings were the observation of complete bone bridging 12 months after implantation in skulls of PLA porous structures seeded with human fetal bone cells, and a strong induction of trabecular bone ingrowth in femoral condyles 2 months after surgery. The osteogenic properties observed in xenogeneic implants might have been reduced due to adverse response of the hosts, as reported with MSCs from rats used in mice, although immunoprivilege of fetal and adult MSCs is described (4). Further studies must be undertaken to evaluate the respective actions of host and donor cells in the healing process observed. A preliminary study showed that human cells were still detectable in cranial implants 4 weeks after surgery. In conclusion, we demonstrate here, the high potential of human fetal bone cells associated with PLA/ceramic composite structures processed by supercritical gas foaming for their use in cortical and trabecular bone repair.

References: 1. Montjovent et al. Bone, 35, 1323, 2004.
2. Montjovent et al. Tiss Eng, 11, 1640, 2005.
3. Mathieu et al. J Biomed Mater Res A, 75, 89, 2005.
4. Wang et al. J Orthop Res, 25, 926, 2007.

Acknowledgements: This study was supported by grants from the Swiss National Science Foundation (FNRS N°2100- 066872.04.01).

FETAL SPINE CELLS FOR INTERVERTEBRAL DISC REGENERATION

[1]Quintin A., [2]Scaletta C., [1]Jaccoud S., [2]Applegate L.-A., [3]Schizas C., [1]Pioletti D.

EPFL-HOSR[1], Orthopedic Cell Unit Therapy, CHUV[2], Hôpital Orthopédique de la Suisse Romande[3]

INTRODUCTION: Degeneration of the intervertebral disc (IVDD) is thought to be one main cause of low back pain. IVDD begins early in the nucleus pulposus (NP) with decreased cellular content and a loss of proteoglycan and water. Our hypothesis is that matrix synthesis could be stimulated by proteoglycan producing cells. Fetal disc cells could be a promising cell source for regeneration of the degenerated disc. The aim of this study was to investigate the feasibility of using fetal disc cells for disc tissue engineering.

METHOD: Fetal spinal column tissues (1 cm) were obtained after voluntary interruption of pregnancy at 14-16 weeks of gestation (n=3). The spinal tissue was cleaned of adherent tissue, dissected and put into culture in tissue culture dishes. Cells were routinely cultured in DMEM with 10% FCS and 200 mM L-Glutamine. Cell proliferation in monolayer was measured with the CellTiter colorimetric method and compared to adult NP cells (individuals aged 30 to 40 years). Consistency of the cell culture was assessed by measuring expression of galectin-3 and HIF-1 by flow cytometry. Sulphated glycosaminoglycan (sGAG) production by fetal spine cells entrapped in alginate beads was measured by DMMB assay and normalized to DNA content.

RESULTS: Isolated fetal cells proliferated more rapidly than adult NP cells and showed consistent culture. Compared to monolayer culture, fetal spine cells in alginate beads portrayed a rounded morphology. They synthesized matrix as shown by the increase in GAG/DNA ratio during culture in alginate beads up to 26 days.

DISCUSSION: Fetal spine cells can be cultured *in vitro* with minimal requirements and the consistency necessary for a potential clinical application. When cultured in a 3-D environment, they synthesize sGAG, which are responsible for the high water content in NP matrix. It will be of interest to investigate the regeneration capacity of the fetal spine cells in an appropriate animal model.

Acknowledgements: Supported by AO Research Grant 04-S3

Interdisciplinary intervention for Work-related musculoskeletal disorders (MSD)

[1]Kern F., [1]Zuercher K., [1]Gonik V., [1]Danuser B.

IST

The proposed research aims to address the work-related MSD management issue through an interdisciplinary intervention involving clinical and occupational health competencies (rheumatology, occupational medicine, ergonomics).
Workers enduring MSD (especially back-pain) and absent from work are selected from volunteering companies (construction, hospitals, public transport, delivery networks). The workers are randomly placed into two groups : the control group benefits from an usual MSD management strategy and the intervention group benefits from a case-management strategy including work-hardening treatment (work oriented reeducation) and ergonomic intervention in the workplace.

The comparison of health and work-related variables prior and after intervention in the two groups will be used to assess the intervention efficiency and its economic benefits.
We expect to produce new strategies for the management of MSD and workplace rehabilitation as well as guidelines for both authorities and companies.

Keywords : Back-pain, MSD, reeducation, rehabilitation, return to work, interdisciplinary

Whole-Cell Bioprocessing of Human Fetal Cells for Tissue Engineering Applications

[1]Laurent-Applegate L., [1]Scaletta C., [2]Jaccoud S., [2]Quintin A., [2]Pioletti D.

Orthopedic Cell Therapy Unit-CHUV[1], Laboratoire de Biomécanique en Orthopédie[2]

Current restrictions for human cell-based therapies have been related to technological limitations with regards to cellular proliferation capacity (simple culture conditions), maintenance of differentiated phenotype for primary human cell culture and transmission of communicable diseases. We have seen that cultured primary fetal cells from one organ donation could possibly meet the exigent and stringent technical aspects for development of therapeutic products. Master Cell Banks (MCB) of 50 homogenous ampoules of 4-5 million cells each from one fetal organ donation (skin, bone, disc) could be developed in short periods of time compared to other primary cell types. Safety tests were performed at all stages of the cell banking. MCB ampoules could create a Working Cell Bank to be used for clinical or research purposes. For therapeutic use, fetal cells can be used up to 2/3 the life-span in an out-scaling process. These cells should be consistent for several biological properties which could include protein concentration, gene expression and biological activity. As it is the intention that banked primary fetal cells can profit from the prospected treatment of hundreds of thousands of patients with only one organ donation, it is imperative to show consistency, tracability and safety of the process including donor tissue selection, cell banking, cell testing and growth of cells in out-scaling for the preparation of whole-cell tissue engineering products.

Human Fetal Skeletal Muscle Cells for Tissue Engineering

[1]Hirt-Burri N., [1]De Buys Roessingh A., [2]Scaletta C., [2]Applegate L.-A., [1]Hohlfeld J.

Service de Chirurgie Pédiatrique, DMCP, CHUV[1], Orthopedic Cell Therapy Unit, CHUV[2]

INTRODUCTION: Surgical treatment of skeletal muscle loss resulting from trauma, tumor ablation, or inborn tissue defects is hampered by numerous limitations, including early myoblast death, specific immune rejection or the scaricity of functional substitute tissue. Several cell types as well as different matrices have been analyzed to overcome some of these limitations. In our study we aimed to use human primary fetal skeletal muscle cells associated to a clinically approved collagen scaffold to obtain a cellular tissue that could easily be transplanted into injured mice for tissue repair

METHODS: Primary fetal muscle cells were isolated from thigh biopsies from two organ donation after pregnancy termination at 14 and 16 weeks of gestational age. Cells were cultured, frozen and thawed at passage 3 to be marked with a fluorescent cell membrane marker (PKH26). Marked cells were seeded on a collagen scaffold ($1.5x10^6$ cells/cm^2) and implanted in normal C57BL6 mice. Mice were injured on both thighs with a biopsy punch (4 mm diameter), one injured thigh was transplanted with a collagen scaffold disc with human marked fetal muscle cells ($5x10^4$) and the other thigh either with a the scaffold alone or nothing. At 4 days, 2 weeks, 1 month and 2 months post-grafting, implanted and control muscles were harvested for multiple analyses.

RESULTS: Fluorescent labeled human muscular fetal cells were identified at all analyzed time points by fluorescent microscopy. After RNA extraction we found that human beta-actin gene was expressed confirming the viability of the grafted cells.

CONCLUSIONS: Fetal human muscular cells engraft on mice muscle and are still present 2 months after implantation. Further analysis of fetal human muscular cells constructs for the repair of severe muscle loss is warranted.

Granulocyte-macrophage colony-stimulating factor improves mucosal repair in a mouse model of acute colitis

[1]Bernasconi E., [2]Favre L., [2]Bachmann D., [3]Bouzourene H., [4]Croze E., [4]Velichko S., [4]Parkinson J., [1]Michetti P., [1]Velin D.

Department of Gastroenterology and Hepatology - CHUV[1], Department of Gastroenterology and Hepatology, CHUV[2], Institute of Pathology, CHUV[3], Department of Immunology, Berlex Biosciences, Richmond, United States[4]

Background: Granulocyte-macrophage colony-stimulating factor (GM-CSF) has been shown to provide symptomatic benefit in some patients with moderate to severe Crohn's disease. Since GM-CSF was previously reported to improve wound healing, we tested the hypothesis that GM-CSF therapy may exert beneficial effects during acute colitis by promoting regeneration of the injured intestinal mucosa. ***Methods:*** Mice treated with GM-CSF or saline were exposed for 7 days to 4% dextran sulfate sodium (DSS) to induce colitis. On day 5, 7 and 10, mice were subjected to colonoscopy or sacrificed for evaluation of inflammatory reactions and mucosal healing. ***Results:*** DSS exposure resulted in colonic epithelial injury with ulceration. GM-CSF therapy prevented the associated body weight loss and diarrhea, and dampened late inflammatory reactions. Overt signs of mucosal regeneration were observed in GM-CSF-treated mice from day 7 on, both by colonoscopy (ulceration score 1.2 ± 0.3 (GM-CSF-treated mice) vs 3.1 ± 0.5 (untreated mice), p=0.01) and histological analysis (percentage of reepithelialized ulcers 55% ± 4% (GM-CSF-treated mice) vs 18% ± 13% (untreated mice), p=0.01). On day 10, while the crypts at ulcer edges in untreated mice exhibited high cell proliferation indicative of active ongoing mucosal regeneration, we observed a weak proliferation at the ulcer edges of GM-CSF-treated mice suggesting a more advanced regenerative stage. GM-CSF-mediated mucosal repair improvement was accompanied on day 5 by strong expression of mRNA encoding factors implicated in mucosal healing such as hepatocyte growth factor, regenerating gene III beta and gamma, and calgranulin B. ***Conclusions:*** Our study shows that the regenerative activity of the colonic epithelium is improved by GM-CSF administration and suggests that enhanced ulcer healing might contribute to the mechanisms of action of GM-CSF in Crohn's disease.

Neuroprotective Properties of an Anti-VEGF antibody delivered by Gene Transfer in the mouse retina

[1]Cachafeiro M., [1]Bemelans AP., [1]Kostic C., [1]Wanner D., [2]Wenzel A., [1]Arsenijevic Y.

Unit of Gene therapy and Stem cell biology, Jules-Gonin Eye Hospital, Lausanne[1], Laboratory for retinal cell biology, Zürich[2]

In the retina, the balance between pro- and anti-angiogenic factors is critical for angiogenesis control and is involved in cell survival and maintenance. In this study, we describe the effect of an anti-VEGF antibody (scFv-VEGF) local delivery by lentiviral gene transfer.

Balb/c mice received subretinal injections of lentiviral vectors coding scFv-VEGF or a control scFv, and were subjected to a light-induced lesion. Retinal function was tested by electroretinography, and the photoreceptor survival rate was estimated by rhodopsin dosage and transgene expression by Q-PCR.

In vitro data demonstrated that cells transduced by LV-antiVEGF secrete a high amount of scFv-VEGF. We thus treated a group by a subretinal injection of LV-antiVEGF prior to light damage. Control groups received LV-control, vehicle alone, or no pre-treatment. Assessment of the retinal function by ERG showed a decrease of the a-wave amplitude in control groups compared to naïve animals. After LV-antiVEGF treatment, the decrease in a-wave amplitude was only of 37.8 ±6.4%, indicating a better survival rate of the photoreceptors. Rhodopsin content was higher in the LV-antiVEGF group. Q-PCR quantification in the RPE layer demonstrated that the extent of photoreceptor protection correlates with the level of anti-VEGF expression ($R^2=0.781$, $P=0.0194$).

This suggests that anti-VEGF gene transfer may help to fight retinal diseases by both its neuroprotective and anti-angiogenic actions.

From bench to bedside: the reglementation of ex vivo gene therapy

[1]Savioz-Dayer E., [2]Rochat A., [2]Lathion S., [2]Grasset N., [2]Barrandon Y.

Chirurgie expérimentale - CHUV+ Laboratoire de dynamique des cellules souches - EPFL[1], Chirurgie expérimentale - CHUV + Laboratoire de dynamique des cellules souches - EPFL[2]

Recent advances in the field of embryonic and adult stem cells let foresee future clinical applications. Regulatory affairs should be included as early as possible in the design of a cell or gene therapy project as it can seriously impact the decision making process and the feasibility of the project.

Our laboratory is a partner of the Therapeuskin consortium (http://www.omen-graphizm.com/therapeuskin/index.htm), in the 6th framework program of the ECC, aiming to set up foundation to the ex-vivo gene therapy of Recessive Dystrophic Epidermolysis Bullosa (RDEB), an horrendous hereditary skin disease due to deficient collagen VII. RDEB is characterized by continuous and painful blistering, severe scaring resulting in serious handicap, and eventually the formation of squamous cell carcinoma. Treatment is only symptomatic, and the transplantation of genetically corrected autologous stem cells is one of the therapeutic avenues to improve patient's life.

New legal requirements for cell and gene therapy have recently been published in Switzerland and in the European community. In Switzerland, ex vivo gene therapy is under the law on transplants ("Transplantation law") effective from July 1th 2007, and under the supervision of the Federal Office of Public Health (FOPH) and Swissmedic. These agencies will grant permission to experiment only after the project has been approved by the Ethics Committee, and after consultation of the Swiss Expert Committee for Biosafety (SECB), the Federal Office for the Environment (FOEN), and the Swiss Ethics Committee on Non-human Gene Technology (ECNH), and independent experts. Furthermore, genetically corrected cells should be produced in a facility fulfilling the international requirements for good manufacturing practice (cGMP).

Keywords:
Transplantation, cell therapy, ex-vivo gene therapy, clinical trial, legislation, regulatory affairs

RPE65 Lentivirus-Mediated Gene Therapy in Rpe65R91W Mouse Model Improves Cone Survival.

[1]Kostic C., [1]Bemelmans A.-P., [2]Samardzija M., [1]Crippa S., [1]Pignat V., [1]Tekaya M., [1]Wanner D., [1]Cachafeiro M., [2]Wenzel A., [1]Arsenijevic Y.

UGTSCB- Jules-Gonin Eye Hospital[1], Laboratory of Retinal Cell Biology, University Eye Hospital, Zürich[2]

As the gene therapy application to human patients has now started for the treatment of eye diseases, it is of prime importance to precisely document the natural history of candidate diseases for this strategy. Patients suffering from Leber's Congenital Amaurosis (LCA) display a high heterogeneity in the time course of their visual loss, and mouse model technologies offer interesting possibilities to mimic human diseases. We were thus interested in evaluating the effect of a lentivirus-mediated gene transfer of *Rpe65* on cone survival in a new mouse model expressing the mutated $Rpe65_{R91W}$ gene, a mutation found in LCA patients.
$Rpe65_{R91W}$ knock-in mice were treated at P5 or at 1month with an HIV-1-derived lentiviral vector encoding *Rpe65* or GFP under the control of the human 0.8kb *RPE65* promoter. Animals were followed each month by retinal function testing and were sacrificed at 4 months of age for immunohistological analyses to evaluate the expression of different markers in the retina.
The cone-specific markers GNAT2, S-opsin and M/L-opsin in $Rpe65_{R91W}$ retinas are already decreased at 1 month old in comparison to wild type controls and continue to decline severely during the following months. However, after *Rpe65* gene transfer, in the region of *Rpe65* transgene expression, a clear increase in the immunolabeling of cone cells is observed at 4 months old even when the injection of the LV-R0.8-RPE65 was performed at 1 month of age. Moreover, some LV-R0.8-RPE65-injected mice have an improved score at the optomor response test or improved retinal sensitivity as measured by electroretinogram recordings. *Rpe65* gene transfer is able to prolong expression of specific genes that are essential for cone function. This observation is consistent with a functional rescue of $Rpe65_{R91W}$ mice after lentivirus-mediated gene transfer of *Rpe65* in this model. In addition, the therapeutic window to increase cone survival in $Rpe65_{R91W}$ knock-in mouse differs from the one we observed in our previous studies in the $Rpe65^{-/-}$ mouse model (Bemelmans *et al.* PloS Med 2006). Indeed, at four months of age, cone markers were detected after *Rpe65* gene transfer at 1 month of age in $Rpe65_{R91W}$ mice whereas it was inefficient when applied at 1 month in the $Rpe65^{-/-}$ mouse model. These data suggest that treatment in $Rpe65_{R91W}$ patients may similarly benefit of a large therapeutic window for application of a potential gene therapy. However functional analysis has still to be further examined to ensure that not only survival is improved but also cone function is restored. Moreover, additional studies using injections of the LV-R0.8-RPE65 lentiviral vector at an older age will precisely determine the therapeutic window allowing protection of cone photoreceptors in this model.

A COMPARATIVE STUDY OF THE BIOAVAILABILITY OF BROMAZEPAM, OMEPRAZOLE AND PARACETAMOL FOLLOWING ORAL AND NASOGASTRIC ADMINISTRATION TO HEALTHY VOLUNTEERS

[1]Podilsky G., [1]Berger-Gryllaki M., [2]Buclin T., [3]Roulet M., [1]Pannatier A.

Service de pharmacie - CHUV[1], Division de pharmacologie clinique - CHUV[2], Unité de nutrition clinique - CHUV[3]

Introduction: Bromazepam (BMZ), omeprazole (OMZ) and paracetamol (PAC) are frequently administered together to hospitalized patients to decrease anxiety, prevent stress ulcers and fight pain. In enterally fed patients, these drugs are usually administered via a feeding tube. However, their nasogastric bioavailability is uncertain, if only because the pharmaceutical formulation of tablets is altered by grinding. Other causes of concern are gastric emptying and changes in gastrointestinal parameters such as pH and volume of gastric fluid. An examination of the relevant literature reveals that our information on the bioequivalence of the oral and nasogastric routes is replete with gaps and contradictions.

Objectives: To characterize and compare the pharmacokinetic profiles of the three drugs administered by the oral and nasogastric routes in healthy volunteers.

Methods: A prospective, monocentric, randomized and crossover study in 8 healthy volunteers. Each subject was treated via the oral or nasogastric route, followed 28 days later by the other treatment. The protocols were as follows:

- Nasogastric administration: On day 0, insertion of feeding tube, enteral feeding during 24h. On day 1, feeding discontinued, administration of the 3 drugs, then enteral feeding resumed.
- Oral administration: On day 0, 3 standard meals. On day 1, administration of the 3 drugs and 3 standard meals.

Thirteen blood samples were collected during each protocol between t_o and t_{48h}.
The plasma samples were analyzed by HPLC-UV using two validated methods (ISO, ICH and FDA).
Pharmacokinetic parameters were compared statistically: t-paired test of natural log for C_{max}, $AUC_{0-\infty}$, $t_{1/2}$, k_e, and non-parametric test (Wilcoxon) for t_{max}. C_{max}, $AUC_{0-\infty}$ and t_{max} were analyzed for bioequivalence.

Results and discussion: The Table shows the mean $AUC_{0-\infty}$ values, which best represent the pharmacokinetic profile.

	Parameters	Geometric mean	Variation coefficient		Ratio of geometric means	90% confidence limits
BMZ	AUC_{or} [ng/ml·h]	2500	78%			
	AUC_{SNG} [ng/ml·h]	1855	56%	p<0.05	0.74	(0.64 - 0.87)
OMZ	AUC_{or} [ng/ml·h]	579	172%			
	AUC_{SNG} [ng/ml·h]	587	108%	p>0.05	1.01	(0.64-1.61)
PAC	AUC_{or} [µg/ml·h]	37.0	25%			
	AUC_{SNG}[µg/ml·h]	41.3	21%	p>0.05	1.12	(0.98-1.28)

A statistically significant difference is seen in the $AUC_{0-\infty}$ of bromazepam, with nasogastric administration decreasing availability by about 25%. However, this does not appear to be clinically relevant given the usual dosage and the drug's half-life (≈ 30h).
A large inter-individual variability in the parameters of omeprazole prevents any statistical outcome regarding the bioequivalence of the 2 modes of administration. An extended study with a larger number of subjects may perhaps bring clearer answers.
The narrow 90% confidence limits of paracetamol point to an equivalence.

Conclusion: This study shows that the nasogastric route of administration does not appear to cause marked and clinically undesirable alterations in the bioavailability of the tested drugs.

MYOFIBROBLAST DEVELOPMENT IS SUPPRESSED BY HYPOXIA - A CAUSE FOR CHRONIC WOUNDS?

[1]Pietramaggiori G., [1]Modaressi A., [2]Pittet B., [3]Hinz B.

Laboratory of Cell Biophysics, EPFL; department of Plastic Surgery, Genève[1], department of Plastic Surgery, Genève[2], Laboratory of Cell Biophysics, EPFL[3]

Conditions of acute hypoxia support dermal wound healing by promoting inflammation but lead to the development of chronic (non-healing) wounds when persisting; the cause of the latter is unknown. We here investigated how hypoxia influences development and function of myofibroblast, which promote normal wound closure by contraction. Myofibroblasts are specialized fibroblastic cells that generate high contractile activity by de novo expressing smooth muscle actin (SMA) in response to TGFβ1 and mechanical tension. To decipher the direct effect of hypoxia on rat subcutaneous fibroblasts and myofibroblasts in vitro, we assessed SMA expression, cell contraction, proliferation and survival after 5d culture in normoxia (21% O_2) and hypoxia (2% and 5% O_2). Hypoxia significantly increased cell proliferation compared with normoxic conditions. In contrast, the expression levels of the myofibroblast marker SMA as well as myofibroblast contraction on deformable silicone substrates were strongly reduced in hypoxic conditions. Unexpectedly, the level of active TGFβ1 in the culture supernatant in hypoxia was significantly higher compared with normoxia and myofibroblast differentiation was not restored by adding TGFβ1 to the culture. At the same time, expression levels of TGFβ1 receptor type II were moderately down-regulated. Hence, hypoxia appears to uncouple SMA expression in fibroblasts from TGFβ1 signaling. Preliminary results indicate that this hypoxia effect may be due to reduced cell tension, the second pivotal factor for myofibroblast differentiation. We will further elucidate the underlying molecular mechanism with the aim to develop new therapeutic strategies that target altered healing in chronic hypoxic wounds.

OPTIMIZATION CRITERIA IN THE DESIGN OF MEDICAL UWB RADARS IN COMPLIANCE WITH THE REGULATORY MASK

[1]Staderini E., [1]Varotto G.

HEIG-VD, Biomedical Engineering Group[1]

INTRODUCTION: In the present paper we refer to a pulsed UWB radar of the *base-band* type [1-2] which emits very short electromagnetic pulses with a repetition frequency driven by a PRBS generator (Pseudo Random Binary Sequence) performing a synchronous sampling and averaging of the pulses echoed back by the target.
From this analysis a set of constraints will be evidenced and a set of relations linking the various performance parameters of a medical UWB radar will be derived to comply with UWB spectral masks ruled out [2].

METHODS: Once fixed the dynamic range R_m and the process gain G_p, *Eq. (1)* predicts the suitable PRBS frequency f_{prbs} to correctly sample the heart displacement signal modelled as a sinus wave at frequency f_h corresponding to the heart rate in bpm.

$$f_{prbs} = \frac{\pi \cdot f_h \cdot 10^{\frac{G_p}{10}} \cdot 10^{\frac{R_m}{20}}}{60} = \frac{10^{(2G_p + R_m)/20} \cdot \pi \cdot f_h}{60} \quad (1)$$

Eq. (1) defines the family of curves shown in *Fig. 1*.

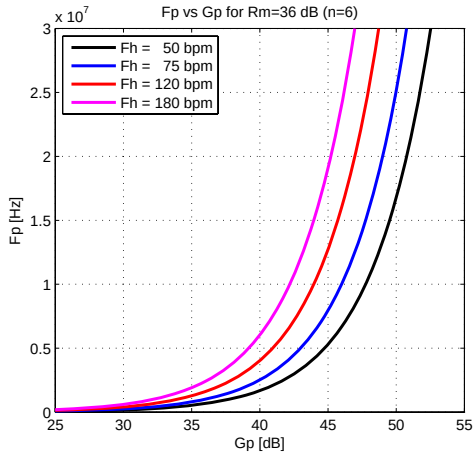

Fig. 1: Pulse repetition rate vs system gain

To maximize the process gain and therefore the signal to noise ratio, we can first minimize R_m, then we can increase f_{prbs}.

$$f_{prbs} \le 4 \cdot \frac{\sqrt{P_{FCC}}}{\tau \cdot A} \quad (3)$$

For a given class of pulses it is possible to express the upper limit for f_{prbs} *(3)*, where P_{FCC} is the FCC maximum power level, τ is the pulse duration and A the pulse amplitude.

RESULTS: *Fig. 2* shows the curves related to *Eqs. (1)* and *(2)* respectively, which have been plotted against f_{prbs}.

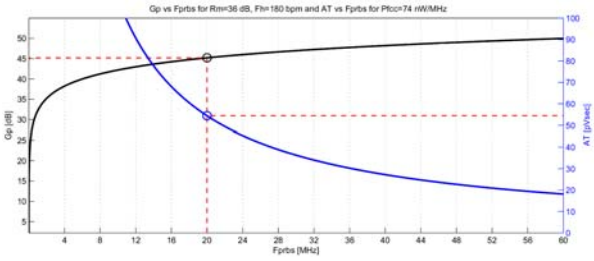

Fig. 4: UWB pulsed radar optimization method

To consider the worst case, f_h =180 bpm, while R_m =36 dB. On the left Y axis we get the process gain, while the right Y axis shows $A \cdot \tau$, corresponding to the pulse shape family.
As result, each given frequency f_{prbs} is associated to an optimum G_p and a sub-family of pulses related to $A \cdot \tau =$ constant and $\tau_{\min} = 430$ps.

DISCUSSION & CONCLUSIONS: This work suggests a general method to optimize the design of a pulse UWB radar system for medical application under FCC mask constraints.
Working at higher f_{prbs} gives better G_p, but the price to pay is a lower $A \cdot \tau$, which means to use a lower energy pulse for a given τ.
The minimum pulse amplitude A which can be employed is function of the noise level, the attenuation path and the kind of used antenna. Is then up to the designer to find the better trade-off depending on the specific application.

iminet, Intelligent Medical Information Network

Jaton M.

HEIG-VD, Biomedical Engineering Group

This project aims to create a usable platform for a virtual medical surgery. Planned over three years, this project means to provide the basis for a suite of new projects with the aim of adding them to the foundation of iminet. It is often difficult to valorise a project in the biomedical field as the context of utilisation is too complex to permit on-going idea implementation. iminet provides the means to access this utilisation context whilst respecting legal and practical conditions.

iminet has been defined using a variety of scenarios, each of which represents a pre-determined situation and highlights a set group of functionalities. A scenario also provides a means of measuring the progress of the project - more specific than the abstract notion of the "workpackage" (also defined in the project) - a scenario has the advantage of being demonstratable and to provide proof of its own advancement. We can define several basic scenarios, used to define the project specifications, but there are many possible scenarios and certainly a number of them will be included as the project progresses - hopefully by professionals in the field of healthcare whom we heartily invite to join however small the contribution they can make.

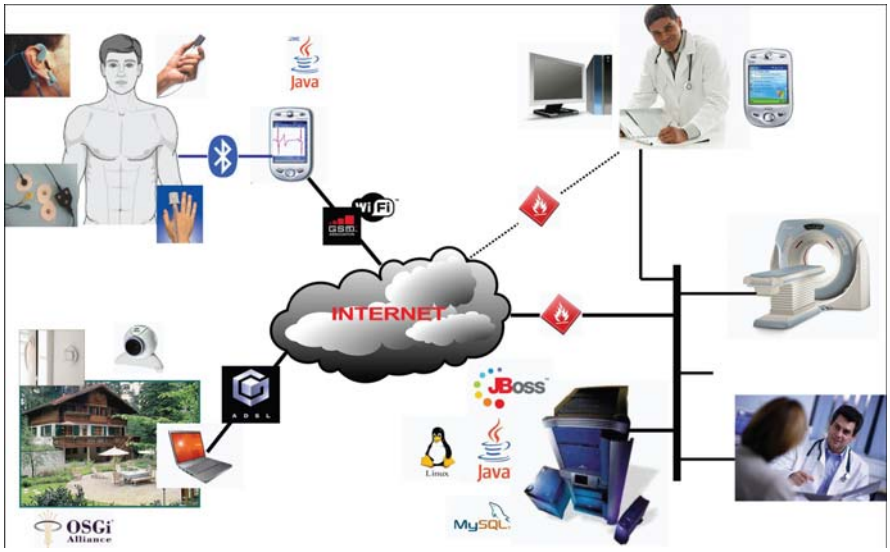

SENSATION: SpO2 Sensor Embedded in a Finger Ring

[1]Castoldi S., [2]Solà J., [1]Correvon M.

HEIG-VD, Biomedical Engineering Group[1], CSEM[2]

In the framework of the European Integrated Project SENSATION (Advanced Sensor Development for Attention, Stress, Vigilance and Sleep/Wakefulness Monitoring) CSEM and HEIG-VD are developing a Finger Ring intended for long-term monitoring of arterial desaturation.

A novel concept of Oxygen Saturation (SpO2) sensor embedded in a finger ring is presented in this paper. Due to the mechanical conception of the probe, the sensor fits any finger topology and assures a constant force applied to the phalanx. Ambient light artifacts are rejected at the analog electronics level. Finally, an innovative distribution of light sources and detectors and a dedicated signal processing procedure resolve the anatomical heterogeneity of different phalanx topologies, compensate low perfusion indexes due to the phalanx anatomy and estimates equivalent pulse oximetry SpO2 indexes. First in-vivo validation results of the novel sensor are discussed at the end of the paper.

Exploring stem cell engraftment

[1]Grasset N., [1]Vannod J., [1]Vermot S., [1]Burki M., [1]Barrandon Y.

Chirurgie expérimentale - CHUV + Laboratoire de dynamique des cellules souches - EPFL[1]

For the last twenty years transplantation of autologous keratinocyte stem cells expanded *ex vivo* (CEA) has been part of the therapeutic arsenal for permanent coverage of extensively third-degree burned wounds. Using this life-saving technique thousands of patients have been treated worldwide. Engraftment is variable, ranging from poor to high, and the number of stem cells needed to sustain long-term renewal of the regenerated epidermis is unknown. Reasons for the lack of this crucial information range from the absence of reliable stem cell markers to the difficulty to experiment on humans. Furthermore, small laboratory animals do not permit to address the question and there is a necessity for a reliable large animal model. With the support of the FP6 EuroStemCell consortium (http://www.eurostemcell.org/), the CHUV and the EPFL, we have demonstrated that the pig is a predictable model to study engraftment of autologous keratinocyte stem cells.

We have first demonstrated that the skin of the pig closely resembles that of the human by all criteria used to characterize keratinocyte stem cells (location, serial cultivation, clonal analysis, transduction of a single keratinocyte stem cell). Second, we have recapitulated all the surgical steps to successfully transplant CEA in the pig, following a procedure that we had previously used in human. Following transplantation clinical examination, routine histology, immunochemistry and clonal analysis were systematically performed to assess CEA engraftment,. Most importantly, these experiments revealed that there was a rapid decrease in the number of transplanted cells that could ultimately result in the loss of the regenerated epidermis, confirming similar observations in the human (unpublished results). Results of Ki-67 and caspase-3 immunostaining indicated that the regenerated epithelium was not apoptotic and remained proliferative. Therefore, it is likely that the transplanted stem cells responded by differentiating to the drastic change in their environmental niche, i.e. from a pampered cell culture to an aggressive grafting bed).

We are now designing a new generation of CEA to improve stem cell engraftment.

Generating thousands of hair follicles from a single multipotent keratinocyte stem cell

[1]CLAUDINOT S., [1]NICOLAS M., [1]ROCHAT A., [1]BARRANDON Y.

Chirurgie expérimentale - CHUV + Laboratoire de dynamique des cellules souches - EPFL[1]

Adult stem cells are crucial for tissue renewal, regeneration and repair. In the skin, they contribute to the constant epidermal renewal and the hair cycling. In the human, keratinocyte stem cells can be extensively expanded in culture and can permanently engraft when autologously transplanted, but the regeneration of hair follicles and sweat glands has never been observed. We have recently demonstrated that the whisker follicle contains multipotent epithelial stem cells that are able to respond to morphogenetic signals to form epidermis, hair follicles and sebaceous glands (Oshima et al., 2001). Most importantly, these stem cells, that are located in the hair follicle niche (the permanent upper part of the whisker) but also in the variable part of the follicle (outside the niche) where they contribute to the regeneration of the hair bulb, can extensively expanded in culture and serially transplanted (Claudinot et al., 2005). Thus, a single epithelial stem cell can generate thousands of hair follicles. These results demonstrate that stemness and multipotency can be maintained in long-term culture and strongly suggests that the absence of hair follicle regeneration is not a consequence of cultivation, but rather due to the absence of inductive morphogenetic signals.

Ex vivo gene therapy to treat recessive dystrophic epidermolysis bullosa: the single cell approach

[1]LATHION S., [1]Rochat A., [2]Vermot S., [1]Barrandon Y.

Chirurgie Expérimentale-CHUV+Laboratoire de dynamique des cellules souches[1], Chirurgie Expérimentale-CHUV[2]

Recessive dystrophic epidermolysis bullosa (RDEB) is caused by loss of function mutations in *COL7A1* encoding type VII collagen, the major component of anchoring fibrils, which are key structures for dermal-epidermal adherence. RDEB patients suffer from skin blistering and develop severe complications resulting in cancer. Lacking a specific treatment for RDEB, *ex vivo* gene transfer to epidermal stem cells shows therapeutic potential. Within the Therapeuskin consortium (http://www.omen-graphizm.com/therapeuskin/index.htm) in the 6th framework program of the ECC, we are setting up an approach to anticipate safety concerns required by regulatory affairs and propose a clonal strategy to fully characterise corrected cells before transplantation (integration site, copy number, absence of rearrangement). We show a proof of principle set of experiments demonstrating the feasibility of the approach and will ask permission for a first clinical trial.

Skin biopsies from an RDEB patient contain stem cells (holoclones) with a life span and quality similar to those of healthy donors. Furthermore, transducing cells via self inactivating (SIN) retrovirus bearing the *COL7A1* cDNA under a human promoter, does not alter their original quality. Transduced cells were cloned and expanded to identify corrected holoclones that express *COL7A1* at a level similar to that of healthy donors and have a normal life span *in vitro*. We are currently investigating the ability of stem cells to engineer a corrected skin equivalent that can regenerate *in vivo*.

In conclusion, we have demonstrated the potential of a single cell approach for *ex vivo* gene therapy to treat RDEB, which should fulfil the regulatory requirements for a first clinical trial to demonstrate safety and feasibility.

RAINBOW: Challenging life-style, chronic and age-related health problems

[1]Staderini E., [1]Varotto G.

HEIG-VD, Biomedical Engineering Group[1]

Western health care faces growing challenges in the years to come. Dramatic increases in chronic diseases such as obesity, cardiovascular diseases and diabetes are already occurring due to factors related to lifestyle and are further exasperated by an aging population. For example, people of age 65 or older account for almost 40% of Americans with diabetes. At the same time, this increase in the number of patients needing care has been complicated by more informed health consumers and influential patient-interest organisations that have increased expectations towards the healthcare system. Together these factors make the prevention and treatment of chronic diseases a crucial issue for Western health care systems.

Sensor technology, wireless communication, miniaturization of patient terminals, and special physical activity monitors have gained broad attention among the public, in academia and in the industry as a strategy for meeting challenges related to chronic diseases including such issues such as improvements lifestyle. Three principal ways in which these technologies can play an essential role in this regard are described in the following. First, sensor technologies may improve the expertise of patients when dealing with their own health. This will enable 'self-care', where patients manage their own health condition and lifestyle-related problems in order to prevent and treat health problems and thus ease burdens on health services. Second, the combination of sensor technologies installed in people's homes and wearable sensor systems on patients will make it possible for health personnel to regularly monitor chronically ill patients or the disoriented elderly. This will allow patients to live at home for a longer period than they otherwise might have been able to. Third, the continuous gathering of patient data may serve as an input to sophisticated medical decision support systems in hospitals and healthcare support centers. This will allow accurate, rapid and individualized feedback to be given to patients about their current health condition and population-based (statistically processed) feedback to be given to health authorities.

However, there are still some crucial problems within sensor technology that must be dealt with. For example, current sensor technology generally suffers from a lack of functionality, low reliability and poor wireless communication interfaces. Other problems, making them largely unfit for routine use, often include the inability to monitor their own working condition and be self-adaptive or context sensitive. Moreover, integration with existing medical information sources is needed in order to make proper use of the knowledge embodied in smart devices.

The unifying concept between all these issues is the collection, processing and sharing of medical information. This is a complex and heterogeneous problem that will require an interdisciplinary approach. RAINBOW is proposed as a collaborative project that will proceed with innovation-based research along the three complementary areas involved in the process sketched above. These three areas are *sensor-based technologies for vital signs and surveillance*, *computer aided diagnostics and extended decision support*, *computer supported cooperative work and medical radio networking*. These three areas will work in conjunction and help create new products and services related to the prevention and treatment of chronic diseases in the future.

These research challenges are extremely complex, thus requiring a multidisciplinary approach. We draw on fields such as medical informatics, computer supported collaborative work, microelectronics and signal and image processing.

Thymic epithelial cells have skin potency

[1]Bonfanti P., [1] Claudinot S., [2]Farley A., [1]Amici A., [2]Blackburn C., [1] Barrandon Y.

Chirurgie expérimentale - CHUV & Laboratoire de dynamique des cellules souches - EPFL[1], Institute for Stem Cell Research, University of Edinburgh[2]

In its function as primary lymphoid organ, the thymus provides the essential environment for maturation and selection of functional T lymphocytes. Thymic epithelial cells (TECs) derive from the endoderm, and more specifically, from the third pharyngeal pouch. The thymic epithelium is organized in a three-dimensional architecture that does not easily fit into standard classifications of simple or stratified epithelia. Moreover, the mechanisms that maintain the epithelial compartment in the post-natal thymus remain unclear. On the other hand, clonogenicity has been shown to be an essential property of adult multipotent stem cells (SCs) in the skin and other stratified epithelia. Epidermal clonogenic keratinocytes can be propagated for several generations *in vitro* and can permanently engraft when transplanted onto patients. In the absence of reliable molecular markers to identify and purify multipotent SCs, the demonstration that they can self-renew *in vitro* and *in vivo* represents, to date, the best method to assess stemness. Likewise, the thymus contains epithelial cells that express genes usually only expressed in the skin or other stratified epithelia, thus indicating a possible relationship. We are investigating the potentialities of post-natal human and rat primary TECs using clonal analysis and functional assays. We demonstrate that post-natal human and rat primary TECs have a clonogenic growth pattern *in vitro*. It has been possible to analyze the molecular signature of subtypes of thymic keratinocytes and to investigate the post-natal role of developmentally regulated genes which are commonly expressed in skin and thymus. Clones of rat TECs have been transplanted onto developing skin in order to evaluate their response to skin morphogenetic signals. Similarly, the response of these clones, as well as of clones obtained from hair follicles, to a thymic environment is being investigated. We demonstrate that cultured TECs share morphological, phenotypic and functional characteristics with skin multipotent stem cells. Moreover, uncovering the relationship of TECs with stem cells of stratified epithelia may provide important insights into the molecular basis of diseases involving both thymus and skin.

Mammalian TOR Modulates Transcription through TORRID Sequences

[1]Brouard M., [1]Nanba D., [1]Azzabi F., [1]Lathion S., [2]Schmid C., [1]Barrandon Y.

Laboratoire de dynamique des cellules souches - EPFL + Chirurgie expérimentale - CHUV[1], Swiss Institute of Bioinformatics[2]

The epidermis, the outermost layer of the skin and the cornea are directly in contact with the outside environment, thus keratinocytes and corneal stem cells need to adapt to environmental changes constantly. Therefore, we have investigated the effect of small temperature variations on human keratinocyte stem cells.

We have identified mammalian target of rapamycin (mTOR) as a major transcriptional modulator in response to physiological variations of temperature in human keratinocytes and demonstrated that the promoter regions of mTOR responsive genes share a common sequence termed TORRID *that comprises two to five 20 base pairs consensus motifs. We defined a minimal DNA sequence that regulates transcription and confers temperature sensitivity. In addition, mTOR is part of a transcriptional complex that associates with* TORRID *sequences. This complex includes the human orthologs of the yeast TOR transcriptional complex and members of the mTORC1 and mTORC2 complexes (RAPTOR or RICTOR respectively). Altogether, our results demonstrate that mTOR transcriptional activity plays a crucial role in fine-tuning of stem cells by their microenvironment.*

Downregulation of p63 enhances fibrinolysis

[1]Volorio C., [1]Nicolas M., [1]Delacour A., [1]Barrandon Y.

Chirurgie expérimentale-CHUV and Laboratoire de dynamique des cellules souches-EPFL[1]

The epidermis, the outermost compartment of the skin, is a stratified and squamous epithelium that constantly self-renews. Keratinocytes, which represent the main epidermal population, are responsible for cohesion and barrier function. Epidermal renewal necessitates a fine equilibrium between proliferation and differentiation of keratinocytes. The keratinocyte stem cell, located in the basal cell layer, is responsible for this epidermal homeostasis and has to decide which fate to adopt through asymmetric division. The p63 transcription factor, belonging to the p53 superfamily, is expressed in basal cell layer of stratified epithelia and is thought to be important in determining stem cell fate. By using a shp63 mediated RNA interference approach, we established an *in vitro* model of the p63 deficiency in human keratinocyte stem cells. Knockdown of endogenous p63 induces cell detachment and downregulation of cell-adhesion genes as previously reported, and results in a loss of clonogenicity. Interestingly, replating of p63 knockdown cells on a fibrin matrix, induces extended fibrinolysis, suggesting that p63 regulates the fibrinolytic pathway. This result was confirmed by quantitative PCRs and shows that p63 modulates members of the fibrinolysis pathway at the transcriptional level.

These results strongly suggest that part of the phenotype observed in knockout p63 mice may result from dysregulation of the fibrinolysis pathway also known to be important for self-renewal, differentiation and wound healing.

Keywords: epidermis, stem cell, p63, RNA interference, fibrinolysis.

Building an artificial corneal: a cocktail of stem cell biology and material sciences

[1]Tobler C., [1]Barrandon Y.

Chirurgie expérimentale - CHUV + Laboratoire de dynamique des cellules souches - EPFL[1]

Clarity of vision requires a transparent and intact cornea. According to the World Health Organization, 45 million people worldwide are estimated to be bilaterally blind and 135 million suffer from severely impaired vision in both eyes. The most efficacious treatment for corneal blindness is the transplantation of a cornea obtained from a human donor, but the demand for corneal transplants largely exceeds availability and the situation is worsening. An alternative may be to replace the damaged cornea with an artificial device. Although considerable progresses have been made in designing transparent biomaterials for ocular applications, many problems remain to be solved to ensure acceptance and proper function of an artificial cornea. Our laboratory has recently demonstrated the presence of stem cells in the corneal epithelium, the function of which is to maintain the integrity of the epithelium that protect the corneal stroma from environmental aggressions. Assessing the impact of biomaterials on stem cell renewal and differentiation is thus crucial.

Efficient computational solutions for bioinformatics and computational biology

Peña C.

HEIG-VD, Biomedical Engineering Group

Bioinformatics and computational biology are tools that biologists and medical researchers use regularly and extensively. Generally speaking, bioinformatics and computational biology make intensive application of well-established algorithms (or variations of them) to huge amounts of data contained in large databases. However, in spite of the continuous growth of computing power, these domains are increasingly experiencing performance bottlenecks that prevent efficient exploitation of the collected data. In response to this situation, we intend to apply our computer-engineering know-how for developing efficient computational solutions for bioinformatics and computational biology.
To attain such a goal we explore two applied-research avenues which are described below: software and hardware solutions.

(1) **Software solutions:** Applying, adapting, and conceiving advanced adaptive methods for processing biological data (analysis, modelling, simulation, etc.) so as to improve existing solutions and/or to solve new problems. Example projects include using bio-inspired algorithms to better search for sequence alignments or applying inference methods to build semi-quantitative models of gene regulatory networks or cell signalling pathways with acceptable predictive power.

(2) **Hardware solutions:** Accelerating, on specialized hardware platforms, the execution of computationally-intensive algorithms in order to build data-processing tools that approach the high-throughput performance of modern experimental biology platforms (-omics). An example application consists in implementing on hardware the highly-sensitive but very-slow Smith-Waterman algorithm for sequence alignment so as to obtain similar processing speeds than for the less-sensitive BLAST family of algorithms. In addition, such specialized platforms are cheaper and more energy-efficient than the high-performance computing facilities being used nowadays.

Combining AFM and calcium imaging to correlate micro-contractile events with calcium flashes

[1]Buscemi L., [1]Hoffmann A., [1]Meister J.-J., [1]Hinz B.

Laboratory of Cell Biophysics. Ecole Polytehnique Fédérale de Lausanne[1]

During wound healing and tissue repair fibroblasts differentiate into myofibroblasts. Expressing alpha-smooth muscle actin, myofibroblasts are able to develop strong contractile forces thereby contributing to wound closure. As in smooth muscle cells, myofibroblast contraction appears to be regulated by the variation of intracellular calcium concentration. We have recently shown that cultured myofibroblasts exhibit spontaneous oscillations of intracellular Ca^{2+} (flashes). In an attempt to provide direct evidence that small contractile events follow Ca^{2+} transients in myofibroblasts and to correlate both events, we used an atomic force microscope (AFM) mounted on the stage of an inverted microscope equipped with epifluorescence illumination. With this setup, the Ca^{2+} flashing of the cell monolayer was recorded simultaneously with the micro-contractile activity transmitted to the AFM force probe. With its ability to record events with nanometer and piconewton resolution the AFM is especially suited to assess the relation between intracellular calcium variation and nanoscale cell contraction.

The mammalian cornea is self-renewing

[1]MAJO F., [1]ROCHAT A., [1]NICOLAS M., [2]ABOUJAOUDE G., [1]BARRANDON Y.

Chirurgie Expérimentale - CHUV + Laboratoire de Dynamique des Cellules Souches - EPFL[1], EPFL[2]

Exceptionally, the corneal epithelium is thought to renew by committed cells generated in and migrating laterally from the limbus, a transition zone between the cornea and the bulbar conjunctiva, a mechanism in striking opposition to regular squamous epithelial renewal. Here, we show that the corneal epithelium of the mouse is self-maintained without limbal contribution, contains oligopotent stem cells that can be serially transplanted and have the capacity to generate goblet cells if provided with a conjunctival environment. In addition, the entire ocular surface of the pig, including the central cornea, contains stem cells (holoclones) that share the same ocular signature, are oligopotent and can generate individual colonies of corneal and conjunctival cells. Hence, we demonstrate that the corneal epithelium is not different from other squamous epithelia, which challenges the popular paradigm that the limbus is the niche for corneal stem cells. We propose that stem cells throughout the mammalian ocular surface have equal potency and that a differing stromal environment determines a corneal or a conjunctival fate.

MERKEL CELLS DO NOT HAVE EPITHELIAL STEM CELLS PROPERTIES

[1]Cattin V., [1]Amici A., [1]Bonfanti P., [1]Brouard M., [1]Barrandon Y.

Chirurgie expérimentale - CHUV + Laboratoire de dynamique des cellules souches - EPFL[1]

Merkel cells are specialised neuro-epithelio-endocrine cells present in pluristratified epithelia of most vertebrates; their epithelial or neural crest origin is still debated. Merkel cells, which specifically express the transcription factor Math1, are scattered in the basal layer of the epidermis and are more numerous in the palm and sole skin, in sensory receptors called touch domes as well as in hair follicle bulges. Their anatomical location close to nerve endings and their function in touch sensation suggest a pivotal role in the interface between the epidermis and the nervous system, possibly in signal transduction. In this study, we have attempted to characterise the relationship between Merkel cells and bulge epithelial stem cells using rodent whisker as models. Clonal analysis and transplantation assays strongly suggest that Merkel cells are not derived from epithelial stem cells. Moreover, Math1-expressing cells sorted from the epidermis are unable to form colonies and to participate in epidermal lineages when transplanted, failing to show stemness properties. Furthermore, when the cells are cultured in conditions that favour the growth of neuro-spheres, they are unable to proliferate, revealing a different behaviour than that of neural crest stem cells. We are further investigating the origin of Merkel cells using neural crest specific lineage tracing.

Stratified Epithelia Stem Cells: A Generic Stem Cell?

[1]Littman D., [1]Claudinot S., [2]Oshima H., [1]Rochat A., [1]Nicolas M., [1]Barrandon Y.

Chirurgie expérimentale - CHUV + Laboratoire de dynamique des cellules souches - EPFL[1], Department of Plastic and Reconstructive Surgery, Kumamoto Medical Center, Kumamoto, Japan[2]

Squamous stratified epithelia are self-renewing tissues, which implies the existence of stem cells. In skin, the existence of *bona fide* multipotent stem cells has been demonstrated in long-term, serial grafting assays. Clonogenic epithelial cells present in the stratified epithelia of the rat (cornea, hairy and glabrous skin, oesophagus, buccal cavity and vagina) are also able to respond to skin and hair morphogenetic signals, thereby forming *de novo* cycling hair follicles, sebaceous glands and contributing to skin formation. Our results show that, irrespective of their germ layer origin, the ability of clonogenic cells from stratified epithelia to respond to skin and hair morphogenetic signals is part of their intrinsic competence. Cell culture acts as a revealer of this competence and does not reprogram the cells. These observations strongly suggest that stem cells of stratified epithelia, irrespective of their germ layer origin, share common characteristics, are closely related, if not identical, and therefore may be interchangeable, opening the door for therapeutic use of one stratified epithelium to heal another.

Acquisition of clonogenicity in rat keratinocyte stem cells

[1]Nicolas M., [1]Delacour A., [1]Barrandon Y.

LDCS - EPFL - CHUV[1]

Mammalian skin contains adult keratinocyte stem cells that are able to self renew and maintain skin function for life. These stem cells are localized in the basal layer of the epidermis and in the upper permanent part of the hair follicle (the bulge). These keratinocyte form colonies under defined culture conditions and are termed “clonogenic” or “keratinocytes colony forming cells” (K-CFCs). Some, named holoclones, have an extensive growth potential and can be serially propagated in culture at least for 180 doublings, whereas others have a growth potential limited to a maximum of 15 divisions (paraclones). Our laboratory has recently demonstrated that clonogenic keratinocytes isolated from the whisker of the rat are bona fide multipotent stem cells that can be serially cultivated, have the capacity to generate hair follicles and sebaceous glands for years when serially transplanted (Claudinot et al., 2005). Hence, clonogenicity seems to be an intrinsic property of adult keratinocyte stem cells. However, keratinocyte colony forming cells can only be detected around E14.5 in the developing skin of the rat, whereas cells with the capacity to form hair follicles already exist in the primitive epidermis at E9.5. These precursor cells were termed fetal keratinocyte stem cells (F-KSCs). Our aim is to characterize these precursor cells and to understand which molecular mechanisms are involved in the acquisition of the clonogenic phenotype in the adult keratinocyte stem cells.

Image acquisition and processing in Epithelial Stem Cell Biology

[1]Fête N., [1]Delacour A., [2]Abou-Jaoudé G., [3]Thiran J.-P., [1]Barrandon Y.

Chirurgie expérimentale - CHUV + Laboratoire de dynamique des cellules souches - EPFL[1], Computer and visualization laboratory - School of Architecture - EPFL[2], Signal processing institute 5 - School of Engineering - EPFL[3]

Images play a key role in biology research. Nevertheless, the information they contain is often underexploited because its collect requires extra technical competences in addition to biological knowledges.
By concentrating on image quality enhancement and on image post -processing fine tuning, hidden important information can be revealed. Moreover, by developing self-made algorithms and implementing resulting computer tools, special treatments that general software are unable to successfully complete, are made possible.
These concepts are carried out here in a growth factor study, FGF-5, which is supposed to have an action on dermal papilla mesenchymal cells; these cells in turn have an action on the mouse vibrissa layers growth. The objective is to identify if the FGF5 expression results in a mesenchymal cells proliferation or in a mesenchymal cells extracellular matrix production increase.

Controlling mesenchymal stem cells response to biomaterials with recombinant integrin-specific fibronectin fragments

[1]Martino M., [1]Mochizuki M., [2]Barker T., [1]Hubbell J.

Institute of Bioengineering, EPFL[1], Georgia Institute of Technology[2]

Introduction: Biomaterials have been modified by the addition of integrin ligand motifs derived from the natural extracellular matrix (ECM). The most simplified and abundantly used being the RGD peptide motif derived from the ECM protein fibronectin (FN). However, even if ECM-derived peptides such as RGD have demonstrated their utility for supporting cell adhesion, their lack of biological information is thus far not optimal to control other cellular processes. At the opposite pole, biomaterial modification with full-length ECM proteins presents significant complications in working with macromolecules that have a complex biology. Ideally, biomaterial scientists would be able to harness the dynamics of the integrin-binding and thus cell-instructive behavior of ECM protein with more simplified systems. Hence, small fragments of ECM proteins, containing specific integrin binding sites, could be used instead of full-length proteins displaying low levels of specificity or small peptides with low bioactivities and poor integrin specificities[1]. In this study, we hypothesized that integration of variants of FN 9th and 10th Type III repeats (FN III9-10) into biomaterials would provide more integrin-specific instructions than full-length FN, while keeping similar adhesion and spreading capacities. As models, we used fibrin matrix, because it is an ideal protein/cell delivery vehicle for repairing damaged tissues, since the polymer is derived from the normal haemostatic pathway. Finally, we used mesenchymal stem cell (MSC) osteoblastic differentiation (OD), as a cell model, since literature suggests that integrins are implied in their differentiation, and because these cells have a strong potential in regenerative medicine.

Materials and Methods: To confirm that α5β1 integrin is a potential target, integrin expression during OD was analyzed. MSCs were cultured with standard OD-inducer medium until 14 days. Percentage of positive cells stained for the subunits α5, α2, αv, β1 and β3 as well as median fluorescence intensities were mesured by flow cytometry. FN III10 and FN III9-10 were cloned into a bacterial expression vector, and addition of the a_2-plasmin inhibitor transglutaminase-sensitive sequence at the N-terminus allowed covalent crosslinking into fibrin matrices[2]. A point mutation on FN III9 (FN III9*-10) was made, in order to increase the specificity for α5β1[3]. Proteins were produced in *E.coli* BL21 and purified with *ÄKTA*FPLC. Cell adhesion and spreading in response to FN fragments as well as their integrin-specificities were assessed in 2D by adhesion, Electrical Cell Impedance Sensing, and immunostaining assays. FN fragments ability to sustain proliferation or differentiation was first evaluated in a 2D model. MSCs were plated on ECM-coated plate with or without α5β1 functional blocking antibody (FBA) in normal or OD-inducer media. Cell number was quantified with alamar blue and cell OD state by alkaline phosphatase activity and qPCR. For the 3D model, fibrin matrices were made to obtain 1-5 molecules of fibrinogen per molecule of FN fragments. MSCs were seeded into the matrices with or without FBA and cultured with OD-inducer media. Proliferation and OD were quantified as in 2D.

Results: Within the first 2 weeks of MSC OD, the surface expression of α5 and β1 subunits were upregulated in parallels showing that α5β1 is likely important during the first steps of OD. Cell adhesion with FBA and immunostaining assays confirmed that FN III9*-10 is more specific for the integrin α5β1 compared to full-length FN and other FN fragments (FN III9*-10 > FN III9-10 > full-length FN > FN III10). Moreover, FN III9*-10 showed similar cell adhesion and spreading rates to full-length FN demonstrating that this fragment keeps adhesion and spreading capacities of the native protein. In 2D, MSC proliferation on full-length FN, FN III9-10, and FN III9*-10 was significantly better than on FN III10 and demonstrated to be dependant of α5β1 engagement. In both 2D and 3D models, MSC OD was significantly accelerated on FN fragments compared to full-length FN, as demonstrated by an increase of alkaline phosphatase activity and by an upregulation of the expression of osteoblastic-specific genes such as the transcription factor CBFA-1, bone sialoprotein and alkaline phosphatase (FN III9*-10 > FN III9-10 > FN III10 < full-length FN). Again, α5β1 engagement showed to be responsible of enhancing OD, since blocking this integrin significantly reduced MSC differentiation.

Conclusions: With a molecular stabilization of FN III9, we generated a specific FN fragment for the integrin α5β1, FN III9*-10. Full-length FN replacement by FN III9*-10 provides more integrin-specific instructions to MSCs and direct proliferation and/or differentiation in both 2D and 3D models, while maintaining similar attachment and spreading capacities to full-length FN. Hence, FN III9*-10 represents a more simplified model for ECM signaling molecule incorporation into biomaterials, limiting ECM information to cells such that cell behavior may be more efficiently controlled. This FN fragment could be used to functionalize fibrin matrix or other biomaterials, in order to specifically control cellular processes that require α5β1 integrin engagement such as MSCs differentiation.

References:

[1]Petrie TA et al. Biomaterials. 2006 Nov;27(31):5459-70.
[2]Schense JC and Hubbell JA. Bioconjug Chem. 1999 Jan-Feb;10(1):75-81.
[3]Altroff H et al. J Biol Chem. 2003 Jan 3;278(1):491-7.

Drops in pulse wave amplitude, a microarousal scoring surrogate

[1]Delessert A., [1]Espa F., [1,2]Rossetti A., [1,3]Lavigne G., [1,4]Tafti M., [1,5]Heinzer R.,

Centre d'investigation et de recherche sur le sommeil. CHUV, Lausanne[1]. Service de neurology. CHUV,Lausanne[2]. Faculté de médecine dentaire, Université de Montréal. Québec, CA[3]. Centre intégratif de génomique, UNIL, Lausanne[4]. Service de pneumologie, CHUV, Lausanne[5]

Rationale: During sleep, sudden drops in pulse wave amplitude are commonly observed simultaneously with microarousals. Their presence are thought to result from a vasoconstriction induced by an autonomic central nervous system activation. We sought to determine if pulse wave amplitude are associated with cortical activation as quantified by EEG spectral analysis.

Methods: EEG spectral analysis was performed over 5 consecutive epochs of 4-seconds before, #1+2: during #3 and after # 4+5 the pulse wave amplitude drops(> 20%). A total of 1084 events, from 10 consecutive sleep polygraphic recordings were analysed. The presence or absence of visually scored EEG arousals was also determined (according to AASM criteria). EEG spectral analysis was done over five wave lengths: (beta 17-30 Hz, alpha 8-12 Hz, theta 4-8 Hz, sigma 12-16 Hz and delta). The power density of each type of EEG wave was compared between the five epochs using repeated measures ANOVA with a Tukey post hoc test.

Results: The global analysis of all drops in pulse wave revealed a significant increase in EEG power density of all EEG wave for the epoch #3 in comparison to the preceding (#1-2) and subsequent (#4-5) ones ($p<0.001$). Further analysis of pulse wave drops not associated with a visually recognized microarousal also revealed a significant increase in EEG power for all types of waves during the pulse wave drops (epochs #3; $p< 0.001$).

Conclusion: Pulse wave amplitude drops, observed on polygraphic sleep recordings, are associated with a sudden increase in EEG power density in all wave length. This suggests that drops in pulse wave amplitude are concomitant to central nervous system activation , even in absence of microarousal.

Supported by the Swiss Pulmonary Society fund for research

Index des auteurs

Remarque: Auteur principal en gras

BEERMANN FRIEDRICH IMI-23
BELLI DOMINIQUE NEU-23
BEMELMANS ALEXIS-PIERRE THE-18/THE-20
BENARD JEAN ODE-10
BENOÎT DAMIEN EHU-1
BERGER METTE M. IMI-30/MCV-26/MCV-27/MCV-29
BERGER THOMAS NEU-25
BERGER-GRYLLAKI MARKOULINA THE-21
BERGMANN SVEN GEN-8
BERNARD MATHIEU **ODE-28**
BERNASCONI ERIC **THE-17**/IMI-31
BERTA TEMUGIN NEU-19
BERTELLI CLAIRE **IMI-28**
BERTHET CAROLE **NEU-34**
BERTHET SERGE THE-1/
BERTHONNECHE CORINNE MCV-21
BERWERT LORENZO MCV-7
BESSON JACQUES THE-8
BEYER VALÉRIE ODE-7/ODE-26
BEZZI PAOLA MCV-4
BIANCHI NICOLETTA NEU-23
BILLE JACQUES IMI-12/IMI-5/IMI-7/IMI-8
BILLE THIERRY IMI-1
BIOLEY GILLES IMI-19
BIOLLAZ JEROME ODE-6/THE-3
BISCHOFDELALOYE ANGELIKA /MCV-31/MCV-39/MCV-40/MCV-47/MCV-7/NEU-28/ODE-14/ODE-15/ODE-21/ODE-24/ODE-25/ODE-4/ODE-5
BIZE VINCENT **MCV-34**
BLACKBURN CLARE THE-39
BLOCH JOCELYNE THE-6
BLOCH JONATHAN **MCV-10**
BOBST MARTINE IMI-22
BOCHUD FRANÇOIS O. ODE-1/ODE-11/ODE-20
BOCHUD MURIELLE MCV-45
BOLARD GRÉGORY MCV-31
BOLAY SASKIA IMI-1/IMI-4
BONAFE LUISA NEU-23
BONFANTI PAOLA **THE-39**/THE-49
BORGEL DELPHINE IMI-34
BOUBAKER ARIANE **MCV-7**/**ODE-5**
BOUFERRACHE KAHINA THE-5
BOUGEON SANDRINE ODE-7/ODE-26
BOUGORSKI ROUSLAN MCV-23/MCV-24
BOULAT OLIVIER NEU-23
BOURBAN PIERRE-ETIENNE THE-11
BOURQUIN CÉLINE EHU-14
BOURQUIN ISABELLE NEU-27
BOUTREL BENJAMIN NEU-30
BOUZOURENE HANIFA THE-17
BOVET PASCAL **MCV-1**/MCV-15/MCV-43/**MCV-44**
BRAISSANT OLIVIER **NEU-22**/NEU-23/NEU-7
BREIDEN BERNADETTE IMI-23
BRIOSCHI ANDREA NEU-27
BRON LUC ODE-18/ODE-22
BRON SYLVIAN GEN-6

BROUARD MICHEL **THE-40**/THE-49
BRUGGIMANN LAURE NEU-13
BRUNET JEAN-FRANCOIS **THE-6**/ NEU-29
BRUYNINX MARC IMI-39
BUCHEGGER FRANZ ODE-21/ODE-4
BUCLIN THIERRY IMI-1/THE-21/THE-3
BULAT NATASA **MCV-25**/MCV-33
BURGER CYRIL MCV-40
BURKI MARCO THE-33
BURNIER LAURENT **IMI-34**/ODE-19
BURNER M MCV-14
BUSCEMI LARA **THE-46** /
BUSSO NATHALIE IMI-33/IMI-40/IMI-41
BUTCHER STEVE ODE-12
BUTTICAZ CHRITOPHE ODE-2
BUTTY ANNE-CHRISTINE MCV-33
CACHAFEIRO MAITE **THE-18**/ THE-20
CAGNON LAURÈNE **NEU-7**
CALANDRA THIERRY IMI-1/IMI-10/IMI-16/IMI-17/IMI-34/IMI-38/IMI-4/IMI-5/IMI-7/IMI-8
CAPLAZI A MCV-18
CARDINAUX JEAN-RENÉ NEU-30
CARIA-DEKHISSI SOUMIA NEU-11
CARMAN GEORGE M. NEU-15
CARMELIET PETER IMI-34/ODE-19
CARNAL BÉATRICE NEU-4
CARPENTIER YVON A. MCV-26/ MCV-29
CARRUZZO EMMANUELLE **THE-8**
CASPAR FRANZ NEU-25
CASTALDO SANDRA NEU-28
CASTELLA CYRIL **ODE-1**
CASTELLA VINCENT **GEN-1**
CASTOLDI SERGE **THE-31**
CATTIN VINCENT **THE-49**
CAVASSINI MATTHIAS **IMI-14**/**IMI-31**/**IMI-32**/NEU-14
CENGELLI FERIDE **THE-10**
CESSON VALERIE **ODE-18**/ODE-22
CHANSON ANNE-LAURE IMI-16/IMI-17
CHANSON MARC IMI-34
CHAPUIS-TAILLARD CAROLINE **IMI-8**
CHARDOT CHRISTOPHE NEU-23
CHARLES ROCH PHILIPPE IMI-23/ GEN-7
CHARRIÈRE NICOLE ENA-1
CHAVE J.P. NEU-14
CHIOLERO ARNAUD MCV-15
CHIOLÉRO RENÉ IMI-25/IMI-30/IMI-34/ MCV-26/MCV-28/MCV-29
CHOBAZ V IMI/33
CHRAST ROMAN NEU-15/NEU-8/NEU-9
CIUFFI ANGELA **IMI-27**
CLARKE PETER G.H. NEU-26
CLAUDINOT STÉPHANIE **THE-34/**THE-39/THE-50
COLLYN FRANÇOIS IMI-28
COMETTA ALAIN IMI-14
COMPTE-PERRET S MCV-35
CONRAD CHRISTIAN THE-1
CORDEY MYRIAM **NEU-32**

CORNUZ JACQUES THE-5
CORREVON MARC THE-31
CORTHESY PATRICIA IMI-39
COULON AURÉLIE ODE-3/**ODE-17**/ODE-23
CRETTAZ DAVID MCV-3
CRIPPA SYLVAIN NEU-21/THE-20
CROQUELOIS ADRIEN MCV-46
CROXATTO ANTONY IMI-15
CROZE ED THE-17
CUTTELOD MELANIE IMI-14
DAHAN E MCV-34
DANON-HERSCH NADIA **MCV-15**
DANUSER BRIGITTA EHU-1/EHU-11/EHU-7/EHU-8/THE-47
DAPHNE REEVES EHU-16
DARWICHE JOELLE EHU-2
DAWSON KEITH ODE-12
DE COULON NICOLAS NEU-16
DE PREUX CHARLES ANNE-SOPHIE **NEU-9**/NEU-15
DEBUYS ROESSINGH ANTHONY THE-15
DECEAURRIZ JACQUES MCV-19
DECOSTERD ISABELLE NEU-19
DECOSTERD LAURENT-ARTHUR GEN-10/ODE-6/THE-4/THE-3
DECRAUSAZ LOANE **IMI-22**
DELACOUR ALEXANDRA THE-42/THE-51/THE-52
DELALOYE JULIE **IMI-10**/**IMI-38**
DELESSERT A THE-57
DENYS ALBAN ODE-14
DEROTEN YVES ODE-28/NEU-16
DERRÉ LAURENT **IMI-21**/MI-26
DESMARCHELIER AURELIEN MCV-19
DESMEDT THIBAUT IMI-41
DESPLAND JEAN-NICOLAS ODE-28/NEU-16/THE-8
DESSEN PIERRE MCV-10
DEVEVRE ESTELLE IMI-21/IMI-39
DI IULIO JULIA **GEN-10**
DIDON JOACHIM MCV-44
DING XAVIER IMI-16
DIXON BRANDON **MCV-41**
DJOJOSUBROTO META **ODE-8**
DO KIM Q. NEU-2
DOMENIGHETTI ANDREA MCV-46
DOVAT M EHU-12
DROZ PIERRE-OLIVIER ENA-1
DUBUIS ALEXANDRE EHU-4
DUC MÉLANIE IMI-22
DUCHOSAL MICHEL IMI-14
DUCHOSAL MICHEL A. ODE-12
DUDLER JEAN IMI-19/IMI-41
DUPASQUIER RENAUD IMI-18/IMI-20/NEU-14
DUPLAIN HERVE MCV-10
DUPUIS MARC ODE-12
DUPUIS PAULINE MCV-31/ODE-15
DYSON PAUL J THE-7
EAP CHIN BIN GEN-10
ECKSTEIN MIGUEL P. ODE-1

EDITH HUMMLER GEN-12
EDWARDS TONY MCV-13
EGGER BERNARD ODE-24
EGGIMANN PHILIPPE IMI-1/IMI-30/IMI-7/MCV-27/MCV-28
ESCHER ANETTE ODE-18
ESPA F THE-57
ESTEBAN MARIANO IMI-10/IMI-38
FAEH DAVID MCV-1
FALCONNIER C MCV-17
FAOUZI MOHAMED EHU-7
FARLEY ALISON THE-39
FAVEZ NICOLAS EHU-2
FAVRAT BERNARD EHU-12
FAVRE BERTRAND **GEN-11**/GEN-4
FAVRE DIMITRI **MCV-36**
FAVRE LAURENT ODE-24/THE-17
FAVRE NATHALIE ODE-28
FAYET AURELIE ODE-6/**THE-3**
FEIHL FRANÇOIS IMI-24/IMI-25/IMI-29/IMI-34/MCV-27
FELLEY ALLISON **MCV-21**/MCV-6
FERBER MATHIAS IMI-21
FEROLDI VERONICA IMI-13
FERRARI SÉLÈNE **GEN-13**
FIUMELLI HUBERT **NEU-1/NEU-20**
FLACTION LAURENCE MCV-47
FLAHAUT MARJORIE ODE-13/ODE-17/**ODE-3**
FLORENCE FAUCHERRE EHU-16
FODSTAD HEIDI **GEN-6**
FOLLONIER LYSIANNE **MCV-37**
FORETAY DIDIER ODE-27
FORNARI ELEONORA **NEU-27**
FRANCIS VERDUN ODE-15
FRATESCHI SIMONA **IMI-23**
FROIDEVAUX CÉLINE IMI-17
FUCHS SEBASTIAN ODE-17
FUMEAUX THIERRY IMI-34
FURRER H IMI-31
FÊTE NICOLAS **THE-52**
GABRIEL ANNE MCV-43/MCV-44
GAEGGELER HANSPETER GEN-6
GAILLARD R NEU-6
GAMBA MARCELLA **NEU-6**
GANTELET EMILIEN NEU-11
GARCIA MIGUEL IMI-18
GARCIA ROSA-EMMA ODE-5
GARDIER STEPHANY MCV-8
GAY CHRISTELLE **NEU-16**
GENTON B THE-4
GERMOND MARC EHU-2
GESSLER A MCV-17
GHIKA JOSEPH NEU-27
GIACOBINI EZIO NEU-14
GIJS M MCV-34
GINET VANESSA **NEU-26**
GIRARDIN ERIC NEU-23

GOGNIAT CÉLINE ODE-7/ODE-26
GOLSHAYAN DELA **IMI-9**/MCV-14
GOMEZ PATRICK **EHU-11**
GONIK VIVIANE EHU-8/THE-47
GONSETH SEMIRA **THE-5**
GONZALES CHRISTINE **MCV-30**
GONZALEZ-RODRIGUEZ ELENA GEN-6
GOURDON GENEVIÈVE NEU-11
GOVINDASWAMY PADAVATTAN THE-7
GOY GENEVIÈVE **IMI-15**
GRASSET NICOLAS THE-19/**THE-33**
GRATA ELIA EHU-13
GREANEY PETER ODE-12
GREMION ISABELLE ODE-25
GREUB GILBERT **IMI-13**/IMI-15/IMI-28
GROSS NICOLE ODE-10/ODE-13/ODE-17/ODE-23/ODE-3
GRUETTER ROLF NEU-34
GRZYB JUSTYNA THE-10
GRÈS SANDRA NEU-15
GUDINCHET FRANÇOIS ODE-11/ODE-5
GUERRY FRÉDÉRIC **GEN-15**
GUEX PATRICE EHU-14/EHU-2
GUIDI RAFFAELLA **NEU-30**
GUIGNARD LAURENCE IMI-20
GUILLEMIN MICHEL EHU-10/EHU-7
GUISAN BARBARA GEN-6
GUTIERREZ DANIEL **ODE-11**
GYSIN RENÉ **NEU-2**
HABRE WALID NEU-23
HAEFLIGER JACQUES-ANTOINE MCV-36
HALFON OLIVIER NEU-30
HAN GIL-SOO NEU-15
HANESSIAN STEPHEN THE-10
HAYOZ DANIEL MCV-15
HEINZER R **THE-57**
HENRY HUGUES EHU-5/MCV-26/MCV-29/NEU-22
HINZ BORIS MCV-37/MCV-38/MCV-42/THE-22/THE-46
HIRSCHEL BERNARD NEU-14
HIRT LORENZ **NEU-24**/NEU-29/NEU-34
HIRT-BURRI NATHALIE **THE-15**
HODEL EM THE-4
HOEFFLINGHAUS THOMAS MCV-40
HOFFMANN ANNICK THE-46
HOFMANN HEINRICH THE-10
HOHL DANIEL GEN-11/GEN-4/ODE-16
HOHLFELD JUDITH THE-15
HONEGGER PAUL NEU-7
HORISBERGER JEAN-DANIEL GEN-6/MCV-34
HOVIUS RUUD NEU-10
HUBBELL JEFFREY IMI-35/ THE-56
HUBER MARCEL ODE-16
HUGUENIN-ELIE ANAÏS **NEU-19**
HUMMLER EDITH GEN-7/ IMI-23
HUYNH CONG KHANH **EHU-4**
IANCU EMANUELA MARINA **IMI-39**

IRESON CHRISTOPHER ODE-12
ISELIN H.U. MCV-18
JACCOUD SANDRA THE-12/THE-14
JACQUEMONT SEBASTIEN GEN-15
JANDUS CAMILLA **IMI-19**
JAQUIÉRY EMILIE **IMI-18**
JATON MARKUS **THE-24**
JATON-OGAY KATIA IMI-12/IMI-5/IMI-8
JAUNIN JEROME **MCV-45**
JEANNET PIERRE-YVES GEN-15
JEROME BADAUT NEU-24
JILEK SAMANTHA IMI-18/**IMI-20**
JOSEPH JEAN-MARC ODE-13/ODE-23/ODE-3
JOTTERAND MARTINE ODE-7/ODE-26
JUILLERAT-JEANNERET LUCIENNE THE-10/THE-7
KADI LINDA **ODE-19**
KAMBER MATTHIAS EHU-5
KAPPENBERGER LUKAS MCV-20
KARABABA MAHIR **IMI-40**/**IMI-41**
KAUFMANN PHILIPPE MCV-40
KEISER J THE-4
KELLENBERGER STEPHAN NEU-10
KELLER U MCV-17/MCV-18
KELLINY CLARA **MCV-43**
KERN FABIENNE **THE-13**/**THE-47**
KERN ILSE NEU-23
KINKEL KAREN ODE-1
KLEEBERG JOERG IMI-20/NEU-13
KNAUPREYMOND MARLIES IMI-16/IMI-17/IMI-38
KNYAZEVA MARIA G. NEU-27
KOLLY LAETICIA **IMI-33**/IMI-41
KOSINSKI MAREK MCV-39/MCV-40/ODE-21/ODE-4
KOSTIC CORINNE THE-18/**THE-20**
KOURTIS IRAKLIS IMI-35
KRAFTSIK RUDOLF NEU-11/NEU-4
KRAMER UELI **NEU-25**
KSONTINI RIADH IMI-1/IMI-7
KUNTZER THIERRY NEU-11/NEU-9
LAHAUSSOIS ANNE MCV-19
LAHRICHI SABINE ODE-6
LAMBELET MARTINE **ODE-9**
LAMON SÉVERINE **EHU-5**
LAMOTH FREDERIC **IMI-12**/**IMI-4**/**IMI-5**
LATHION STÉPHANIE THE-19/**THE-37**/THE-40
LAURENT-APPLEGATE LEE ANN **THE-14/**THE-11/THE-12/THE-15
LAVIGNE G THE-57
LECHLER ROBERT IMI-9
LEGOFF GÉRALDINE IMI-18/IMI-20
LEHR HANS-ANTON IMI-9/MCV-20/MCV-14
LEHNERT T MCV-34
LEI HONGXIA NEU-34
LEIMBRUGER ANTOINE IMI-21
LEMKE G ODE-19
LEPORE MARIO **MCV-12**/MCV-46
LEROY DIDIER IMI-17/IMI-34

LETOVANEC IGOR ODE-24/ODE-25
LEUBA GENEVIÈVE NEU-3/**NEU-4**/NEU-5
LEVRAND SANDRA **IMI-24**/IMI-25/IMI-29
LEVY FREDERIC IMI-21
LEYVRAZ SERGE ODE-14
LIAUDET LUCAS IMI-24/IMI-25/**IMI-29**/**IMI-30**/IMI-34/**MCV-27**
LIBERMAN JULIE **ODE-23**
LIMACHER MONIKA NEU-32
LITTMAN DANIEL **THE-50**
LJUBICIC SANDA **MCV-4**
LOCHERBACH CLAUS **THE-1**
LUBOMIROV RUBIN GEN-10
LUTOLF MATTHIAS EHU-9/NEU-32
MACH JEAN-PIERRE ODE-4
MADRID CARLOS THE-5
MAEDER PHILIPPE NEU-27
MAGISTRETTI PIERRE J. NEU-30/NEU-34
MAGNIN GUYLÈNE NEU-26
MAILLARD CAROLINE ODE-16
MAILLARD DIDIER MCV-47/**ODE-15**
MAILLARD FLORINE **EHU-2**
MAJD HICHAM **MCV-42**
MAJO FRANÇOIS **THE-48**
MALTERRE JEROME MCV-39/NEU-28/ODE-14
MAMIE CHANTAL NEU-23
MANGIN PATRICE EHU-18/EHU-3/EHU-5/EHU-12/GEN-1/GEN-5
MANSUY V NEU-6
MANUEL O IMI-8
MARCHETTI OSCAR IMI-1/IMI-12/IMI-4/IMI-5/IMI-7/IMI-8
MAREK DIANA **GEN-8**
MARQUES-VIDAL PEDRO MCV-15/MCV-45
MARTIN JEAN-LUC NEU-1/NEU-20
MARTINET DANIELLE **GEN-3**
MARTINEZ RAQUEL IMI-27
MARTINO MIKAËL **THE-56**
MASTOUR NABIL NEU-29
MATEUS-AVOIS LIDIA EHU-13
MATHIEU CAROLINE MCV-10
MATSUSHIMA GK ODE-19
MAURI DAVIDE IMI-17
MEIER ROLAND ODE-10/ODE-17/ODE-23/ODE-3
MEINHARDT ANDREA MCV-20/MCV-22
MEISTER JEAN-JACQUES MCV-37/MCV-38/THE-46
MEISTER RAFAEL **MCV-35**
MEMBREZ MATHIEU IMI-23
MERCANTON NICOLE ODE-7
MERCIER T THE-4
MERILLAT A.M. GEN-12
MERMOD NICOLAS THE-9
MEULI RETO MCV-32/NEU-27
MEYLAN P IMI-8
MICHEL PATRIK MCV-44
MICHETTI PIERRE THE-17
MICHIELIN OLIVIER IMI-21
MICONNET ISABELLE IMI-40

MIHAESCU ANCA ODE-25
MILLER BENJAMIN F. MCV-13
MITTAZ-CRETTOL LAUREANE NEU-23
MOCHIZUKI MAYUMI THE-56
MODARESSI ALI THE-22
MODOLO LUCA **MCV-31**/**MCV-32**/MCV-39/MCV-40 **MCV-47**
MOECKLI RAPHAËL ODE-20
MOIX JEAN BERNARD EHU-4
MONNEY ANITA MCV-10
MONNIER PHILIPPE ODE-22
MONNIN PASCAL MCV-32
MONTET XAVIER THE-10
MONTJOVENT MARC-OLIVIER THE-11
MONTORO AUXIA THE-10
MOOSER VINCENT MCV-15/MCV-45
MORICONI N MCV-17
MUNOZ MIGUEL IMI-27
MÉCHIN NATHALIE MCV-19
MÉDARD JEAN-JACQUES NEU-15/NEU-9
MÜHLEMATTER DOMINIQUE ODE-7/ODE-26
MÜHLETHALER-MOTTET ANNICK **ODE-13**/ODE-17/ODE-3/ODE-10
NADRA KARIM **NEU-15**
NAHIMANA AIMABLE **ODE-12**
NANBA DAISUKE THE-40
NARDELLI-HAEFLIGER DENISE IMI-22
NARDOU KATYA ODE-13
NEBIKER-PEDROTTI P MCV-18
NEMIR MOHAMED MCV-12/**MCV-46**
NGUYEN SYLVAIN **MCV-11/**MCV-35
NICOD LALONDE MARIE **ODE-24**
NICOD PASCAL MCV-10
NICODLALONDE MARIE ODE-25
NICOLAS MICHAEL THE-34/THE-42/THE-48/THE-50/**THE-51**
NIEDERHAUSER GUY MCV-36
NIEL FLORENCE GEN-3
NIGGLI FELIX ODE-3
O'NEIL CONLIN IMI-35
OBARZANEK-FOJT MAGDALENA GEN-11/**GEN-4**
OBENAUS ANDRÉ NEU-33
ODDO MAURO IMI-30/MCV-27/MCV-28
OGAY SANDY MCV-6
OPPLIGER ANNE **ENA-1**
OPRAVIL M IMI-31
ORCURTO MARIA-VICTORIA ODE-24/ODE-25/ODE-5
ORTIZ MILLAN **GEN-9**
OSHIMA HIDEO THE-50
OSIH REGINA IMI-14/IMI-31/IMI-32
OVERNEY JAN **ODE-27**
PACCAUD FRED MCV-15/MCV-43/MCV-44/MCV-45
PAERLI K MCV-18
PANAITE PETRICA ADRIAN **NEU-11**
PANNATIER ANDRÉ THE-21
PANTALEO GIUSEPPE IMI-18/IMI-20
PARKINSON JOHN THE-17
PARLIER VALÉRIE ODE-7/ODE-26

PARVEX PALOMA NEU-23
PASCAL SINGY EHU-15/EHU-16
PASCUAL ANDRES **IMI-1**/IMI-14/IMI-4/IMI-7
PASCUAL MANUEL IMI-9
PATRICE GUEX EHU-15/EHU-16
PEDRAZZINI THIERRY MCV-12/MCV-21/MCV-30/MCV-6/MCV-46
PEDRETTI SARAH **MCV-8**
PERILLO FLORENCE ODE-21
PERRENOUD LAURENT EHU-13
PERRIARD JEAN-CLAUDE MCV-23/MCV-24
PERTIN MARIE NEU-19
PESSE BENOIT ODE-6
PETREMAND JANNICK **MCV-33**
PETTER ALAIN **EHU-6**
PEÑA CARLOS-ANDRÉS **THE-45**
PIETRAMAGGIORI GIORGIO **THE-22**
PIGNAT VÉRÈNE THE-20
PIOLETTI DOMINIQUE **THE-11**/THE-12/THE-14
PIOTET ELSA ODE-18
PITTET BRIGITTE THE-22
PITTET VALERIE NEU-23
PLAISANCE VALÉRIE MCV-36
PODILSKY GRÉGORY **THE-21**
PORRET ANDRÉE IMI-23/**GEN-12**
PORTER SARAH **ODE-7/**ODE-26
POUSSIN CARINE MCV-33
PRALONG F NEU-6
PREISSMANN DEPHINE **NEU-5**
PRICE MELANIE NEU-29
PRIKHODKINE ALEXEI EHU-14
PRIOR JOHN O. ODE-14/MCV-31/MCV-39/MCV-40/MCV-47/NEU-28/ODE-15/ODE-24/ODE-25
PROD'HOM GUY IMI-12/IMI-5
PUDER JARDENA **MCV-17**/**MCV-18/**MCV-35
PUGIN JÉRÔME IMI-34
PUTTINI STEFANIA THE-9
PUYAL JULIEN NEU-26
PÉCOUD ALAIN MCV-15
QUADRONI MANFREDO **GEN-2**
QUAGLIA XAVIER **NEU-17**/NEU-18
QUE YOK-AI IMI-30/MCV-27
QUINN THOMAS M. MCV-42
QUINTIN AURELIE **THE-12** /THE-14
RADDATZ ERIC MCV-8
RADTKE FREDDY ODE-8
RAGHUNATHAN SANDEEP MCV-41
RAGUENEZ GILDA **ODE-10**
RANGA ADRIAN **EHU-9**
REDDY SAI **IMI-35**
REDMOND D. EUGENE THE-6
REGAZZI ROMANO MCV-36/MCV-4/MCV-5
REGLI LUCA MCV-28
RENNER PASCAL IMI-16
REVELLY JEAN-PIERRE IMI-30/MCV-27/MCV-28
RIBORDY VINCENT MCV-27
RIEDERER BEAT M. NEU-1/NEU-2/**NEU-3**/NEU-4/NEU-5

RIEDERER IRÈNE M. NEU-1/NEU-2/ NEU-3/NEU-4
RIEDIKER MICHAEL EHU-10
RIFKIN DANIEL B. MCV-38
RIGNAULT STÉPHANIE IMI-34
RIMBAULT ABRAHAM ALINE NEU-14
RIMOLDI DONATA ODE-22
RINSOZ THOMAS ENA-1
RIVALS JEAN-PAUL ODE-18/**ODE-22**/IMI-19
ROBINSON NEIL EHU-5/**GEN-5**
ROCHAT ARIANE THE-19/THE-34/THE-37/THE-48/THE-50
ROCHAT BERTRAND IMI-1/**ODE-6**
ROEHRICH MARC-ESTIENNE **MCV-22**
ROGER THIERRY IMI-10/**IMI-16**/**IMI-17**/IMI-34/IMI-38
ROGGLI ELODIE **MCV-5**
ROHRER MARCEL **MCV-26**/**MCV-29**
ROLLI JOËLLE IMI-24/**IMI-25**/IMI-29
ROMERO PEDRO IMI-19/IMI-21/IMI-26/IMI-39/ODE-18/ODE-22
ROSENBLATT-VELIN NATHALIE **MCV-6**
ROSSETTI ANDREA MCV-27/THE-57
ROSSI MICHEL J. EHU-10
ROSSIER BERNARD C GEN-6
ROTGER MARGALIDA GEN-10
ROTHENBERGER SYLVIA ODE-2
ROTMAN SAMUEL IMI-23
ROUGEMONT BUECKING ANSGAR THE-8
ROULET MICHEL THE-21
RUBIN OLIVIER **MCV-3**
RUCHET MARIE-CHRISTINE ODE-7
RUDAZ SERGE EHU-13
RUFER NATHALIE IMI-26/IMI-39
RUFFIEUX CHRISTIANE NEU-13
RUIZ JUAN MCV-11/MCV-17/MCV-18/MCV-35
SALVI ROBERT IMI-41
SAMARDZIJA MARIJANA THE-20
SANDHOFF KONRAD IMI-23
SANGLARD DOMINIQUE GEN-13/GEN-14
SARTORI CLAUDIO MCV-10
SAUDAN CHRISTOPHE **EHU-3**
SAUGY DAMIEN THE-9
SAUGY MARTIAL EHU-13/EHU-3/EHU-5/GEN-5/MCV-19
SAULNIER-BLACHE JEAN-SÉBASTIEN NEU-15
SAUVAIN JEAN-JACQUES EHU-10
SAVIOZ ARMAND NEU-4
SAVIOZ-DAYER EMMANUELLE **THE-19**
SCALETTA CORINNE THE-11/THE-12/THE-14/THE-15
SCHAEFER STEPHAN IMI-9/MCV-14
SCHAFFTER MANUEL EHU-14
SCHALLER MARIE-DENISE IMI-30/MCV-11/MCV-27
SCHAPIRA MARC IMI-34/ODE-19
SCHAUB SÉBASTIEN MCV-37
SCHENK FRANÇOISE NEU-5
SCHERRER URS MCV-10
SCHIFFER VÉRONIQUE NEU-14
SCHIZAS CONSTANTIN THE-12
SCHLUEP MYRIAM IMI-18/IMI-20/NEU-13

SCHMID CHRISTOPH THE-40
SCHMID P IMI-31
SCHMITT FREDERIC **THE-7**
SCHOMBOURG KARIN **ODE-20**
SCHRAG BETTINA EHU-18
SCHWAB MARCOS MCV-10
SEELENTAG WALTER ODE-22
SENGSTAG THIERRY ODE-23
SENN LAURENCE IMI-12/IMI-5/**IMI-7**
SETYAN ARI **EHU-10**
SHELTON EARP H ODE-19
SIMEONI ELEONORA IMI-35
SIMIONI SAMANTA **NEU-13/NEU-14**
SINGY PASCAL **EHU-14**
SO ALEXANDER IMI-33/IMI-40/IMI-41
SOGUEL LUDIVINE MCV-26/MCV-29
SOLÀ JOSEP THE-31
SOMMER LUKAS ODE-17
SOTTAS PIERRE-EDOUARD EHU-5
SPEISER DANIEL IMI-19/ IMI-21/IMI-26/IMI-39/ODE-18/ODE-22
SPENCER BRENDA EHU-14
SPICHER ALBERT MCV-22
SPORKERT FRANK EHU-12/**EHU-18**
STADERINI ENRICO **THE-23/THE-38**
STALDER MICHÈLE ODE-7
STEEL GRAEME MCV-13
STEHLE JEAN CHRISTOPHE IMI-23
STEIMANN MYRIAM NEU-30
STEINER-TARDIVEL QUYNH-GIAO IMI-10
STIEFEL FRÉDÉRIC ODE-28
STUDER REGINA EHU-11
SUAREZ PHILIPPE **GEN-7**
SUGAMELE ROCCO IMI-34/ODE-19
SULSTAROVA BRIKELA EHU-15
SUSS-FINK GEORG THE-7
SWARTZ MELODY IMI-35/MCV-41/ODE-27
TAFTI M THE-57
TALAMO BLANDIN ANNA **ODE-26**
TANGER ELLEN NEU-21
TAPPY LUC MCV-26/MCV-29
TARDIF ERIC NEU-4
TARR PHILIP GEN-8
TEKAYA MERIEM NEU-21/ODE-8/THE-20
TELENTI AMALIO GEN-10/GEN-8/GEN-9/IMI-27/ODE-2/THE-3
THERRIEN BRUNO THE-7
THEUMANN NICOLAS MCV-32
THIRAN JEAN-PHILIPPE THE-52
THORENS BERNARD MCV-33
THORSTENSEN ERIC MCV-13
TICHELLI ANDRÉ ODE-7
TISSOT JEAN-DANIEL MCV-3
TOBLER CÉLINE **THE-43**
TOUVREY CEDRIC IMI-21/**IMI-26**
TRUEB LIONEL MCV-11
TRUTTMANN ANITA C. NEU-26

TSCHOPP JÜRG IMI-17
TSCHUDI-MONNET FLORIANE THE-10
TURNER VINCENT **GEN-14**
VALENTA INES MCV-40
VAN TULDER LAURENCE **MCV-28**
VANDERVLIES ANDRE IMI-35
VANLOHUIZEN MAARTEN NEU-21
VAN MELLE GUY ODE-26
VANNOD JEANNE THE-33
VANZWIETEN RUTHGER **THE-9**
VAROTTO GRAZIANO THE-23/THE-38
VASSALLI GIUSEPPE **MCV-20**/MCV-22/**MCV-23**/**MCV-24**
VELICHKO SHARLENE THE-17
VELIN DOMINIQUE THE-17
VENETZ JEAN-PIERRE MCV-7
VERDIER VALERIE **NEU-8**/NEU-9
VERDUN FRANCIS R. MCV-47/MCV-31/MCV-32/ODE-1/ODE-11/MCV-39/MCV-40
VERMOT STEEVE THE-33/THE-37
VERNAY ANDRÉ NEU-4
VEUTHEY JEAN-LUC EHU-13
VICTORIA ORCURTO **ODE-14**
VIERTL DAVID **ODE-21**/ODE-4
VINGERHOETS FRANÇOIS IMI-20/NEU-28
VOELTER VERENA ODE-14
VOIROL PIERRE MCV-26/MCV-29
VOLLENWEIDER PETER MCV-15/MCV-45
VOLORIO CHRISTELLE **THE-42**
VORA SAMIR IMI-4
WAEBER BERNARD IMI-24/IMI-25/IMI-29
WAEBER GÉRARD MCV-11/MCV-15/MCV-33/MCV-36/MCV-45
WANG Q MCV-14
WANNER DANA NEU-21/ODE-8/THE-18/THE-20
WASELLE LAURENT **NEU-18**
WEBER OREST **EHU-15**/**EHU-16**
WENZEL ANDREAS THE-18/THE-20
WIDMANN CHRISTIAN MCV-25/MCV-33
WIDMER NICOLAS ODE-6
WIEGLER KARINE NEU-29
WIPFF PIERRE-JEAN **MCV-38**
WIRAPATI PRATYAKSHA ODE-8
WYNIGER JOSIANE ODE-2
WYSS JEAN-CHRISTOPHE IMI-9/MCV-14
YANG JIANG-YAN MCV-33
ZAMBELLI PIERRE-YVES THE-11
ZANOLARI BORIS **THE-4**
ZENCAK DUSAN **NEU-21**
ZHANG KUNLIN GEN-9/IMI-27
ZIMMERMANN G THE-8
ZOETE VINCENT IMI-21
ZOSSO NATHALIE IMI-22
ZUERCHER EMILIE **ODE-2**
ZUERCHER KARIN THE-47
ZUFFEREY C THE-8
ZURN ANNE NEU-17/NEU-18